SYNTHESIS AND CHARACTERIZATION OF

POLY(ETHYLENE GLYCOL) AND POLY(ISOBUTYLENE)

BASED IONIC LIQUIDS

AND SAXS INVESTIGATIONS OF

THEIR HIERARCHICAL INTERNAL STRUCTURE

DISSERTATION

Zur Erlangung des

Doktorgrades der Naturwissenschaften (Dr. rer. nat.)

der

Naturwissenschaftlichen Fakultät II

der Martin-Luther-Universität Halle-Wittenberg,

vorgelegt

von **Parvin Zare**

geb. am 03. August 1981 in Tabriz/Iran

ausgeführt unter der Leitung von

Prof. Dr. Wolfgang H. Binder

Professor für Makromolekulare Chemie

Martin-Luther-Universität Halle-Wittenberg

Gutachter: Prof. Dr. Piotr Stepnowski

Tag der Verteidigung: 08.07.2015   Halle (Saale), den 29.07.2015

i

Acknowledgements

I would like to express my gratitude to:

Abstract

Owing to the unique characteristics of the ionic liquids, incorporation of the ionic moieties to the polymer structure results in a new class of materials, so called polymeric ionic liquids (POILs), with enhanced mechanical stability, improved processability, durability, and spatial controllability. Simple tuning of the physicochemical and mechanical properties of POILs via modifying their molecular features such as nature of the anion, cation, and the associating polymeric compartment, flourishes their sophisticated utilization in the various fields of applications.

This thesis describes the synthesis and characterization of two class of POILs based on poly(ethylene glycol) (**PEGILs**) and poly(isobutylene) (**PIBILs**) accompanied by morphological investigations of the products in which self assembly of the material is observed. Both of the selected polymers are biocompatible, with low T_g, and tunable viscosity via varying polymerization degree or modifying functional end groups. In this respect, series of **PEG** and **PIB** were reacted with the selected amines (an aliphatic, a cyclic, and an aromatic amine) or their alternative derivatives. Different synthetic approaches and conditions were performed to achieve the facile and efficient route toward the designed products. Azide/alkyne "click" reaction was acquired as a successful method for efficient synthesis of the two novel series of **PEGILs** and **PIBILs** with different molecular weights accompanied with various cations. Subsequent alteration on the associating anion was carried out via anion exchange reaction. All synthesized materials were characterized via spectroscopic methods (NMR, ESI and MALDI-TOF-MS). Furthermore, physical and mechanical behavior of the prepared materials with respect to the type of cation, anion, and molecular weight were evaluated. According to the results, all synthesized POILs demonstrated a higher thermal stability in comparison to the nonionic initial polymers. Tribological investigations on **PEGILs** exhibited their potential as lubricants due to low friction and reduced wear. ESI-TOF-MS analysis of the synthesized **PEGILs** proved the formation of the small aggregates, while SAXS analysis revealed a strong self-organizing attitude of the synthesized **PIBILs** due to high polarity difference between the polymer chain and ionic head groups resulted in formation of the ordered structures in the range of meso-scale. However, increasing the molecular weight and exchanging the anion from Br$^-$ to poorly coordinating Tf$_2$N$^-$ resulted in weakening and even loss of the ordered structures. Variable temperature in situ SAXS measurements showed a temperature dependent order-disorder transition in most of the synthesized **PIBILs**. The required relaxation time to recover the initial ordered structure in some **PIBILs** was very short. Hence, **PIBILs,** with a proper choice of cation and anion can be a potential candidate in the field of self healing materials.

Kurzfassung

Der Einbau von ionischen funktionellen Gruppen in eine Polymerkette ermöglicht, basierend auf den herausragenden Eigenschaften von ionischen Flüssigkeiten (engl. ionic liquids, IL), das Design von neuartigen Materialen, den so genannten polymeren ionischen Flüssigkeiten (engl. polymeric ionic liquids, POILs). Diese zeichnen sich durch eine erhöhte mechanische Stabilität, verbesserte Verarbeitbarkeit, Langlebigkeit sowie gezielte (Mikro-)Strukturierbarkeit aus. Physikalisch-chemische sowie mechanische Eigenschaften polymerer ionischer Flüssigkeiten können durch zielgerichtete Modifizierung ihrer molekularen Merkmale wie die Natur des Anions, des Kations oder des zugrundeliegenden Polymergerüstes in einem breiten Rahmen variiert werden und ermöglichen dadurch eine große Bandbreite unterschiedlicher Anwendungsmöglichkeiten in den verschiedensten Einsatzgebieten.

Diese Arbeit beschreibt die Synthese und Charakterisierung zweier Klassen polymerer ionischer Flüssigkeiten, welche auf Poly(ethylenglykol) (**PEGILs**) und Poly(isobutylen) (**PIBILs**) basieren. Der Fokus der vorliegenden Arbeit liegt im Besonderen auf den morphologischen Analysen der hergestellten Materialien und deren Selbstorganisationsverhalten. Beide Polymerklassen sind biokompatibel, weisen eine niedrige Glasübergangstemperatur (T_g) auf und ermöglichen das Einstellen der Viskosität durch die Variation des Polymerisationsgrades oder durch Modifikation der funktionellen Endgruppen. Dem entsprechend wurde eine Reihe von verschiedenen Poly(ethylenglykol)en und Poly(isobutylen)en mit ausgewählten Aminen (aliphatisch, zyklisch und aromatisch) sowie deren Derivaten umgesetzt, wobei verschiedene Synthesemethoden und Reaktionsbedingungen getestet wurden, um eine möglichst einfache und effiziente Syntheseroute für die Herstellung der gewünschten Produkte zu entwickeln. Dabei stellte sich die kupferkatalysierte Azid-Alkin-"Click"-Reaktion als eine erfolgreiche Methode für die effiziente Synthese zweier neuer Gruppen von **PEGILs** und **PIBILs** mit verschiedenen Molekulargewichten sowie verschiedenen Kationen heraus. Im Anschluss erfolgte die Variation des assoziierten Anions durch Anionenaustauschreaktionen. Alle hergestellten Verbindungen wurden mittels spektroskopischer Methoden (NMR, ESI und MALDI-TOF-MS) charakterisiert, wobei das physikalische und mechanische Verhalten der hergestellten Materialien in Abhängigkeit von der Art des Kations und des Anions, sowie in Abhängigkeit vom Molekulargewicht untersucht wurde.

Alle synthetisierten POILs wiesen eine höhere thermische Stabilität als die entsprechenden Ausgangspolymere auf. Außerdem zeigten die tribologischen Untersuchungen auf Grund guter

Gleiteigenschaften und vermindertem (thermischen) Verschleiß von **PEGILs** das Potential dieser Materialen für die Anwendung als Schmiermittel auf. Die Analyse der hergestellten **PEGILs** mittels ESI-TOF-MS bestätigte die Bildung von kleinen Aggregaten, während SAXS Untersuchungen die starke Selbstorganisationstendenz der synthetisierten **PIBILs** zeigten. Diese beruht auf den starken Polaritätsunterschieden zwischen der Polymerkette und der ionischen Kopfgruppe und führte zur Bildung von geordneten Strukturen im Meso-Größenbereich. Die Erhöhung des Molekulargewichtes und der Anionenaustausch des Br^- zum schwach koordinierenden Tf_2N^- resultierten jedoch in der Abschwächung oder sogar im Verlust der geordneten Struktur. Temperaturabhängige SAXS Messungen zeigten für fast alle synthetisierten **PIBILs** einen temperaturabhängigen Übergang von geordneter zu nichtgeordneter Struktur. Die dabei beobachtete Relaxationszeit bis zur Wiederherstellung der ursprünglichen Struktur war für manche **PIBILs** relativ kurz. Folglich können **PIBILs**, nach geeigneter Auswahl des Kations und des Anions, als potentielle Kandidaten für selbstheilende Materialien betrachtet werden.

Results of this dissertation have been published

Parts of the chapters 2.1 have been published in Zare, P.; Mahrova, M.; Tojo, E.; Stojanovic, A.; Binder, W. H., Ethylene glycol-based ionic liquids via azide/alkyne click chemistry. *J. Polym. Sci. Pol. Chem*. **2013**, *51*, 190-202. Text, Figures 2.1- 2.11, and Tables 2.1-2.3 adapted with permission from *J. Polym. Sci. Pol. Chem.* Copyright 2013 John Wiley and Sons.
DOI: 10.1002/pola.26362.

Parts of the chapters 2.1 have been published in Pagano, F.; Gabler, C.; Zare, P.; Mahrova, M.; Dörr, N.; Bayon, R.; Fernandez, X.; Binder, W.; Hernaiz, M.; Tojo, E.; Igartua, A., Dicationic ionic liquids as lubricants. *Proc. Inst. Mech. Eng. J J. Eng. Tribol* **2012,** *226* (11), 952-964.Text and Figures 2.11 and 2.12 adapted with permission from SAGE Journals (http://online.sagepub.com).
DOI:10.1177/1350650112458873

Parts of chapter 2.2 have been published in Zare, P.; Stojanovic, A.; Herbst, F.; Akbarzadeh, J.; Peterlik, H.; Binder, W. H., Hierarchically Nanostructured Polyisobutylene-Based Ionic Liquids. *Macromolecules* **2012,** *45*, 2074-2084. Figures 2.13, 2.16, 2.17, 2.22, 2.25, part of Tables 2.6 adapted with permission from (Zare, P.; Stojanovic, A.; Herbst, F.; Akbarzadeh, J.; Peterlik, H.; Binder, W. H. *Macromolecules* 2012, 45, 2074-2084.) Copyright 2012 American Chemical Society.
DOI:10.1021/ma202736g

Parts of chapter 2.2 have been published in Stojanovic, A.; Appiah, C.; Dohler, D.; Akbarzadeh, J.; Zare, P.; Peterlik, H.; Binder, W. H., Designing melt flow of poly(isobutylene)-based ionic liquids. *J. Mater. Chem. A* **2013,** *1* (39), 12159-12169. Figures 2.26, 2.30, 2.32, 2.33 and part of Tables 2.6 2.17, 2.22, 2.25, part of Tables 2.6 [*J. Mater. Chem. A*, **2013**, *1*, 12159-12169] reproduced by permission of The Royal Society of Chemistry. DOI:10.1039/C3TA12646C

List of abbreviations

ATMS   allyltrimethylsilane

ATRP   atom transfer radical polymerization

BCP   Block copolymer

BPB   3-(bromopropoxy)benzene

CNT   carbon nanotube

CuBr   copper (I) bromide

DCM   dichloromethane

DIPEA   diisopropyethylamine

DMF N,N-dimethylformamide

DMSO   dimethyl sulfoxide

DSC   differential scanning calorimetry

DtBP   2,6-di-tert-butylpyridine

EHM   Eisenberg-Hird-Moore

ESI-TOF-MS   electrospray ionization time-of-flight mass spectroscopy

FSDP   first sharp diffraction peak

GPC   gel permeation chromatography

HEXIL   hexaethylene glycol-based ionic liquid

IB   isobutylene

IL   ionic liquid

IR   infrared

LC   liquid-crystalline

LCCP   living carbocationic polymerization

MALDI-TOF-MS   matrix-assisted laser desorption/ionization time-of-flight mass spectrometry

MeOH   methanol

MIM   1-methylimidazole

MPy   1-methylpyrrolidine

MWCNT   multiwalled carbon nanotube

NMR   nuclear magnetic resonance

ODT   order-disorder transition

OOT   order-order transition

PDI   polydispersity

PEGIL   poly(ethylene glycol)-based ionic liquid

PIB	poly(isobutylene)
PIBIL	poly(isobutylene)-based ionic liquid
PIL	polymerized ionic liquid
PIL-BCP	ionic liquids block copolymer
POIL	polymeric ionic liquid
PS	polystyrene
RAFT	reversible addition-fragmentation chain transfer polymerization
RDF	distribution function
ROMP	ring opening metathesis polymerization
RTIL	room temperature ionic liquids
SAXS	small angle X-ray scattering
TEA	*N,N,N*-triethylamine
TEGIL	tetraethyleneglycol-based ionic liquid
TGA	termogravimetric analysis
THF	tetrahydrofuran
TLC	thin-layer chromatography
TMPCL	2-chloro-2,4,4-trimethyl-1-pentyl chloride
TSIL	task-specific ionic liquid

Table of contents

1.0. Ionic liquids (ILs)

Excellent thermal stability, high heat capacity, negligible vapor pressure, low flammability, conductivity, extended electrochemical window, solvation ability of materials with widely varying polarity but mainly tunability via precise selection of its constructive components are the very well known characteristics of "ionic liquids".[1] Ionic liquids (ILs) are constructed of an organic cation, mainly quaternary ammonium, imidazolium, pyridinum, pyrrolidinium or phosphonium and a weakly coordinating anion such as halides, acetates, tetrafluoroborate, hexafluorophosphate which makes them to be considered as molten salts.[2] However, these compounds are characterized by weak interactions as result of the combination of a large cation and a charge-delocalized anion which lead to a significant decline in their melting point in comparison with classical molten salts. Eventually, the physical and chemical properties of ILs are highly dependent on both, the nature of the cation and the anion.[3] Thus, a proper choice of the cation and associating anion can lead to ionic liquids with melting point at or even below room temperature named as room temperature ionic liquids (RTILs).[2,4] Further, task-specific ionic liquids (TSILs) are another category of ionic liquids which are designed and synthesized for a particular application.[5]

It is noteworthy to mention that, since Paul Walden[6] reported the synthesis of the very first ionic liquid as a side product of Friedel-crafts reaction in 1914, there is an exponential growth in the number of research being conducted in this field. Although this new class of material was neglected in its early discovery years, the topic was revolutionized after almost half a century until 2000s when ILs entered their glorious time.[7]

Today, owing to their unique physicochemical properties, ILs are still on the spotlight of many research fields. They have a wide range of applications from solvents as reaction media of numerous organic syntheses[1] and polymerizations,[8-9] electrolytes[10] in fuel cells,[11] batteries[12] and sensors,[13] ionic matrices[14] in analytics, separation via gas sorption,[15] membranes and metal extractions,[16] catalysts,[17-19] lubricants in tribology,[20-21] and many others.[22-23]

1.1. Polymeric ionic liquids (POILs)

Although, ionic liquids initially came across polymer chemistry as a reaction media,[24] recently, due to great demands toward especially new electrolytes, investigations on ionic moieties chemically bonded to polymer structures, so called polymeric ionic liquids (PILs) became more dominant.[25-29] Revealing of the fascinating characteristics of ionic liquids encouraged polymer scientists to explore the possibility of designing a new class of polymeric materials via introducing these ionic compartments to the body of polymers. Hence, a new class of materials was invented with durability, processability, and mechanical stability inherited from the preliminary polymer and thermal stability, high polarity, and conductivity of the original ionic liquids.[29-30] But most importantly, PILs, can be tailored and tuned via different modification of the polymer chain in addition to numerous combinations of the cation and the anion. Obtaining an extensive overview on these novel materials require a proper classification which can be done after an appropriate definition. Shaplov[31] defined PILs as "polymers which contain at least one ionic center, similar by composition to the structure of commonly used ionic liquids (ILs), as a covalently bonded part of their constitutional repeating (monomer) unit" and provided a comprehensive classification of these materials. In this regards, polymeric ionic liquids can be classified via three different approaches[32] accordingly: a) the type of mobile ion[33-34] b) the type of polymer structure, and c) the location of ionic center.[32]

| | poly cation | poly anion | copolymer | zwitterion |
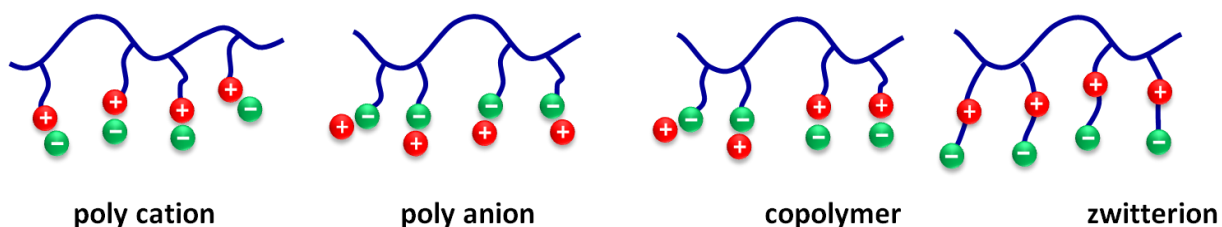
Figure 1.1. Schematic representation of variety of structures of synthesized PILs.

a) The type of mobile ion: This category covers all polymeric ionic liquids which consist of ionic moieties as their repeating unit. Depending on the structure of IL monomer there are four different possibilities. If the polymerizing center is located only on the cation, it generates a polycation with mobile anions[35-37] while the inverse structure results in a polyanion accompanied by mobile cations.[38] Furthermore, the mixture of the first and the second case can produce an ionic copolymer[39,40]

bearing both kinds of mobile ions while the zwitterionic monomers which contain both cation and anion on the same structure leading to a polyzwitterion[41] without any mobile ions (Figure 1.1). Such PILs are also called polyelectrolytes due to the presence of cations and anions. However, contrary to traditional polyelectrolytes which dissolve in water and dissociate in aqueous solutions, PILs are mainly soluble in organic polar solvents.[29]

b) The type of polymer structure: Based on the structure of the polymer PILs can be divided to linear,[36] hyperbranched,[42] and dendritic.[43,44] Linear PILs are the most abundant type among others in this category.[32] However, it can be divided to different sub-classes depending on the structure of the monomer, whether there is a hetero atom,[45] a cycle,[45] or a heterocycle[46] in the polymer chain, as described in the literature.[32]

c) The location of ionic center: There are three different locations where ionic moieties can be found on PILs. It can be hanged from the polymer body as a side chain,[36] located in the body of the main chain,[46] or attached to the end of the polymer chain.[47,48]

As the structures has been described in this research is mainly focused on telechelic polymers bearing ionic moiety as terminal groups, despite some deviations in the structure, it can still be classified according to the ionic center location under last sub-category, as described before.

1.2. Synthesis of POILs

Synthesis of variety of POILs, regardless of the efficiency and final structure of the product, can be carried out through two main strategies. Starting from an ionic liquid with defined structure and then introducing the polymer chain via different synthetic routes or subsequent chemical modification on a tailor-made polymer which contains suitable functional groups. Both of these methods have advantages or disadvantages. But, in general, they have a lot in common with synthetic chemistry of monomeric ILs.[1] Depending on the application, one can decide whether to compromise the desired features of the intended material to compensate for the sake of efficiency or the vice versa.

As the number of POILs, which are synthesized via polymerization of the monomeric ILs, designated as PILs, is significantly high among all others, it is noteworthy to mention about two main approaches which are established to achieve these polymers. PILs can be obtained either via polymerization of

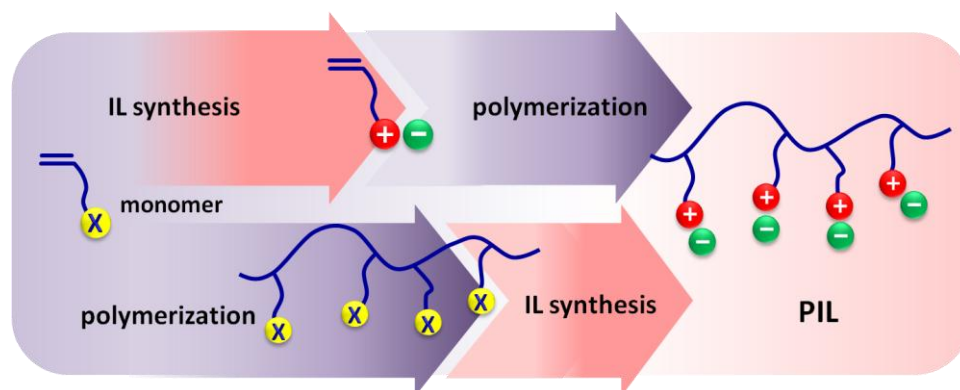the monomeric IL or the modification of the functional groups of the already synthesized polymer (Figure 1.2).

Figure 1.2. Schematic representation of the general pathway toward synthesis of PILs.

To synthesize PILs via polymerization of the monomeric ILs, the initial step is to provide the relevant IL bearing a moiety that can go through the polymerization. The most common type of these monomers are ILs containing either C-[49-51] or N-vinyl groups.[34,36,52] Monomeric ILs can be obtained via synthetic methods very similar to classical ILs.[1] As it is described in the literature,[1] in principle there are two main steps to attain an IL. First is to obtain the desired cation which can be performed either via protonation with an acid or quaternization of an amine, phosphine, or sulfide. Second step is to transform the structure of already synthesized or purchased IL via anion exchange, if it is required. Exchanging the anion can be carried out via e.g. the anion metathesis or direct reaction of the halide salt with Lewis acids.[1] Once the monomeric IL was successfully acquired during the initial step, it can undergo almost all common type of polymerization reactions, such as free radical polymerization,[36,40,52] atom transfer radical polymerization (ATRP),[53-54] ring opening metathesis polymerization (ROMP),[45,55] reversible addition-fragmentation chain transfer polymerization (RAFT),[56-58] and photopolymerization[59,60] to result in desired PILs.

However, it should not be ruled out that the polymerization of the monomers containing charges can be complex due to the electrostatic repulsion of the similar charges whereby it can lead to PILs with lower molecular weight or induces dissolubility in the reaction media.[61,62] Despite these limitations which can influence the conversion, efficiency and even properties of the produced material, yet, polymerization of the monomeric ILs is a very popular approach which provides a variety of novel PILs with well-defined structures due to the possibility of initial design of IL monomer.

Besides the polymerization of the monomeric ILs to produce PILs, the second approach is the reverse strategy. PILs can be synthesized via post modification of the already synthesized polymers. The polymer with proper functional group on its repeating unit can go through transformation in a same way as classical ILs.[63-68] Quantitative conversion during the quaternization or alkylation is the main drawback of this method[64,69-70] which can become even more robust when further anion exchange is required.[71] Additionally, while the electrostatic repulsion is not an issue to achieve higher molecular weights, the introduced ionic moieties can reduce the solubility of the polymer in the reaction solvent and thus, suppress the transformation.[72-73]

1.2.1. Synthesis of telechelic POILs

Contrary to common PILs which consist of IL monomers as repeating unit, telechelic POILs are, indeed, telechelic polymers with their end groups attached to the charged moieties via modification of the primary polymer. In this regard, the structure of POILs is more likely to some ionomers as they are also low in ion content.[74] (Further details regarding ionomers will be provided in chapter 1.3)

In general, later modification on a commercially available or synthesized polymer is a major approach toward synthesis of POILs. To afford such modification, the existence of an appropriate functional group on the body of the polymer is essential. The polymer undergoes the transformation via alkylation or quaternization of such groups similar to the monomeric ILs.[1] The success of such reaction highly depends on the strength of the alkylation or quaternization agent and the functional group from the polymer which can be described as following: I>Br>>Cl in the case of halides. Acquiring this method to synthesize POILs provides the opportunity to tune an already known polymer with defined structure and particular properties for the intended application which is very advantageous. However, quantitative conversion of the functional groups in such reactions is quite a challenge. Although, there are plenty of reports on synthesis of oligomeric ILs and POILs following the above mentioned procedure, the method confronts obstacles where the increasing polymer chain length results in declining efficiency. The ionic polymerization in the presence of bifunctional initiator and proper quenching agent can lead to some ion containing telechelic polymers which is not an easy task due to crucial requirements of living polymerization. Thus, developing efficient strategies to produce the designated structure is inevitable.
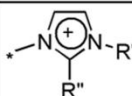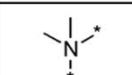
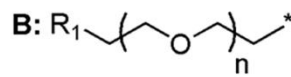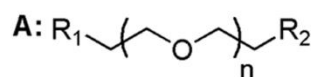**1.2.2. Synthesis of poly(ethylene glycol)-based ionic liquids (PEGILs)**

Poly(ethylene glycol)-based ionic liquids are the most abundant synthesized POILs[75] due to favorable thermal and electrochemical features,[76-80] physicochemical properties dependence (such as viscosity) on the chain length,[81] and coordinative ability of the oxygen atom[71,82] accompanying with intrinsic characteristics of PEG such as biocompatibility,[83] wide range of solubility,[84] and lack of toxicity.[85]

In this respect, a series of poly(ethylene glycol)-based phosphonium POILs were synthesized via direct transformation of the bromo- telechelic polymers. The intention was to provide low ion content charged polymers, similar to ionomers, in order to investigate their ionic aggregations as described for ionomers.[86-88] Meanwhile, mono- and bis- substituted poly(ethylene glycol) were synthesized via the reaction of bromo-telechelic polymer with saturated solution of ethanol/ammonia, at elevated temperature and pressure in a glass autoclave. The trimethylammonium based polymeric ionic liquids with variety of molecular weights were synthesized to be attached to the biochemical compounds such as enzymes for biological studies.[89] In order to generate ion conducting poly(ethylene oxide)s (PEO) bearing charged end groups,[47,90-91] imidazolium containing PEOs were synthesized via quaternization of bromo- derivative polymers. The hybrid system of the synthesized charged polymers proved to exhibit high ion conductivity in broader range of temperature due to decreasing T_g of the polymer comparing to unfunctionalized PEO/salt hybrid.[47-48] However, the synthesis of poly ether based POILs thrived in 2000s by dramatic growth of the interest in ILs especially in the field of "green chemistry".[23] In this respect, eco-friendly synthesis of oligomeric mono-substituted poly(ethylene glycol)s with imidazolium derivatives accompanied by fluorinated anions was reported to be used in liquid-phase combinatorial chemistry. The reaction was performed via quaternization under microwave irradiation in minutes and followed by the anion metathesis.[82] On the account of new findings,[92-94] implicated in higher thermal stability of the geminal dicationic ILs which flourished their implantation in tribology,[95] a novel series of dicationic poly(ethylene glycol) bearing alkyl or polyfluoroalkyl imidazolium and triazolium cations were designed and synthesized. The reaction was performed via quaternization and subsequent anion metathesis.[96] However, in order to addition of extra alkyl or polyfluoroalkyl, the bromo- substituted polymer, first, reacted with imidazole in the presence of NaH and further quaternization of the amine resulted in designed products. The high thermal stability of the materials particularly imidazolium derivatives in comparison with triazolium was proved.[96] Similar structures containing hydroxy- and

phenyl substituted imidazolium were synthesized and characterized via linear solvation method[97] to investigate their ability as stationary phase in GC. The produced POILs demonstrated a high separation attitude and unique selectivity in comparison to commercial stationary phases such as polysiloxan and poly(ethylene glycol) based stationary phases.[97] Following the prosperous results of catalytical hydrosilylation reactions in the presence of ionic liquids,[98-101] monometoxy poly(ethylene glycol)-based ionic liquid containing imidazolium and hexafluorophosphate were synthesized via alkylation of 1-butylimidazole with methanesulfonate attached to the polymer chain followed by anion exchange.[102] Applying the attained POIL as a reaction media for the hydrosilylation of variety of alkenes resulted in enhanced catalytic activity and selectivity[102] comparing to unfunctionalized PEG.[103] Another dicationic poly(ethylene glycol)-based IL with imidazolium was synthesized via treatment of germinal chloro-substituted PEG with imidazole in the presence of a base. Further reaction of the product with 1,3-propanesultone resulted in an acidic POIL which was used together with toluene as recyclable temperature dependent phase separation system in one pot synthesis of benzopyranes.[104] A similar structure was also acquired in metal free, selective oxidation of toluene derivatives,[105] regioselectivity nitration of aromatics,[106] and solvent free synthesis of amidoalkyl naphthol[107] as catalyst. Similar system was developed by using POILs bearing tetrafluoroborate anion for hydrolysis of organic halides, epoxides, and esters.[108] Bifunctional PEO bearing imidazolium and TEMPO in either side of the polymer was also produced which was accompanied by Cl⁻ and later on converted to $CuCl_2^-$ via anion exchange for aerobic oxidation of alcohols.[109] Another series of monomethoxy poly(ethylene glycol) POILs were synthesized via quaternization of iodine terminated polymer with imidazole as potential electrolytes for energy conversion and storage devices.[76] A new ammonium-based poly(ethylene glycol)-ionic liquid was synthesized to be used as solvent in peptide synthesis. In this respect, two brominated methoxy poly(ethylene glycol) were attached to one *N,N*-dimethylamine (gaseous) at -15 °C in ethanol.[110] Another tailor-made POIL, bis- and mono-hexaethylene glycol based imidazolium ionic liquids, synthesized as multifunctional catalyst for specific organic reactions such as nucleophilic fluorination with alkali–metal fluorides.[111] To achieve water soluble palladium catalyst for Suzuki reaction, NHC precursors bearing PEG was synthesized via alkylation of mesylate terminated methoxy poly(ethylene glycol) with 1-alkyl-imidazole.[112] An efficiently recyclable ligand for palladium catalyzed Heck reaction was obtained by poly(ethylene glycol) bridged dicationic imidazolium ionic liquid which was functionlized with 8-hydroxyquinoline as an excellent bidentate chelating ligand.[113] Another poly(ethylene glycol) bridged dicationic imidazolium ionic liquid bearing diol functionalities were synthesized as copper catalyst ligand.[114]

Table 1.1. Summary of the structures of synthesized **PEGILs** described in the literature.

polymer	cation			anion	n	ref.
A	$P^+(Ph)_3$	$R_1= R_2$		Br	n~7, 9,14,22,34,77	87
	$N^+(CH_3)_3$	$R_1= R_2$ $R_2=OCH_3$		Br	n~34,89,135,226,453	89
		$R_1= R_2$	R'=H, R"=CH_2H_5	Br	n= 2,6,11	47
		$R_1= R_2$	R'= CH_3 , R"= CH_3	$(CF_3SO_2)_2N$	n=3	96
		$R_1= R_2$	R'=H, R"=CH_3	$(CF_3SO_2)_2N$	n=1-4	
		$R_1= R_2$	R'= H , R"= C_3H_7		n=3	
		$R_1= R_2$	R'= H , R"= $C_2H_4CF_3$		n=3	
		$R_1= R_2$	R'= H , R"= C_4H_9		n=3	
		$R_1= R_2$	R'= H , R"= $C_3H_6CF_3$		n=3	
		$R_1= R_2$	R'=H, R"=C_6H_{13}		n=3	
		$R_1= R_2$	R'= H , R"= $C_2H_4C_4F_9$		n=3	
		$R_1= R_2$	R'=H, R"=CH_3	$(CF_3SO_2)_2N$	n=3-5	97
		$R_1= R_2$	R'=H, R"=$CH_2(C_6H_5)$			
		$R_1= R_2$	R'=H, R"=C_2H_4OH			
		$R_1= R_2$	R'=H, R"=C_2H_4OH	CF_3SO_3	n=3,4	
		$R_2=OCH_3$	R'=H, R"=C_4H_9	PF_6	n=6	103
		$R_1= R_2$	R'=H, R"=$C_3H_4SO_3H$	HSO_4	n~22 n~3	105, 106
		$R_1= R_2$	R'=H, R"=$C_3H_4SO_3H$	HSO_4 BF_4 PF_6 CF_3SO_3	n~12,7,22 n~22 n~22 n~22	107
		$R_2=$TEMPO	R'=H, R"=$C_3H_4SO_3H$	$CuCl_2$	n~22	109
		$R_2=OCH_3$	R'=H, R"=CH_3	CH_3SO_3	n~11	112
		$R_2=OCH_3$	R'=H, R"=n-C_3H_7		n~11	
		$R_2=OCH_3$	R'=H, R"=iso-C_3H_7		n~11	
		$R_1= R_2$	R'=H, R"=quinoline, 8-propoxy	BF_4	n~22	113
		$R_1= R_2$	R'=H, R"=2,3-dihydroxypropyl	PF_6	n~22	114
B		$R_1=OCH_3$		CH_3SO_3	n=5	111
		$R_1=OCH_3$		Br	n~6	110

A: **B:**

1.2.3. Synthesis of other poly ether-based ionic liquids

Beside poly(ethylene glycol)-based ionic liquids, there are some reports on synthesis of POILs based on other poly ethers. Poly ethers bearing ionic moieties are one of the first reported POILs. In this respect, phosphonium based polymers were generated to convert less stable tertiary oxonium to quaternary phosphonium cation via "ion trapping" method in order to investigate the structure and concentration of the active species during the polymerization of THF and some other cyclic ethers. [115-117] Besides, some other polymeric structures, covalently bonded to ionic moieties were also developed.[116] Following the previous research on synthesis of telechelic terephthalate polyester ionomers via a new polycondensation reaction,[118] synthesis of imidazolium based telechelic poly(butylene terephthalate)s POILs for antimicrobial applications was reported.[119] In this research, the desired ionic liquids were precisely designed and synthesized. The attachment of the ionic moiety to polymer proceeded by addition of the ionic liquid to the mixture of 1,4-butanediol and dimethyl terephthalate monomers and subsequent poly condensation.[119] Similar series of imidazolium based terephthalate polyesters were also synthesized as telechelic POIL and randomly distributed ionomers.[120]

α,ω-Difunctionalized poly(ethylene glycol) and poly(ethylene glycol)-b-poly(ϵ-caprolactone) block copolymers were synthesized via N-heterocyclic carbene-Induced zwitterionic ring-opening polymerization of ethylene oxide using 1,3-bis-(diisopropyl)imidazol-2-ylidene as NHC initiator. Even though the research was not intended to synthesize a POIL but a zwitterionic poly(ethylene oxide) chain bearing imidazolium moiety was generated as an intermediate.[121] Cationic polymerization of L,L-lactide in the presence of 1-butyl-2-hydroxymethyl-3-methyl imidazolium resulted in a medium molecular weight monovalent poly(L,L-lactide) containing imidazolium derivative as an end group in order to stabilize carbon nanotubes (CNTs) suspension.[122]

1.3. Self assembly in PILs

Self organization phenomenon as point of view of chemistry is construction of well-defined structures resulted from spontaneous arrangement of the components of the system by noncovalent forces. Today, due to sophisticated use of self-organizing materials in numerous fields of developing technology, from research to industry, the importance of such systems became enormously significant.[123] Ordered structures in synthetic materials can be created via incorporation of different interactions such as coulombic, van der Waals, hydrophobicity and hydrophilicity, and hydrogen bonding effects. Combination of these interactions can result in a self assembly of a material over a wide range of length scale from nano- to meso- and even macroscopic scales.[124]

In this regard, ion containing polymers, regardless of the position of the ion, can promote aggregations which can results in different levels of hierarchies similar to microphase separation in BCPs.[124] To have a better understanding about formation of the ordered structures in the case of POILs, it is essential to have an insight of ionic liquids aggregations first. Hence, the following sub-chapter starts with the simulation and experimental findings about induced assemblies in monomeric ionic liquids concluding the similarity of such organizations with microphase separation behavior between polar and nonpolar domain in amphiphiles or block copolymers. Further on, the theoretical background on microphase separation phenomena lead to justification of the induced self assemblies in poly(ionic liquids) homo- and block copolymer via Flory–Huggins parameters as defined for classical BCPs.[124] However, due to low ion content, in contrast to poly(ionic liquids), self assembly in POILs is more similar to telechelic ionomers where Eisenberg-Hird-Moore (EHM) theory[125] is used instead, as a comprehensive model to explain not only the generated hierarchies via formation of, so called, multiplets and clusters but also the physical and mechanical behavior of the polymers as such. Therefore, the chapter will be continued firstly by more detail about ionomers and then the history of the development of Eisenberg-Hird-Moore theory to justify the experimental findings obtained from the ordered assemblies in ionomers.
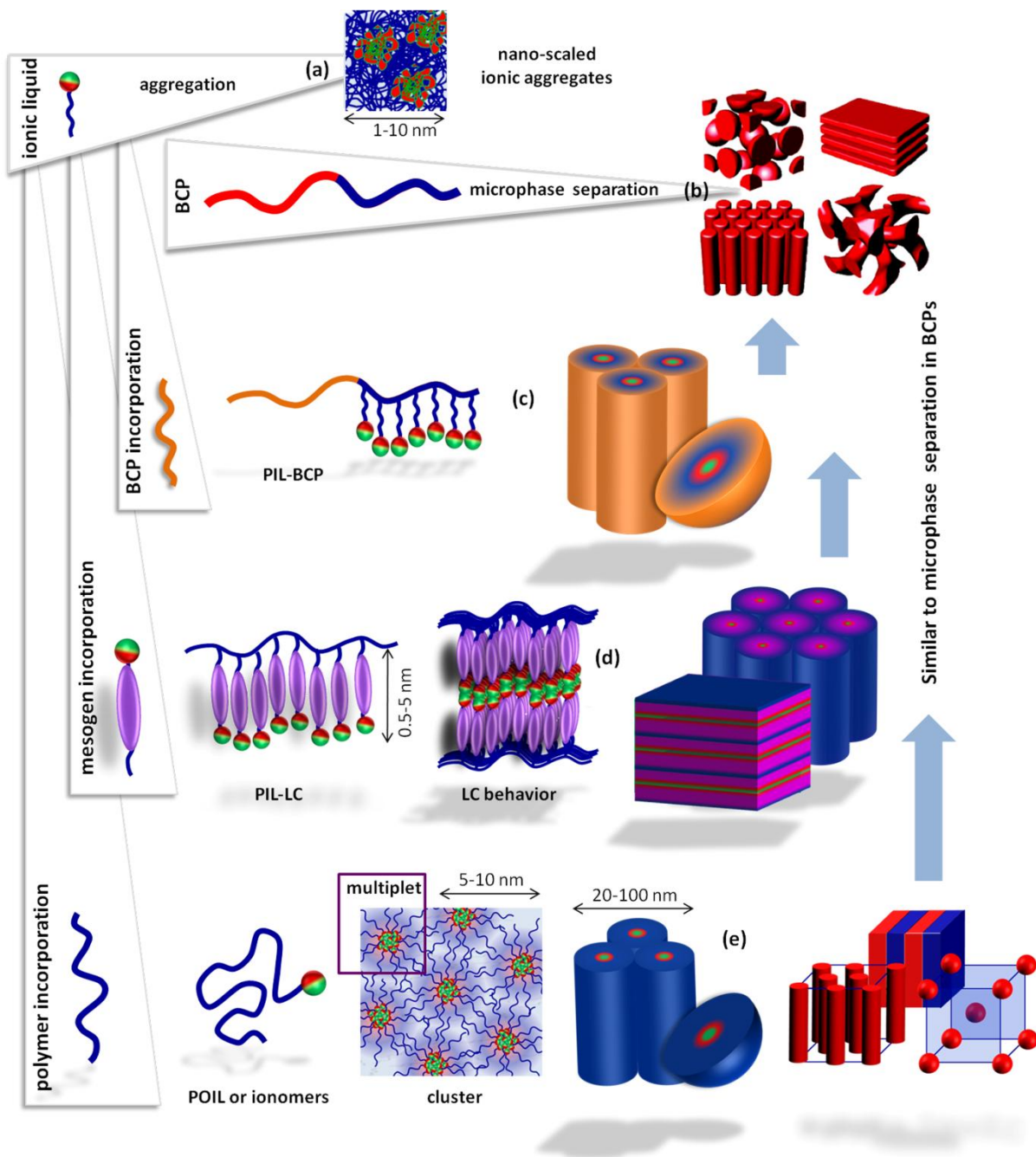
Figure 1.3. Schematic representation of different levels of hierarchies in ionic liquids, BCPs, PIL-BCs, PIL-liquid crystals (PIL-LC), and POILs. **a)** Fomation of nano-scaled ionic association due to aggregation of ionic liquids. **b)** Microphase separation in BCP resulted in variety of the morphologies from body centered cubic spheres to hexagonally packed cylinders, bicontinuous gyroids, and lamellae (The schematic illustration of the self assembled supramolecular architectures has been taken from the reference).[126] **c)** Microphase separation in BCP containing PIL block (PIL-BCP). **d)** Mesophase formation in PILs containing mesogen moiety in their repeating unit (PIL-LC). **e)** Formation of multiplets and clusters due to aggregation of POILs or ionomers resulted in meso-scaled ordered structures.

1.3.1. Nano-scaled organizations in ILs

Besides their unique properties, ionic liquids are also desired materials due to their high structuring order in the nanometer scale.[127] The reciprocation between Coulombic and van der Waals interactions in ILs result in medium range ordered structures.[128] An IL is composed of charged head group and uncharged tail which leads to atomic polarization. The interactions between head groups are electrostatic while the tails are interacting mainly through the collective short-range interactions. The competition between these two interactions leads to formation of heterogeneities. The presence of such heterogeneities in RTILs was first revealed via computer simulations[129] and confirmed with experiments later on.[130]

Molecular dynamic simulation was a valuable method as the numerous industrial applications of ILs demand a more detailed microscopic view on the interplay between structure and dynamics in these systems. However most of the simulation studies performed so far was focused on the local scale considering only given cation or anion or to prove the results retrieved from the scattering experiments.[131,132] In 2004, Urahata and Ribeiro[133] used a united-atom model of imidazolium ILs to investigate the long-range structure of ionic liquids on the basis of computer simulation. Their investigations revealed the appearance of low wave-vector peaks which became more pronounced specially with growing alkyl chain.[133] This feature was inconsistent with characteristic of simple molten salts and it was indication of long-range ordering. Shortly after, in 2005, Wang and Voth[134] announced their observation regarding tail aggregation in imidazolium ILs with homogeneous distribution of anion and cation head group where the alkyl chain length was above C_4. They applied multiscale coarse-grained model for their simulations and regarding to the findings they proposed the presence of tail aggregations in most of the organic ILs.[134]

Padua and Lopes,[135] in 2006, for the first time used atomistic simulation to study the effect of chain length (n=2-12) of the side chain attached to the cation in series of alkyl imidazolium ILs in the liquid phase. They were targeting to investigate the nanoscale organizations of these materials on the long-range structures. Site- site intermolecular radial distribution function (RDF) based on terminal carbon atom of alkyl chains was the first evidence of tail aggregation. The appearance of the first peak in C_4, C_6, and C_8, while it was absent for C_2, was the primary indication of the nonpolar chain clustering in pure ionic liquids. Analyzing RDFs belong to anion-anion center of mass demonstrated the

consistency of the anion-anion distance for different chain length which indicated the sustainability of the polar structure as no disruption occurred in the cation-anion network due to increment of the methylene groups. Cation-cation center of mass RDF's did not reveal much information, yet the consistency in the peak position for C_4 and C_6 was observable whereas it was diminished for longer chains. However, increasing the proportion of the part that did not belong to the polar part and migration of the mass center due to the flexibility of the cation containing longer chain were justifying the attained results. To compensate this drawback, cation-cation, RDF was recalculated considering the center of the mass of only imidazolium rings and adjacent atoms which lead to a similar conclusion as anion-anion RDF. All these findings including the results drawn out of the RDFs belong to the center of the mass between anion and imidazolium ring strongly emphasized on the precision of the primary hypothesis. Eventually, computer simulation along with all-atom force field calculations revealed that in the pure ionic liquids of alkylimidazolium the charged domain forms ionic channels in a tridimensional network pattern while nonpolar domain constructs a dispersed microphase (in the case of C_2) or a continuous one (in the case of C_4, C_6, C_8) which is analogues to **microphase separation** behavior between polar and nonpolar domain in amphiphiles or block copolymers.[135] The appearance of the first sharp diffraction peaks (FSDPs)[136] in X-ray[137] as well as neutron diffraction structure functions,[138-139] indicates the presence of the intermediate range order (~5-10 Å).

1.3.2. Microphase separation in PILs

Microphase separation is a thermodynamically induced phenomenon in materials containing incompatible compartments which result in a variety of microstructures in the size of nanometers. Block copolymers (BCPs) are one of the simple classic examples of these materials. The incompatibility between two components of A and B is the most characteristic feature of BCPs. Due to the repulsion which is originated from the immiscibility of these components they tend to segregate but as they are covalently bonded no macroscopic separation occurs. However, when the incompatibility reaches to the particular point microphase separation takes place and lead to the transformation from an amorphous homogeneous structure to highly ordered assemblies in the form of lamellae, hexagonally packed cylinders, body centered cubic structures composed of spheres or a gyroid.[140] Numerous experiments and calculations were performed to define the criteria to interpret and control the complexity of the structures originated from microphase separation.[140-143] These

criteria were declared as: the chemical composition of the BCP, which can be represented by volume fraction of each A and B blocks as f_A and f_B ($f_A+f_B=1$), the overall degree of polymerization ($N=N_A+N_B$) and the inherent difference between two blocks that induces incompatibility and can be well defined via Flory–Huggins parameter (χ_{AB}).[123]

In this regard, some of the ionic liquids block copolymers (PIL-BCPs), considering the presence of highly polar ionic moieties in the body of the polymer chain can undergo microphase separation phenomenon similar to the way explained for BCPs (Table 1.2). Hence, the theory developed for the microphase separation can be applied to justify the formation of complex structures in such polymers.

Imidazolium functionalized polystyrene (PS) was one of the first synthesized PIL-BCPs which according to scattering data was in the form of micelles in dilute toluene. Following investigations revealed the dependency of the size and geometry of the micelles to length of the IL block.[144] Furthermore, ion conduction behavior in several PIL-BCPs composed of PS and Imidazolium functionlized PS was investigated as function of morphology which lead to hexagonally packed cylindrical, mixture of cylindrical and lamellar, and lamellar morphology depending on the mol% of IL block (below 7.1 and above 17 mol%).[145] A report on series of imidazolium based methacrylate IL-BCPs demonstrated anion and solvent responsive self assembly[57-58] while another series of imidazolium based methacrylate PIL-BCPs which also went through microphase separation lead to high ion conductivity as a result of anion exchange and decreasing T_g.[39] Gradual adjustment of morphology of the BCP via anion exchange was reported for PS and poly(2-vinylpyridine) (P2VP) through partial quaternization of the P2VP block. Subsequent exchange of the anion from bromid to Tf_2N^- resulted in similar lamellar morphology with increasing the domain size.[146] Norbornene based block copolymers containing alkyl imidazolium in PIL segment and dodecyl ester in the nonionic block was another nanostructured PIL-BCP, which was synthesized via sequential ring opening metathesis polymerization. Morphological phase behavior of a set of these BCPs and its variation with respect to the changes of volume fraction of both blocks in melt state was investigated. The results revealed the formation of variety of highly ordered structures including lamellae, hexagonally packed cylinders, and spheres on a body-centered cubic lattice.[147] Poly(vinyl acetate)-*b*-poly(N-vinyl-3-butylimidazolium bromide) PIL-BCP formed micelle in THF and vesicle in water while exchanging the anion to bis(trifluorosulfunyl)imide resulted in ordered lamellar structure, in the bulk polymer.[148]

The investigations on morphology of a four-armed star shape PIL-BCP composed of poly(N-vinylimidazolium salt) and poly(N-isopropylacrylamide) which were the opposite in the sequence of PIL segments exhibited different morphology changes above LCST temperature. While BCP containing PIL in the outer shell rapidly aggregated to form bigger micelles in water the other BCP with thermoresponsive segments in the outer shell formed smaller micelles that tended to create dehydrated clusters.[149] Another series of PIL-BCP based on PS and imidazolium functionalized acrylate were synthesized and the relation between their ionic conductivity and morphology was investigated. SAXS and TEM results revealed the existence of variety of ordered structures from hexagonally packed cylinders to lamellae, and coexisting lamellae, and network morphologies changing with the composition of the BCP.[150] The conductivity of the synthesized PIL-BCPs was varied depend on the degree of the microphase separation. The higher degree of incompatibility leads to stronger microphase separation resulting in improved ion transport properties. [150]

Besides BCPs as multicomponent systems, homopolymers also can experience microphase separation where the incompatibility between charged moieties is in contrast with hydrophobic body of the homopolymer. PILs composed of ionic liquids as their repeating units as mentioned below can be examples of such homopolymers. Cryogenic TEM image obtained from poly (3-alkyl-1-vinylimidazolium bromide) nanoparticles bearing different alkyl chains exposed the nanodomains which formed a mesostructure during the polymerization. The morphology of the highly ordered PIL can be tuned by varying the alkyl chain from multilamellar to unilamellar vesicles (Table 1.2).[151]

Incorporation of mesogenic moiety into IL monomers results in PILs with promoted meso-scaled self assembly exhibiting liquid-crystalline (LC) behavior (Table 1.2). Construction of such ordered structures originated from intermolecular interactions, such as hydrogen bonding, ionic interactions, π-π, and charge transfer interactions. Hence, controlling these interactions is a key feature in development of these materials.[152] The presence of the ionic moieties in the structure of the mesophase results in low-dimensional (anisotropic) materials with ion conductivity.[153] It was reported that a molecular block of ionic and none ionic structure based on imidazolium salt established one dimensional (1D) ion transport in self assembled columnar morphology.[153] In situ photopolymerization of methacrylate monomer carrying biphenyl imidazolium derivatives resulted in a liquid-crystalline PIL with layered nanostructure which functions as 2D ion conductor.[154] Following the idea of enhancing anisotropy via fixation of the orientation through post polymerization of the constructing ionic moieties, Ohno et al.[155] presented a new imidazolium based 1D ion-conductive film

with vertical and parallel alignment of the channels to the surface of the film. Recently, they developed another 1D ionic channel constructed of self assembly of imidazolium based wedge-shaped molecule bearing dihydroxyl groups functionalized with polymerizable diene moieties.[156] Other examples of PILs exhibiting LC behavior can be found in the literature.[28,157]
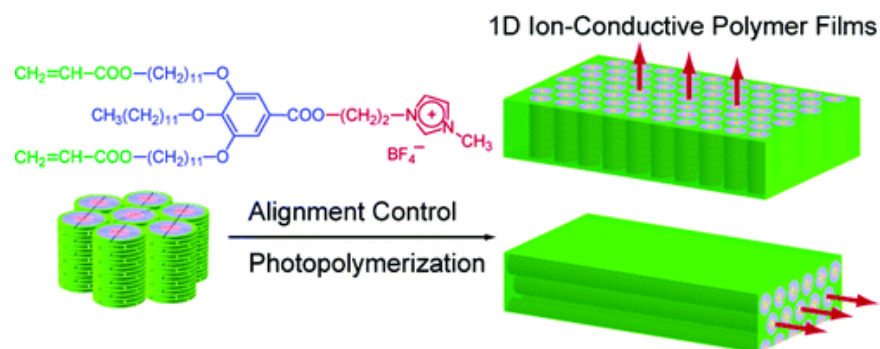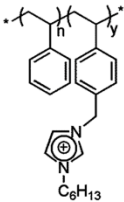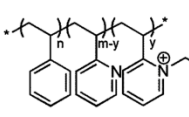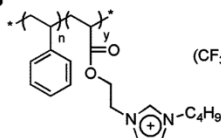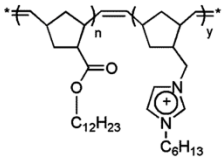

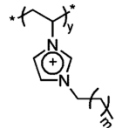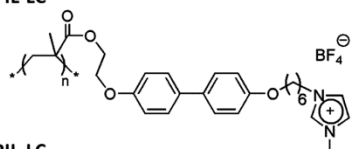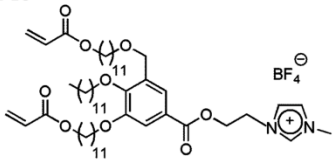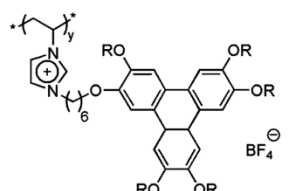**Figure 1.4.** Schematic representation of self assembly of mesogen incorporated imidazolium based monomer (The image has been taken from the literature). [156]

Table 1.2. Microphase separation in **PIL-BCPs**, **PIL**, and **PIL-LC.**

polymer	PIL (mol%) or m	morphology	domain spacing (nm)	phase separation	ref.
PIL-BCP	2.7	cylindrical	42	micro-	145
	7.1	cylindrical	42		
	8.6	cylindrical+lamellea	35/37		
	15.6	lamellea	39		
PIL-BCP	17.0	lamellea	35		
		lamellea	34	micro-	146
	~20	lamellea	48		
		lamellea	73		
PIL-BCP	6.6	cylindrical	18-20	micro-	150
	12.2	cylindrical	20.8		
	17.0	lamellea	25		
PIL-BCP	23.6	lamellea	30		
	30	lamellea	28.6	nano-	147
	40	lamellea	29.4		
	47.9	lamellea	32.1		
PIL m=10, 12, 14, and 16	m = 10	multilamellar	3.4	meso-	151
	m = 12	multilamellar	3.8		
	m = 14	multilamellar+unilamellar	4.0		
PIL-LC	m = 16	unilamellar	3.9		
PIL-LC		lamellea	layer spacing 4.9	meso-	154
		hexagonal columnar	intercolumnar spacing 4.2	meso-	155
PIL-LC		columnar rectangular	lattice parameters a = 3.71 nm b = 1.54 nm	meso-	156

17

1.3.3. Self assembly in POILs regarding Eisenberg-Hird-Moore (EHM) model

As it was described before, polymerized ionic liquids can go through self assembly in different size scale from nano- to meso-scale structures.[151] However, POILs are quite different as the volume fraction of the ionic moiety is far too low in comparison to the volume fraction of the hydrophobic moiety which constitutes the body of the polymer.[158] Therefore, POILs can be categorized as charged polymers, so called ionomers, regarding their self assembly behavior where EHM theory was developed.[125] In this respect, it is necessary to define some terminologies regarding ionomers and their aggregates. Hence, in the following section, firstly, ionomers will be defined. Consequently, the theory will be explained by comprehensive interpretation of "multiplets" and "clusters".

1.3.3.1. Ionomers

The term "ionomer" was used in 1965, for the first time, to designate a class of olefin-based polymeric materials that accommodate a relatively small amount of ionic content.[159] To avoid any complexity between ionomers and polyelectrolytes, the definition was revised in 1990 by Eisenberg and Rinaudo.[74] According to the new definition, ionomers are polymers with an ion content of less than 15 mole %. Their structure consists of nonionic repeating unit which is accompanied with ionic groups and alkali metals or transition metals as most common counter ions. The position of the ionic fraction can be varied from, randomly or systematically distributed to, the polymer backbone, anchored moieties to the copolymers, or to the end groups in the polymer chain.[74] The existence of the ionic fraction, regardless of its position, can promote the aggregation which can results in microphase separation similar to BCPs. Microphase separation in ionomers is urged due to the strong attraction between ions and dipoles which are small and few thus the dimension of the microdomains are not as vast as BCPs. Though, ionomers, in contrast to BCPs, contain less ordered microstructure and no long range orders.[125]

Conducting numerous experiments on a wide variety of ionomers along with recruiting spectroscopic and scattering techniques gave rise to the development of different theories concerning the possible models describing the morphologies of random ionomers, but none of them was fully congruent with all of the obtained experimental results. In 1970, Eisenberg[160] presented another theoretical model using mechanical data based on electrostatic versus elastic forces, instead of X-ray scattering studies,

which was coincided and developed shortly after by introducing hard-sphere[161] and core-shell[162] models, but yet carrying several inconsistencies. Finally, in 1990, Eisenberg, Hird, and Moore[125] reported a new model for clustering of multiplets in random ionomers called Eisenberg-Hird-Moore (EHM) model. Before any detailed explanation about clustering of random ionomers based on EHM model it is necessary to introduce two main terms as "multiplet" and "cluster".
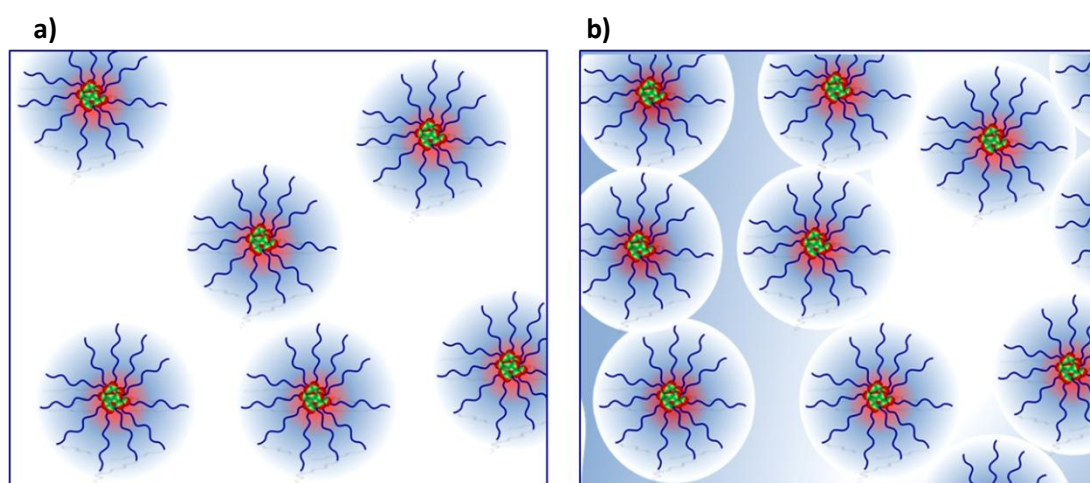

Figure.1.5. Schematic representation of morphology of ionomers at increasing ion content; **a)** low ion content, individual multiplets, **b)** high content, formation of clusters (The picture is redrawn from the literature).[163]

1.3.3.2. Multiplets[125]

Ion pairs tend to aggregate and constrain assemblies called multiplets.[125] The formation of these multiplets is strongly influenced by ion content and electrostatic interactions between ion pairs as well as characteristics of the accompanying polymer such as dielectric constant and T_g. In the other words, if the electrostatic interactions between ion pairs become strong enough to overcome the elasticity, which is originated from the associating polymer, multiplets will be formed. Besides, regarding the nature of the polymer, the lower the dielectric constant and T_g the most probable is the multiplet formation. The size of the multiplet, where the aggregation is a privileged process, is highly restricted due to steric hindrance. Hence, polystyrene based ionomers generate small, but firm multiplets whereas ionomers bearing charged moieties as end groups procreate larger aggregates. The shape of the multiplets can be spherical or non-spherical according to the different reports on various ionomers. Remarkably, while a multiplet being constructed via aggregation of the ion pairs, the mobility of the joint polymer chain in the proximity of the multiplet become highly restrained as a result of its strong attachment to the ion pair, while by increasing the distance from the multiplet

this restriction declines. It is worth to mention that the stated mobility restricted section so called "skin" does not have a precise boundary to isolate it from the rest of the polymeric matrix, but its thickness is strongly dependent on the mechanical properties of the polymer chain. Rigid polymers induce a thicker skin while flexible chains lead to thinner one.[125]

1.3.3.3. Clusters[125]

When the distance between two or more independent multiplets become smaller, their mobility restricted regions overlaps and forms a broader zone compiled of these restrained areas. The process continues by growing the size of the zone until it rises above the limit of the independent phase behavior (50-100 Å) where the new T_g emerges, and cluster formation occurs. The size of the region where the material undergoes the phase separation is not determined, though the maximum distance between two neighboring multiplets should not exceed the twice thickness of the "skin" layer in a cluster. The accumulation of multiplets composed of ion pairs and their surrounding nonionic polymers constructs clusters.[125]
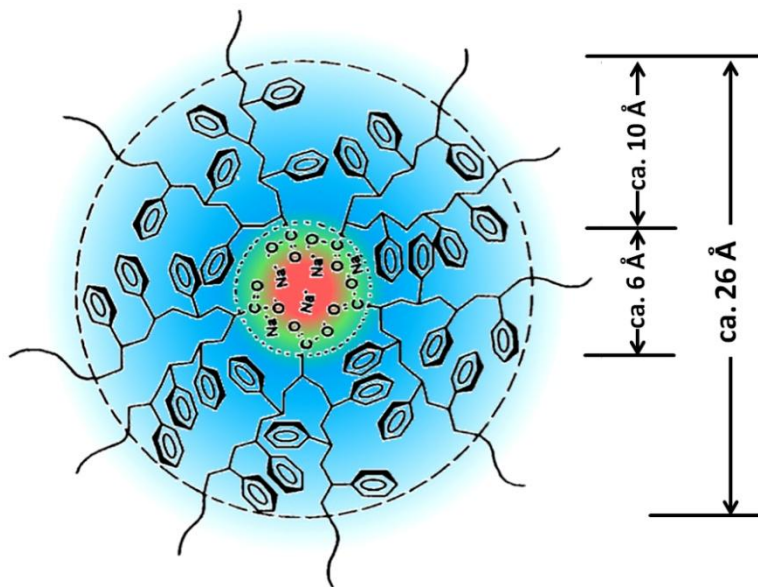

Figure 1.6. Illustration of the mobility restricted region of ionomers within a multiplet structure. The image has been taken from the reference.[125]

Although, the definition of the multiplets and clusters remained similar to the previous models,[160] according to EHM model,[125] clustering occurs due to the adjacency of the multiplets and not the

intra-multiplet electrostatic interactions, as they are not strong enough to stimulate the clustering, which is in contrast with previous models. Furthermore, the new model does not compel the clusters into a defined geometry or number of ion pairs and multiplets. Introducing the mobility restricted region for the multiples is another important feature of EHM theory which makes is it an outstanding model among others. Indeed, after two decades of research on random ionomers, despite the fact that exact structure of multiplets and clusters is still not fully discovered, EHM model was the most comprehensive answer to explain physical behavior of such polymers and similar structures.[125] Thus, the recorded results from small-angle X-ray and neutron scattering and dynamic mechanical results obtained from various structures, which were not fully in agreement with the previous models, became the satisfactory evidences of the existence of the clustering in ionomers.[164-165] According to the model, the origin of the so called "ionomers peak" emerged at the low wave-vector, found in all ionomers, can be interpreted as inter-multiplet distances within the clusters. The results attributed also on weak dependence between Bragg spacing and ion contents in the random ionomers.[162,166] The new model accounted for numerous experimental observations and was used as a strong foundation of the new investigations. [167,168] In this respect, a series of α,ω-metal sulfonato and carboxylato polyisoprenes telechelic ionomers associated with variety of cations (Na, K, Rb, Cs, Mg, Ca, Sr, and Ba) synthesized and investigated via X-ray scattering.[169] The obtained SAXS data were analyzed from the point of view of ionic peak position and its dependence on the molecular weight, ion pair structure, neutralization degree of the acid end group, and the nature of the polymer.[169]

1.3.3.4. Rheology of ionomers

Ion containing polymers, represented mostly by ionomers, exhibit different physical and mechanical properties in comparison to their non-ionic analogous polymers.[170] As it is postulated, introducing a small amount of the ionic moieties into the body of the polymer can results in dramatic alteration of the physical and mechanical characteristics of the material due to formation of the ionic association centers, called multiplets. The formation of such organizations is well molded by EHM theory[125] and granted with X-ray scattering results. [169] These aforesaid nanophase separated ionic domains can induce an increasing of the T_g and boosting viscosity in the melt and solution in the order of magnitudes by hindering the chain motion and acting as physical cross-links.[170] However, the flow of the material is not limited to complete disruption of these cross-links as the SAXS results implicated in endurance of the aggregates to higher temperatures, up to even 300 °C in the case of molten

salts.[171-172] The flow behavior of the ionomers is featured by ion hopping and increased relaxation time (t_d).[170] Ion hopping is a localized relaxation process of the polymer chain via interchanging between aggregates in a dynamic equilibrium state. Assuming a finite life time (denoted with τ) for the ionic aggregates, designated as the average of the residing time of an ionic group in a particular multiplet, the ionic group can diffuse (hop) to another aggregate in the time duration of τ. This process leads to relaxation of the polymer chain segments which are attached to the ionic associations and allowing the whole polymer to diffuse without simultaneous rupture of the all ionic associations along the chain. Consequently, elevated temperature may not destroy the ionic associations but it can result in acceleration of the interchanges between these organizations accompanied with the stress relaxation of the polymer yielding to melt flow of the material.[172] Thus, the presence of the ionic associations in the polymer chain, acting as temporary cross-links, results in reduction of the overall diffusion coefficient of the polymer leading to increase of the viscosity and terminal relaxation time.[170]
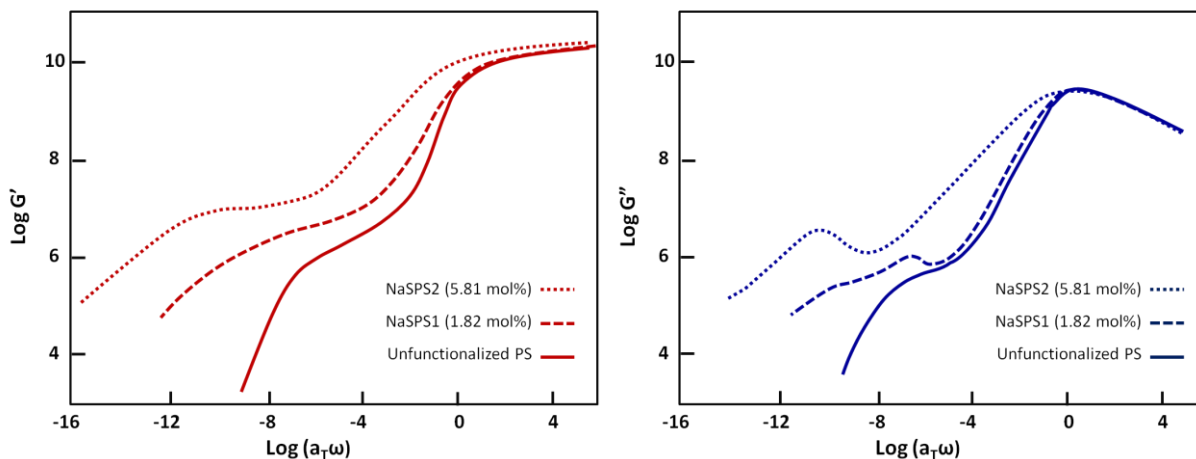

Figure 1.7. G' and G'' modulus-frequency master curves for unfunctionalized PS and NaSPS. Reference temperature for each material is T_g. The graphs are redrawn from the literature.[173]

Determination of the rheological characteristics of the ion containing polymers due to enhanced viscosity and long lasting relaxation time (t_d) is convoluted. The measurement of zero-shear viscosity η_0 with conventional rheometers for materials with low-shear Newtonian behavior can be problematic, as the required shear rate $\dot{Y}$ must be less than $1/t_d$.[170] In addition, interpretation of the data can be complex due to entanglement effect, where it exists. However, various measurements were performed on mainly sulfonated and craboxylated ionomers in order to determine the effect of

the ionic group, molecular weight of the polymer, and neutralization degree on the rheological behavior of the ionomers.[174-176]

Figure 1.7 demonstrated dynamic responses measured for lightly sulfonated polystyrene (SPS) samples and unfunctionalized polystyrene (PS). Shear storage (G') and loss (G") modouli were measured for samples which were subjected to an oscillatory deformation at a frequency ω. The depicted master curves in Figure 1.7 are obtained from time-temperature superposition of NaSPS1 (1.82 mol% sulfonation), NaSPS2 (5.81 mol% sulfonation), and unfunctionalized PS. According to the results, at very low frequencies, unfunctionalized PS exhibits nearly a terminal behavior indicated by G' α ω and G" α ω^2, as it was expected for materials without permanent cross-links. With increasing the frequency, G' forms a rubbery plateau due to entanglement and then glass transition occurs at higher frequencies. Addition of the ionic moiety results in an increase of the value of G' in the plateau region in comparison to non-ionic polymer as a result of presence of ionic associations and entanglement, while increasing the ion content leads to the appearance of second G", which attributes to the break of the ionic associations. Furthermore, investigations on mechanical properties of variety of the ionomers proved that exchanging the cation affects the rheological behavior of the ionomer, though there was no correlation found to simply relate it to the valance of the cation.[177-178] The neutralization level was also determined as a crucial factor in controlling of the rheological behavior of the synthesized materials via changing the ion content.[178]

1.4. Application of PILs

Similar to their monomeric analogous, PILs also have received enormous attention due to their unique tailored characteristics which candidates them for a wide range of application from electronic devices to catalytic membrane, CO_2 absorbent, stabilizer, carbon nanostructures dispersant, tribology, self healing, and biomaterials.

Undoubtedly, electrochemical devices are one of the most important fields of the applications of PILs. This can explain why a broad range of PILs are being categorized as polymer electrolytes although, contrary to classical polyelectrolytes which are producing ions due to dissociation in aqueous solvents, most of PILs are not soluble in water. Traditional liquid electrolytes which are being used in batteries and fuel cells are prone to be disadvantageous due to the leakage, toxicity,

flammability, and instability while these drawbacks are eliminated in the case of solid state polyelectrolytes due to the combination of characteristics of the ionic liquid moiety and associating polymer.[12,33]

To obtain a polymeric ionic liquid for different electronic approaches one should carefully consider their ionic conductivity and mechanical stability. High ion conductivity is an important factor for PILs being used as electrolytes which can be achieved by addition of higher ionic moiety to the body of polymer, but it can have an inverse influence on mechanical stability of the PIL. Morphology of the PILs can also play a role on their performances. The presence of nanostructured domains, introducing nanofillers, or block copolymer to the body of PILs can result in more tuned materials for specific tasks.[179] Ohno's innovative work was one of the first reports on ionic conductivity of PILs.[33] Their latter investigations on influence of incretion of flexible spacers between polymerized monomer via addition of small amount of cross-linker before polymerization of IL monomer resulted in a flexible transparent PIL film with higher ionic conductivity.[37] Further investigations in synthesis, design and evaluation of new PILs in this field of application are published in some review articles.[9,151,179-180]

Supporting solid materials covalently attached IL to polymers demonstrated an outstanding performance either as a recyclable catalyst or in separation processes.[181, 182] In this respect synthesis of some polymer-supported N-heterocyclic carbene (NHC) compounds containing imidazolium moieties have been reported. Poly isobutylene based imidazolium salts synthesized to be used as polymer supports for Pd and Pt in Suzuki cross coupling, respectively.[183, 184] Chiral and achiral poly imidazolium particles were synthesized as a precursor of –NHC polymers to be used in asymmetric catalysis and separation.[185] Intrinsic structural advantages of ILs, prompted their application in gas capture, mainly focused on CO_2 due to reversible sorption of it. Consequent investigations revealed significant capacity of several ammonium[15] and specially imidazolium[186] based synthesized PILs in fast, reversible, and selective absorption of CO_2. Recent studies on low cost poly(urethane) based imidazolium PILs lead to new absorbent with improved practical performance.[187]

Improving dispersibility of carbon materials specially carbon nanotubes (CNTs) and graphene sheets as well as other nanoparticles is a major issue of surface scientists in further modification and processing of such materials. Capability of imidazolium based ionic liquids in π-π stacking lead to investigation of ILs[188] and further on PILs[189] as potential dispersant for carbon material. Non covalent interaction between imidazolium ring and CNT surfaces resulted in CNT supported nanoparticles of

Ru and Pt with better dispersity and catalytic activity.[32] Later on covalent attachment of PILs to CNTs via grafting from and grafting to reactions lead to significant improvement in their solubility in variety of solvents from water to polar organic ones.[190,191] Recent studies reported on synthesis of imidazolium based treelike PILs grafted onto graphene nanosheets which was dispersed in water without obstacles associating crude graphene nanosheets.[192]

During the last decade, the research on usage of IL in tribology also gained significant importance. High thermal stability and nonflammability as well as other physicochemical and environmental features of ILs nominated them as a good candidate for lubricating oil or lubricating additives.[20] The variety of combinations of cations and anions with different bridging chains were investigated. Evidences on improved tribological properties of polyether embedded structures[95] resulted in synthesis of imidazolium based poly(ethylene glycol)ionic liquids (PEGILs). Detailed investigations suggested the capability of polyfluoroalkyl substituted imidazolium PEGIL as high temperature lubricant.[96] Further researches[193] revealed that some PIL brushes can provide a proper boundary layer. The synthesized imidazolium based PIL grafted multiwalled carbon nanotubes (MWCNTs) exhibited anti-wear and low friction performance as an additive for base oil lubricating systems.[190]

Self healing appears to be another emerging application field of PILs.[163] Recently Mecerreyes[194] reported on some supramolecular ionic polymers which combined ionic conductivity and rheological features and exhibited self-healing behavior as the materials were capable of generating reversible network in the polymer matrix resulting in drastic changes of the mechanical and physical behavior controlled with temperature.[194] This was similar to previous reports on self-healing behavior observed in some ionomers regarding thermo mechanical properties of the material. According to their study dynamic mechanical analysis revealed that due to the presence of ionic clusters these materials demonstrated different properties from an elastic to a molten polymer varying with the temperature.[195]

1.5. Aim of the work

The aim of this work is to design and synthesize new polymeric ionic liquids (POILs). The designed POILs can be created through modification of the end functional groups of the polymer chain resulting novel telechelic polymers covalently attached to the ionic liquids. A variety of structural combinations can be obtained just by a simple choice of cation and anion or the nature and molecular weight of the polymer backbone. Introduction of a small amount of the ionic moiety in the structure of the polymeric materials is expected to have a high impact on their physical and mechanical properties. Thus, the investigation on physical, chemical, and mechanical properties of the synthesized POILs to determine the influence of the above mentioned variables (nature of cation, anion, molecular weight, and chemical structure of the primary polymer) is another crucial aspect of this work. Two different types of polymers, hydrophilic and hydrophobic, with distinctive molecular weight accompanied with different cations and anions are aimed to be synthesized.
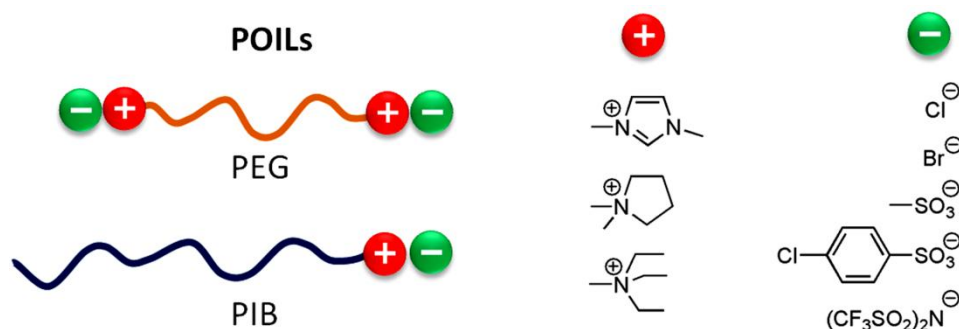

Figure 1.8. Schematic representation of the structure of the designed POILs.

Poly(ethylene glycol) and poly(isobutylene) are selected as the constituent polymers to react with a aromatic, a cyclic, and an aliphatic amine to explore the role of the hydrophilicity or hydrophobicity in addition to the chemical structure of the ionic moiety in the formation of the self assemblies in the final products (Figure 1.8). Different synthetic methods and conditions are acquired to achieve the designed products in an efficient process. An elaborative characterization of the products is performed via spectroscopic methods. Once the accuracy of the structures is confirmed, further investigations can be conducted to monitor their thermal behavior as well as other physical and mechanical properties.

2.0. Concept

The aim of this work is synthesis, characterization and internal structure assessment of the polymeric ionic liquids. For this propose poly(ethylene glycol) and poly(isobutylene) with different molecular weights were chosen to react with three different amines, 1-methylimidazolium, 1-methylpyrrolidinium, and *N,N,N*-triethylammonium, associated with variety of anions such as, chloride, bromide, mesylate, tosylate, and bistriflimide. The synthetic concept of this research consists of two main parts: Synthesis of poly(ethylene glycol)-based ionic liquids (**PEGILs**) and synthesis of poly(isobutylene)-based ionic liquids (**PIBILs**).

Part 1: poly(ethylene glycol)-based ionic liquids (PEGILs)
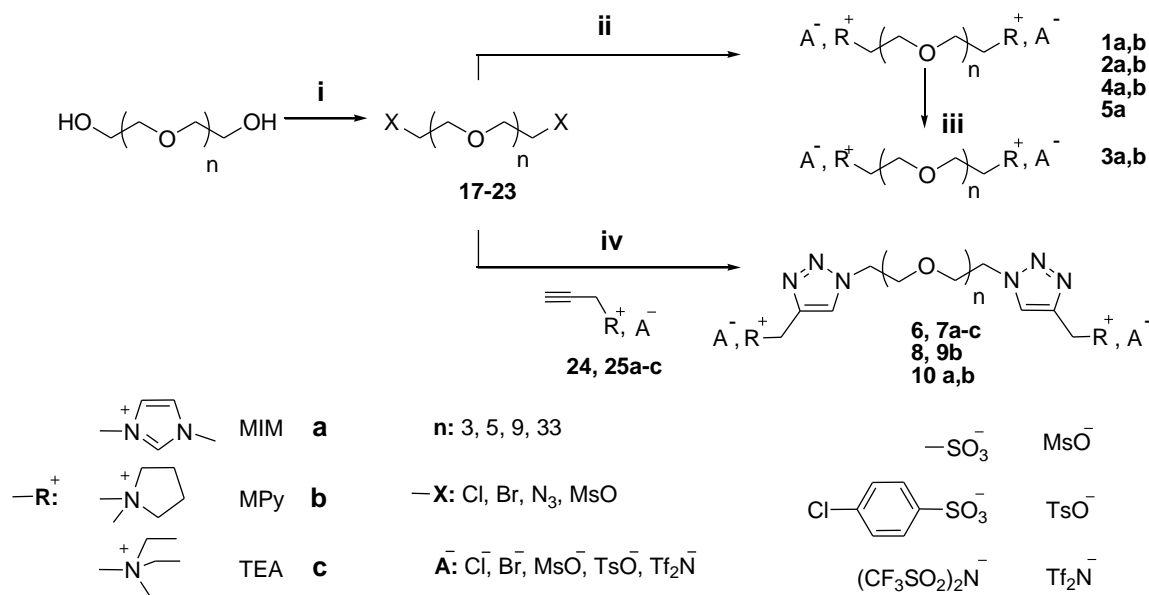
i: SOCl$_2$ (X: Cl); MsOCl (X:MsO); PBr$_3$ (X: Br); PBr$_3$/ NaN$_3$ (X; N$_3$)
ii: MIM or MPy/ toluene
iii: (CF$_3$SO$_2$)$_2$NLi/ methanol:water (1:10)/ RT/ 72 h
iv: Cu(I) catalyst/ DIPEA/ Cu(I) catalyst/ DIPEA/ toluene:water:isopropanol (2:1:1)/ MW or heat under condition described in Table 2.2.

Scheme 2.1. General pathway toward synthesis of the designed **PEGILs**.

The most common way to synthesize ionic liquids is quaternization. The nucleophilic substitution reaction of the chosen nucleophile (amine here) with an organic compound containing an appropriate leaving group (most commonly halides) can result in designed ionic liquids (**ii**). Further

tuning of the structure can be accomplished via anion exchange reaction (**iii**). To investigate the applicability of the above mentioned synthetic strategy to for preparation of poly(ethylene glycol)-based ionic liquids which contain a long organic chain with a variable number or repeating units, a very short analogous of the same polymer was selected. Even though, the physical and chemical properties of the polymer could be dramatically changed with increasing the number of the repeating unit in comparison to the model system, it could be still very useful to evaluate the reaction condition and to predict the properties of the products (Scheme 2.1).

In order to overcome the shortcomings of the quaternization reaction for efficient synthesis of **PEGILs**, the reaction was replaced with azide/alkyne "click" reaction (**iv**). The obtained products, after elaborative characterization via NMR spectroscopy, were subjected to ESI-MS-TOF to investigate the presence of the ionic liquid aggregates. Thermal behavior of synthesized materials were also monitored to determine the main transition points (Scheme 2.1)

Part 2: Poly(isobutylene)-based ionic liquids (PIBILs)
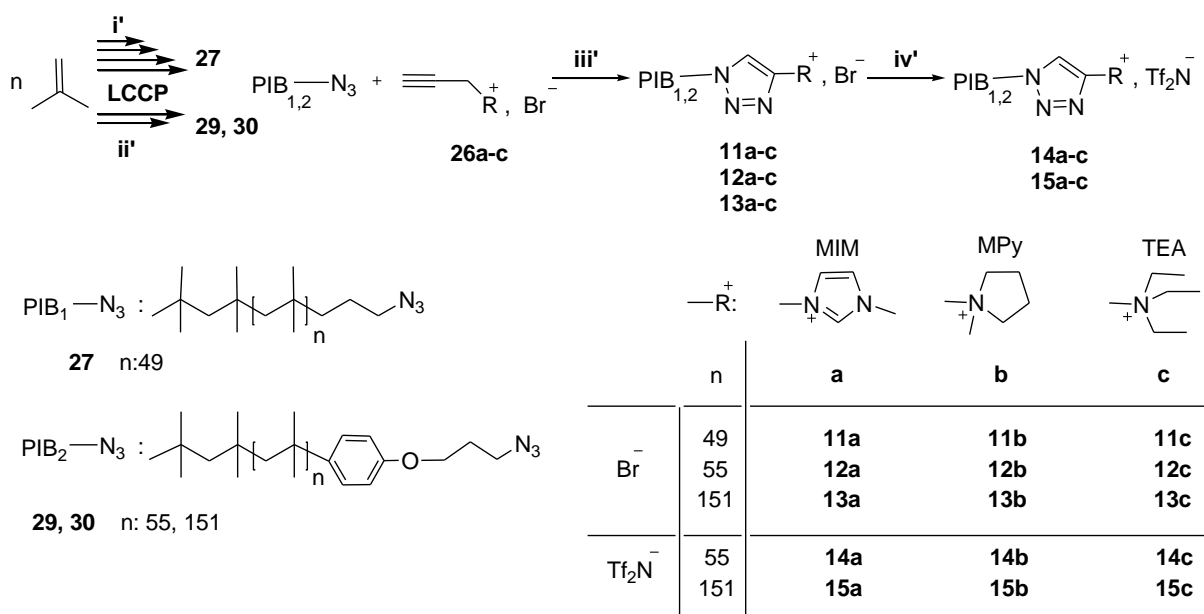
i': TMPCl/ TiCl$_4$/ DMA/ DtBP/ATMS/Hexane:DCM (3:2); 9-BBN/MCPBA/THF; CBr$_4$/ PPh$_3$/DCM; TMSA/TBAF/THF
ii': TMPCl/ TiCl$_4$/ DMA/ DtBP/BPB/Hexane:DCM (3:2); NaN$_3$/DMF:Heptane (1:1)
iii': Cu(I) catalyst/ DIPEA/ toluene:water:isopropanol (2:1:1)/ MW irridation under condition described in Table 2.5.
iv': (CF$_3$SO$_2$)$_2$NLi/ methanol:water (1:10)/ RT/ 72 h

**Scheme 2.2.** General pathway toward synthesis of the designed **PIBILs**.

The synthesis of poly(isobutylene) based-ionic liquids via direct quaternization of the end functionalized PIB with the corresponding amine did not seem as a feasible synthetic pathway considering the very long chain length of the polymer and declined activity of the leaving group attached to the end of the polymer chain. Hence, similar to the previous part, "azide/alkyne click" reaction (**iii'**) and consequent anion exchange (**iv'**) was selected as a quantitative method to synthesize the designed **PIBILs**.

As depicted in Scheme 2.2, to perform such reaction it was necessary to insert the alkyne moiety to the selected amine, which was carried out via nucleophilic substitution of propargyl bromide with corresponding amine. Meanwhile, azido- functional group was introduced via a multi-step functionalization of poly(isobutylene), which was synthesized via living carbocationc polymerization. All synthesized products were characterized by means of NMR spectroscopy. The accuracy of the structures was proved via MALDI. Furthermore, the materials were subjected to SAXS and rheology measurements to detect the presence of the hierarchies in the polymer matrix and their change with variation of the temperature. Additionally, the effect of molecular weight of the polymer, type of the cation, and anion on the formation of self assemblies was studied.

.

2.1.Poly(ethylene glycol)-based ionic liquids (PEGILs)

2.1.1.1.Synthesis of tetraethylene glycol-based ionic liquids (TEGILs)

Tetraethylene glycol was modified via converting the hydroxyl end groups to chloro- or mesylate- to enhance the activity of the starting material for further nucleophilic substitution reaction (via route **i** as demonstrated in Scheme 2.1).[196-197] As depicted in Scheme 2.3, the reaction between the amines (MIM or MPy) and modified tetraethylene glycol (route **ii**) under the reaction condition described in the literature,[96,198] was resulted in the desired ionic liquids (**1-2a,b**) in a reasonable yield. The results of the synthesized tetraethylene glycol ionic liquids (**TEGILs**) are summarized in Table 2.1.
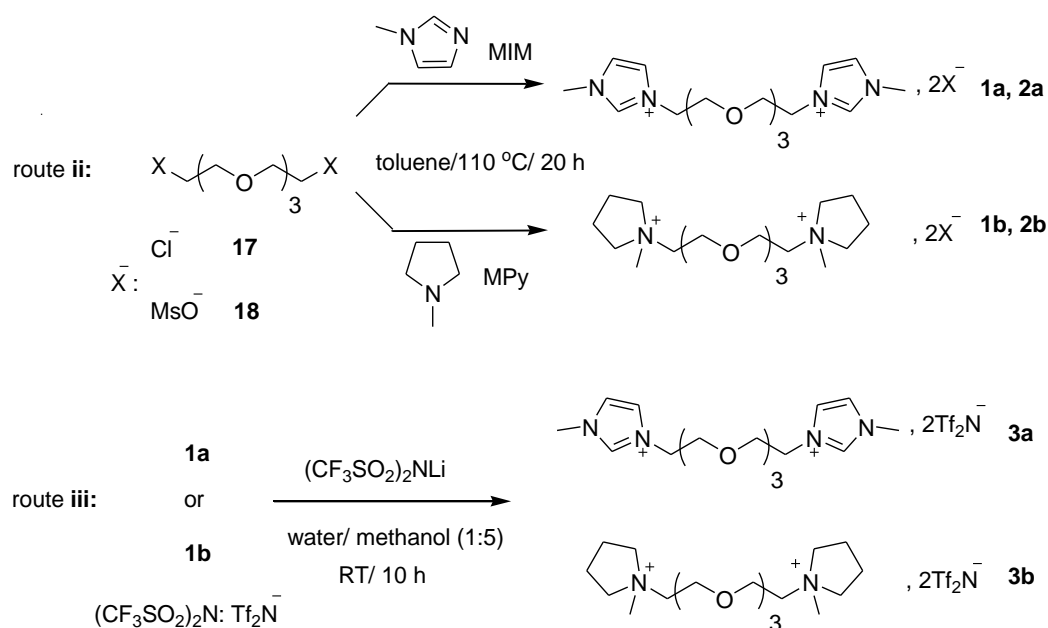
Scheme 2.3. Synthesis of **TEGILs** (**1a**, **1b**, **2a,** and **2b**) via quaternization reaction (route **ii**). Subsequent anion exchange yielded to **3a** and **3b** (route **iii**).

Scheme 2.1 illustrates the general reaction route toward the expected **PEGILs**. To obtain ionic liquids with broader range of counteranions, anion exchange reaction (route **iii**) is the simplest method to acquire. In this respect, as reflected in the scheme 2.3, compounds **3a** and **3b** were synthesized due to the reaction between the previously synthesized ionic liquids (**1a** and **1b**) and lithium bis(trifuoromethanesulfonyl)imide salt via exchanging the chloride anion with bistriflimide salt,

according to the procedure described else in the literature.[96] The yield of the synthesized ionic liquids **3a** and **3b** is mentioned in Table 2.1
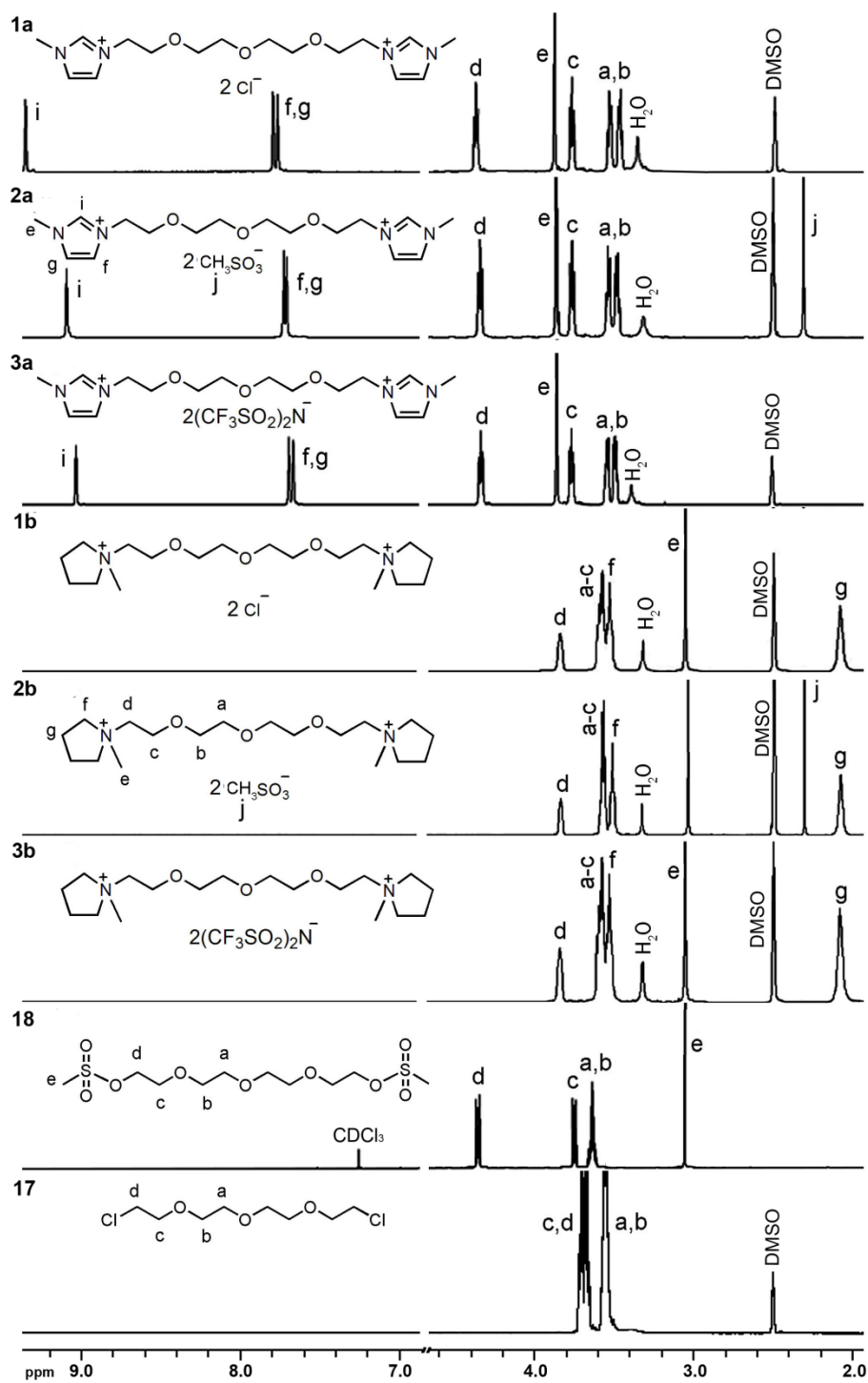

Figure 2.1. ^{1}H NMR spectra of synthesized **TEGILs (1-3a** and **1-3b)** in comparison with modified **TEG (17, 18)**.
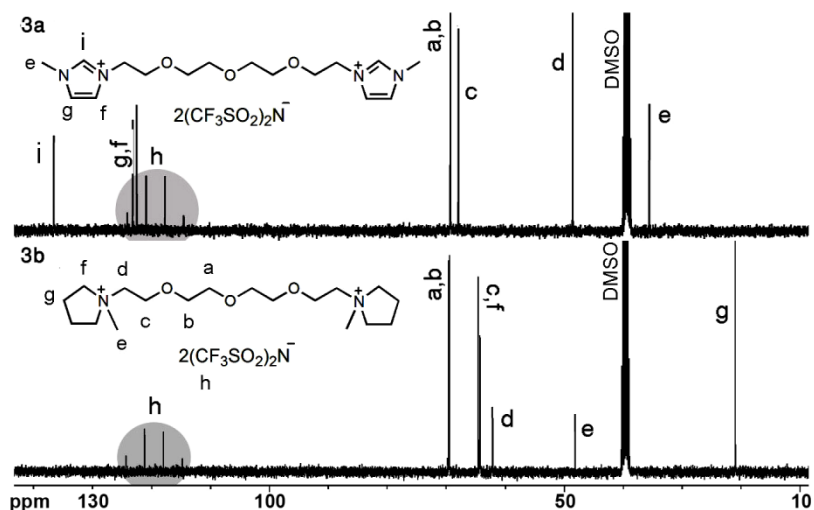
Figure 2.2. ^{13}C NMR spectra of the synthesized **TEGILs 3a** and **3b** via anion exchange reaction.

All of the synthesized tetraethylene glycol based-ionic liquids were characterized using ^{1}H and ^{13}C NMR. As it is shown in Figure 2.1, which depicts the ^{1}H NMR spectra of compounds **1-3a,b**, replacing chloro- or mesylate groups with a quaternary amine (**a** or **b**) resulted to a shift in the resonance of the very last -CH$_2$- groups. The disappearance of this signal along with the emerging resonances of the corresponding end groups such as aromatic proton signals of imidazolium ring around 7-9 ppm or aliphatic proton signals of pyrrolidinium cycle around 2-4 ppm proved obtaining of the designed structures. Comparison of the integration ratio of the signals belonging to the end groups and ethylene glycol chain confirmed the complete conversion of the attained products. Figure 2.2 represents the ^{13}C NMR spectra of the compounds **3a** and **3b**. The most significant proof of the exchange is the appearance of the quartet resonance from CF$_3$- due to ^{13}C-^{19}F coupling.

Table 2.1. Reaction results of synthesis of **TEGILs 1-2a,b** (route **ii**) and **3a**, **3b** (route **iii**).

entry	product	-R$^+$	A$^-$	reaction condition temp. (°C)/time (h)	Yield (%)
1	**1a**	MIM	Cl$^-$	110 °C/20 h	85
2	**1b**	MPy	Cl$^-$	110 °C/20 h	82
3	**2a**	MIM	MsO$^-$	110 °C/20 h	78
4	**2b**	MPy	MsO$^-$	110 °C/20 h	80
5	**3a**	MIM	Tf$_2$N$^-$	25 °C/10 h	71
6	**3b**	MPy	Tf$_2$N$^-$	25°C/10 h	66

2.1.1.2. Synthesis of poly(ethylene glycol)-based ionic liquids (PEGILs)

A similar strategy was followed to synthesize **PEGILs**. First, poly(ethylene glycol) (400 and 1500 g/mol) was converted to bromo- end caped polymer in the presence of PBr_3 as described in the literature. Then, the modified polymer was exposed to the chosen amine to precede the quaternization reaction under the reaction condition depicted in Scheme 2.4.
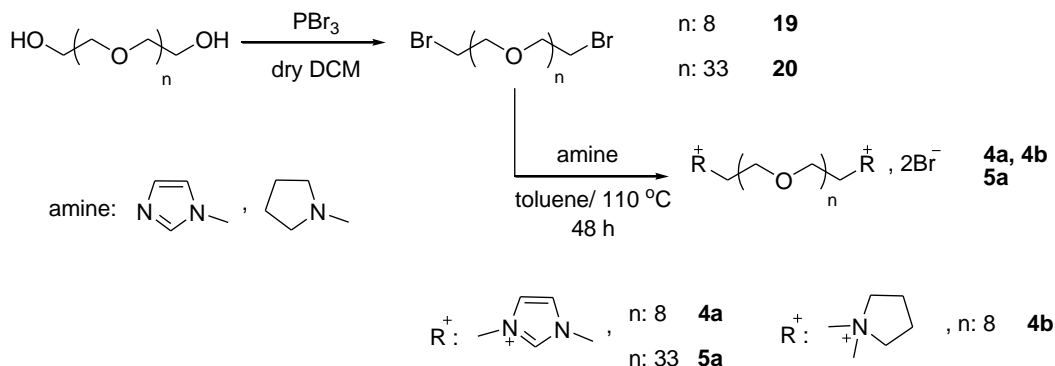
Scheme 2.4. Synthesis of **PEGILs (4a**, **4b,** and **5a)** via quaternization reaction (route **ii**).

The structure of the synthesized **PEGILs** (**4a**, **4b,** and **5a**) was characterized using ^{1}H and ^{13}C NMR. As it is shown in Figure 2.3 which demonstrates the ^{1}H NMR spectra of compounds **4a**, **4b**, and **5a**, replacing bromo- group with a quaternary amine (**a, b**) , similar to **TEGILs**, resulted in a shift in the resonance of terminal -CH$_2$- groups. The emerging resonances of the aromatic proton signals of imidazolium ring around 7-9 ppm in the case of **4a** and **5a** and aliphatic proton signals of pyrrolidinium cycle around 2-4 ppm for **4b** proved obtaining of the designed structures. However, characterization of the produced polymer via NMR spectroscopy revealed the presence of unreacted polymer end groups in the product (Figure 2.3). Despite of the pronounced signals of the ionic moieties attached to the polymer (assigned as e, f, g, and h), the minor signal of the terminal -CH$_2$- (assigned as d) was still detectable. Besides the mismatch of the integration ratio between the signals from the attached amine groups, terminal –CH$_2$- groups (assigned as c, d) and the signals from the polymer chain (assigned as a) was another evidence of existing of mono- substituted polymer from 10-18% (calculated via integration data obtained from ^{1}H NMR). To achieve the full conversion of the polymer, the reaction time was extended from 48 h up to 120 h. However, this resulted in appearance of more impurities in the product mixture. Eventually, the quaternization reaction

between poly(ethylene glycol) (400 and 1500 g/mol) and the corresponding amines resulted in a mixture of bi- and mono- functionalized polymer. Evidently, the increase in polymer chain length resulted in the decrease of the activity in neclueophilic substitution reaction and subsequently the reaction efficiency. Furthermore, with increasing molecular weight of the polymer, the physical properties of the products were more dominated by characteristics of the polymer than the ionic end group. Therefore, separation of mono- and bi- functional polymer via classical purification methods was not feasible. Thus, the quaternization pathway was replaced with a different synthetic strategy to boost the conversion.
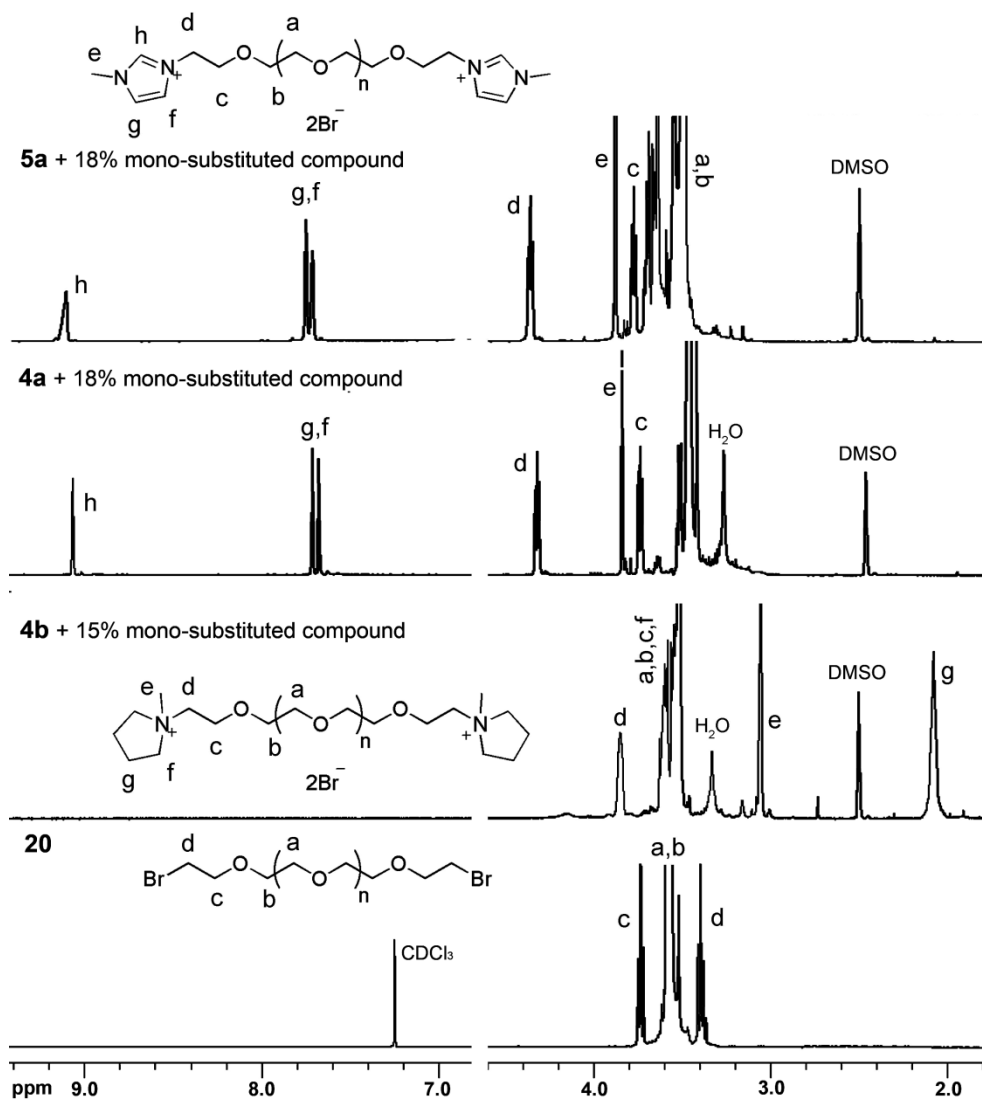

Figure 2.3. ^{1}H NMR spectra of the synthesized **PEGILs** (**4a**, **4b**, and **5a**) in comparison with modified **PEG** (**19, 20**).

In this respect, azide/alkyne "click" reaction was selected as a promising method to achieve the desired products in shorter period of time with considerably higher efficiency.

2.1.1.3. Synthesis of hexaethylene glycol-based ionic liquids (HEXILs) via click reaction

Azide/alkyne "click" reaction is based on Huisgen 1,3-dipolar cycloaddition[199-200] which nowadays is frequently being termed as "Sharpless-type click reaction".[201-202] Quantitative yield, high tolerance to variety of functional groups, solvents, and interfaces, insensitivity to water and simple reaction approach settled this recently re-discovered "click" reaction as one of the main routes toward modification of variety of polymers.[203-210] Hence, to investigate the feasibility of synthesis of **PEGILs** via azide/alkyne "click" reaction, the method was probed starting from the smaller molecules such as hexaethylene glycol (**HEX**). For this purpose, hexaethylene glycol was modified via nucleophilic substitution of terminal hydroxyl-s to azido- end groups.[211] Meanwhile, the alkyne functionality was introduced to the selected tertiary amines via simple quaternization of these compounds with propargyl derivatives according to the literature. [212]
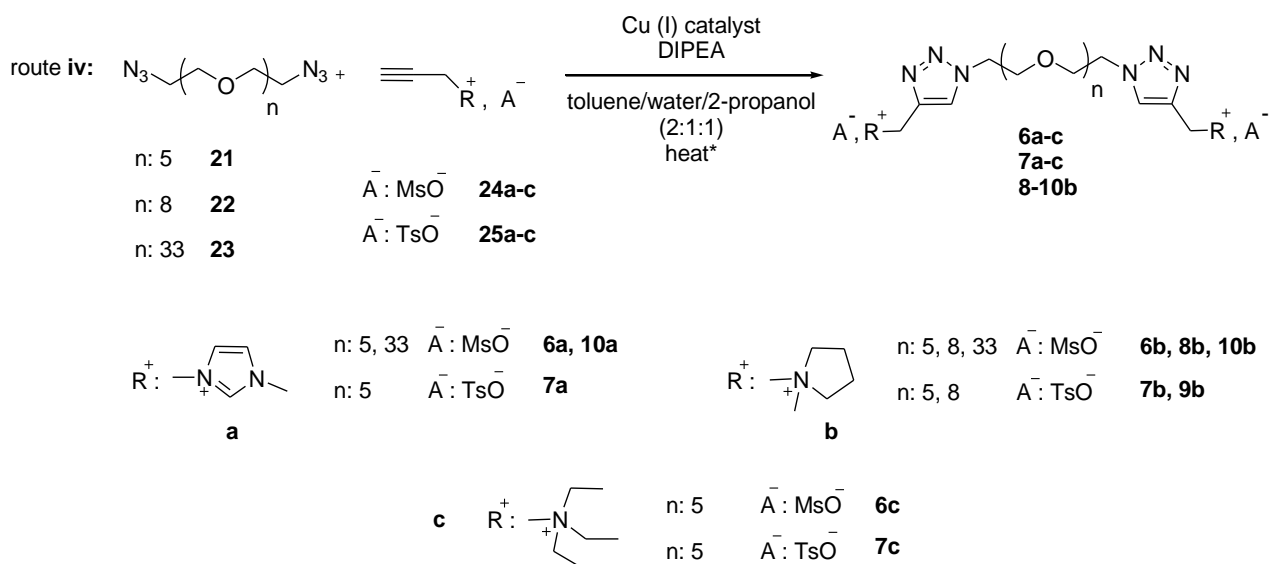
* Microwave irradiation (MW) or conventional heating via oil bath under the condition described in Table 2.2.

Scheme 2.5. Synthesis of **HEXILs** (**6a-c** and **7a-c**) and **PEGILs** (**8-10b**) via azide/alkyne "click" reaction (route **iv**).

The click reaction was conducted in the presence of catalytic amount of CuBr accompanied by excess of diisopropyethylamine (DIPEA) base to generate copper(I)-acetylide species. The elimination of oxygen from the reaction medium before addition of the catalyst was very crucial to avoid the deactivation of the catalyst due to oxidation of Cu(I) to Cu(II). Thus, **HEXILs** (**6a-c**) were successfully synthesized via introducing 1,3-triazole ring due to azide/alkyne "click" reaction not only in short time but also with almost complete conversion (see Table 2.2). Further work up was necessary to remove the excess of the alkyne moiety and copper catalyst but due to complete conversion the mono- and bi- functional polymer mixture issue was resolved.
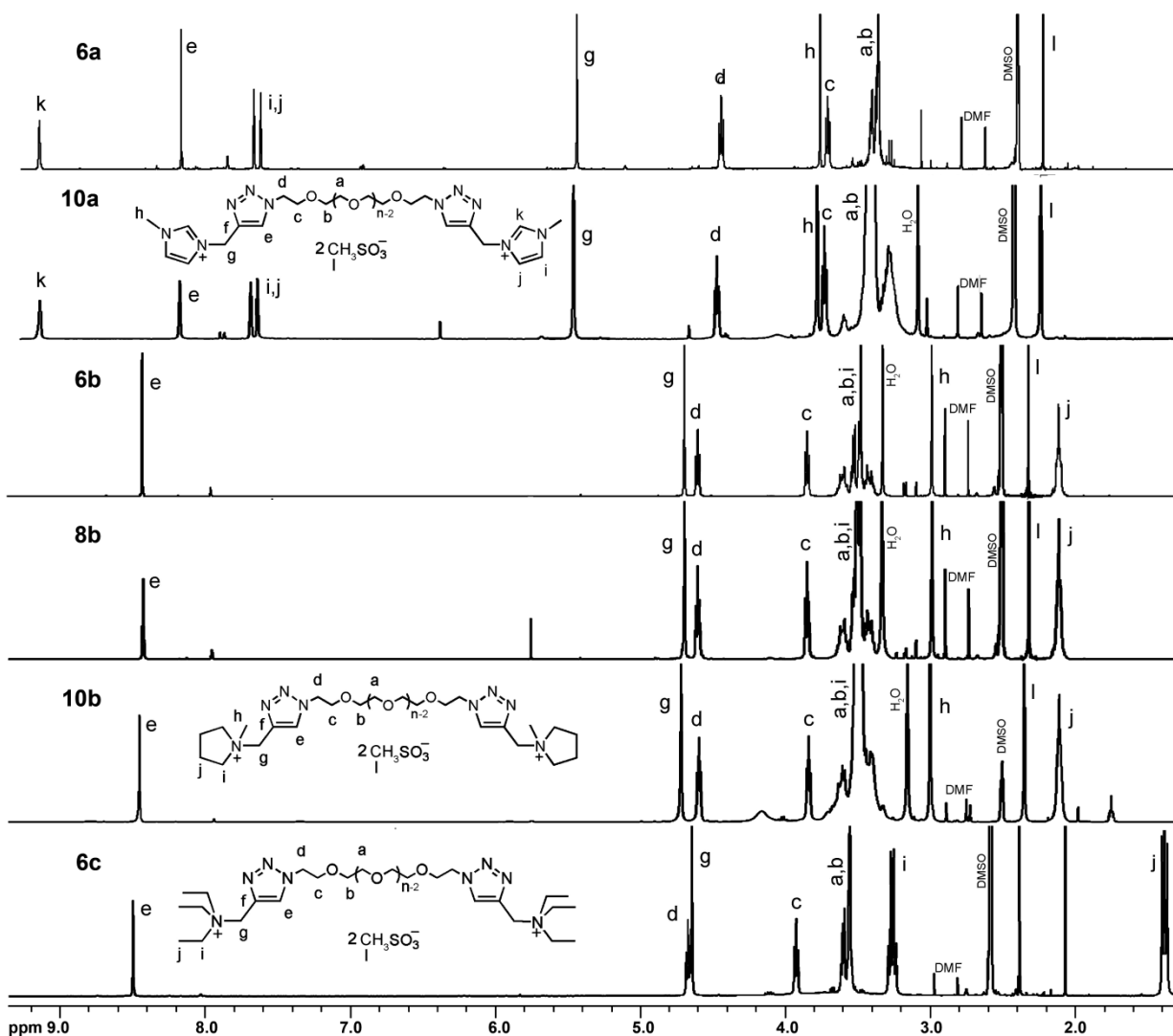

Figure 2.4. ^{1}H NMR spectra of the synthesized **HEXILs** (**6a-c**) and **PEGILs** (**8b** , **10a** and **10b**) via azide/alkyne "click" reaction (route **iv**).

Figure 2.4 demonstrates ^{1}H NMR spectra of the synthesized polymeric ionic liquids via click chemistry. The construction of 1,4-triazole ring was clearly confirmed due to the appearance of the singlet resonance around 8.1-8.3 ppm (assigned as e in Figure 2.4). Arising of the new resonances from the corresponding amines was coincided with the chemical structure of the expected products. The complete conversion of the azido- functionalized hexaethylene glycol was firmly justified considering the absence of $-CH_2-N_3$ signal of the starting material and precise match of the integration ratio of the signals of head groups (assigned as k, i, and j in Figure 2.4) in comparison to the terminal $-CH_2-$ (assigned as d in Figure 2.4) and other resonances from the polymer chain. These results were reassured once more after complete assignment of the ^{13}C NMR spectra signifying the disappearance of the resonance of the carbon atom attached to the nitrogen of the azido- group.

Table 2.2. Reaction results of synthesis of **HEXILs** (**6a-c** and **7a-c**) and **PEGILs**,(**10 a** and **8-10b**) via azide/alkyne "click" reaction in the presence of CuBr as catalyst (route **iv**).

entry	product	-R$^+$	A$^-$	n	reaction condition power(W)/temp. (°C)/time (h)*	Isolated yield (%)
1	**6a**	MIM	MsO$^-$	5	70 W/70 °C/12 h	98
2	**6b**	MPy	MsO$^-$	5	70 W/70 °C/12 h	95
3	**6c**	TEA	MsO$^-$	5	70 W/70 °C/12 h	97
4	**7a**	MIM	TsO$^-$	5	70 W/100 °C/10 h	74
5	**7b**	MPy	TsO$^-$	5	70 W/100 °C/10 h	95
6	**7c**	TEA	TsO$^-$	5	70 W/70 °C/12 h	98
7	**8b**	MPy	MsO$^-$	8	70 W/70 °C/12 h	93
8	**9b**	MPy	TsO$^-$	8	70 W/70 °C/12 h	95
9	**10a**	MIM	MsO$^-$	33	50 °C/72 h	95
10	**10b**	MPy	MsO$^-$	33	50 °C/48 h	92

* The reaction was performed either under MW irradiation or oil bath.

2.1.1.4. Synthesis of poly(ethylene glycol)-based ionic liquids (PEGILs) via click reaction

After successful synthesis of hexaethylene glycol based ionic liquids via click reaction, a similar approach was employed toward the synthesis of poly(ethylene glycol)-ionic liquids. Accordingly, azido- functionalized poly(ethylene glycol) was synthesized from commercially available poly(ethylene glycol) (400 and 1500 g/mol). Subsequently, azido- functionalized polymer and tertiary

amine bearing alkyne moiety was brought together following the same procedure described before. As expected, 1,3-dipolar cycloaddition reaction occurred in the presence of catalytical amount of copper (I). Adversely to the previous pathway (route **ii**), the reaction was proceeded under a mild condition and lead to the expected structure with complete conversion rate. This experiment was carried out using both microwave irradiation (MW) as well as oil bath as heating source. These methods, both, microwave irradiation and oil bath, were resulted in fully converted bi-functional polymeric ionic liquids within 12 hours to 4 days, depends on the heating source, respectively. The reaction condition and yield of the products are summarized in Table 2.2. As exhibited in Figure 2.4 ^{1}H NMR spectra of the achieved poly(ethylene glycol) based-ionic liquids were comparable to hexaethylene glycol based products. The sharp singlet signals around 8.1-8.3 ppm (e) resembled the formation of triazole ring while the vanished resonances of -CH_2-N_3 were evidence of complete conversion of the primary polymer. Additionally, arising of the resonances from the corresponding amines around 7.50 ppm (i, j), and 9.15 ppm (k) in the case of imidazolium, 2.15 ppm (j) for pyrrolidinium, and 1.40 ppm (j) and 3.25 ppm (i) for ethylammunium together with their integration ratio values which was in agreement with the other resonances from the polymer chain (c, d, and g) were coincided with the chemical structure of the expected products.

2.1.2. ESI-MS analysis of the synthesized PEGILs

Besides NMR spectroscopy the structural features of the synthesized poly(ethylene glcol) based ionic liquids were investigated by means of electrospray ionization mass spectroscopy (ESI-MS) as well. This technique was performed via direct transfer of the ionic molecules to the gas phase in both positive and negative modes which allows us to assay the associations of the ionic liquids. To facilitate the interpretation of the attained results $[C^{2+}, 2\ A^-]^z$ was appointed as the notation for the synthesized ionic liquids where C^{2+} was representing the polymer chain bearing quaternary amines with 1+ charge in each end and $2A^-$ was standing for two anions which were accompanying the molecule in neutral state where z was zero. This means z is the overall sum of the charges inside of the bracket.

Figure 2.5 illustrates the recorded ESI-MS spectra of tetraethylenglycol based-ionic liquids in negative mode. **1a** exhibited a signal with significantly higher intensity at 429.1 m/z designated to the neutral ionic liquid accompanied by one extra Cl^- counteranion which can be shown as $[C^{2+},3A^-]^-$. Besides the

medium height signal at 393.13 m/z which represents **1a** after a proton abduction, [C2$^+$,2A$^-$-H]$^-$, the rest of the signals were very weak, and they appeared only after expanding the intensity.
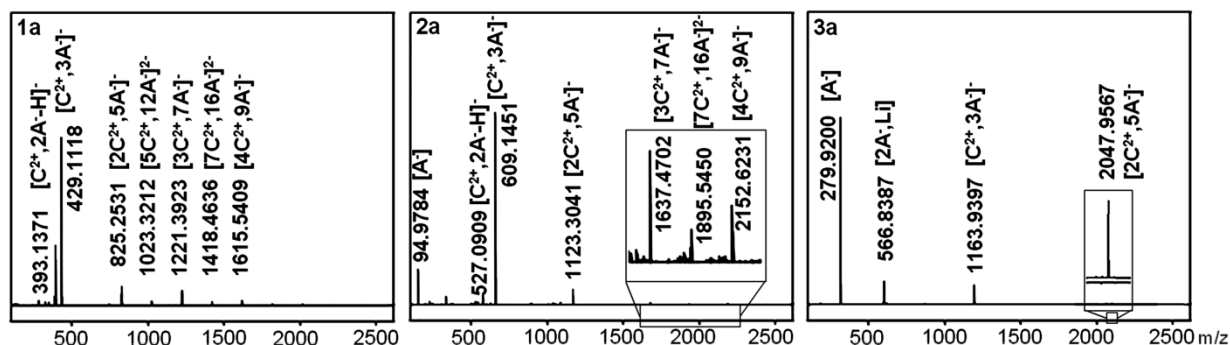

Figure 2.5. ESI-MS spectra of **TEGILs (1-3a)** in negative mode. The signals in the framed areas appeared after magnifying the intensity.

As it is demonstrated in Figure 2.5, variety of structures are assigned in the range of 800 to 2500 m/z which are bearing either single or double charge and their structure can be formulated as [yC^{2+}, (2y+1)A$^-$]$^-$ and [yC^{2+}, (2y+2)A$^-$]$^{2-}$ respectively (y=2,3,4). The formation of such clusters is due to the aggregation of the ionic liquids which was proved by other research groups.[213-217] Similarly, **2a** showed a high intensity signal at 609.14 m/z assigned for [C2$^+$,3A$^-$]$^-$ where A$^-$ was a mesylate anion. However, the presence of mesylate anion was also coincided with the detected signal at 94.97 m/z. The expansion of the intensity vector clarifies the formation of the aggregates of **2b** in the similar pattern of [yC^{2+}, (2y+1)A$^-$]$^-$ and [yC^{2+}, (2y+2)A$^-$]$^{2-}$ (y= 2, 3, 4). In the case of **3a**, the main signal appears at 279.92 m/z belongs to bistriflimide anion.
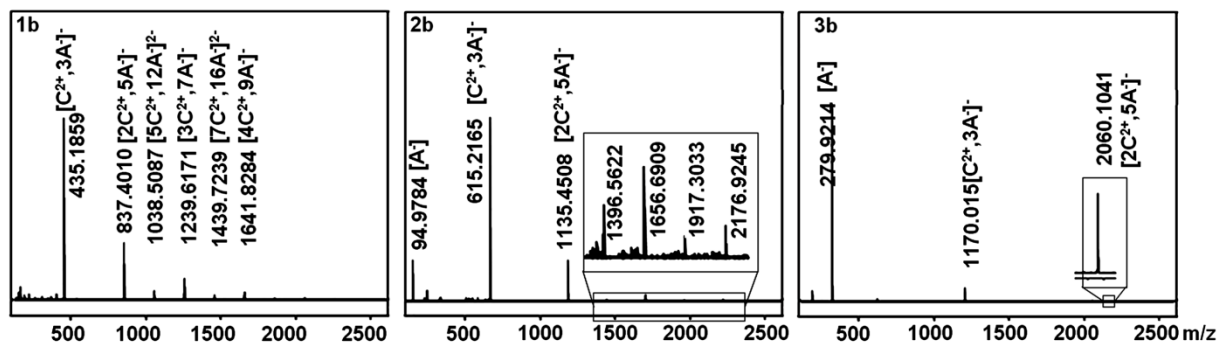

Figure 2.6. ESI-MS spectra of **TEGILs (1-3b)** in negative mode. The signals in the framed areas appeared after magnifying the intensity.

This can be occurred due to a weaker cation-anion interactions between bistriflimide anion and the cation.[217] Furthermore, as it was expected, $[C2^+, 3A^-]^-$ and $[2C^{2+}, 5A^-]^-$ signals were detected at 1163.93 m/z and 2047.95 m/z, respectively (see Figure 2.5). Due to the increasing of the molecular weight, the probable aggregates of **3a** with higher value of y would appear out of the measured range. The ESI-MS spectra of the ionic liquids bearing pyrrolidinium cation (**1b**, **2b**, and **3b**) behave almost in the same pattern (See Figure 2.6). $[yC^{2+}, (2y+1)A^-]^-$ and $[yC^{2+}, (2y+2)A^-]^{2-}$ aggregates were observed for **2a** and **2b** up to y=7. In the case of **3b**, besides the bistriflimide anion and $[C^{2+}, 3A^-]^-$, only a dimeric structure of the product surrounded by 5 counteranion ($[2C^{2+}, 5A^-]^-$) was detectable. **HEXILs** were also examined via ESI-MS under similar circumstances resulted in comparable patterns of the single anion and the aggregates. As expected, the highest intensity signals in the negative mode for the products **6a-c** were $[C2^+, 3A^-]^-$, and $[A^-]^-$ which stands for MsO$^-$ anion , while the **7a-c** were distinguished only with a very pronounced signal at 171.01 m/z assigned for the tosylate anion probably due to the weak interactions between TsO$^-$ anion and the cation (similar to Tf$_2$N$^-$) comparing to Cl$^-$ or MsO$^-$ (Figure 2.7).[217]
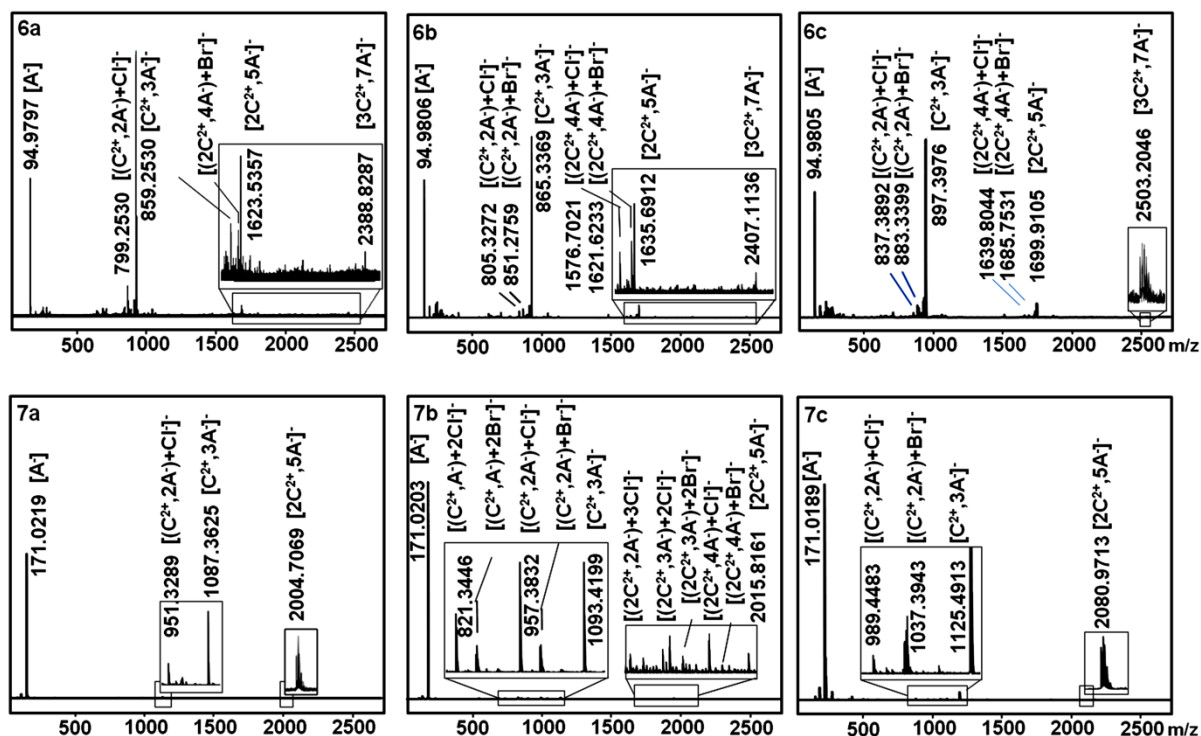

Figure 2.7. ESI-MS spectra of **HEXILs** (**6a-c** and **7a-c**) in negative mode. The signals in the framed areas appeared after magnifying the intensity.

40

As depicted in Figure 2.7, magnification of the intensity revealed the presence of the singly (-1) charged aggregates in **6a-c** and **7a-c**, though there were some signals of detected doubly (-2) charged larger structures which was buried under the signals of singly charged smaller clusters due to the lack of intensity. Besides the clusters formulated as [yC^{2+}, $(2y+1)A^-$]$^-$, where y=1, 2, 3 for **6a-c** and, y= 1, 2 for **7a-c**, there were aggregates detected in all **HEXILs** following the similar formula while 1 or 2 of the counteranions, [A^-], were replaced with Br^- or Cl^- anions. The accuracy of the all assignments of the detected signals was confirmed by comparison of the isotopic pattern of each measured signal with simulated pattern for the expected formula. Figure 2.8 represents the comparison between simulated and measured isotopic patterns of some of the selected signals from **1a**, **2b**, and **6c** as an exemplary. As it is depicted in the Figure, the detected signals at 1656.6 m/z from **2b**, were, in fact, resulted from overlapping of two signals originated from two different series of aggregates. One was belonged to a singly (-1) charged trimer of the cationic moiety, associated with 7 counteranions, [$3C^{2+}$, $7C^-$]$^-$, while the other was detected from a doubly charged (-2) aggregation of 6 cations
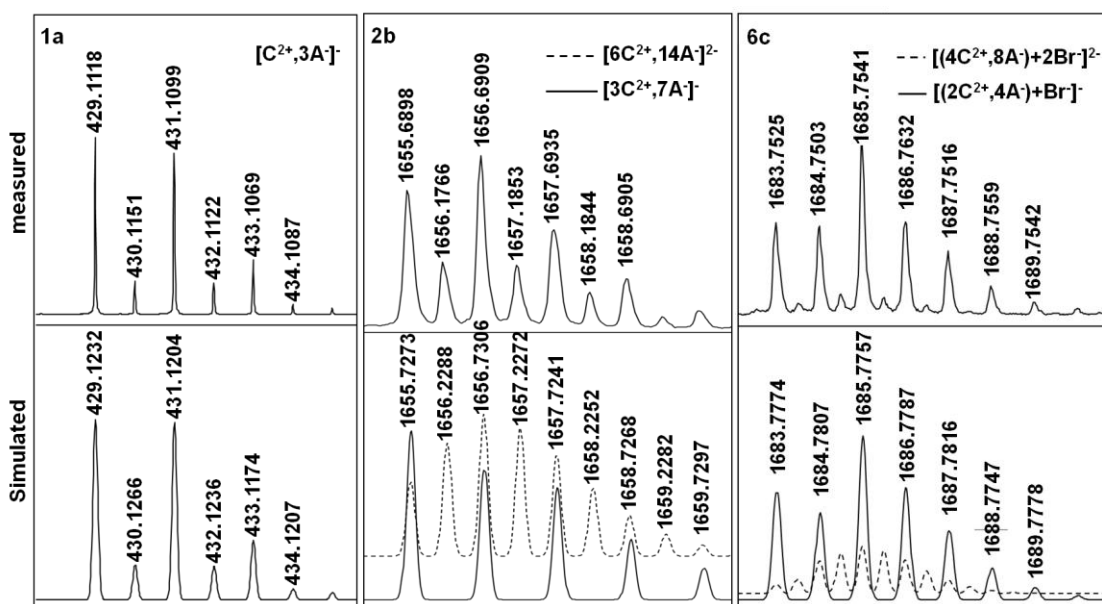

Figure 2.8. Comparison of the expanded spectrum of the exemplary selected signals from **1a**, **2b**, and **6c** with simulated isotopic pattern.

surrounded by 14 numbers of counteranions. Figure 2.8, **6c** displays a similar condition which was observed for **2b** where there was an overlap between the signals recorded from the dimer and the tetramer while there were 1 and 2 counteranions replaced by Br^-, respectively.
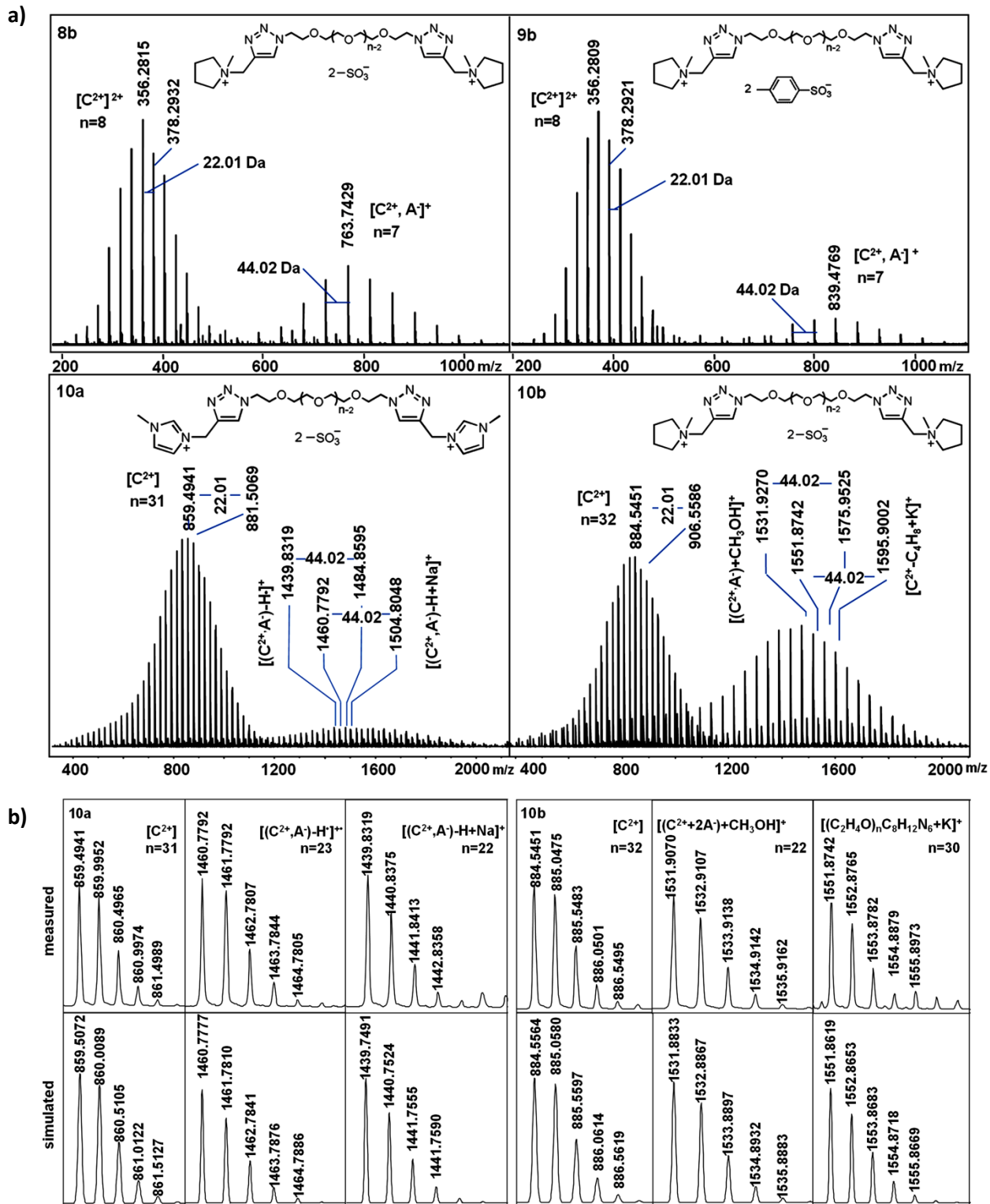
Figure 2.9. a) ESI-MS spectra of the synthesized **PEGILs (10a, 8-10b)** in positive mode; **b)** Comparison of the expanded spectra of the measured and simulated isotopic pattern selected from **10a** and **10b**.

ESI-MS analysis of the **PEGILs** (**10a, 8-10b**) in the positive mode demonstrated a different arrangement (see Figure 2.9). The spectra of all four polymers consist of 2 main series of singly and doubly charged species with signal spacing of 44 Da and 22 Da, respectively which stands for the molecular weight of ethylene glycol fragments. The selected signals detected at 356.28 m/z from the major series of the both ionic liquids, **8b** and **9b**, were assigned to the structure of the naked cation denoted as $[C^{2+}]^{2+}$, while the less pronounced signals were precisely assigned for $[C^{2+}, A^-]^+$. As indicated in Figure 2.9, ESI-MS spectra of **10a** and **10b** exhibited three different series of signals. In both polymers, the main series of the fragments were assigned to a doubly (+2) charged structure of the ionic liquid bearing no anions $[C^{2+}]^{2+}$. In the case of **10a**, the singly charged minor series belonged to the structure of the corresponding ionic liquid, after removal of the counteranion (MsO^-) and a $H^\bullet$, denoted as $[(C^{2+}, A^-)- H^\bullet]^+$, and its Na adduct, denoted as $[(C^{2+}, A^-)-H+Na]^+$. Beside the $[C^{2+}]^{2+}$ signals assigned for the major series of **10b**, the remaining fragments specified in the Figure 2.9 were assigned for the corresponding ionic liquid with methanol and K^+ adducts formulated as $[(C^{2+},2A^-)+CH_3OH+H]^+$ and $[(C^{2+}-C_4H_8+K]^+$, respectively. Figure 2.9 (**b**) demonstrated the comparison of expansion of the selected signals which were designated in Figure 2.9 (**a**) with the corresponding simulated isotopic patterns.

2.1.3. Thermal analysis of the synthesized PEGILs

As ionic liquids have negligible vapor pressure, the thermal degradation temperature (T_m) is the upper limit where an ionic liquid can be found in liquid state and it can be determined by TGA analysis. This range is restricted due to glass transition temperature as the lower limit which can be detected via DSC. Many applications of ionic liquids are owing to their high thermal stability. therefore it is necessary to investigate thermal properties of ionic liquids to define their efficient operating temperature. The thermal degradation temperatures of all synthesized ethylene glycol based-ILs which are listed in Table 2.3, are determined as onset temperature which is the interception of two linear functions.

Literature survey on thermal stability of amine based ionic liquids with variety of structures reveals some key features[218] which can be concluded as following: the anion plays the most important role in the stability of the IL where the structures are identical.[219-220] Thermal stability of an ionic liquid containing pyrrolidinium cation is slightly higher than imidazolium or tetraalkyl ammonium cations,

where the anions are alike.[221-222] Furthermore, studies have demonstrated that geminal dicationic ionic liquids are more stable than their monocationic analogous.[223-224] It appears that chain length of the linkage between two cations can also have slight influence on thermal stability of the ionic liquid as the longer the chain length the lower the decomposition temperature.[71,225] Furthermore, the type of linker also has a significant effect on the thermal stability[226], though geminal dicationic ionic liquids linked with PEG were proved to exhibit the similar thermal resistance as hydrocarbon linkers.[97]
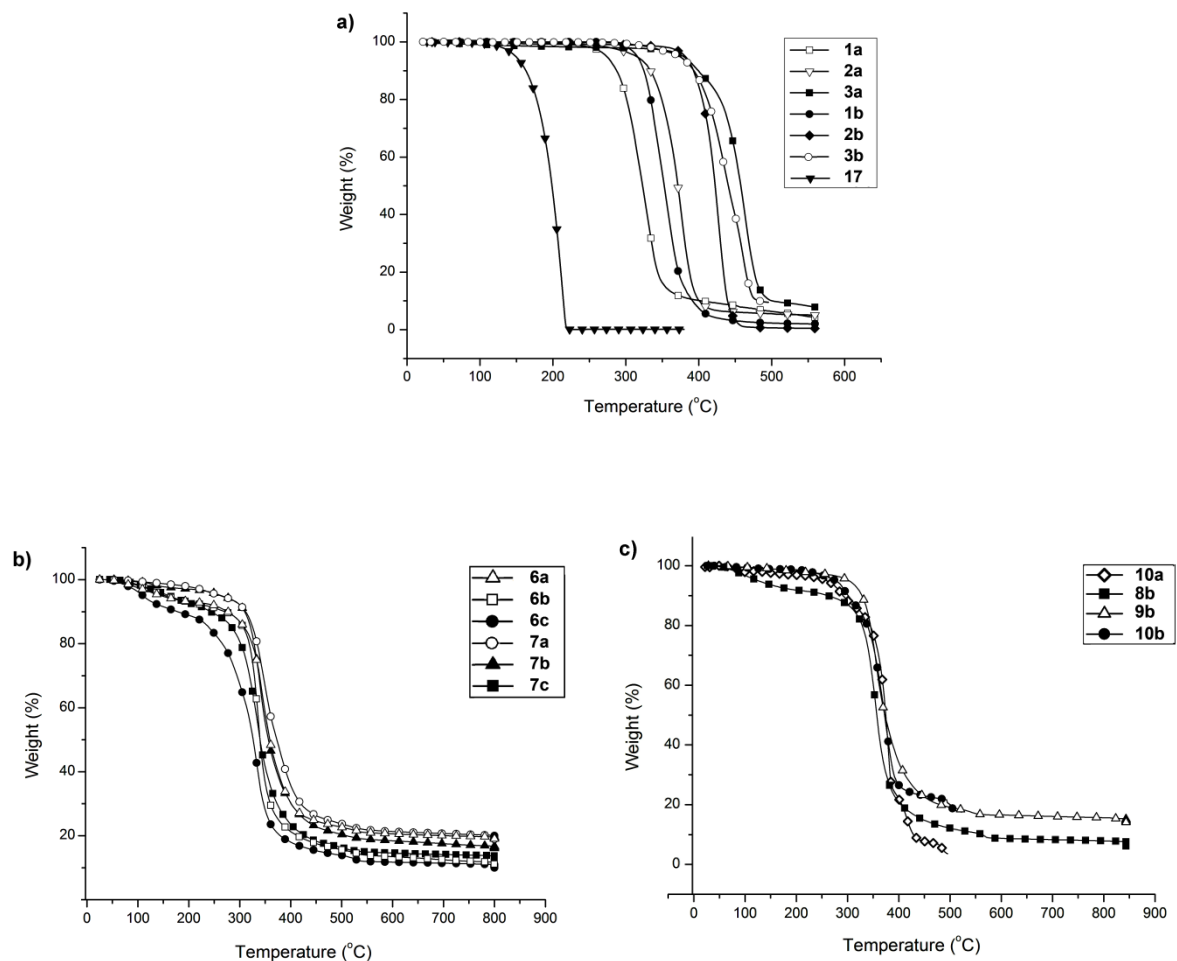

Figure 2.10. TGA results of the synthesized ionic liquids. **a) TEGILs**; **b) HEXILs**; **c) PEGILs**.

Figure 2.10 illustrates the TGA plots of all **TEGILs** where the structure of the linkage is identical and cations and anions are divergent. The results clearly reveal the strong dependence of the thermal stability values on the structure of the attributed anions. Expectedly ionic liquids containing bistriflimide counterion (**3a**, **3b**) demonstrated higher thermal stability where Cl⁻ (**1a**, **1b**) and MsO⁻

(**2a**, **2b**) decomposed at lower temperature. In the case of the cation effect, beside the distinctive higher thermal stability of pyrrolidinium chloride (**2a**, **2b**), a closer study of TGA graphs confirmed that the actual decomposition temperature, where the weight loss begins, was also slightly higher in the case of pirrolydinum ILs comparing to imidazolium analogous which was in agreement with results obtained from the literature.[96,221-222] TGA results of **HEXILs** which are represented in Figure 2.10 (**b**) show a decomposition temperature in the range of 290-315 °C. In general, there was a slight decrease in the thermal stability which can be due to slight increase in the length of the spacer. Introducing triazole ring did not seem to have a strong influence on this decline as it has a stable structure. Similarly, pyrrolidinium-ILs (**6b**, **7b**) demonstrated higher thermal resistance while there was no significant effect of the anions is observed.

Table 2.3. Thermal analysis results of all synthesized **TEGILs**,.**HEXILs**, **PEGILs**.

entry	product	-R$^+$	A$^-$	n	T_g (°C)	T_m (°C)	T_d (°C)
1	**1a**	MIM	Cl$^-$	3	-18	-	293
2	**1b**	MPy	Cl$^-$	3	-32	-	400
3	**2a**	MIM	MsO$^-$	3	-34	-	346
4	**2b**	MPy	MsO$^-$	3	-43	-	324
5	**3a**	MIM	Tf$_2$N$^-$	3	-52	-	431
6	**3b**	MPy	Tf$_2$N$^-$	3	-67	-	403
7	**6a**	MIM	MsO$^-$	5	-5	-	305
8	**6b**	MPy	MsO$^-$	5	-14	-	318
9	**6c**	TEA	MsO$^-$	5	-15	-	290
10	**7a**	MIM	TsO$^-$	5	-6	-	313
11	**7b**	MPy	TsO$^-$	5	-5	-	320
12	**7c**	TEA	TsO$^-$	5	-6	-	297
13	**8b**	MPy	MsO$^-$	8	-7	-	315
14	**9b**	MPy	TsO$^-$	8	-8	-	308
15	**10a**	MIM	MsO$^-$	33	-41	30	345
16	**10b**	MPy	MsO$^-$	33	-30	38	310

The DSC results of all synthesized **ILs** are summarized in Table 2.3. According to the results the glass transition temperature of the **ILs** is in the range of -67 °C up to -5 °C. **TEGILs** exhibited significantly lower T_g values (-67 °C up to -18 °C) in comparison with analogous oligomers bearing triazole ring (-15 up to -5 C). Moreover, **PEGILs** (**10a**, **10b**) demonstrated a melting point around 30-40 °C and lower T_g (-41 and -30 °C) comparing to **TEGILs** and **HEXILs**.

2.1.4. Tribological analysis of the synthesized PEGILs

In recent decades, ionic liquids, due to their high thermal stability, negligible volatility, none flammability, low melting point, broad liquid range, and miscibility with organic compounds, as well as other physicochemical and environmental characteristics received a significant attention in the field of tribology.[227-233] Ionic liquids in the field of tribology can be employed either as base oils,[232-234] additives[235-238] or as a thin films.[239-243] Accordingly, variety of structures were designed and synthesized and their tribological performances were investigated.[228] Meanwhile, investigation on dicationic ionic liquids revealed the higher capability of such materials as lubricant in comparison with their asymmetrical mono-valent analogous.[92,244] Additionally, the presence of polyether chain in the ionic liquid structure resulted in improved tribological performance.[95,226] Hence, it was worthwhile to evaluate tribological behavior of the all synthesized poly(ethylene glycol) based ionic liquids regarding the anion, the cation, and polymer chain length effects. The materials were studied as neat lubricants and additives for synthetic base oil using a Schwing–Reib–Verschleiss (SRV) tribometer with reciprocating ball-on-disc configuration. The tribological behavior of the products were evaluated at 50 °C, 100 °C, and 150 °C by measuring the friction coefficient and wear. This research was performed in tribology laboratories of Fundacion TEKNIKER, Eibar, in Spain and Austrian centre of competence for tribology (AC^{2}T) research GmbH, Wiener Neustadt, in Austria. The result of this work is published elsewhere[245], in detail. The major findings obtained from this research can be concluded as following:

The tribological performance of **PEGILs** was investigated on steel–steel surface. Friction and wear reduction in the presence of neat IL, depends on both anion and chain length of the poly(ethylene glycol). According to the results demonstrated in Figure 2.11, the longer chain yielded to better tribological behavior. Hence, the synthesized dicationic **PEGILs**, exhibited reasonable performance as potentials lubricant, even without additives. In particular, **10a** and **10b** demonstrated significant

reduction of the friction at higher temperatures while their measured wear formation was among the lowest (Figure 2.11).
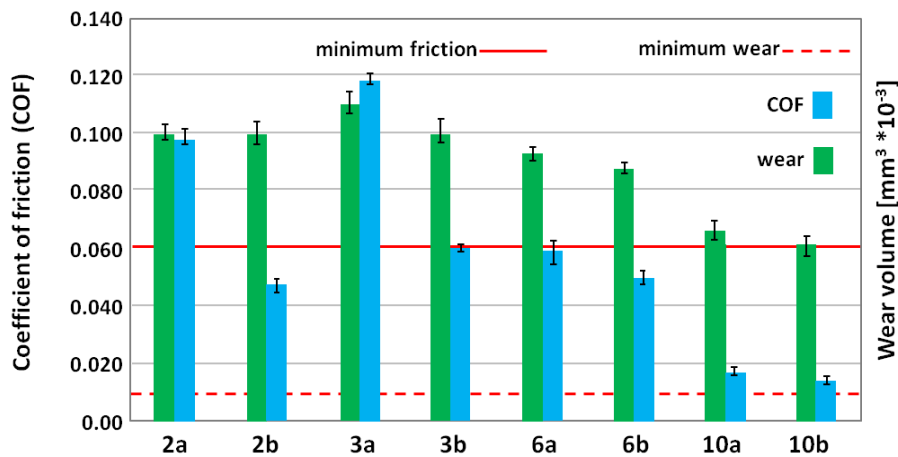

Figure 2.11. Friction and wear results of neat ionic liquids **2a**, **2b**, **3a**, **3b**, **6a**, **6b**, **10a**, and **10b** measured on steel-steel surface at 150 °C.[245]
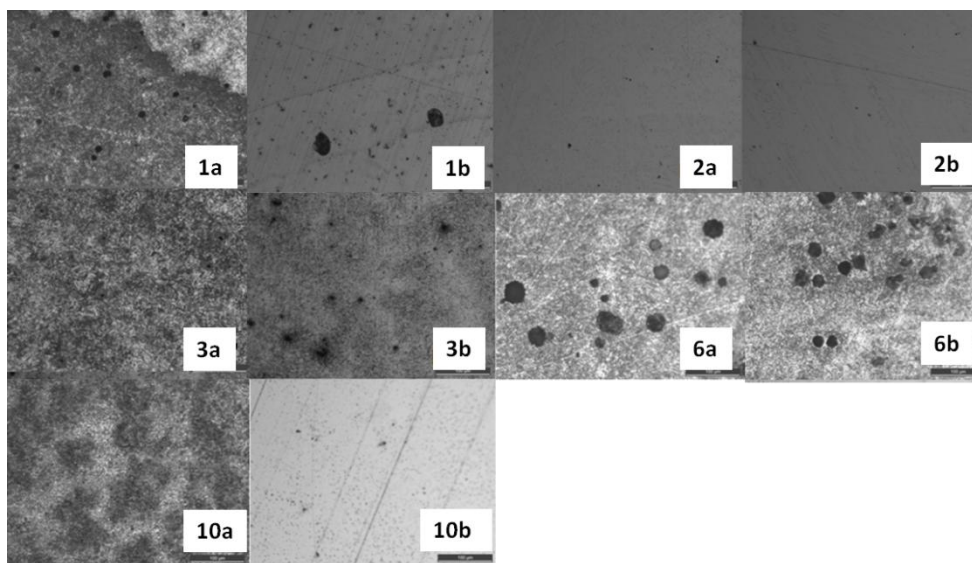

Figure 2.12. Surfaces of SRV discs after exposure to the neat ionic liquids **1-3 a**, **1-3b**, **6a**, **6b**, **10a**, and **10b**. All images obtained with an optical microscope have a width of 400 mm.[245]

For corrosion experiment, the degradation of the steel surface in contact with a drop of synthesized ionic liquids at 100 °C, after 7, was investigated. Figure 2.12 exhibited the contact surface of the steel disk after the experiment. According to the results, the longer chain regardless of its attachment to

the cation or the anion exhibited corrosion inhibiting properties. As an additive, there was an improvement in tribological performance of mixture of Synalox™ as the base oil and 1% (w/w) of **3a**. However, the corrosion caused by ILs is still one of the major issues which need to be solved via appropriate design of the structure of the ionic liquid.

2.2. Poly(isobutylene)-based ionic liquids (PIBILs)

2.2.1. Synthesis of azido- functionalized PIB (27)

Synthesis of poly(isobutylene) can be achieved via carbocationic polymerization.[246] The developments in the polymerization techniques resulted in attainment of highly controlled and precise macromolecules via so called "living polymerization".[247] In this regard, owing to the significant features of living polymerization, isobutylene (IB) was successfully polymerized via living carbocationic polymerization (LCCP) of the monomer, in the presence of 2-chloro-2,4,4-trimethyl-1-pentyl chloride (TMPCl) as initiator associated with $TiCl_4$ as co-initiator.[248] The polymerization was quenched with allyltrimethylsilane (ATMS) following the procedure described in the literature, which introduced the alkyne group to the polymer chain ends as initial functional groups for further post-polymerization modifications (Scheme 2.6).[248]
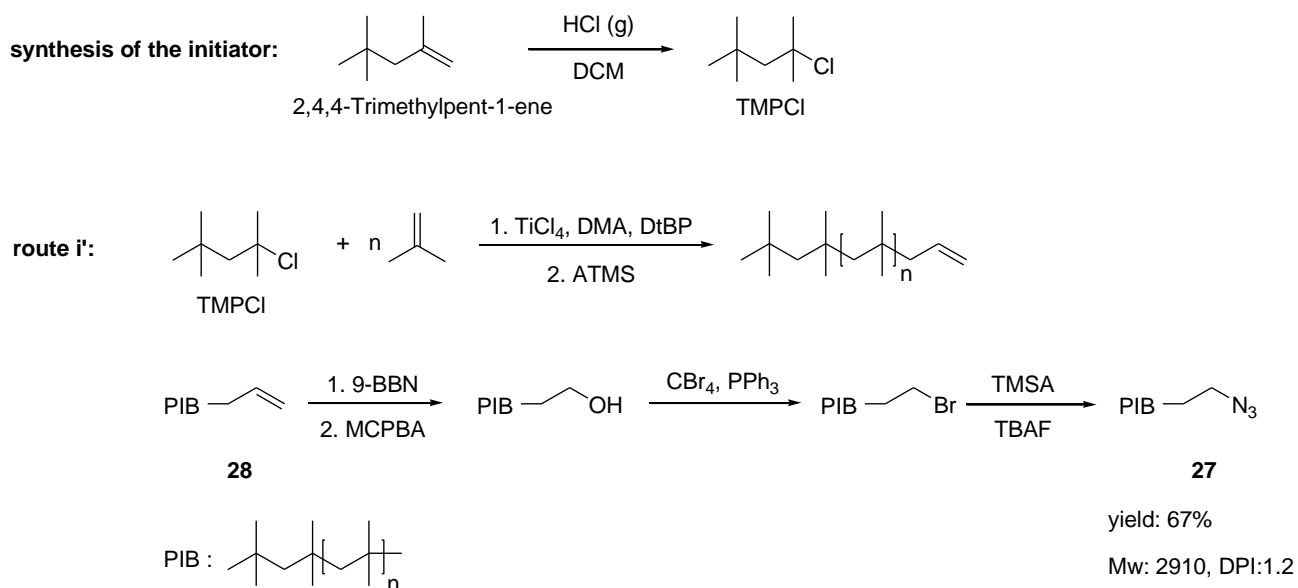
Scheme 2.6. Synthesis of **PIB-N₃** via LCCP, ATMS quenching, and further modifications (route **i'**).

2.2.2. Synthesis of azido- functionalized PIB (29, 30)

The synthesized PIB (**28**) bearing alkyne end group must be converted to the azide moiety which was achieved via hydroboration/oxidation to introduce an OH group and subsequent substitution reaction to replace it with -Br and then -N₃.[249-250] Thus, PIB containing azido end group (**27**) was

obtained with a narrow polydispersity (PDI) and an overall yield of 67% after a chain of modification reactions as shown in Scheme 2.6.[251] Meanwhile, the alkyne moiety was introduced to the selected amines by substitution reaction of propargyl bromide and corresponding amines under a moderate condition as described in the literature.[212]

Synthesis of **PIB-N$_3$ (27)** via subsequent modification of the alkene moiety introduced by ATMS quenching agent, despite the efficiency of the quenching step and reasonable yield of the final product costs a lot of time, chemicals, and efforts due to sequential steps. Owing to the work of Storey[252] using 3-(bromopropoxy)benzene (BPB), as quenching agent, during LCCP of IB can result in high yield of azido- functionalized PIB in a very short time by reducing the steps from five to only two steps. The termination of the polymerization of IB with BPB results in direct insertion of a bromo-group by attaching 4-(3-bromopropoxy)benzyl group. Further modification of this product can be simply performed via substitution reaction in the presence of sodium azide to achieve the desired azido- functionalized PIB.[253] Thus, two series of telechelic PIB (**29**, **30**) with low and high molecular weights were synthesized following the above mentioned pathway (Scheme 2.7).
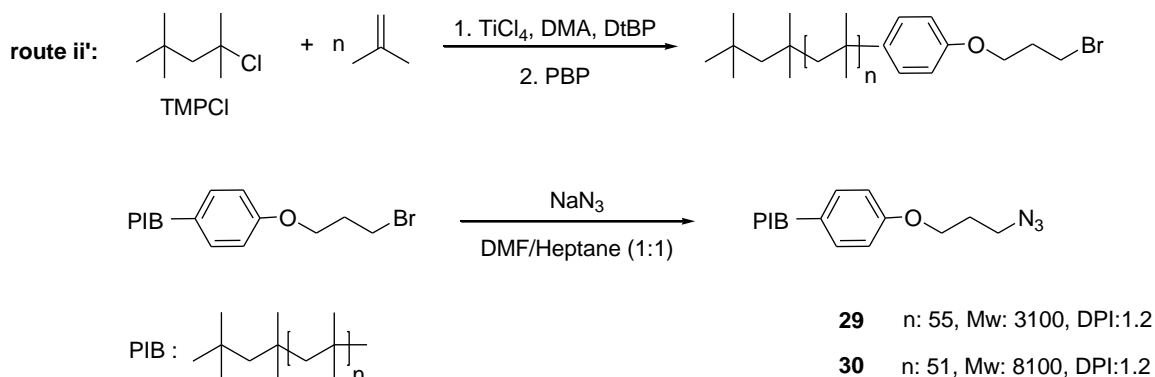

Scheme 2.8. Synthesis of **PIB-N$_3$ (29, 30)** via LCCP, BPB quenching, and further modification (route **ii'**).

2.2.3. Synthesis of PIBILs 11a-c

PIBILs 11a-c were synthesized via microwave irradiation of the solution of **PIB-N$_3$ (27)** and corresponding propargyl (**26a-c**) which was synthesized according to the procedure described elsewhere,[254] in the presence of DIPEA as N-base and copper catalyst, where oxygen was eliminated. Several experiments were conducted in order to determine the optimized condition of the click reaction (see Appendix A27). According to the results, among all three copper catalysts which have

been used CuI, was the best choice of the catalyst. The click reaction in the presence of CuI was reached to the conversion level of 86% while Cu(PPh₃)Br resulted in only 30% and CuBr lead to none. Additionally, moderated reaction condition referring to microwave irradiation criteria (power, time, temperature) was selected to obtain the maximum efficiency.
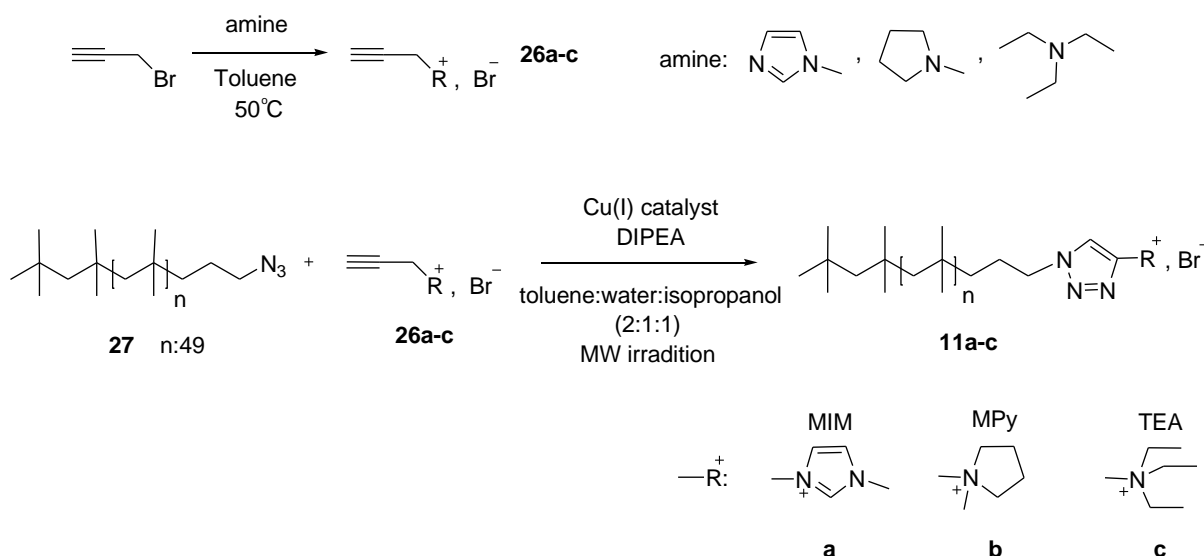
Scheme 2.8. Synthesis of **PIBILs (11a-c)** via click reaction (route **iv'**).

PIBILs **11a**, **11b**, and **11c** were successfully synthesized according to the conditions described in Table 2.4. Despite the high conversion rate of the performed click reactions, the yield of the all three products were around 50% due to the partial loss of the product during the work up through column chromatography.

Table 2.4. The reaction condition and isolated yield of the synthesized **PIBILs 11a-c** via click reaction, in the presence of CuI as catalyst.

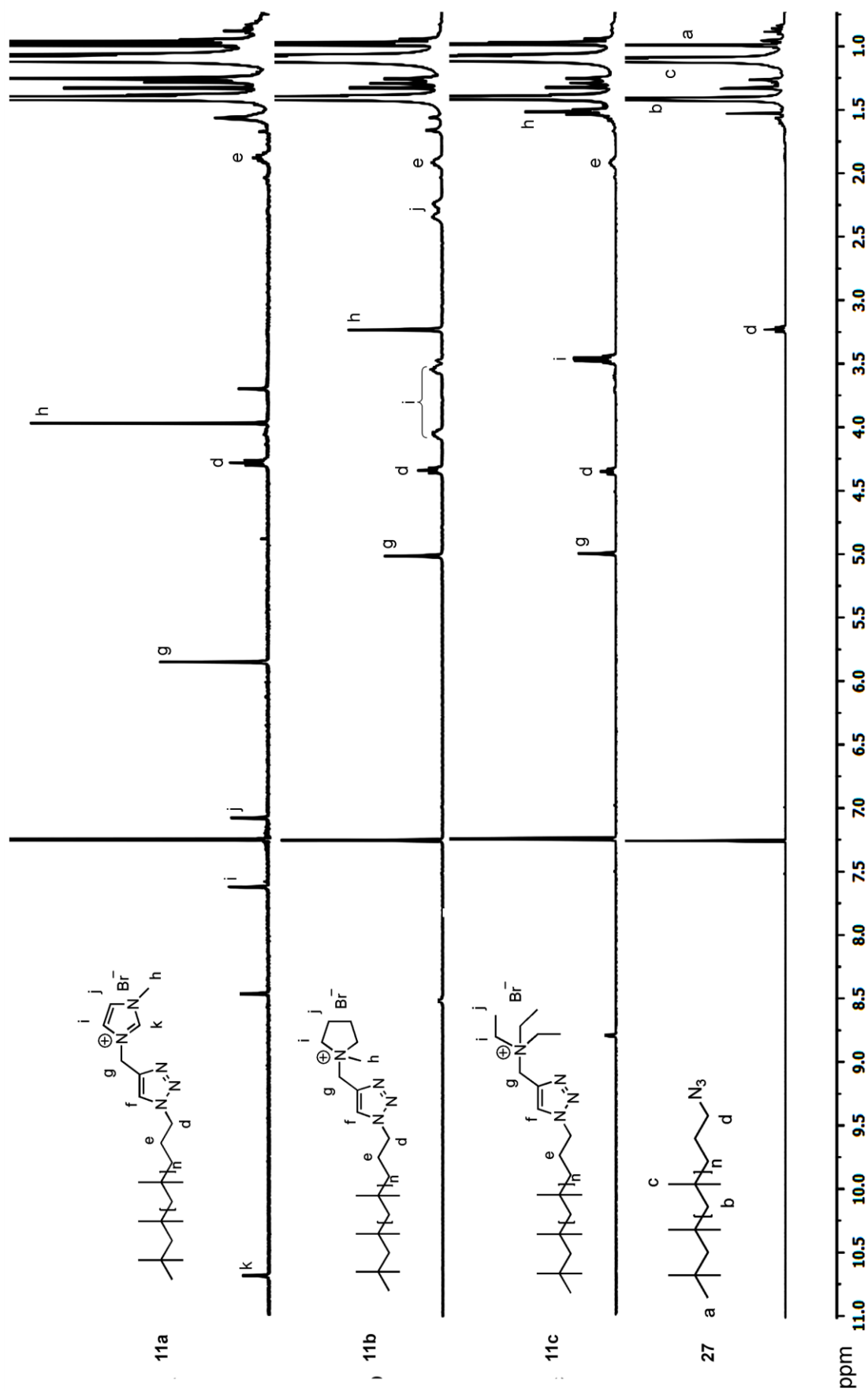| entry	product	-R⁺	A⁻	reaction condition power (W)/temp. (°C)/time (h)	M_n (g/mol)	(GPC)M_n (g/mol)	(NMR)PDI	Yield (%)
1	**11a**	MIM	Br⁻	75 W/75 °C/16 h	3256	3241	1.2	58
2	**11b**	MPy	Br⁻	75 W/75 °C/16 h	3259	3207	1.2	52
3	**11c**	TEA	Br⁻	70 W/75 °C/16 h	3334	4700	1.2	48

Figure 2.13. ^{1}H NMR spectra of **PIBILs 11a-c** in comparison with the corresponding **PIB-N$_3$·(27)**.

The accuracy of the chemical structure of the attained products (**11a-c**) was investigated via spectroscopic methods. Figure 2.13. illustrates the ^{1}H NMR spectra of three synthesized **PIBILs 11a-c** in comparison to **PIB-N$_3$ (29)**, as the initial polymer. The distinct singlet resonance of triazole ring emerged around 8.5-8.9 ppm associated with the corresponding resonances assigned for quaternary amine groups attached to the polymer prove the formation of the expected structures. The resonances of methylimidazolium in **11a** denoted as i, j, k, and h, all are well distinguished. The intensity ratio of the aromatic ring signals originated from three protons around the imidazolium are in accordance with the double intensity signal of the linkage between triazole and imidazolium rings, denoted as g, as well as the single proton signal of the triazole ring (denoted as f) itself. Similar results were observed after comparison of the specific signal intensities for **11b** and **11c**. Furthermore, the significant shift of the triplet resonance assigned to CH$_2$-N (denoted as d) from 3.2 ppm to around 4.5 ppm due to the formation of triazole ring is another evidence of constructed new structures. All these hints, along with complete vanishing of CH$_2$-N$_3$ resonance from 3.2 ppm and the perfect match between integration ratios of terminal CH$_2$ resonances from the polymer chain (d and e), proton from triazole ring (f), and attached amine resonances confirm the purity of the achieved products from any starting material or side products.

2.2.4. Synthesis of PIBILs 12a-c and 13a-c

PIB-N$_3$ (29, 30) which were synthesized via route **ii'** were reacted with propargyl derivatives of the corresponding amines (**26a-c**) via click reaction under similar circumstances as described earlier (Scheme 2.9). The yield and the conversion of both high and low molecular weight **PIBILs** are listed in Table 2.5.
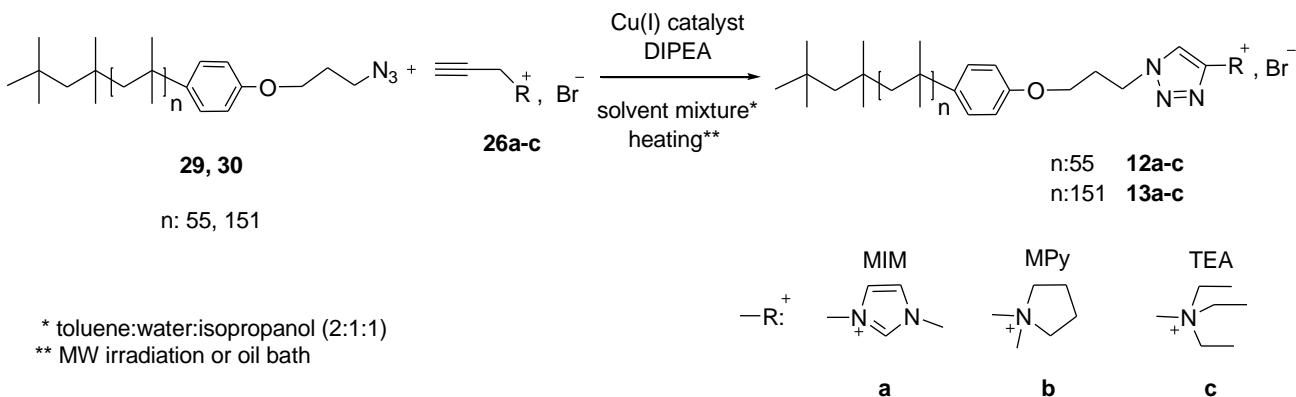
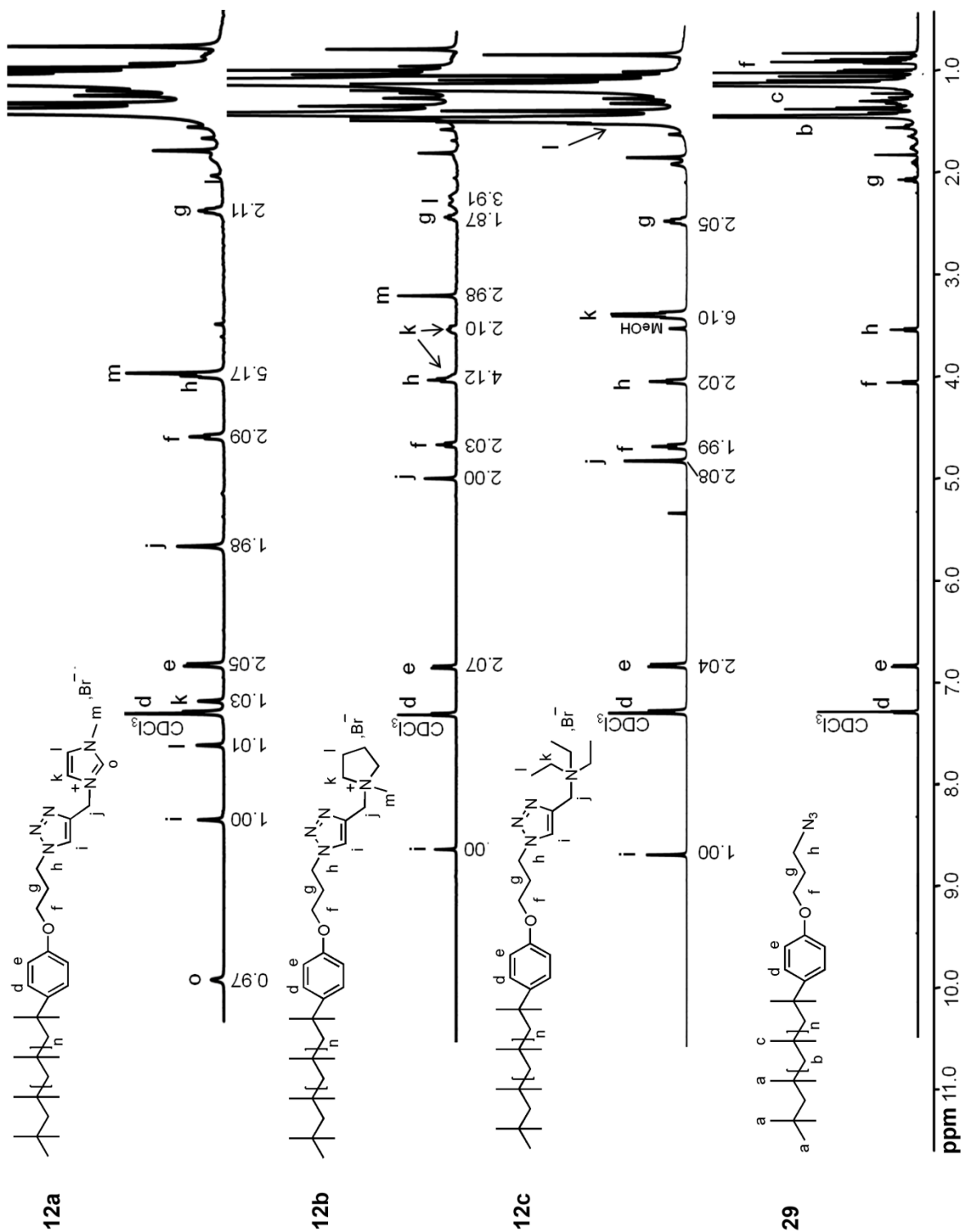**Scheme 2.9.** Synthesis of **PIBILs 12a-c** and **13 a-c** via click reaction (route **iii'**).

53

Figure 2.14. ^{1}H NMR spectra of **PIBILs 12a-c** in comparison with the corresponding **PIB-N₃-(29)**.

All of the synthesized **PIBILs 12a-c** and **13a-c** were characterized via ^{1}H and ^{13}C NMR. Figure 2.14 exhibits the ^{1}H NMR spectra of compounds **12a-c** in comparison to the azido-PIB (**29**) as starting material. Similar to previously synthesized **PIBILs 11a-c**, the resonance of the single proton of the triazole ring around 8 ppm is an assuring evident of the formation of the click products. Both triplet signals originated from terminal $-CH_2-$ groups of **PIB-N$_3$** (**29**), which are indicated as g and h (according to Figure 2.14) were shifted toward low fields due to transformation of $-N_3$ to triazole ring. Besides, all other detected resonances which were belonged to the corresponding ionic moieties are fully assigned. The coherency between the integration ratio of the critical resonance assigned to the inserted ionic moieties (k in the case of **12c** and k, l, m, and o for **12a** and **12b**) and terminal $-CH_2$ groups (indicated as f, g, and h) from the polymer chain plus comprehensive removal of the resonances dedicated to **PIB-N$_3$,** justifies the purity of the produced materials. Similar findings were deducted from ^{1}H and ^{13}C NMR of compounds **13a-c** (See Appendix A29-33)

Table 2.5. The reaction condition and the yield of the synthesized **PIBILs** (**12a-c** and **13a-c**) via click reaction, in the presence of CuI as catalyst.

entry	product	-R$^+$	A$^-$	reaction condition* power(W)/temp. (°C)/time(h)	M$_{n\,(GPC)}$ (g/mol)	M$_{n\,(NMR)}$ (g/mol)	PDI	Yield (%)
1	**12a**	MIM	Br$^-$	80 °C/96 h	3760	3449	1.3	51
2	**12b**	MPy	Br$^-$	80 °C/96 h	3280	3054	1.3	73
3	**12c**	TEA	Br$^-$	80 W/85 °C/16 h	3240	3142	1.3	82
4	**13a**	MIM	Br$^-$	80 °C/96 h	9500	9046	1.2	44
5	**13b**	MPy	Br$^-$	80 °C/96 h	8990	8421	1.2	58
6	**13c**	TEA	Br$^-$	80 W/85 °C/16 h	8860	7923	1.2	64

*The reactions were performed either via conventional heating (**12-13a,b**) or MW irradiation (**12c, 13c**).

2.2.5. Synthesis of PIBILs 14a-c and 15a-c via anion exchange reaction

Anion exchange is the main strategy toward generating variety of ionic liquids containing divergent anions which can be performed via a simple one step reaction of the already synthesized ionic liquid, with a proper choice of salt which generates the desired anion. To investigate the effect of large

anions with higher stability in comparison to weakly coordinating symmetrical bromide anion a series of **PIBILs** (**14a-c** and **15a-c**) bearing bistriflimide counteranion were synthesized via anion exchange of the previously synthesized **12a-c** and **13a-c** in the presence of lithium bistriflimide salt as shown in Scheme 2.10 (rote **iv'**). The results of this reaction are summarized in Table 2.6.
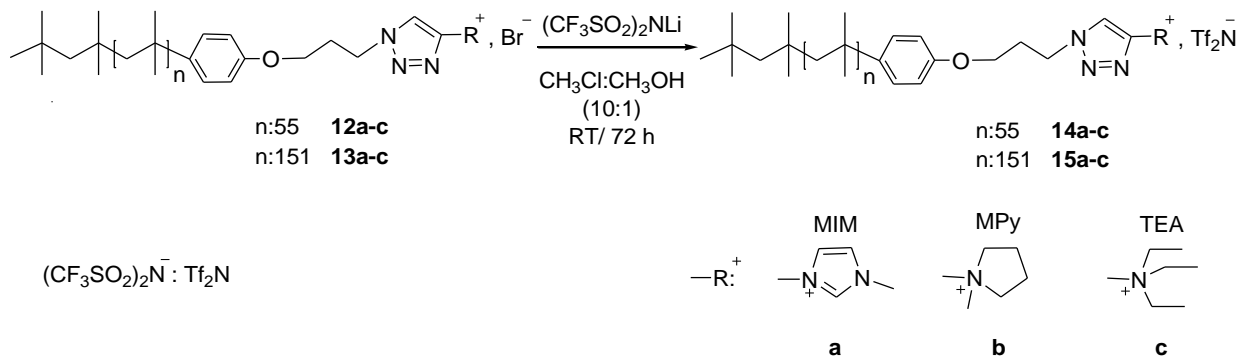
Scheme 2.10. Synthesis of **PIBILs** (**14a-c** and **15a-c**) via anion exchange reaction (route **iv'**).

After synthesis, **PIBILs 14a-c** and **15a-c** were characterized via ^{1}H, ^{13}C, ^{19}F NMR, and IR spectroscopy. The ^{1}H NMR spectra of the all synthesized products were almost identical with their bromo-containing analogous as there was no change in the structure of the primary ionic liquid. Besides, the exchanged anion did not contain a proton, therefore, there was no new signal introduced to the ^{1}H NMR spectra of the product. However, occurrence of the exchange was confirmed due to emerging a quartet resonance (indicated as t) as a result of C-F coupling in ^{13}C NMR spectra. Figure 2.15 represents the ^{13}C NMR spectra of the synthesized **PIBILs** (**14a-c** and **15a-c**) after anion exchange. Beside all other signals which were assigned to the corresponding carbon atoms in the body of polymer, cationic moiety, and triazole ring, there was a quartet resonance of ^{13}C-^{19}F coupling detected around 135 ppm with a very high J_{C-F} coupling constant as a proof of the exchange reaction. However, it was difficult to visualize the full quartet, as the side signals were too weak and one of them was overlapping with the neighboring signal from the phenyl ring of the polymer (denoted as f). Furthermore, the detected signal at 78.8 ppm in ^{19}F NMR spectra (see Appendix A35), as well as the appearance of several characteristic bands in the IR-spectra between 1350 cm^{-1}, 1058 cm^{-1}, 511 cm^{-1}, and 656 cm^{-1}, which were attributed to the presence of $(CF_3SO_2)_2N^-$ anion, as a result of the C–F stretching and bending vibrations of the trifluoromethyl groups (–CF$_3$) coincided the fulfillment of the anion exchange reaction (see Appendix A37-38).
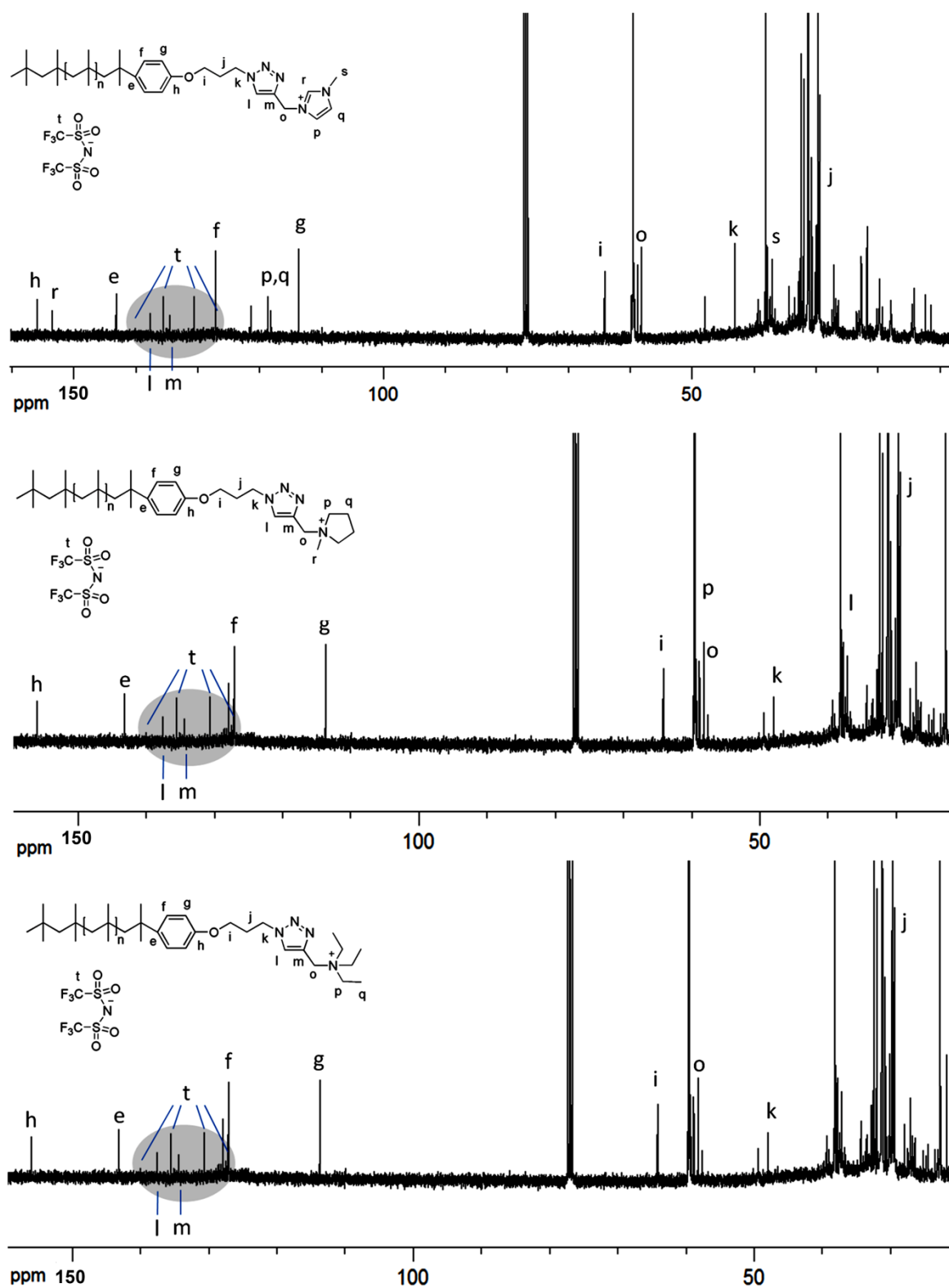
Figure 2.15. ^{13}C NMR spectra of synthesized **PIBILs** (**14a-c** and **15a-c**) via anion exchange.

Table 2.5. The reaction condition and the yield of the synthesized **PIBILs** (**14a-c** and **15 a-c**) via anion exchange reaction

entry	product	-R$^+$	A$^-$	reaction condition temp.(°C)/time (h)	M$_{n\,(GPC)}$ (g/mol)	M$_{n\,(NMR)}$ (g/mol)	PDI	yield (%)
1	**14a**	MIM	Tf$_2$N$^-$	RT/ 72 h	3670	3460	1.4	96
2	**14b**	MPy	Tf$_2$N$^-$	RT/ 72 h	3340	3403	1.4	95
3	**14c**	TEA	Tf$_2$N$^-$	RT/ 72 h	3180	3315	1.4	98
4	**15a**	MIM	Tf$_2$N$^-$	RT/ 72 h	8950	9326	1.4	93
5	**15b**	MPy	Tf$_2$N$^-$	RT/ 72 h	9240	9453	1.4	94
6	**15c**	TEA	Tf$_2$N$^-$	RT/ 72 h	8120	8321	1.4	98

2.2.6. MALDI analysis of synthesized PIBILs

Further investigations on the chemical structure of all synthesized **PIBILs** were carried out by means of MALDI-TOF-MS analysis. Figure 2.16 represents the MALDI-TOF-MS spectra of compounds **11a**. The spectra contains a single series of signals with the distance of 56.06 Da which stands for the molecular weight of the repeating unit of poly(isobutylene).
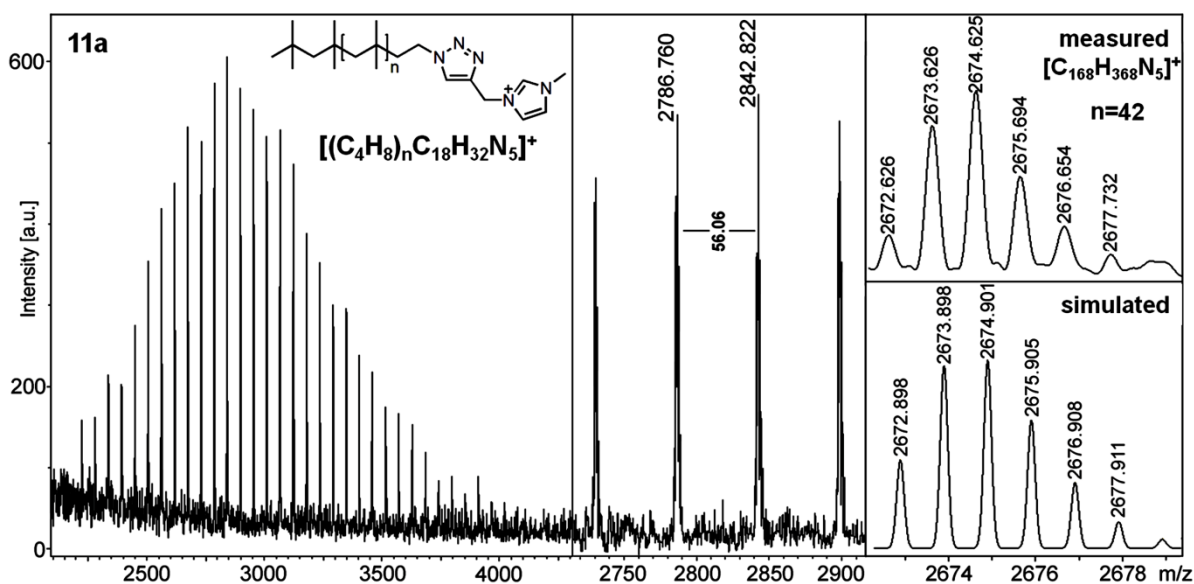
Figure 2.16. MALDI-TOF-MS sepectra of **11a**

Expansion of the selected signal at 2674.62 m/z is depicted in Figure 2.16 to compare it with the simulated isotopic pattern for the deducted structure. In this respect, the isotopic pattern was simulated for the possible polymeric structures. The comparison of the simulated pattern for $[(C_4H_6)_nC_{18}H_{32}N_5]^+$ was in agreement with the measured signal. Thus, the deducted structure was assigned to the synthesized polymeric ionic liquid bearing imidazolium cation (**11a**) after extraction of the bromide anion where n was 42.
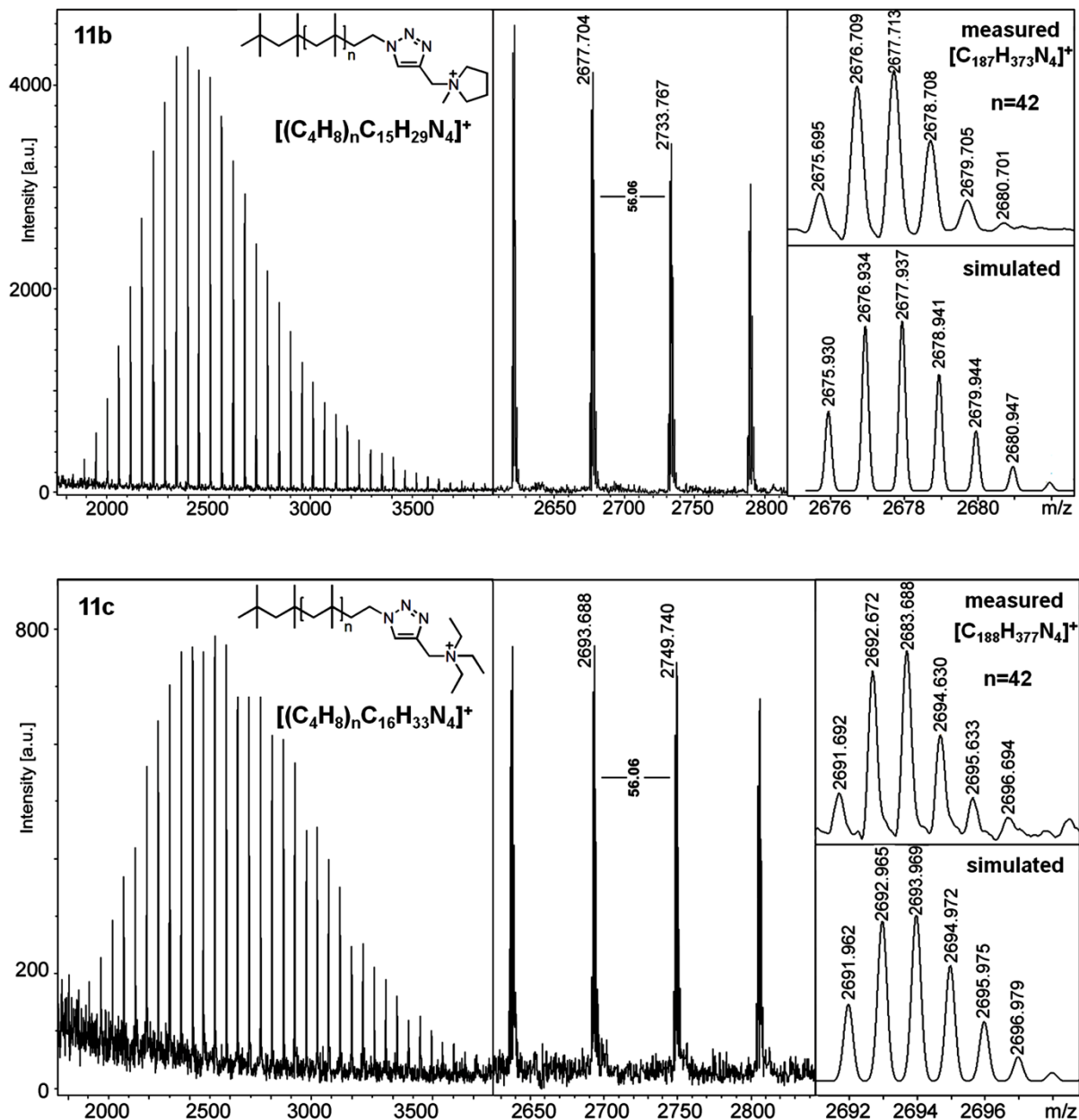
Figure 2.17. MALDI-TOF-MS spectra of **PIBILs** (**11b, 11c**)

Figure 2.17 represents the MALDI-TOF-MS spectra of compound **11b**. Similarly, there is only one main series of signals with the spacing of 56.06 Da, related to isobutylene repeating unit. The signal detected at 2677.71 m/z is selected as an exemplary to compare with the simulated pattern obtained for $[(C_4H_6)_nC_{19}H_{37}N_4]^+$. As shown in Figure 2.17 the simulated isotopic pattern is in accordance with the selected measured spectra which is designated for the structure of poly(isobutylene) bearing pyrrolidinium cation without the bromide counteranion (n=42).

Furthermore, similar result was observed for compound **11c**. As exhibited in Figure 2.17, the recorded spectrum is composed of series of signals appearing repeatedly with 56.06 Da of distances. The expanded signal detected at 2683.68 m/z was designated to $[(C_4H_6)_nC_{20}H_{41}N_4]^+$ which represents the polymeric ionic liquid **11c** while it contains no associating anion. Comparing the simulated isotopic pattern of the deducted formula coincide the accuracy of the assigned structure.
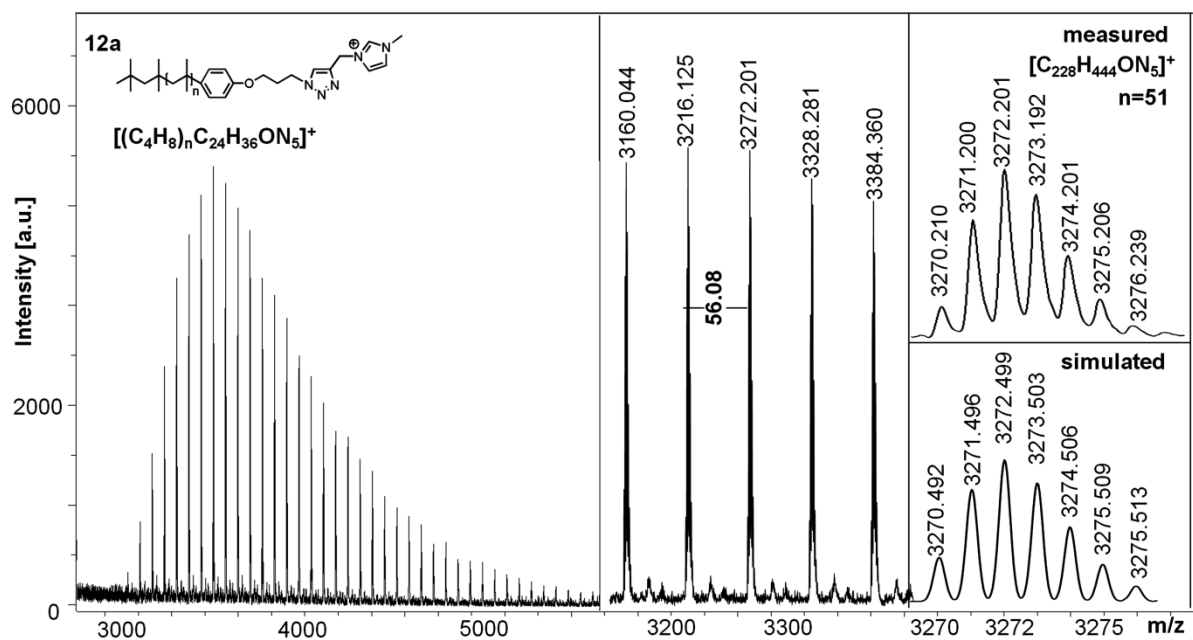
Figure 2.18. MALDI-TOF-MS spectra of **PIBILs 12a.**

Compounds **12a-c** were also subjected to MALD-TOF analysis. Likewise, the elaborative assignment of the signals was performed via comparison of a measured signal with the isotopic pattern of the simulated structure. Figure 2.18 represents the spectrum of compound **12a** which consists of a well pronounced single series corresponds to poly(isobutylene) derivatives. The comparison between the expansion of the selected signal which was recorded at 3272.20 m/z and the isotopic pattern

simulated for $[(C_4H_6)_nC_{24}H_{36}N_5]^+$ verified the presence of compound **12a** after elimination of the counteranion. Comparative results were observed in the case of **12b** and **12c** as shown in Figure 2.19. The detected minor series for **12b** were assigned to the structure of the synthesized ionic liquid after removal of one hydrogen atom.
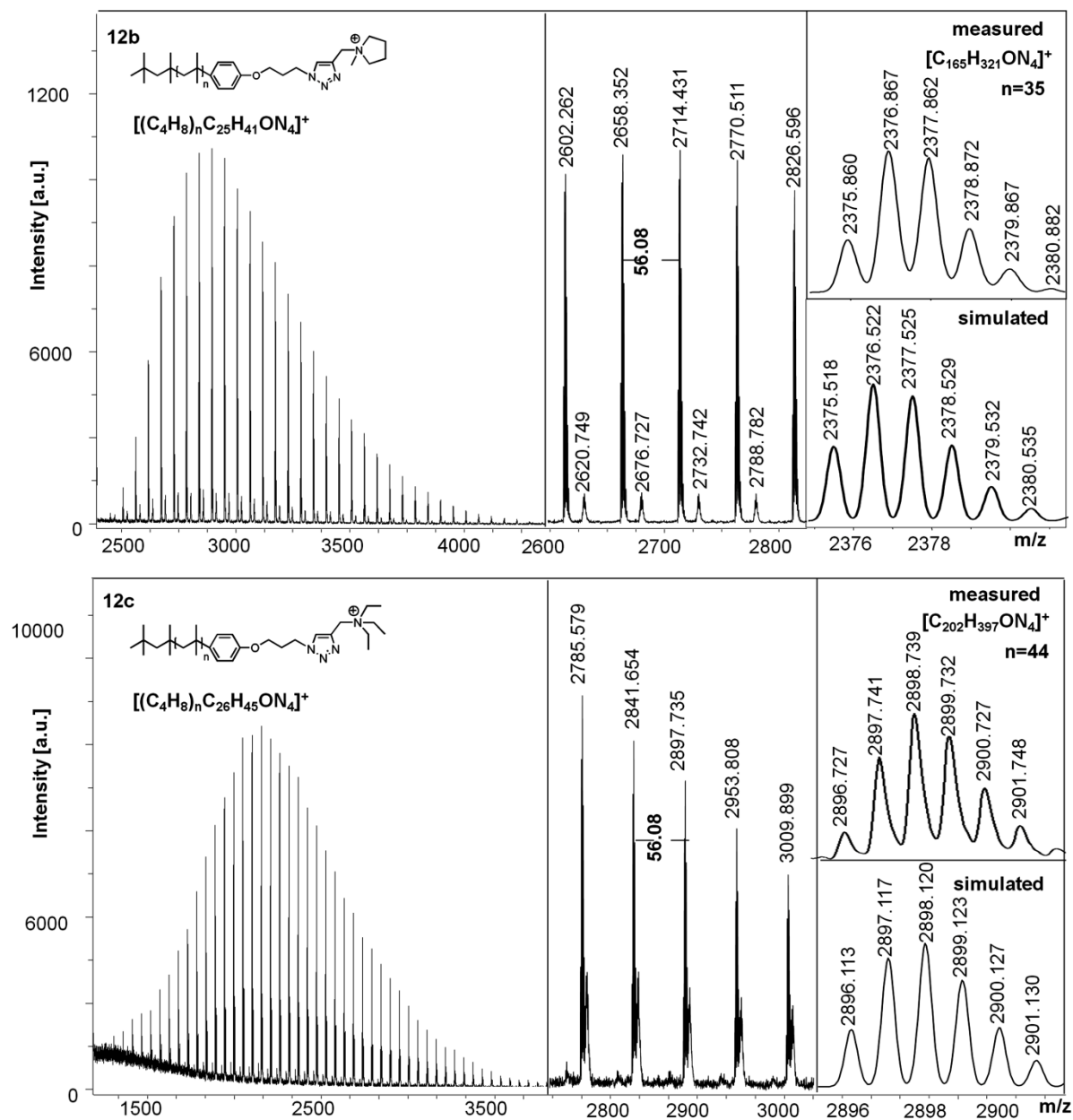

Figure 2.19. MALDI-TOF-MS spectrum of **PIBILs 12b**, **12c**.

MALDI-TOF-MS analysis on **PIBILs** bearing bistriflimide anion (**14a-c**) generated comparable pattern of signals. All three compounds exhibited only one distinct series with signal spacing of 56.06 Da, corresponds to the repeating unit of the acquired polymer.
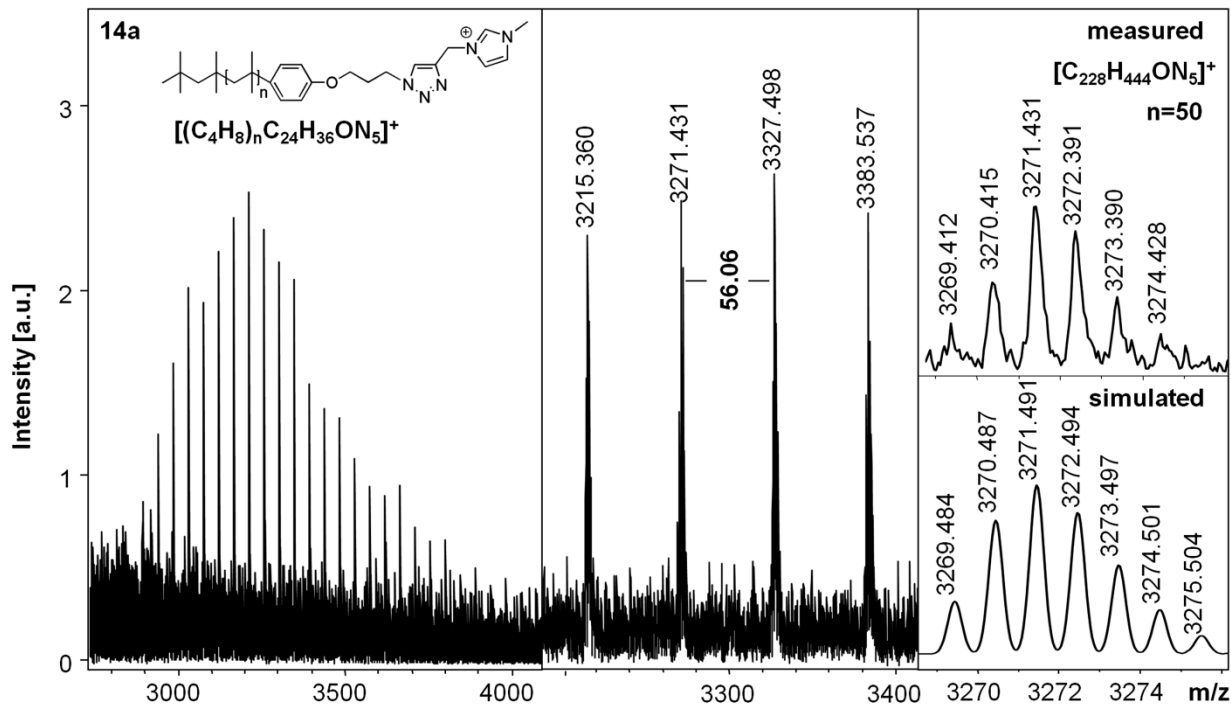
Figure 2.20. MALDI-TOF-MS spectra of **PIBILs 14a.**

Figure 2.20 represents the obtained spectrum from compound **14a**. The peak with the highest intensity at 3271 m/z was enlarged and compared to the theoretically calculated mass distribution of the corresponding ionic liquid without triflamide anion where the repeating unit was 50. The compatibility between the measured and simulated distribution which was formulated as $[(C_4H_6)_nC_{24}H_{36}N_5]^+$ confirmed the accuracy of the assignment.

MALDI-TOF-MS spectra obtained from compounds **14b** and **14c** are shown in Figure 2.21. In accordance with the simulated isotopic pattern, the selected peak with the highest intensity at 2657.78 m/z was precisely assigned to the poly(isobutylene) bearing pyrrolidinium moiety (n=39) which was formulated as $[(C_4H_6)_nC_{19}H_{37}N_4]^+$. Meanwhile, the resulted spectrum from **14c** was designated to the synthesized polymeric ionic liquid without associating anion. The consistency of the simulated distribution for the predicted structure which was formulated as $[(C_4H_6)_nC_{20}H_{41}N_4]^+$ for

62

n=25 with the highest intensity peak recorded at 1887.985 m/z confirmed the formation of the predicted structure.
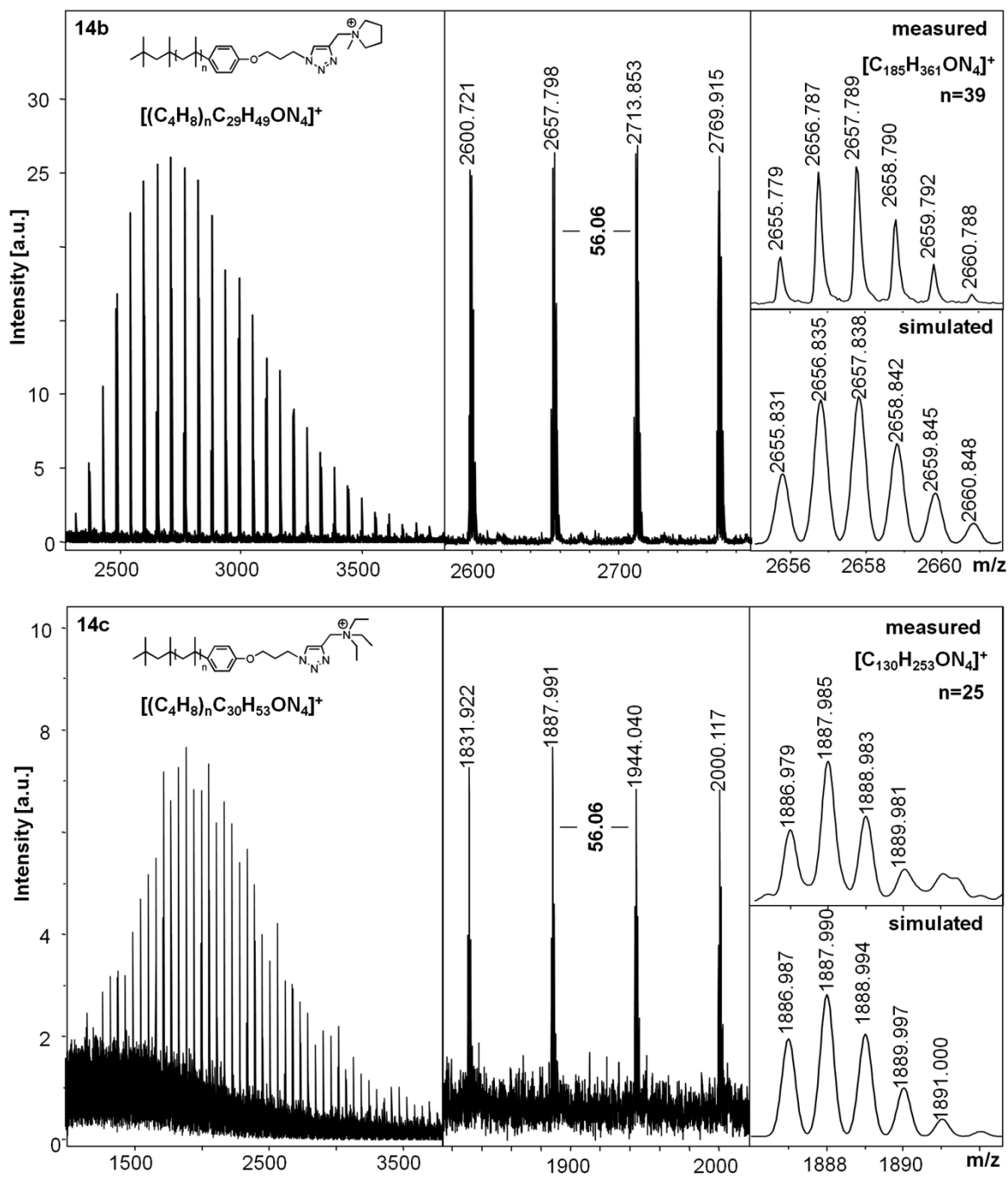

Figure 2.21. MALDI-TOF-MS spectra of **PIBILs 14b, 14c**.

MALDI-TOF-MS analysis on the synthesized **PIBILs 13a-c** and **15a-c** which contain the polymer with higher molecular weight (~8000 g/mol) resulted in broad peaks with low resolution. Thus, the characterization of these compounds was not possible via MALDI spectroscopy.

2.2.7. Thermal analysis of PIBILs

TGA measurement was conducted for all synthesized **PIBILs** to evaluate their thermal stability by determining their degradation temperature which has been reported as onset temperature. First series of **PIBILs** (**11a-c**) exhibited a one step degradation process with the onset temperature in the range of 310-398 °C which was higher in comparison to the primary **PIB** analogues. According to Figure 2.22, while **11a** exhibited the lowest thermal stability with a slight slope extending to higher temperatures, **11b**, and **11c** degraded in higher temperatures respectively, with a sharp drop in the slope of the degradation curves. The slight weight loss detected in the case of **11b** and **11c** was due to the presence of small amount of the solvent.[255-256]
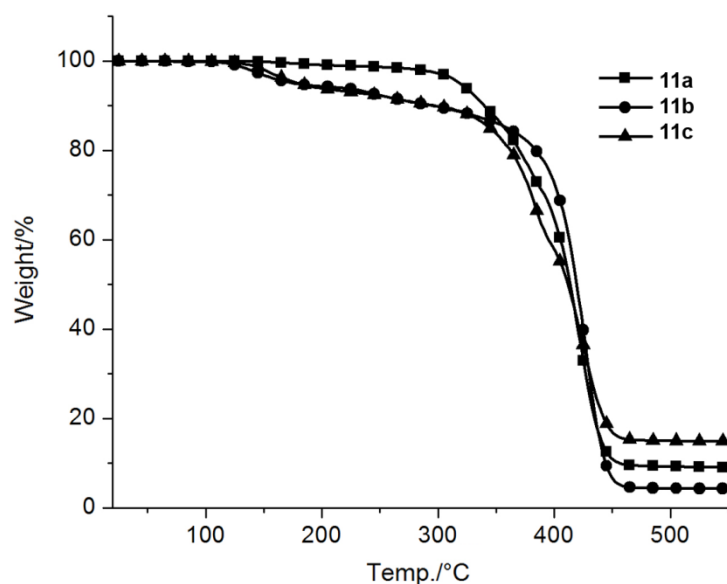

Figure 2.22. TGA results of **PIBILs** (**11a-c**)

The obtained results revealed the strong dependence of the thermal stability of the synthesized **PIBILs 11a-c** on the structure of the incorporated cation to the polymer chain end where the counteranions were identical. Further TGA analysis on the second series of **PIBILs** (**12-15a,b,c**) provided the possibility to investigate the effect of the anion and molecular weight in addition to the

structure of the cation. According to Figure 2.23, **12a-c** and **13a-c** exhibited two step degradation processes. Although the main weight loss occurred in the temperature range of 366 °C to 395 °C, there were slight weight losses around 120 °C- 200 °C which can be attributed to the loss of water molecules from highly hygroscopic ionic liquids.[145] In the case of higher molecular weight polymers, similar behavior was observed only for bistriflimide associating polymers emphasizing on its role as a hygroscopic molecule. Conclusively, the increase in the chain length of the polymer resulted in highly hydrophobic polymer body which resisted against hygroscopycity.
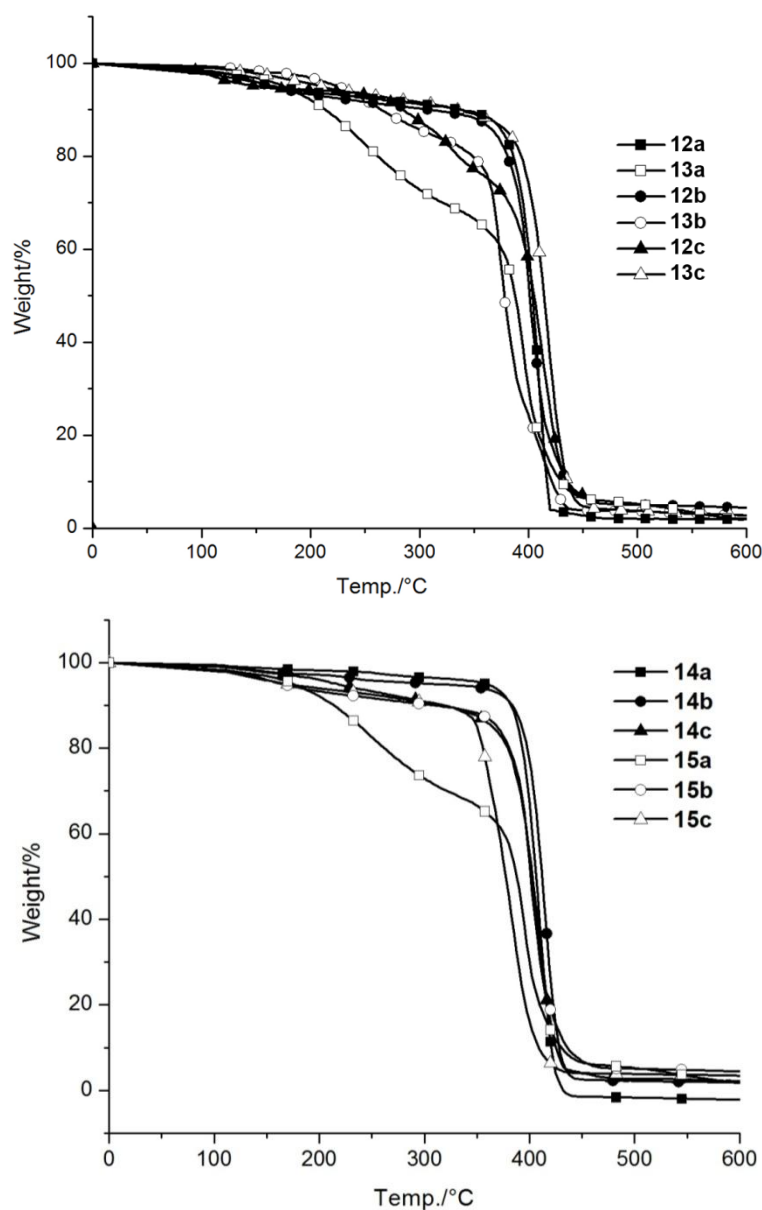

Figure 2.23. TGA results of **PIBILs** (**12a-c** and **13a-c**)

Comparing the degradation temperatures of the synthesized PIBILs, revealed the following points: In general, all synthesized **PIBILs** (**12-15a,b,c**) showed a higher thermal stability comparing to the previously synthesized **PIBILs 11a-c**, probably due to the insertion of phenoxypropyl group which can lead to π-π interactions. All three cations, regardless of the molecular weight and counteranion, exhibited comparable results. Exchanging the associating anion to bistriflimide did not influence degradation temperature significantly as it was for monomeric ionic liquids, though it resulted in a slight decrease in comparison to bromide anion.
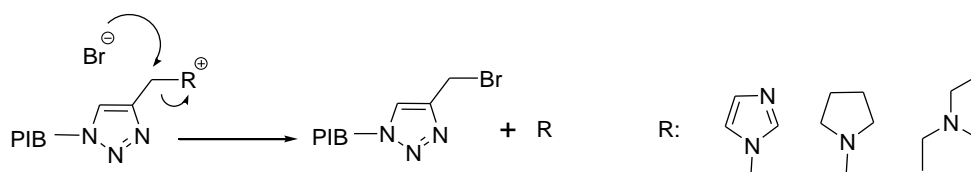
Scheme 2.11: Decomposition mechanism for POILs with nucleophilic bromide anion.

The probable mechanism of the degradation process for the synthesized **PIBILs** can be explained by dealkylation of the cationic moiety via highly nucleophilic bromide anion according to the proposed route which is described in the literature (scheme 2.11).[257] The characterization of the trace of a side product (see Appendix A36) which was retrieved from the reaction media during the synthesis of imidazolium based **PIBIL** (**12a**), supported the possibility of the degradation of all synthesized **PIBILs** (**11a-c**, **12a-c**, and **13a-c**) bearing bromide counteranion following the suggested mechanism. However, the decomposition of the **PIBILs** associated with bistriflimide anion can proceed via degradation of the anion by releasing SO_2 gas rather than dealkylation mechanism (Scheme 2.12).[258]
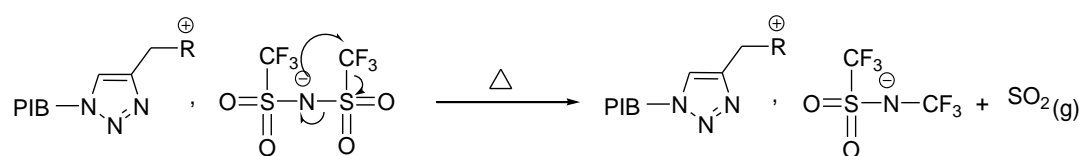
Scheme 2.12. Decomposition mechanism for POILs with non-nucleophilic bistriflimide anion.

All of the synthesized **PIBILs** were subjected to DSC measurement in the temperature range of -120 to 120 °C with a heating rate of 10 K/min to investigate their glass transition temperature (T_g). The transition temperature of the inflection point of the heating curve was reported as T_g.

Table 2.6. Thermal analysis results of the synthesized **PIBILs**

entry	product	-R$^+$	A$^-$	M$_{n(tho.)}$ (g/mol)	T$_{g1}$ (°C)	T$_{g2}$ (°C)	T$_{d1}$ (°C)	T$_{d2}$ (°C)
1	**11a**	MIM	Br$^-$	3000	-70.6	-	-	310
2	**11b**	MPy	Br$^-$	3000	-71.4	-	119	398
3	**11c**	TEA	Br$^-$	3000	-70.9	-	135	352
4	**12a**	MIM	Br$^-$	3000	-67.8	-	124	389
5	**12b**	MPy	Br$^-$	3000	-66.5	64.9	133	387
6	**12c**	TEA	Br$^-$	3000	-67.6	-	202	385
7	**13a**	MIM	Br$^-$	8000	-67.2	-	-	395
8	**13b**	MPy	Br$^-$	8000	-66.4	-	-	391
9	**13c**	TEA	Br$^-$	8000	-67.1	-	-	387
10	**14a**	MIM	Tf$_2$N$^-$	3000	-71.2	66.0	180	373
11	**14b**	MPy	Tf$_2$N$^-$	3000	-69.8	63.8	197	366
12	**14c**	TEA	Tf$_2$N$^-$	3000	-71.4	61.5	181	367
13	**15a**	MIM	Tf$_2$N$^-$	8000	-71.2	66.0	127	385
14	**15b**	MPy	Tf$_2$N$^-$	8000	-69.8	63.8	101	389
15	**15c**	TEA	Tf$_2$N$^-$	8000	-71.2	66.0	-	387

All synthesized samples exhibited a T$_g$ in the temperature range of -66 °C to -72 °C. According to the results (Table 2.6), introducing ionic species to the polymer structure resulted in a slight increase of T$_g$ in comparison to the unfunctionlized PIB. Furthermore, variation in the structure of the cation or chain length of the polymer did not lead to a significant difference in the T$_g$ value. However, all **PIBILs** bearing bistriflimide counteranion (**14a-c** and **15a-c**) and one of the bromides associating **PIBIL** (**12b**) demonstrated an additional T$_g$ in the range of +61.5 °C to +66 °C. It seems that, the formation of the aggregates which leads to the construction of the clusters with restricted mobility regions is the reason of appearance of the second T$_g$.[125-160] This can be an evidence of formation of highly ordered structures in the synthesized **PIBILs**.

2.2.8. Small angle X-ray scattering (SAXS) of PIBILs

In order to investigate morphological behavior of the synthesized **PIBILs**, all samples were examined via small angle X-ray scattering (SAXS). **PIBILs** are formed of an ionic head group covalently attached to a very hydrophobic polymer chain. The distinct polarity difference between the ionic head group and **PIB** chain can be the driving force for microphase separation. The occurrence of such phenomenon was reported for some polymeric ionic liquids in a similar way to ionomers.[28-29,39] Thus, EHM theory,[125] can be used to explain the formation of the nanostructural organizations in such polymeric systems via the new multiplet-cluster model.
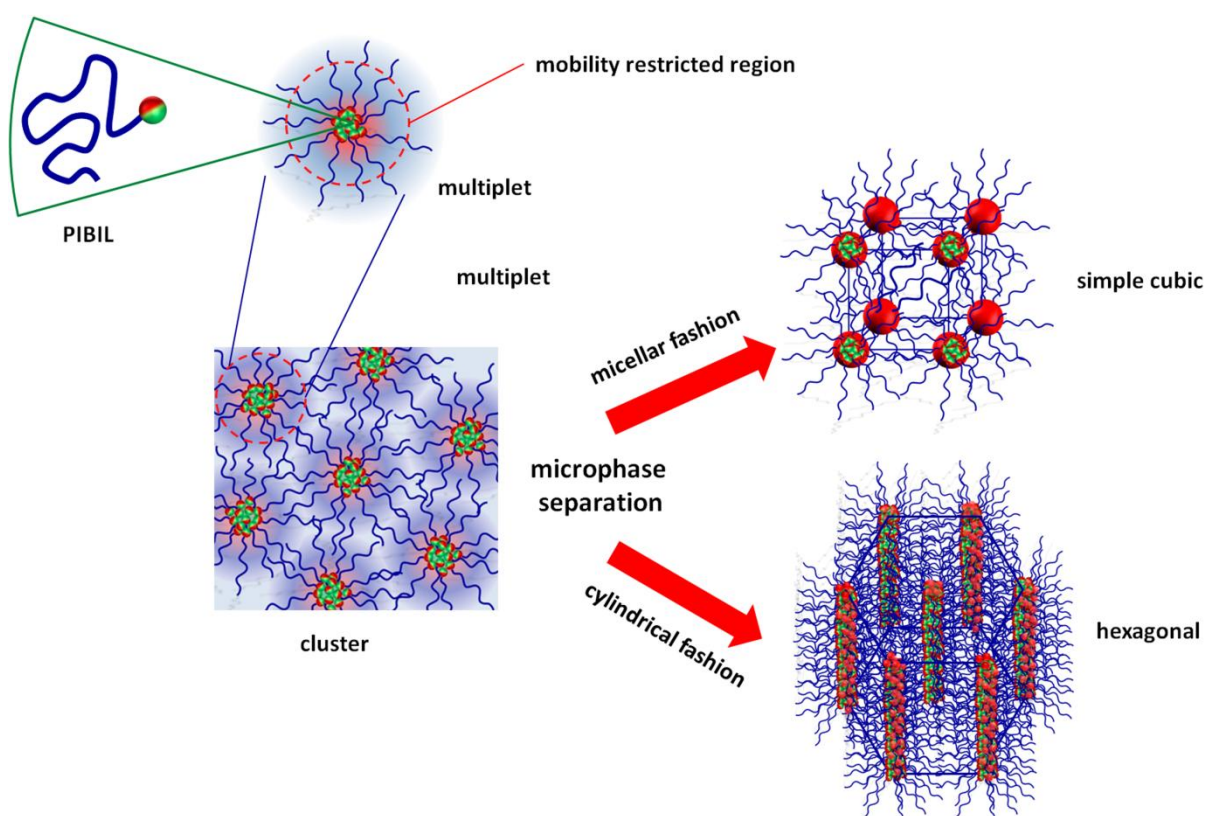
Figure 2.24. The schematic representation of the aggregation of **PIBILs** in the form of multiplet and cluster. The cluster can arrange itself in micellar or cylindrical fashions which can result in simple cubic or hexagonally packed cylindrical confinements.

As depicted in Figure 2.24, **PIBILs** construct "multiplets" due to aggregation of the ionic species as a result of electrostatic forces. The ionic head groups form a central spherical core and **PIB** chains stretch along with a mobility restricted area denoted as "skin". The electrostatic interactions

between the multiplets compel them to aggregate and form the clusters while, the repulsions from the polymer chains (the "skin") restrict the multiplets to approach each other. The mobility of the polymer chain surrounding the ionic core in the multiplets is significantly restrained. Hence, the distance between clusters is highly dependent on the size of this area. However, growing of the ion concentration in the central core of the multiplets reduces the average distance between them as a result of imbrications of the polymer chains from the outer shells of the adjacent multiplets. Thus, the multiplets become closer and their mobility restricted regions overlap and creates a larger area with restrained mobility due to clusterization.[125] Investigation on SAXS data obtained from the synthesized **PIBILs** not only proved the formation of multiplets but also showed a good agreement with the proposed model system.
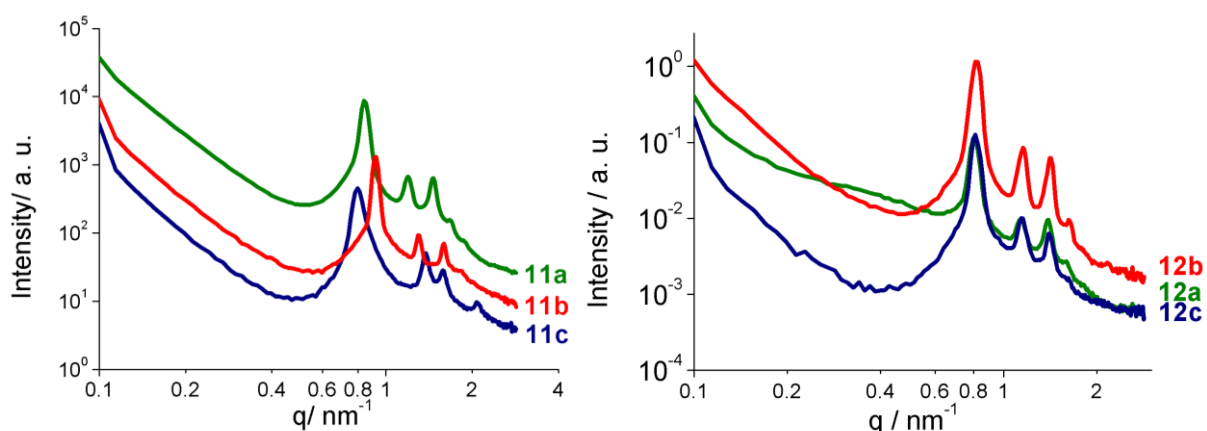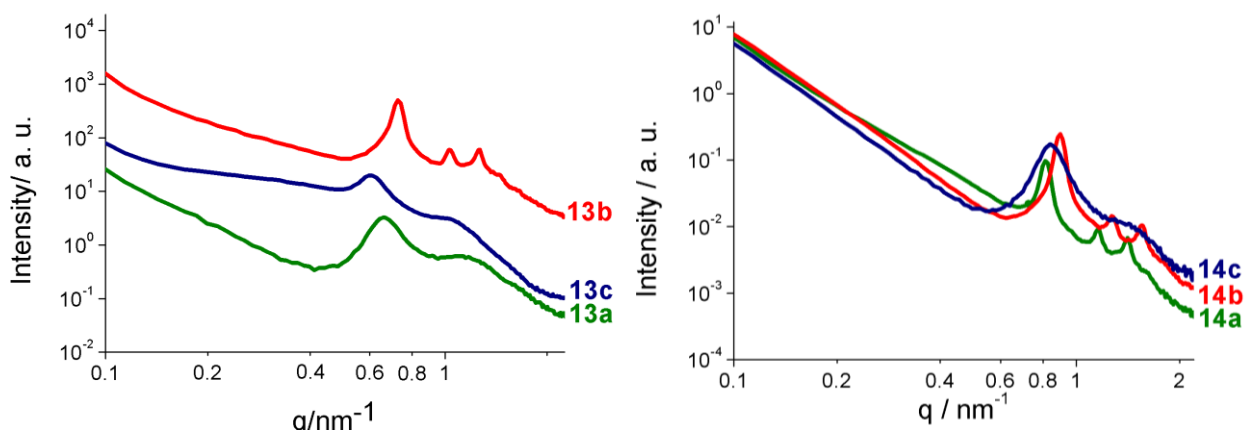

Figure 2.25. SAXS profile from **PIBILs 11a-c** and **12a-c**. For clarity, the peaks are shifted in the axis of intensity.

Figure 2.25 demonstrates the scattering profiles of **PIBILs 11a-c**. All three samples exhibited a distinct primary peak which was associated with multiple reflections verifying microphase separation in the structure. **11a** and **11b** both are identified with five reflections in the order of 1:√2:√3:2:√5 representing their arrangement in a simple cubic structure. Meaning, the multiplets in the form of micelles are arranged together to construct a simple cubic morphology (Figure 2.24). The domain spacings attained from the position of the primary peak reported for **11a** and **11b** as 7.6 nm and 6.9 nm, respectively. The scattering profile of **11c** exhibited four reflections in the order of 1:√2:2:√7 with a domain spacing of 7.95 nm which indicates the rearrangement of the multiplets in a cylindrical pattern to form a hexagonal geometry. Figure 2.25, also, represents the scattering profile of the second **PIBILs** series synthesized via route **ii'-iii'** which contains a phenoxy propyl group in the polymer chain. All three samples demonstrated a primary peak indicating the domain spacing of 7.7,

7.8, 7.9 nm and multiple reflections assigned for cubic morphology. Comparison of the results between these two **PIBILs** (**11a-c** and **12a-c**) series does not declare a significant diversity in the results for **11a** and **11b** in comparison with **12a** and **12b**, though, **11c** was the exception. It seems that the multiplets constructed from triethylammunium (**c**) end groups, had less restrained mobility compared to imidazolium (**a**) and pyrrolidinium (**b**). However, the insertion of phenyl group to the end of the polymer chain resulted in more restriction on the multiplets mobility of this compound (**12c**) as well.

Figure 2.26. SAXS profile from **PIBILs 13a-c**.and **14a-c**. For clarity, the peaks are shifted in the axis of intensity.

Further studies were performed to investigate the influence of the polymer chain length on the morphology of the products (Figure 2.26). Increasing the chain length in accordance with EHM theory[125] resulted in a shift of the primary pick to lower q values (nm^{-1}) due to expansion of the intermutiplet distances (domain size of 8.7-10 nm). These findings were in agreement with the observations for the influence of the alkyl chain length on the structural properties of ionic liquids.[259] Furthermore, besides the general broadening of the scattering peak the loss of the ordered structure was observed for **13a** and **13c** while **13b** still demonstrated a simple cubic confinement with d= 8.7 nm (See Figure 2.19.;a). However, the attained scattering results from **14b** revealed the collapse of the mesostructures in the same manner as a consequence of exchanging anion to Tf$_2$N$^-$.

Figure 2.26 illustrates the scattering profile of **PIBILs** containing Tf$_2$N$^-$ (**14a-c**) to investigate the influence of the counteranion on the morphology of the synthesized **PIBILs**. According to the results, excluding **14c**, there is no significant influence of anion observed on the morphology of the products. **14a** and **14b** both are arranged in the cubic structure with domain spacing of 7.7 and 7.0 nm,

respectively. **14c** in the other hand demonstrated two broad scattering peaks with a domain size of 7.95 nm. The absence of the further multiple reflections suggests a weakly ordered morphology due to increasing flexibility of the structure as a result of poorly coordinating Tf_2N^- counteranion similar to what was described in the literature for classical ionic liquids.[138,146,260-261]

2.2.9. Variable temperature in situ SAXS

According to EHM theory,[125] when the electrostatic forces between ion pairs are strong enough to overcome the elasticity of the anchored polymer they form multiplets and the polymer chains generate a surrounding with restrained mobility due to this opposing forces. Clusterization happens upon the decreasing distance between multiplets as a result of their certain ion content. However the stability of clusters can be restricted due to different factors such as temperature. Apparently heating the matrix higher than a certain temperature where the elastic forces from the polymer chains balance the electrostatic forces of ionic moieties will result in clusters to collapse and the order of the structure will vanish.[125] To investigate the influence of the temperature on the transition of the synthesized materials from order to order or order to disorder and inverse (if the transition is reversible) in situ SAXS measurement was performed in the range of 25 °C up to 300 °C.
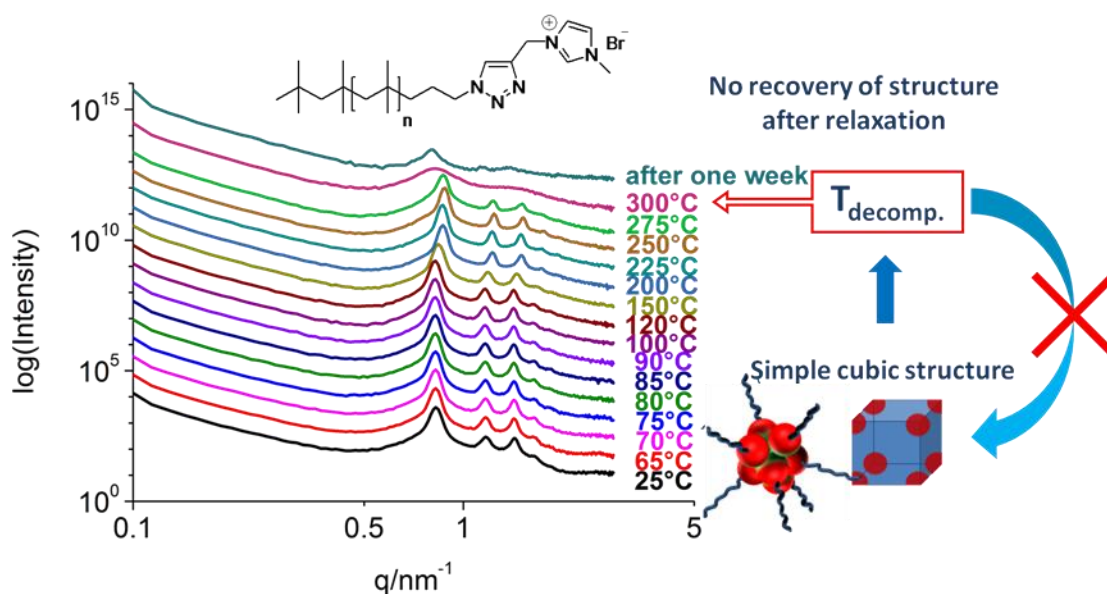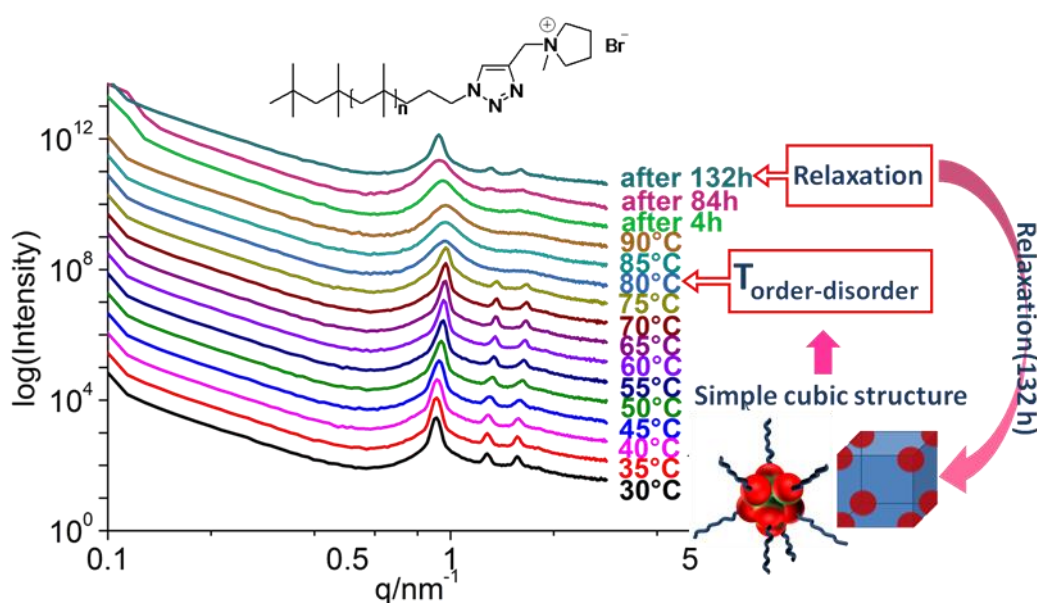

Figure 2.27. SAXS profiles of compound **11a** at different temperatures and after relaxation. The curves are shifted in the intensity axis (y-axis) for clarity.

Figure 2.27 illustrates SAXS profile of **11a** at different temperatures. According to the results, **11a** demonstrates a significant stability against heating up to high temperatures. At 275 °C due to partial loss of the ordered structure the two high order scattering peaks at the higher q values were vanished. Apparently the strong electrostatic interactions originated from π-π stacking of the imidazolium rings in the multiplets resulted in such a distinct strength in the structure of the clusters and co-existing multiplets. The transition from ordered to disordered state was recorded at 300 °C proved by broadening of the primary scattering peak which was due to the decomposition of the product (similar to result obtained from TGA) as the structure was not recovered even one week after cooling down at room temperature.

Figure 2.28. SAXS profiles of compound **11b** at different temperatures and after relaxation. The curves are shifted in the intensity axis (y-axis) for clarity.

Figure 2.28 represents the temperature dependent in situ SAXS measurements of compound **11b**. According to the picture the loss of the ordered structure was detected at 80 °C with broadening of the primary peak and disappearance of the multiple reflections as a result of lattice disorder-order (LDOT) process.[262] As the temperature was increased, due to the gradual weakening of the electrostatic force, the clusters were ruptured. The disruption of the cluster into multiplets resulted in enhanced mobility of the polymer, leading to a shift and broadening of the main peak. Further increasing of the temperature up to complete loss of the multiplets resulted in a homogeneous liquid like state. Such transition was termed as demicellization/micellization transition (DMT) and T_{DMT} was

72

referred to the temperature at which the transition occurred.[262] However, the ordered structure was reestablished 132 hours after cooling down the material to room temperature which was comparable to the relaxation time of to 7 days, reported for some ionomers.[263] The observed attitudes of the synthesized polymeric ionic liquid (**11b**) implied the development of self-healing behavior in the obtained product similar to some classic ionomers. [263-265]
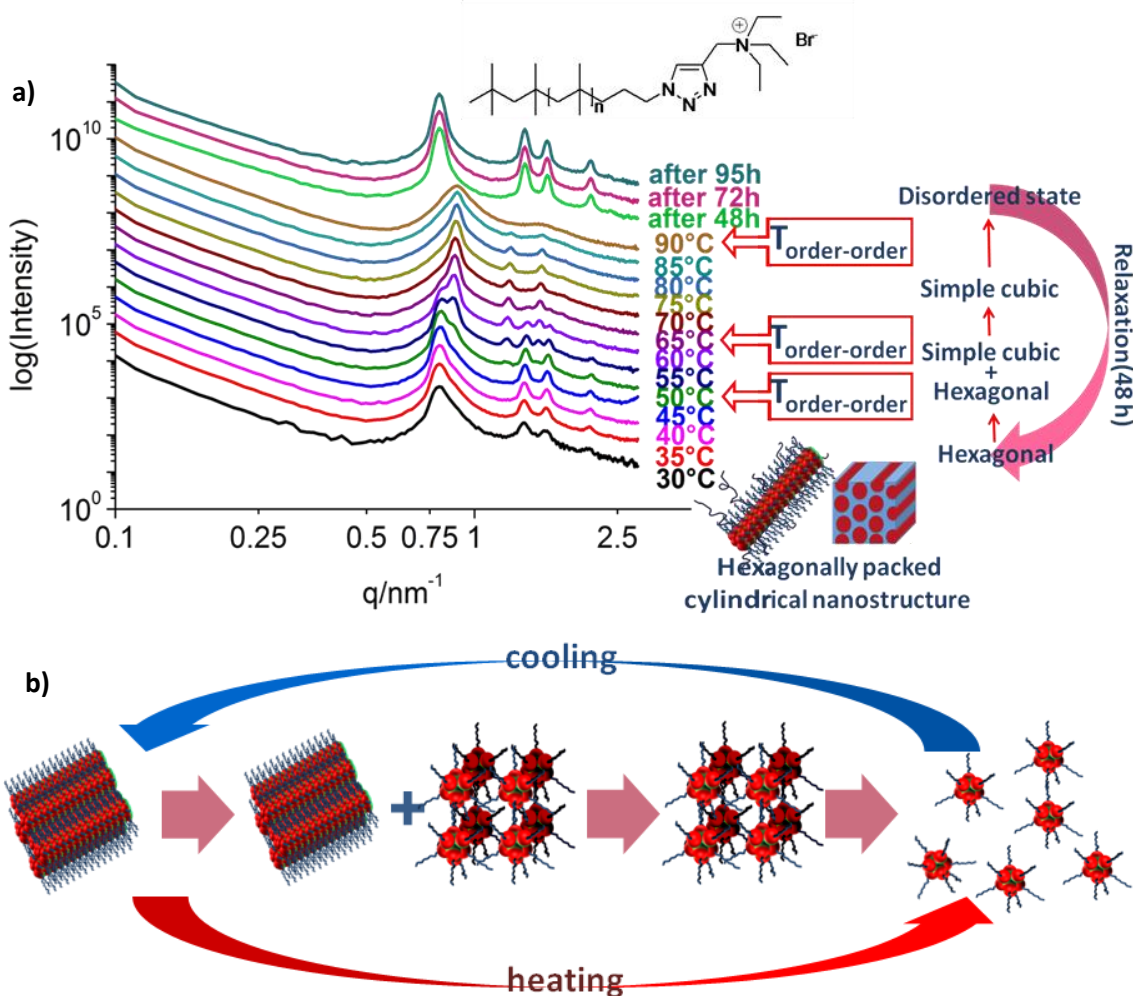

Figure 2.29. a) SAXS profiles of compound **11c** at different temperatures and after relaxation; **b)** Schematic representation of the transitions of **11c** due to the temperature.

Nevertheless, **11c** exhibited a very interesting behavior during the temperature sweep (Figure 2.29). The primary hexagonal geometry of the structure went through rearrangement around 50 °C and generated simple cubic structure. This order-order transition (OOT) was confirmed due to developing of new multiple reflections in the range between 50-65 °C where both hexagonal and simple cubic

structures existed. Second order-order transition was recorded at 65 °C where complete loss of hexagonal structures occurred. The last transition from order to disorder state took place at 90 °C due to falling of the cubic structure, however, it was fully recovered in hexagonal fashion again after only 48 hours. Comparing the results of three **PIBILs 11a-c**, one can conclude the significant influence of the cationic moiety (when the anions are identical) with respect to their transition responses to the temperature and relaxation time. Obviously the multiplets constructed by ethylammonium cations have more flexibility comparing to the other cations as the loss of the primary confined structure occurs at the lower temperatures.

The second **PIBILs** series synthesized via route **ii'-iii'** were exposed to in situ SAXS at variable temperatures in the range of 25-200 °C. Figure 2.30 represents the selected in situ SAXS profiles of **PIBILs 12a-c**. According to the Figure, **12a** demonstrated a lattice disorder-order transition (LDOT) which can be extracted from broadening of the first peak and the progressive decline of the peak at the higher q value due to disordering of the micelles during the heating process.[262] With further increasing of the temperature the electrostatic forces between clusters became weaker until the point of transition temperature where the internal structure was completely vanished. This can be clearly observed with the loss of all four higher order scattering maxima. As a result of destroyed clusters due to continues heating, mobility of the polymer chains were increased which eventually lead to the broadening and shifting of the main peak. However, cooling down the sample resulted in complete restoration of the initial mesostructure. In the case of **12b** there was no loss of the internal structure detected during the heating range possibly due to the interactions between the pyrrolidunium ring of the cation and aromatic rings of the polymer chains (Figure 2.30). Besides, the recovered original structure after the cooling process revealed the scattering peaks with a small shift toward lower q values. Compound **12c** exhibited similar behavior as **12a** (Figure 2.30). The reversible order-disorder transition occurred around 125 °C while, decreasing the temperature to room temperature lead to the immediate recovery of the primary ordered structure. Eventually, introducing longer polymer chain to pyrrolidinium based ionic liquid (**13b**) resulted in an order-disorder transition at 90 °C due to expansion of the intracluster distances.

Exchanging the counteranion from bromide to Tf_2N^- lead to the similar nano-organizations with lower thermal stability in comparison to bromide containing polymers due to the size and symmetry effects. As it is shown in Figure 2.30 the transition from ordered to disordered structure was

observed at 55 °C, 60 °C, and 65 °C for **14a**, **14b**, and **14c**, respectively, while the order was again fully regained after cooling down to room temperature. In the case of **14c**, the reestablished ordered structure after cooling down process exhibited significantly higher and more pronounced scattering signals comparing with initial ones which may be due to rearrangements of the ethyl groups constructing the cation moiety. **14b** also showed a similar behavior of transition and recovery process.
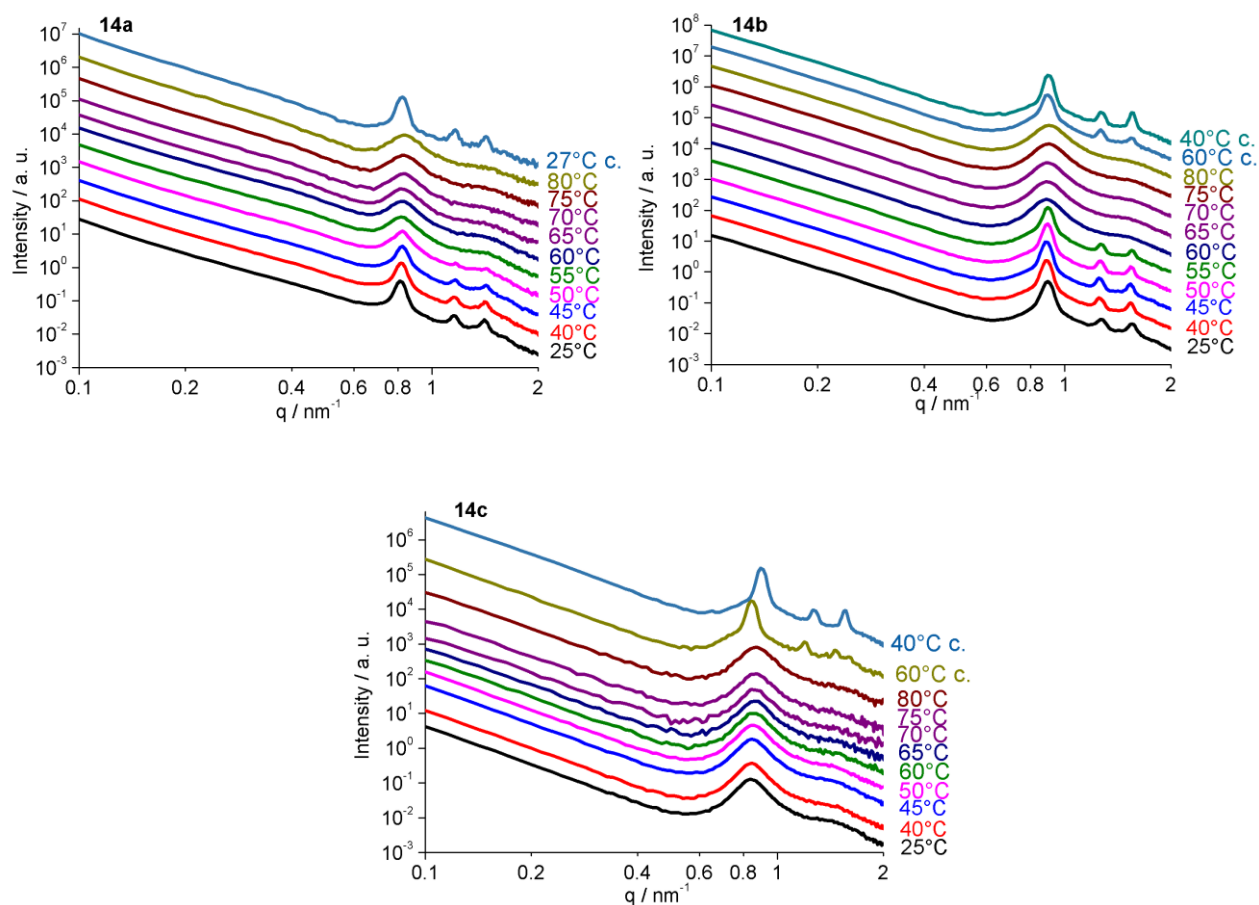

Figure 2.30. SAXS profiles of compound **14a**, **14b**, and **14c** at different temperatures and after relaxation. The curves are shifted in the intensity axis (y-axis) for clarity

According to the results, **PIBILs** synthesized via route **ii'-iii'** (**12a-b, 13b, 14a-b**), constructed nanostructures with shorter relaxation time comparing to the **PIBILs** obtained from **i'-iii'** (**11a-c**) pathway which was described before, as they are reordered almost immediately after cooling. Furthermore, all these synthesized materials exhibited significantly faster relaxation time in contrast

to classical ionomers with up to 7 days of recovery investigated in the literature[263] which can be an advantageous feature to nominate these polymers as self healing materials.[266]

2.2.10. Rheology measurements on PIBILs

To investigate the mechanical behavior of the synthesized **PIBLs** and the authenticity of the results obtained via SAXS measurement all samples were subjected to rheology measurement through monitoring the modulus values as a function of temperature at constant deformation rate.[267] Thus, any deviation from the mechanical properties of the unmodified polymer (**PIB**) can be clearly interpreted due to the presence of ionic moieties expectedly via two different phenomen: microphase separation process which can influence the viscous behavior in similar manner to microphase-separated block copolymers above their T_g and constructed multiplets which suppose to have an strong tendency to retain in the cubic structure.[268-270] Furthermore, the variety of the structures can provide more detailed information regarding the effect of different cation, anion or polymer chain length on the flow properties of the products. Considering the cluster formation based on EHM theory,[125] which was described before and coincided with SAXS results it was assumed that **PIBLs** can behave as crosslinked polymers where the multiples are the associating groups. Hence, the flow behavior of the products can be strongly dependent on the strength of these associations.

As demonstrated in Figure 2.31, the temperature sweep measurement of the series of **PIBILs** (**11a-c**) carrying different cations above their T_g resulted in emerging of different rheological patterns for each polymer which is strongly dependent on the nature of the counterions. While **11a** represented a significant transition at around 140 °C, **11b** exhibited small rubbery plateau and a terminal flow which occurred at far lower temperature (40 °C), indicated by G' ~ ω; G'' ~ ω at ωτ « 1. **11c** on the other hand, underwent a pronounced transition around 50 °C followed by flowing of the material at around 105 °C.
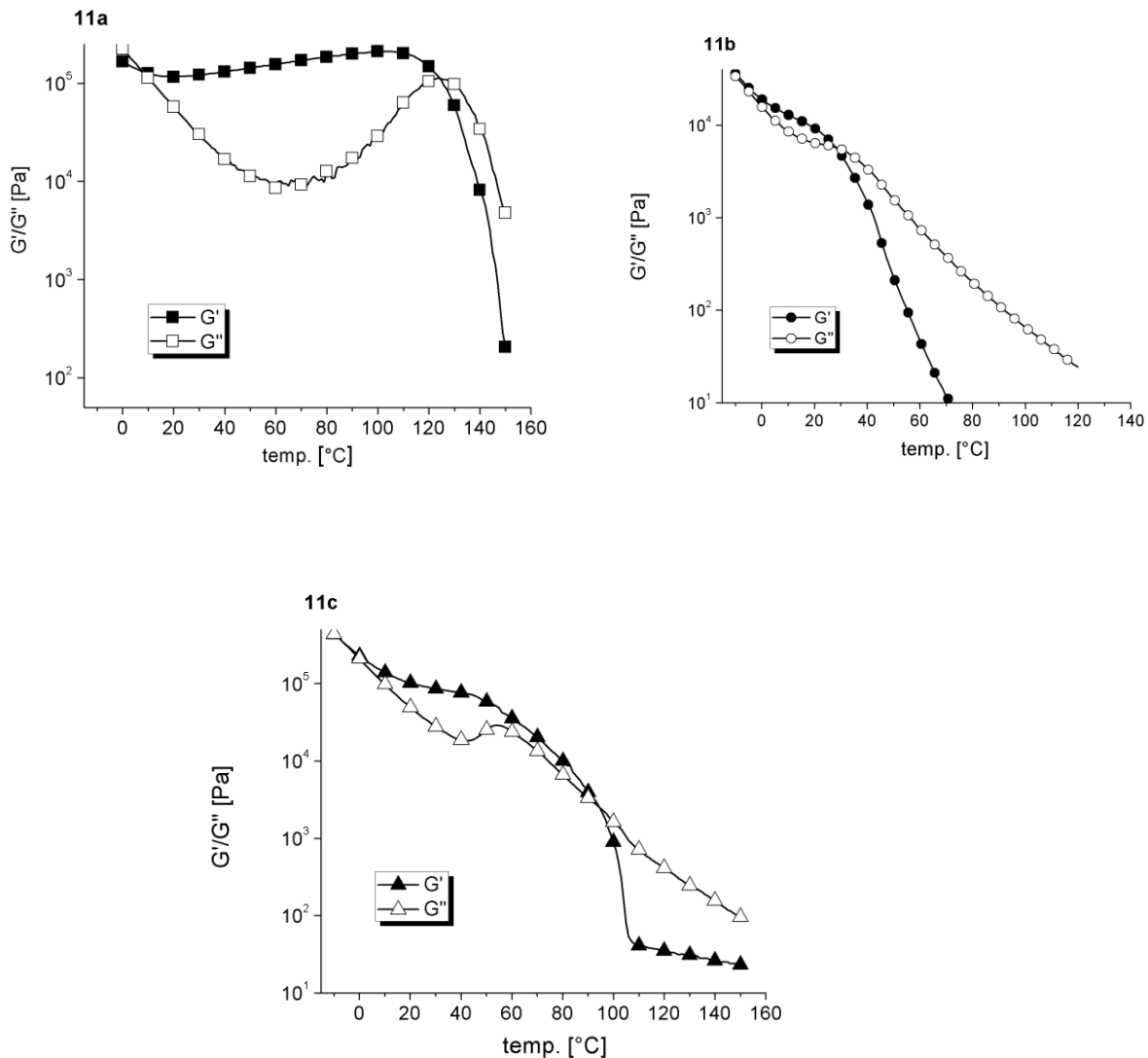
11a

11b

11c

Figure 2.31. Temperature-sweep rheology measurements of **11a**, **11c,** and **11b** with the schematic representation of the suggested sliding of multiplets over each other.

However, the obtained results are entirely different than rheological behavior of classical block copolymers,[269-271] all these experimental findings can be explained with "rubbery nanosphere" model which is described by Antonietti et al.[272] In this respect, a new model was investigated via rheology assessment of small spherical polystyrene microgels which can be successfully applied for our findings. According to this model,[272] it was postulated that the recorded viscous flow for such microgels can only be originated from cooperative movements of the polymer chains. In this respect, to analyze the flow behavior of the synthesized **PIBILs** the multiplets can be assumed as the "rubbery

77

nanosphere"s mentioned in the model. Accordingly, the small rubbery plateau detected in the results can be generated due to sliding of these multiplets as microgels over each other which can result in flow of the material with increasing temperature, due to destruction of the clusters. The detected flow for **PIBILs 11a-c** at 140 °C, 105 °C, and 40 °C is in accordance with the size of the multiples which were determined via SAXS as 7.6, 7.24 and 6.90 nm, respectively. The transition occurred around 50°C in the case of **11c** can be explained due to the order-order transition of its internal structure from hexagonal to cubic as it was concluded from SAXS data previously.
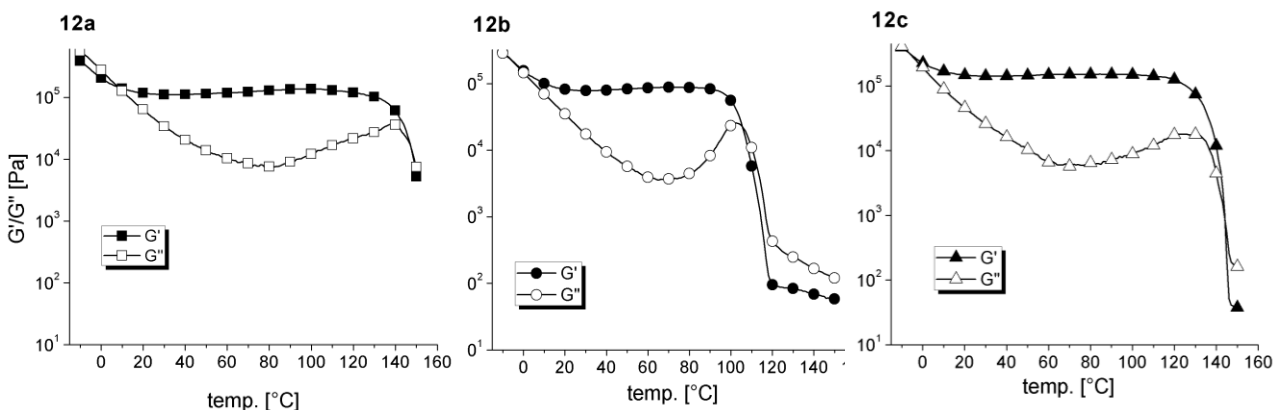
Figure 2.32. Temperature-sweep rheology measurements of **12a**, **12b**, and **12c.**

In accordance to the obtained results from SAXS measurements, increment of the aromatic ring in the structure of the synthesized **PIBILs** affected the dominated influence of the associating cation on the rheological behavior of the **12b** and **12c** and resulted in similar pattern which was observed for **11a**. This can be originated from π-π interactions of the introduced aromatic rings between polymer chains in the multiplets which strengths the thermal stability of the structure. As it is illustrated in Figure 2.32, **PIBILs 12a-c** exhibited a transition followed by flow of the material at around 140 °C, 100 °C, and 130 °C, respectively.

Furthermore, exchanging the counteranion or increasing the molecular weight of the attached polymer due to its effects on the size and strength of the constructed multiplets and clusters, consequently had a significant influence on the rheological performance of the polymers. Weakening of the multiplets and corresponding clusters due to the strong effect of the bistriflimide anion lead to the flow of the polymer in lower temperature in comparison to their bromide containing analogues.

As it has been demonstrated in Figure 2.33, with exchanging the anion from bromide to a large and weakly coordinating Tf_2N^- the flow temperature drops from 105 °C to 68°C. Similar behavior was detected where higher molecular weights of the polymer were implied. Both of these results are in agreement with previously discussed SAXS results which demonstrated the loss of the order due to weakening of the multiplets as a result of larger anion and higher mobility introduced by longer polymer chain.
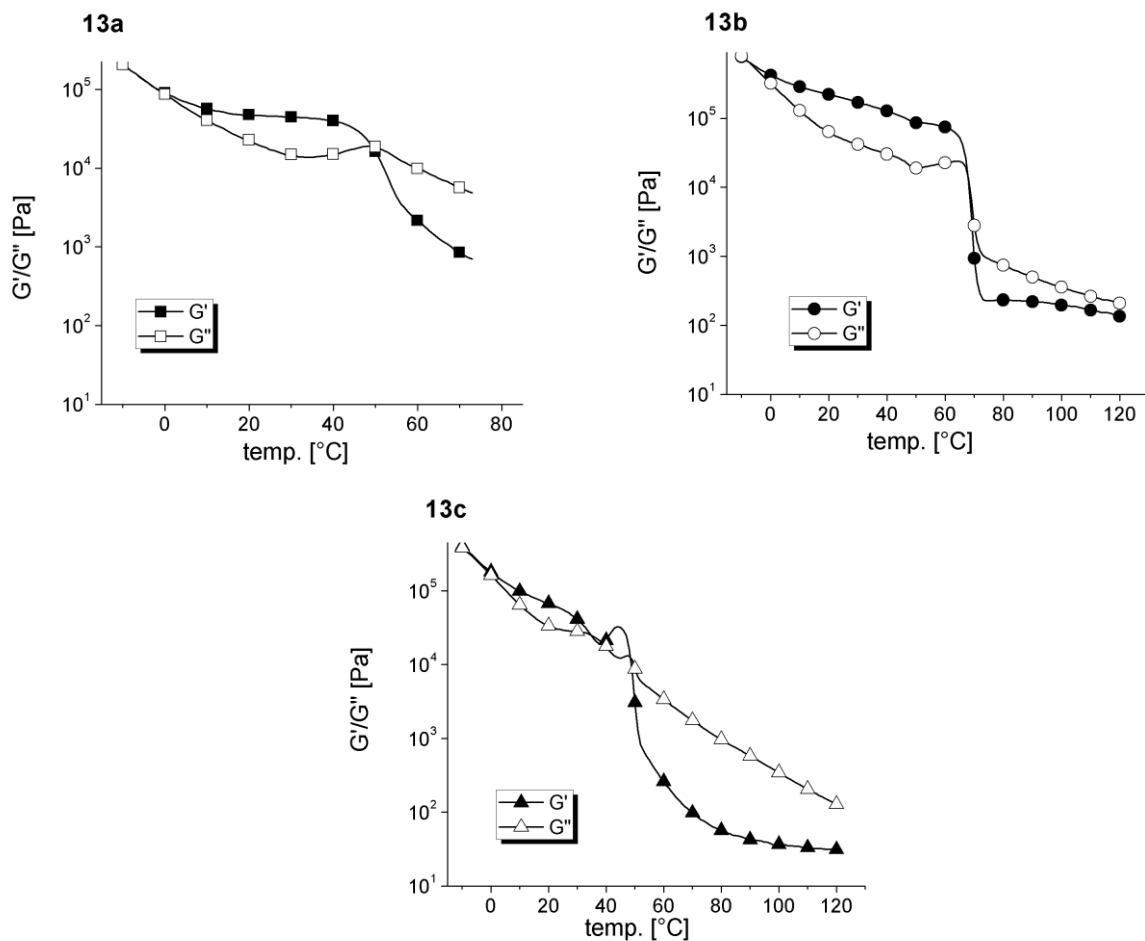

Figure 2.33. Temperature-sweep rheology measurements of **13a**, **13b**, and **13c.**

3.1. Materials

Phosphorous tribromide (≥98%) and propargyl alcohol (≥99%) were purchased from Merk. PEG 400 g/mol and PEG 1500 g/mol, methansulfonyl chloride (≥99%), and toluene-4-sulfonyl chloride (≥99%) were obtained from Fluka. The rest of the materials were purchased from Sigma Aldrich. All of the materials were used without further purification unless otherwise mentioned. 1-Methylimidazole, 1-methylpyrrolidine, and *N,N,N*-triethylamine were distilled over CaH_2 prior to use. Commercial copper (I) bromide (CuBr) was purified by washing with saturated SO_2-water. Tetrahydrofuran (THF) was predried over potassium hydroxide and freshly distilled from sodium and benzophenone under a dry argon atmosphere before use. Isopropanol, dichloromethane (DCM), chloroform, and *N,N*-dimethylformamide (DMF) were freshly distilled from CaH_2 under a dry argon atmosphere before use. Toluene was dried over sodium and benzophenone. *n*-Hexane was heated under reflux conditions with concentrated H_2SO_4 and $H_2SO_4 \cdot (SO_3)_n$ for 48 h in order to remove olefins. The organic layer was washed with concentrated sodium hydrogen carbonate solution and distilled water, dried over Na_2SO_4 and stored over $CaCl_2$. It was freshly distilled from KOH/Na under a dry argon atmosphere prior to use. 2-chloro-2,4,4-trimethyl-pentane (TMPCl) was synthesized according to the literature.[273]

3.2. Instruments and methods

^{1}H NMR, ^{13}C NMR, and ^{19}F NMR spectra were recorded on a Varian Gemini 2000 spectrometer (200 and 400 MHz) at 27 °C. Deuterated chloroform ($CDCl_3$-d_1) and dimethyl sulfoxide (DMSO-d_6) were used as solvents. All chemical shifts (δ) were reported in parts per million (ppm) relative to the solvents $CDCl_3$-d_1 and DMSO-d_6. Coupling constants (*J*) were given in hertz (Hz). MestRec-C software (version 6.0.2-5475) was used for data interpretation.

ATR-IR measurements were performed on a Bruker Tensor VERTEX 70 equipped with a Golden Gate Heated Diamond ATR Top-plate. Opus 6.5 was used for analyzing the data. For all spectra 32 scans were done (distance: 2 cm^{-1}), with the data given in cm^{-1}.

Gel permeation chromatography (GPC) was carried out using THF as solvent on Viscotek GPC max VE 2001 equipped with a styragel linear column GMH_{HR}, with refractive index detector VE 3580 equipped with two polystyrene columns. PIB standards with molecular weight of 340, 1650, 7970,

26300, 61800, and 87600 g/mol were used for calibration. Data were analyzed with the OmniSec (4.5.6) software. The concentration of all samples prepared was 3 mg/mL, and were measured with the flow rate of the instrument set to 1 mL/min.

Thin-layer chromatography (TLC) was performed on Merck TLC aluminium sheets (silica gel 60 F254). Spots on TLC plates were visualized by UV light (254 or 366 nm) or by oxidizing agents like $Ce(SO_4)_2 \cdot 4H_2O$ dissolved in a mixture of distilled water (47.0 mL) and concentrated H_2SO_4 (2.8 mL) or "blue strain" consisting of $Ce(SO_4)_2 \cdot 4H_2O$ and $(NH_4)_6Mo_7O_{24} \cdot 4H_2O$ dissolved in a mixture of distilled water (90.0 mL) and concentrated H_2SO_4 (6.0 mL).

Electrospray ionization time-of-flight mass spectroscopy (ESI-TOF-MS) measurements were conducted at a Bruker Daltonics micrOTOF II. The samples were measured via direct injection, with a flow rate of 300 μL/h. Measurements were done in positive and negative modes with a capillary voltage of 4.5 kV. Calibration was done by measuring Tunemix in a mixture of Acetonitrile/Water (95/5). Data were recorded in the range from 50 to 3000 m/z with a hexapole RF-voltage of 700 V. Recorded spectra were analyzed with Bruker DataAnalysis 4.0 software, and isotopic patterns were simulated with Bruker Compass IsotopePattern.

Matrix-assisted laser desorption/ionization time-of-flight mass spectrometry (MALDI-TOF-MS) experiments were performed on a Bruker Autoflex III Smartbeam equipped with a nitrogen laser (337 nm), operating in reflection and linear modes. DCTB (20 mg/mL in THF) was used as matrix. Ions were formed by laser desorption (smart laser Nd-YAG 355nm). Polymers were dissolved in THF at a concentration of 10 mg/mL; salts sodium trifluoroacetate (NaTFA) and potassium chloride (KCl) were dissolved at a concentration of 10 mg/mL in THF. Solutions of the matrix, the polymer, and the salt were mixed in a volume ratio of 100:10:1 and 1 μL of each mixture was spotted on the MALDI-target plate. Baseline subtraction and smoothing of the recorded spectra were performed using a three point Savitzky-Golay algorithm. Data evaluation was carried out on flexAnalysis software (version 3.0).

Thermogravimetric analysis (TGA) was performed on a Netzsch TG tarsus 209 instrument. The sample was heated in a Pt pan under a nitrogen atmosphere, over a temperature range of 25-700 °C, with a heating rate of 10 K/min. The obtained data were evaluated with the OriginPro8 software.

Differential scanning calorimetry (DSC) was conducted on Netzsch DSC 204 F1 phoenix 240-120-0142-L instrument. The glass transition temperatures were determined by heating the samples to

120 °C and cooling to −120 °C, with a heating ramp rate of 10 K/min. The glass transition temperature was taken as a midpoint of a small heat capacity change upon heating from amorphous glass state to a liquid state.

Small-angle X-ray scattering (SAXS) experiments were carried out under vacuum with a rotating copper-anode X-ray generator (Nanostar, Bruker AXS), Cu Kα radiation (wavelength 0.1542 nm) monochromatized and collimated from crossed Goebel mirrors, and a 2-D position sensitive detector (Vantec 2000). For the in situ SAXS measurements a specially designed X-ray transparent furnace was developed, which allows stepwise heating of the samples from room temperature to 550 °C with an accuracy of ±0.5 °C. The samples were placed either in a Quartz glass capillary with a diameter of 1.5 mm and a wall thickness of 10 µm (from Hilgenberg, Germany) or between commercial aluminum foils. The samples were heated up to the desired temperature, kept at this temperature for 5 minutes to ensure the thermal equilibrium is established, and measured for 15 to 30 minutes depending on the scattering intensity of the respective samples. With a sample to detector distance of 108 cm an accessible q-range from 0.1 to 2.8 nm^{-1} was obtained. The SAXS patterns were radially averaged in order to obtain the scattering intensities I(q), where q = (4π/λ) sin θ is the scattering vector and 2θ the scattering angle. The d_{100} peak (the strongest Bragg reflection) was fitted with a Lorentzian function. This results in numerical values for the peak position (corresponding to the distance of the crystalline units in real space) and the peak breadth (proportional to the domain size).

Rheological measurements were performed on an Anton Paar MCR 101-DSO rheometer using parallel plates (diameter 8 mm). The sample temperature was regulated by thermoelectric cooling/heating in a peltier chamber under a nitrogen atmosphere. Frequency sweep measurements were performed within the LVE (if not mentioned otherwise). Temperature sweep measurements were performed in dynamic mode in the temperature range of -10 to -180 °C with a heating rate of 1 K/min at ω = 10 rad/s.

### 3.3. Synthesis of poly(ethylene glycol)-based ionic liquids

3.3.1. Synthesis of tetraethylene glycol-based ionic liquids

α,ω-Dichlorotetraethylene glycol (17) and α,ω-dimethanesulfonyl tetraethylene glycol ester (18) were synthesized according to the procedure described in the literature.[196-197]
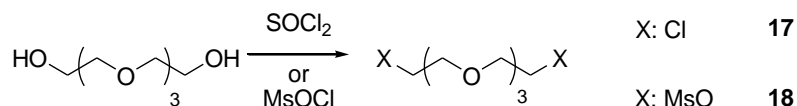
General procedure to synthesis of tetraethylene glycol-based ionic liquids via quaternization reaction (1a, 1b, 2a, 2b)[198]
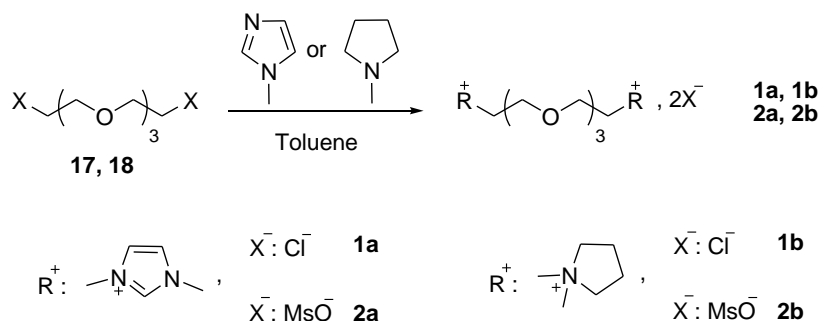
3.0 mmol of corresponding amine (1-methylimidazole or 1-methylpyrrolidine) was added to a solution of 1.0 mmol of functionalized tetraethylene glycol (**17, 18**) in 5 mL toluene. The reaction mixture was heated at 110 °C for 20 h and then cooled down to room temperature. The organic phase was separated via simple decantation and the residue was washed with toluene (3×5 mL). The obtained viscous liquid was dissolved in a small amount of methanol and precipitated in ethyl acetate (3×5 mL). After removing ethyl acetate the y product was dried under high vacuum for 2 days to eliminate the residue of the solvents.

Bis-1,11-[(3-methyl-1H-imidazolium-1-yl)]-(3,6,9-trioxaundecane) dichloride (1a)

The reaction of **17** (0.23 g, 1.0 mmol) with 1-methylimidazole (0.24 g, 3.0 mmol) according to described procedure resulted in 0.32 g (85%) of product **1a**.^{1}H NMR (400 MHz, DMSO-d$_6$, δ ppm): 9.3 (s, 2H), 7.78 (s, 2H), 7.75 (s, 2H), 4.37 (t, J = 4.9 Hz, 4H), 3.88 (s, 6H), 3.77 (t, J = 3.4 Hz, 4H), 3.55–3.52

(m, 4H), 3.48–3.46 (m, 4H). ^{13}C NMR (100 MHz, DMSO-d$_6$, δ ppm): 136.70, 123.12, 122.43, 69.35, 67.99, 48.51, 35.56. ESI-TOF m/z (%), negative mode: found: 429.11 (100) [C$_{16}$H$_{28}$Cl$_2$N$_4$O$_3$Cl$_3$]$^-$, calculated: 429.12.

Bis-1,11-[(1-methyl-pyrrolidinium-1-yl)]-(3,6,9-trioxaun decane) dichloride (1b)

The reaction of **17** (0.23 g, 1.0 mmol) with 1-methylpyrrolidine (0.26, 3.0 mmol) according to the procedure after workup resulted in 0.328 g (82%) of **1b**. ^{1}H NMR (400 MHz, DMSO-d$_6$, δ ppm): 4.39 (t, J = 4.4 Hz, 4H), 3.64 (t, J = 4.4 Hz, 4H) 3.60–3.51 (m, 16H), 3.08 (s, 6H), 2.15 (b, 8H). ^{13}C NMR (δ 100 MHz, DMSO-d$_6$, δ ppm): 69.27, 64.41, 63.91, 61.70, 47.89, 20.81. ESI-TOF m/z (%), negative mode: found: 435.18 (100) [C$_{18}$H$_{38}$Cl$_3$N$_2$O$_3$]$^-$, calculated: 435.19.

Bis-1,11-[(3-methyl-1H-imidazolium-1-yl)]-(3,6,9-trioxaundecane) di(methanesulfonate) (2a)

Compound **18** (0.35 g, 1.0 mmol) and 1-methylimidazole (0.24 g, 3.0 mmol) were reacted following the general procedure to yield 0.40 g (78%) of **2a**.^{1}H NMR (400 MHz, DMSO-d$_6$, δ ppm): 9.11(s, 1H), 7.72 (s, 1H), 7.70 (s, 1H), 4.34 (t, J = 4.8 Hz, 4H), 3.86 (s, 6H), 3.76 (t, J = 4.8 Hz, 4H), 3.46–3.56 (m, 8H), 2.30 (s, 6H). ^{13}C NMR (100 MHz, DMSO-d$_6$, δ ppm): 136.70, 123.12, 122.43, 69.35, 67.99, 48.51, 35.56, 28.30. ESI-TOF m/z (%), negative mode: found: 609.14 (100) [C$_{19}$H$_{37}$N$_4$O$_{12}$S$_3$]$^-$, 94.97 [CH$_3$O$_3$S]$^-$, calculated: 609.15, 94.98.

Bis-1,11-[(1-methyl-pyrrolidinium-1-yl)]-(3,6,9-trioxaundecane) di(methanesulfonate) (2b)

Compound **18** (0.35 g, 1.0 mmol) and 1-methylpyrrolidine (0.26, 3.0 mmol) were reacted following the general procedure to yield 0.41 g (80%) of **2b.** ^{1}H NMR (400 MHz, DMSO-d$_6$, δ ppm): 3.86–3.82 (m, 4H), 3.60–3.55 (m, 12H), 3.54–3.49 (m, 8H), 3.04 (s, 6H), 2.31 (s, 6H), 2.12–2.05 (m, 8H). ^{13}C NMR (100 MHz, DMSO-d$_6$, δ ppm): 69.97, 69.89, 64.98, 64.60, 62.42, 48.48, 21.37. ESI-TOF m/z (%), negative mode: found: 94.97 [CH$_3$O$_3$S]$^-$, 615.21 (100) [C$_{21}$H$_{47}$N$_2$O$_{12}$S$_3$]$^-$, calculated: 94.98, 615.22.

General procedure for the synthesis of tetraethylene glycol-based ionic liquids via anion exchange (3a, 3b)[96]
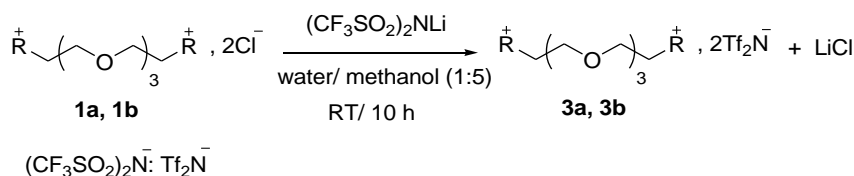
Bis(trifluoromethane)sulfonimide lithium salt (2.2 equivalent) was dissolved in water (0.5 mL). 1.0 equivalent of compound **1a** or **1b** in 5 mL of methanol was added to the solution and stirred at room temperature for 10 h. After removal of the solvent a mixture of 5 mL water and 5 mL ethyl acetate was added to the residue. After separation of the two phases, the ethyl acetate phase was evaporated under vacuum. The obtained product was washed with 5 mL of water and ether (2×5 mL) and dried over magnesium sulfate. After removal of the ether the colorless liquid product was dried under high vacuum for 2 days.

Bis-1,11-[(3-methyl-1H-imidazolium-1-yl)]-(3,6,9-trioxaundecane) di[bis(trifluoromethanesulfonyl)-imide] (3a)

The reaction of **1a** (0.10 g, 0.25 mmol) and bis(trifluoromethanesulfonyl)imide lithium salt (0.16 g, 0.56 mmol)according to the general procedure yield to 0.11 g (71%) of **3a**. ^{1}H NMR (400 MHz, DMSO-d_6, δ ppm): 9.03 (s, 2H), 7.69 (s, 2H), 7.66 (s, 2H), 4.33 (t, J = 4.8, 4H), 3.85 (s, 6H), 3.76 (t, J = 3.4, 4H) 3.55 (m, 8H). ^{13}C NMR (100 MHz, DMSO-d_6, δ ppm): 136.62, 123.19, 122.50, 119.35 (q, $J_{(C, F)}$ = 320 Hz), 69.40, 68.01, 48.67, 35.62. ESI-TOF m/z (%), negative mode: found: 279.92 (100) $[C_2F_6NO_4S_2]^-$, 1163.94 $[C_{22}H_{28}F_{18}N_7O_{15}S_6]^-$, calculated: 279.91, 1163.96.

Bis-1,11-[(1-methyl-pyrrolidinium-1-yl)]-(3,6,9-trioxaundecane) di[bis(trifluoromethanesulfonyl)-imide] (3b)

The reaction of **1b** (0.20 g, 0.50 mmol) and bis(trifluoromethane)sulfonimide lithium salt (0.34 g, 1.20 mmol) according to the general procedure produced 0.29 g (66%) of **3b**. ^{1}H NMR (400 MHz, DMSO-d_6, δ ppm): 3.83 (m, 4H), 3.63–3.42 (m, 20H), 3.02 (s, 6H), 2.08 (m, 8H). ^{13}C NMR (100 MHz, DMSO-d_6, δ ppm): 124.02, 120.83, 117.63, 114.44 (q, J = 319 Hz), 69.33, 64.41, 63.98, 61.81, 47.93, 20.84. ESI-TOF m/z (%), negative mode: found: 279.92 (100) $[C_2F_6NO_4S_2]^-$, 1170.01 $[C_{24}H_{38}F_{18}N_5O_{15}S_6]^-$, calculated: 279.91, 1170.04.

3.3.2. Synthesis of poly (ethylene glycol)-based ionic liquids via quaternization

α,ω-Dibromo poly(ethylene glycol) (19,20) were synthesized with molecular weight of 400 and 1500 g/mol according to the procedure described in the literature.[211]
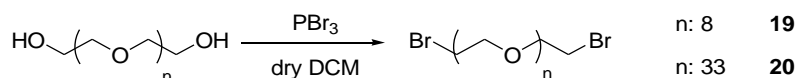
| | n: 8 | **19** |
| | n: 33 | **20** |

General procedure for the synthesis of the poly(ethylene glycol) based ionic liquids via quaternization reaction (4a, 4b, 5a)

The reaction of **19** or **20** (1.0 equivalent) with corresponding amine (2.5 equivalents) was conducted in 5 mL of toluene. After refluxing for 48 h, the reaction mixture was cooled down. Subsequently, the solvent was removed and the residue was dissolved in small amount of methanol and precipitated in diethyl ether (3×5 mL). After removal of the ether, the product was dried under high vacuum.
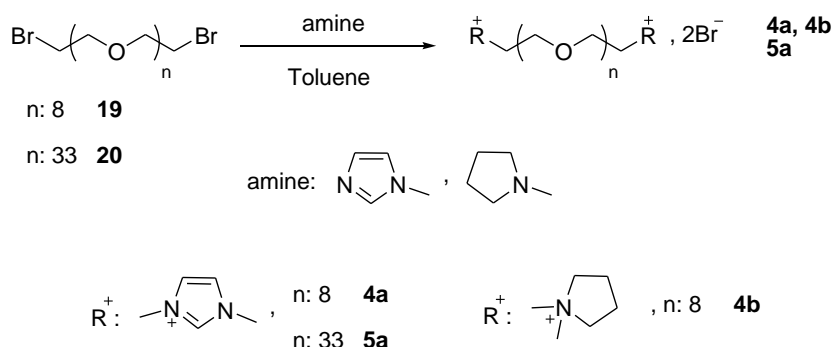
α,ω-Bis-[(3-methyl-1H-imidazolium-1-yl)poly(ethylene glycol)] dibromide (n = 8, Mn= 400 g/mol) (4a)

The reaction of compound **19** (0.22 g, 0.4 mmol) and 1-methylimidazole (0.54 g, 1.0 mmol) according to the general procedure was yielded to 0.58 g of the product **4a** which was containing 10% of mono-substituted polymer. ^{1}H NMR (400 MHz, DMSO-d$_6$, δ ppm): 9.2 (s, 2H), 7.77 (s, 2H), 7.74 (s, 2H), 4.90 (t, J = 4.95 Hz, 4H), 3.87 (s, 6H), 3.74 (t, J = 3.4 Hz, 4H), 3.70–3.42 (m, 54H). ^{13}C NMR (100 MHz, DMSO-d$_6$, δ ppm): 137.4, 123.79, 123.33, 71.04, 70.26, 68.67, 49.19, 36.22.

α,ω-Bis-[(1-methyl-pyrrolidinium-1-yl) poly(ethylene glycol)] dibromide (n = 8, Mn = 400 g/mol) (4b)

The reaction of compound **19** (0.30 g, 0.55 mmol) and 1-methylpyrrolidine (0.13 g, 1.50 mmol) following the general Procedure produced 0.39 g of the product **4b** which was containing 15% of mono-substituted polymer. ^{1}H NMR (400 MHz, DMSO-d$_6$, δ ppm): 3.81, 3.64 (t, 8H) 3.59–3.48 (m, 60H), 3.02 (s, 6H), 2.04 (s, 8H). ^{13}C NMR (100 MHz, DMSO-d$_6$, δ ppm): 69.56, 69.50, 69.27, 69.25 47.88, 39.43, 20.79.

**α,ω-Bis-[(1-methyl-pyrrolidinium-1-yl) poly(ethylene glycol)] dibromide (n = 33, M_n= 1550 g/mol) (5a)**

Compound **20** (1.64 g, 1.0 mmol) and 1-methylimdazole (1.35 g, 2.5 mmol) were reacted according to the general procedure which was resulted in 1.90 g product **5a**, containing 18% of mono-substituted polymer. ^{1}H NMR (400 MHz, DMSO-d_6, δ ppm): 9.1 (s, 2H), 7.74 (s, 2H), 7.70 (s, 2H), 4.35 (t, J= 5.2 Hz, 4H), 3.87 (s, 6H), 3.77 (t, J= 4.0 Hz, 4 H), 3.53–3.46 (m, 208 H). ^{13}C NMR (400 MHz, DMSO-d_6, δ ppm): 136.13, 122.52, 123.29, 69.60, 68.03, 48.70, 35.65.

3.3.3. Synthesis of poly(ethylene glycol)-based ionic liquids via ''click'' reaction

α,ω-Diazido hexaethylene glycol (21) and **α,ω-diazido poly(ethylene glycol) 400, 1550 g/mol (22, 23)** were synthesized following the synthetic method described in the literature.[274]

n: 5   **21**
n: 8   **22**
n: 33   **23**
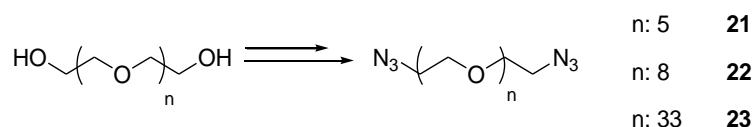
General procedure to synthesis of ionic liquids containing alkyne moiety (24a-c, 25a-c)
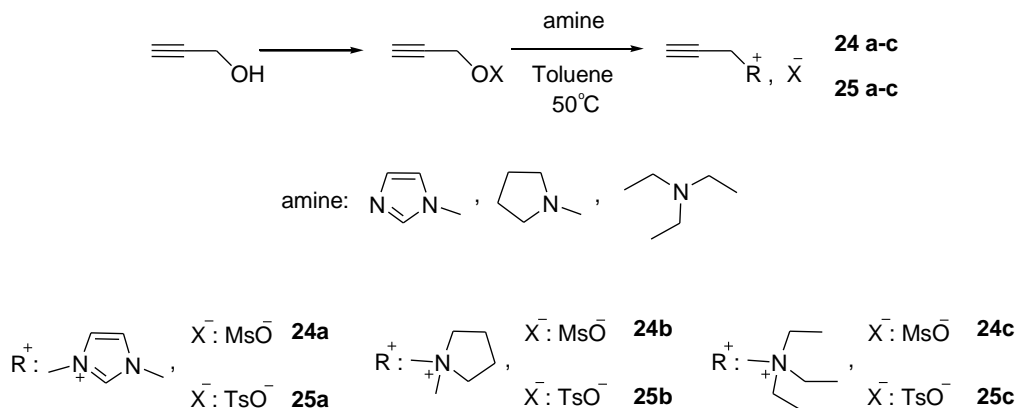
amine:

All alkyne ligands containing corresponding amines (**24a-c, 25a-c**) were synthesized via adopted procedure mentioned in the literature.[254] The selected amine (1.2 equivalents) was added, dropwise, to the solution of propargyl tosylate or propargyl mesylate (1.0 equivalent) in dry toluene. The reaction mixture was stirred at 50 °C for about 1 to 2 days. The desired product was obtained by washing the residue after evaporating the reaction solvent. Afterwards, the obtained product was

dried under high vacuum for 2 days.

1-Propargyl-3-methylimidazolium methanesulfonate (24a)

The reaction of 1-Methylimidazole (1.02 g, 12.43 mmol) and propargyl methanesulfonate (1.39 g, 10.36 mmol) in dry toluene (25 mL) was resulted in 2.20 g (98%) of the product **24a** within 20 h. ^{1}H NMR (400 MHz, DMSO-d$_6$, δ ppm): 9.22 (s, 1H), 7.78 (t, J= 1.8 Hz, 1H), 7.74 (t, J= 1.8 Hz, 1H), 5.18 (d, J= 2.6 Hz, 2H), 3.86 (s, 3H), 3.81 (t, J= 2.6 Hz, 1H), 2.30 (s, 3H). ^{13}C NMR (100 MHz, DMSO-d$_6$, δ ppm): 137.16, 124.55, 122.62, 79.42, 76.60, 40.25, 38.90, 36.41.

1-Propargyl-1-methylpyrrolidinium methanesulfonate (24b)

1-Methylpyrrolidinium (1.74 g, 20.46 mmol) and propargyl methanesulfonate (1.83 g, 13.64 mmol) were reacted in dry toluene (40 mL) for 24h. The yield of the obtained product **24b** was 92% (2.74 g). ^{1}H NMR (400 MHz, DMSO-d, δ ppm): 4.39 (d, J=2.5 Hz, 2H), 3.99 (t, J=2.5 Hz, 1H), 3.51 (m, 4H), 3.10 (s, 3H), 2.29 (s, 3H), 2.10 (m, 4H). ^{13}C NMR (100 MHz, DMSO-d$_6$, δ ppm): 82.36, 73.77, 63.71, 52.80, 49.37, 22.01.

1-Propargyl-*N,N,N*-triethylammonium methanesulfonate (24c)

N,N,N-Triethylamine (1.35 g, 13.34 mmol) and propargyl methanesulfonate (1.19 g, 8.89 mmol) were reacted in dry toluene (40 mL). After 40h the desired product **24c** was obtained with a yield of 88% (1.85 g). ^{1}H NMR (400 MHz, CDCl3, δ ppm): 4.31 (d, J= 2.3 Hz, 2H), 3.47 (q, 6H, J= 7.3 Hz), 2.96 (t, J= 2.2 Hz, 1H), 2.61 (s, 3H), 1.34 (t, 9H, J= 7.3 Hz,). ^{13}C NMR (100 MHz, DMSO-d$_6$, δ ppm): 81.04, 71.24, 53.71, 48.22, 39.50. C NMR

1-Propargyl-3-methylimidazolium *p*-toluenesulfonate (25a)

1-Methylimidazole (0.68 g, 8.34 mmol) and propargyl tosylate (1.46 g, 6.94 mmol) were reacted in dry toluene (40 mL) for 48 h yielding to 1.78 g (87%) of the desired product **25a**. ^{1}H NMR (400 MHz, CDCl3, δ ppm): 9.59 (s, 1H), 7.69 (d, J= 8.1 Hz, 2H), 7.47 (s, 1H), 7.43 (s, 1H), 7.11 (d, J=8.0 Hz, 2H), 5.10 (d, J=2.5 Hz, 2H), 3.86 (s, 3H), 2.78 (t, J=2.5 Hz, 1H), 2.30 (s, 3H). ^{13}C NMR (100 MHz, CDCl3, δ ppm): 143.62, 137.41, 128.79, 125.70, 123.93, 121.90, 77.62, 74.54, 39.15, 36.40, 21.23.

1-Propargyl-1-methylpyrrolidinium *p*-toluenesulfonate (25b)

The reaction of 1-methylpyrrolidinium (1.09 g, 12.84 mmol) and propargyl tosylate (2.25 g, 10.70 mmol) in dry toluene (60 mL) resulted in 3.04 g (96%) of the desired product **25b** after 24 h. ^{1}H NMR (400 MHz, CDCl$_3$, δ ppm): 7.66 (d, J=8.1 Hz, 2H), 7.08 (d, J=8.1 Hz, 2H), 4.50 (d, J=2.3 Hz, 2H), 3.69 (m, 4H), 3.24 (s, 3H), 2.83 (t, J= 2.2 Hz, 1H), 2.27 (s, 3H), 2.10 (m, 4H). ^{13}C NMR (100 MHz, CDCl$_3$, δ ppm): 143.89, 139.32, 128.77, 125.70, 80.21, 72.62, 63.55, 52.97, 49.22, 21.90, 21.36.

1-Propargyl-*N, N, N*-triethylammonium *p*-toluenesulfonate (25c)

N,N,N-Triethylamine (0.74 g, 7.27 mmol) and propargyl tosylate (1.27 g, 6.06 mmol) were reacted in dry toluene (40 mL) for 48 h yielding to 1.69 g (90%) of product **25c**. ^{1}H NMR (400 MHz, CDCl, δ ppm): 7.68 (d, J= 8.1 Hz, 2H), 7.06 (d, J= 8.0 Hz, 2H), 4.23 (d, J= 2.5 Hz, 2H), 3.38 (q, J= 7.3 Hz, 6H), 2.80 (t, J= 2.5 Hz, 1H), 2.26 (s, 3H), 1.25 (t, J= 7.3 Hz, 9H). ^{13}C NMR (100 MHz, CDCl$_3$, δ ppm): 144.25, 139.01, 128.55, 125.90, 80.68, 71.23, 53.70, 48.13, 21.29, 7.94.

General procedure for the synthesis of poly(ethylene glycol)-based ionic liquids via ''click'' reaction
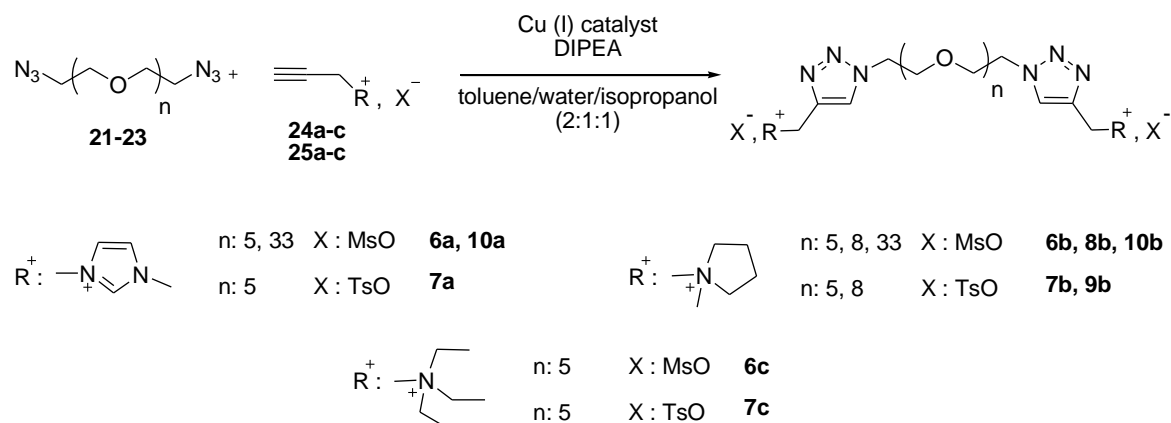
α,ω-Diazido poly(ethylene glycol) (21-23) (1.0 equivalent), corresponding amines bearing alkyne moiety (**24a-c**, **25a-c**) (2.0 equivalents), DIPEA (6.0 equivalents) and copper(I) bromide (CuBr) (0.2 equivalents with respect to **21-23**) were dissolved in the solvent mixture of H$_2$O/DMF (1:1) under nitrogen flow. Afterwards, the reaction mixture was subjected to either microwave irradiation or heating in oil bath. Later when the reaction was accomplished the solvent was removed. The obtained crude product was dissolved in methanol, and filtrated through Al$_2$O$_3$ to remove the excess of CuBr. Subsequently, the solvent was evaporated and the product was purified via precipitation with methanol: ethyl acetate (0.5:5). The desired product was dried under high vacuum for 2 days.

Bis-1,17-[4-(3-methyl-1H-imidazolium-1-yl)-1H-1,2,3-triazole-1-yl]-(3,6,9,12,15-pentaoxahepta-decane) di(methanesulfonate) (6a)

A mixture **24a** (0.19 g, 0.90 mmol), compound **21** (0.15 g, 0.45 mmol), DIPEA (0.35 g, 2.70 mmol), and CuBr (0.01 g, 0.09 mmol) in H_2O/DMF (4 mL) was subjected to microwave irradiation at 70 W (70 °C) for 15 h and purification method described in general procedure. The yield of the obtained brown viscous liquid (0.34 g) was 98%. ^{1}H NMR (400 MHz, DMSO-d_6, δ ppm): 9.23 (s, 2H), 8.25 (s, 2H), 7.75 (t, J = 1.8 Hz, 2H), 7.70 (t, J = 1.8 Hz, 2H), 5.53 (s, 4H), 4.53 (t, J = 5.3 Hz, 4H), 3.85 (s, 6H), 3.79 (t, J = 5.3 Hz, 4H), 3.47 (m, 16H), 2.31 (s, 6H). ^{13}C NMR (100.6 MHz, DMSO-d_6, δ ppm): 140.81, 137.16, 125.42, 124.29, 122.76, 109.86, 70.03, 69.06, 50.01, 43.97, 36.28, 15.62. ESI-TOF m/z (%), negative mode: found: 859.26 (100) $[C_{29}H_{51}N_{10}O14_S_3]^-$, 94.97 $[CH_3O_3S]^-$, calculated: 859.27, 94.98.

Bis-1,17-[(1-methyl-pyrrolidinium-1-yl)-1H-1,2,3-triazole-1-yl]-(3,6,9,12,15-pentaoxaheptadecane) di(methanesulfonate) (6b)

A mixture of **24b** (0.20 g, 0.90 mmol), compound **21** (0.15 g, 0.45 mmol), DIPEA (0.35 g, 2.70 mmol), and CuBr (0.01 g, 0.09 mmol) in H_2O/DMF (4 mL) was irradiated at 70 W (70 °C) for 12 h and the resulted mixture was treated according to the general procedure. The yield of the obtained yellow viscous liquid (0.35 g) was 98%. Conducting the same experiment with conventional heating (48 h at 50 °C) resulted in same product with 95% yield.^{1}H NMR (400 MHz, DMSO-d_6, δ ppm): 8.4 (s, 2H), 4.67 (s, 4H), 4.58 (t, J = 5.2 Hz, 4H), 3.82 (t, J = 5.2 Hz, 4H), 3.49 (m, 24H), 2.96 (s, 6H), 2.30 (s, 6H), 2.09 (m, 8H). ^{13}C NMR (100.6 MHz, DMSO-d_6, δ ppm): 136.41, 128.69, 70.15, 69.03, 63.33, 56.74, 50.18, 48.64, 21.70. ESI-TOF m/z (%), negative mode: found: 865.34 (100) $[C_{31}H_{61}N_8O_{14}S_3]^-$, 94.97 $[CH_3O_3S]^-$, calculated: 865.35, 94.98.

Bis-1,17-[(*N,N,N*-triethylammonium-N-yl)-1H-1,2,3-triazole-1-yl]-(3,6,9,12,15-pentaoxahepta-decane) di(methanesulfonate) (6c)

A mixture of **24c** (0.21 g, 0.90 mmol), compound **21** (0.15 g, 0.45 mmol), DIPEA (0.35 g, 2.70 mmol), and CuBr (0.01 g, 0.09 mmol) in H_2O/DMF (4 mL) was irradiated at 70 W (70 °C) for 12 h and subsequently was purified as it was described in general procedure. The yield of the obtained yellow viscous liquid (0.36 g) was 97%. ^{1}H NMR (400 MHz, DMSO-d_6, δ ppm): 8.59 (s, 2H), 4.75 (t, J= 5.3 Hz, 4H), 4.73 (s, 4H), 4.01 (t, J= 5.3 Hz, 4H), 3.68 (m, 16H), 3.35 (q, J= 7.2 Hz, 12H), 2.47 (s, 6H), 1.47 (t, J= 7.2 Hz, 18H). ^{13}C NMR (100.6 MHz, DMSO-d_6, δ ppm): 134.58, 128.32, 69.61, 68.49, 52.03, 50.45,

49.61, 7.38. ESI-TOF m/z (%), negative mode: found: 897.4 (100) $[C_{33}H_{69}N_8O_{14}S_3]^-$, 94.97 $[CH_3O_3S]^-$, calculated: 897.41, 94.98.

Bis-1,17-[4-(3-methyl-1H-imidazolium-1-yl)-1H-1,2,3-triazole-1-yl]-(3,6,9,12,15-pentaoxahepta-decane) di(*p*-toluenesulfonate) (7a)

A mixture of **25a** (0.20 g, 0.90 mmol), compound **21** (0.15 g, 0.45 mmol), DIPEA (0.35 g, 2.70 mmol), and CuBr (0.01 g, 0.09 mmol) in H_2O/DMF (4 mL) was irradiated at 70 W (70 °C) for 12 h. Following the above mentioned general procedure resulted in brown viscous liquid (0.30 g) with a yield of 74%. ^{1}H NMR (400 MHz, DMSO-d$_6$, δ ppm): 9.19 (s, 2H), 8.23 (s, 2H), 7.73 (t, J= 1.9 Hz, 2H), 7.69 (t, J= 1.8 Hz, 2H), 7.09 (d, J= 7.7 Hz, 4H), 5.51 (s, 4H), 4.52 (t, J= 5.3 Hz, 4H), 3.83 (s, 6H), 3.78 (t, J= 5.3 Hz, 4H), 3.47 (m, 16H), 2.27 (s, 6H). ^{13}C NMR (100 MHz, DMSO-d$_6$, δ ppm): 145.68, 140.25, 137.47, 136.58, 127.97, 125.42, 124.87, 123.78, 122.29, 69.52, 68.55, 49.57, 48.48, 43.54, 35.79, 20.71. ESI-TOF m/z (%), negative mode: found: 171.0 (100) $[C_7H_7O_3S]^-$, 1087.36 $[C_{47}H_{63}N_{10}O_{14}S_3]^-$, calculated: 171.01, 1087.36.

Bis-1,17-[(1-methyl-pyrrolidinium-1-yl)-1H-1,2,3-triazole-1-yl]-(3,6,9,12,15-pentaoxaheptadecane) di(*p*-toluenesulfonate) (7b)

A mixture of **25b** (0.26 g, 0.90 mmol), compound **21** (0.15 g, 0.45 mmol), DIPEA (0.35 g, 2.70 mmol), and CuBr (0.01 g, 0.092 mmol) in H_2O/DMF (4 mL) was irradiated at 70 W (100 °C) for 10 h. After workup on the crude product following the general procedure, 0.39 g (95%) of a viscous liquid was obtained. ^{1}H NMR (400 MHz, DMSO-d$_6$, δ ppm): 8.40 (s, 2H), 7.47 (d, J = 8.0 Hz, 4H), 7.10 (d, J = 7.9 Hz, 4H), 4.66 (s, 4H), 4.58 (t, J= 5.1 Hz, 4H), 3.83 (t, J= 5.3 Hz, 4H), 3.50 (m, 28H), 2.28 (s, 6H), 2.09 (m, 8H). ^{13}C NMR (100.6 MHz, DMSO-d$_6$, δ ppm): 146.31, 138.02, 136.39, 128. 57, 125.91, 79.08, 69.00, 63.16, 50.08, 48.67, 21.66, 21.2. ESI-TOF m/z (%), negative mode: found: 171.0 (100) $[C_7H_7O_3S]^-$, 1093.42 $[C_{49}H_{73}N_8O_{14}S_3]^-$, calculated: 171.01, 1093.44.

Bis-1,17-[(*N,N,N*-triethylammonium-N-yl)-1H-1,2,3-triazole-1-yl]-(3,6,9,12,15-pentaoxahepta-decane) di(*p*-toluenesulfonate) (7c)

According to the general procedure a mixture of **25c** (0.28 g, 0.90 mmol), compound **21** (0.15 g, 0.45 mmol), DIPEA (0.35 g, 2.70 mmol), and CuBr (0.01 g, 0.09 mmol) in H_2O/DMF (4 mL) was irradiated at 70 W (70 °C) for 12 h and purified as described. The yield of the obtained yellow viscous liquid (0.43

g) was 98%. ^{1}H NMR (400 MHz, DMSO-d$_6$, δ ppm): 1.31 (t, J= 6.8 Hz, 18H), 2.26 (s, 6H), 3.23 (m, 12H), 3.50 (m, 16H), 3.81 (t, J= 5.1 Hz, 4H), 4.50 (t, J= 5.2 Hz, 4H), 4.60 (s, 4H), 7.05 (d, J= 7.8 Hz, 4H), 7.65 (d, J= 8.0 Hz, 4H), 8.56 (s, 2H). ^{13}C NMR (100.6 MHz, DMSO-d$_6$, δ ppm): 144.33, 139.04, 135.09, 129.12, 128.57, 125.78, 70.29, 68.87, 53.19, 51.72, 50.33, 21.18, 7.90. ESI-TOF m/z (%), negative mode: found: 171.0 (100) $[C_7H_7O_3S]^-$, 1125.49 $[C_{51}H_{81}N_8O_{14}S_3]^-$, calculated: 171.01, 1125.50.

α,ω-Bis-[(1-methyl-pyrrolidinium-1-yl)-1H-1,2,3-triazole-1-yl]-[poly(ethylene glycol)] di(methane-sulfonate) (n =8, M$_n$ = 400 g/mol) (8b)

A mixture of compound **22** (0.15 g, 0.37 mmol), **24b** (0.16 g, 0.75 mmol), DIPEA (0.30 g, 2.25 mmol), and CuBr (0.01 g, 0.092 mmol) in H$_2$O/DMF (4 mL) was irradiated at 70 W (70 °C) for 12 h. The subsequent treatment of the crude product according to the procedure resulted in 0.31 g (93%) of product as brown viscous liquid. ^{1}H NMR (400 MHz, DMSO-d$_6$, δ ppm): 8.40 (s, 2H), 4.67 (s, 4H), 4.58 (t, J= 5.2 Hz, 4H), 3.82 (t, J= 5.3 Hz, 4H), 3.48 (m, 32H), 2.96 (s, 6H), 2.30 (s, 6H), 2.09 (m, 8H). ^{13}C NMR (100.6 MHz, DMSO-d$_6$, δ ppm): 136.38, 128.71, 70.11, 69.07, 63.34, 56.74, 50.12, 48.65, 21.73. ESI-TOF m/z (%), positive mode: found: 356.28 (100) $[C_{34}H_{64}O_8N_8]^{2+}$ n = 8, 763.74 $[C_{33}H_{63}N_8O_{10}S]^+$, calculated: 356.24, 763.44. negative mode: found: 94.97 $[CH_3O_3S]^-$, calculated: 94.98.

α,ω-Bis-[(1-methyl-pyrrolidinium-1-yl)-1H-1,2,3-triazole-1-yl]-[poly(ethylene glycol)] di(p-toluenesulfonate) (n =8, M$_n$ = 400 g/mol) (9b)

A mixture of compound **22** (0.15 g, 0.37 mmol), **25b** (0.25 g, 0.75 mmol), DIPEA (0.29 g, 2.24 mmol), and CuBr (0.01 g, 0.092 mmol) in H$_2$O/DMF (4 mL) was irradiated at 70 W (70 °C) for 12 h. Afterwards, the resulted mixture was purified following the method described in general procedure which resulted in 0.35 g (95%) of brown viscous liquid. ^{1}H NMR (400 MHz, DMSO-d$_6$, δ ppm): 2.08 (m, 8H), 2.27 (s, 6H), 2.95 (s, 6H), 3.45 (m, 36H), 3.81 (t, J= 5.3 Hz, 4H), 4.57 (t, J= 5.2 Hz, 4H), 4.65 (s, 4H), 7.09 (d, J= 7.9 Hz, 4H), 7.46 (d, J= 8.0 Hz, 4H), 8.38 (s, 2H). ^{13}C NMR (100.6 MHz, DMSO-d$_6$, δ (ppm): 146.18, 138.02, 136.38, 128.69, 128.47, 125.88, 70.09, 69.03, 63.35, 50.16, 48.72, 21.67, 21.20. ESI-TOF m/z (%), positive mode: found: 356.28 (100) $[C_{34}H_{64}O_8N_8]^{2+}$ n = 8, 839.47 $[C_{39}H_{67}N_8O_{10}S]^+$, calculated: 356.24, 839.47; negative mode: found: 171.0 (100) $[C_7H_7O_3S]^-$, 1181,49 $[C_{53}H_{81}N_8O_{16}S_3]^-$, calculated: 171.01, 1181,51.

α,ω-Bis-[4-(3-methyl-1H-imidazolium-1-yl)-1H-1,2,3-triazole-1-yl]-[poly(ethylene glycol)] di(methanesulfonate) (n= 33, M$_n$= 1550 g/mol) (10a)

A mixture of **23** (M_{theory}= 1550 g/mol) (2.0 g, 1.29 mmol), compound **24a** (0.55 g, 2.58 mmol), DIPEA (1.0 g, 7.74 mmol), and CuBr (0.04 g, 0.26 mmol) in H_2O: DMF 1:1 (40 mL) was stirred under nitrogen atmosphere for 72 h at 50 °C. Afterwards, the crud product was treated as described in general procedure which resulted in 2.52 g (95%) of brown gel like polymer (M_n = 1982 g/mol). ^{1}H NMR (400 MHz, DMSO- d$_6$, δ ppm): 9.23 (s, 2H),8.25 (s, 2H), 7.75 (t, J = 1.8 Hz, 2H), 7.70 (t, J = 1.8 Hz, 2H), 5.53 (s, 4H), 4.53 (t, J = 5.3 Hz, 4H), 3.85 (s, 6H), 3.79 (t, J = 5.3 Hz, 4H), 3.47 (m, 130H), 2.31 (s, 6H). ^{13}C NMR (100.6 MHz, DMSO-d$_6$, δ ppm): 140.31, 136.66, 124.98, 122.30, 70.21, 69.15, 49.55, 43.48, 39.01, 35. ESI-TOF m/z (%), positive mode: 859.50 (100) $[(C_2H_4O)_{31}C_{16}H_{22}N_{10}]^{2+}$, calculated: 859.51.

α,ω-Bis-[(1-methyl-pyrrolidinium-1-yl)-1H-1,2,3-triazole-1-yl]-[poly(ethylene glycol)] di(methanesulfonate) (n=33, M$_n$= 1550 g/mol) (10b)

A mixture of compound **23** (M_{theory}= 1550 g/mol) (2.70 g, 1.74 mmol), **24b** (0.76 g, 3.48 mmol), DIPEA (1.34 g, 10.44 mmol), and CuBr (0.05 g, 0.35 mmol) in H_2O: DMF 1:1 (40 mL) was stirred under nitrogen atmosphere for 48 h at 50 °C. After removing of the solvent, the crude product was purified according to the general procedure. The desired product was obtained as 3.18 g of yellow oil with a yield of 92% (M_n = 1988 g/mol). ^{1}H NMR (400 MHz, DMSO-d$_6$, δ ppm): 8.47 (s, 2H), 4.72 (s, 4H), 4.60 (t, J= 5.2 Hz, 4H), 3.84 (t, J = 5.3 Hz, 4H), 3.51 (m, 138H), 3.16 (s, 8H, H_2O), 3.00 (s, 6H), 2.36 (s, 6H), 2.11 (td, J= 3.5 Hz, J= 7.0 Hz, 8H).^{13}C NMR (100.6 MHz, DMSO-d$_6$, δ ppm): 136.48, 128.78, 70.11, 69.00, 63.29, 56.69, 50.16, 49.04, 21.69. ESI-TOF m/z (%), positive mode: 884.54 (100) $[(C_2H_4O)_{32}C_{16}H_{22}N_{10}]^{2+}$, calculated: 884.55.

3.3.4. Synthesis of poly(isobutylene) based ionic liquids

### Synthesis of azido telechelic poly(isobutylene) (27, 29, 30)
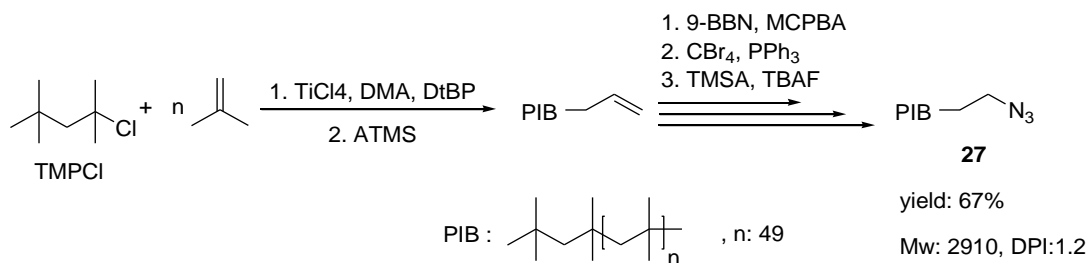
Isobutylene was polymerized via living carbocationic polymerization (LCCP) in the presence of 2-

chlor-2,4,4-trimethylpentane (TMPCl) as initiator and TiCl$_4$ as co-initiator.[248] Quenching of the polymerization with allyltrimethylsilane (ATMS) and further modification of the alkene moiety according to the procedure which is known from the literature,[251] resulted in bromo telechelic poly(isobutylene) (PIB). The bromo- group was subsequently converted to azido- using tetrabutylammoniumfluoride (TBAF) and azidotrimethylsilane (TMSA) following the procedure described in the literature to obtain azido telechelic PIB (**27**). [251,275]
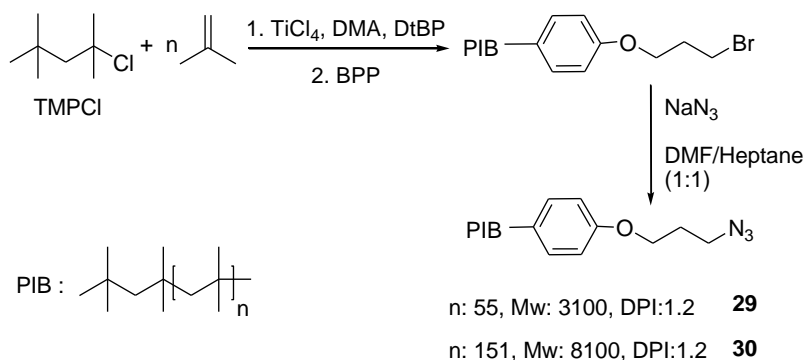
Meanwhile, changing the quenching agent from ATMS to 3-(bromopropoxy)benzene (BPB), according to the work of Storey et al.[252] resulted in bromo telechelic PIB which was containing an extra phenoxy propyl group in comparison to the polymer obtained from the method described earlier. Azido telechelic PIB bearing phenoxy propyl (**29**, **30**) were synthesized via further modification of the obtained bromo telechelic PIBs, with different molecular weights, in the reaction with sodium azide as described in the literature.[251,253]

General procedure to synthesis of ionic liquids containing alkyne moiety (26a-c)
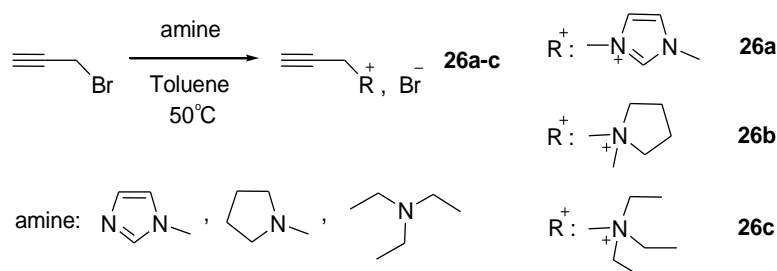
To a solution of propargyl bromide (1.0 equivalent) in dry toluene corresponding amine (1.2 equivalents) was added dropwise. The reaction mixture was stirred at 50 °C. Then, the solvent was

removed from reaction mixture under reduced pressure and the obtained crude product was washed with ethyl acetate.

1-Propargyl-3-methylimidazolium bromide (26a)

1-Methylimidazole (1.02 g, 12.43 mmol) was added dropwisely to a solution of propargyl bromide (1.23 g, 10.36 mmol) in dry toluene (25 mL). After stirring the reaction mixture for 20 h, the obtained product was purified by washing with ethyl acetate. Yield of (**26a**): 1.74 g (8.70 mmol), 84%, as a brownish powder.^{1}H NMR (400 MHz, DMSO-d_6, δ ppm): 9.29 (s, 1H), 7.81 (t, J= 1.8), 7.78 (t, J= 1.8, 1H), 5.24 (d, J= 2.56, 2H), 3.89 (s, 3H), 3.84 (t, J=2.6, 1H). ^{13}C NMR (100 MHz, DMSO-d_6, δ ppm): 136.2, 123.7, 121.8, 78.8, 75.9, 38.4, 35.8.

1-Propargyl-1-methylpyrrolidinium bromide (26b)

After additoin of 1-methylpyrrolidine (1.06 g, 12.43 mmol) to a solution of propargyl bromide (1.23 g, 10.36 mmol) in dry toluene (25 mL) the reaction mixture was stirred for 24 h. After purification, the product (**26b**) was obtained as slightly yellow solid with yield of 88% (1.69 g, 8.28 mmol). ^{1}H NMR (400 MHz, DMSO-d_6, δ ppm): 4.50 (d, J = 2.5, 1H), 4.01 (dt, J = 2.45, 0.74, 2H), 3.63 − 3.49 (m, 4H), 3.15 (s, 3H), 2.18-2.05 (m, 4H). ^{13}C NMR (100 MHz, DMSO-d_6, δ ppm): 81.6, 72.9, 63.0, 52.3, 48.7, 21.4.

1-Propargyl-*N,N,N*-triethylammonium bromide (26c)

According to the general procedure, *N,N,N*-triethylamine (1.25 g, 12.72 mmol) was added to a solution of propargyl bromide (1.23 g, 10.36 mmol) in dry toluene (20 mL) and it was stirred for 16 h. The purification of the product (**26c**) resulted in a white solid with 82% (1.87 g, 8.49 mmol) yield. ^{1}H NMR (400 MHz, DMSO-d_6, δ ppm): 4.34 (d, J = 2.56, 2H), 4.01 (t, J = 2.53, 1H), 3.30 (q, J = 7.2, 6H), 1.23 (t, J=7.2, 9H). ^{13}C NMR (100 MHz, DMSO-d_6, δ ppm): 82.1, 71.9, 52.9, 30.5, 7.3.

General procedure for the synthesis of poly(isobutylene) based ionic liquids via "click" reaction (11a-c, 12a-c, 13a-c)

Azido telechelic PIB (**27**, **29**, **30**) (1.0 equivalent) and corresponding amines containing alkyne moiety (**26a-c**) (2.0 mol equivalents) were dissolved in a solvent mixture of toluene/water/isopropanol (2:1:1) and placed in a microwave vial. After addition of *N,N*-diisopropylethylamine (DIPEA) (10.0

equivalent), the vial was closed with a rubber septum and the solution was purged with nitrogen for 30 min. Afterwards, copper(I) iodide (CuI) (0.2 equivalents) was added to the mixture and the solution was again purged with nitrogen for more than 30 min. Subsequently, the vial was sealed and placed in a microwave reactor, and irradiated under 70-80 W for several h. After termination of irradiation, the organic phase was separated and washed with water (3 times). The crude product obtained after removal of the solvents was purified by column chromatography (stationary phase: SiO_2, eluent: chloroform, $R_f= 1$) to eliminate the unreacted azido telechelic PIB. Then, the eluent was changed to chloroform/methanol (15:1) and the fraction with $R_f= 0.2$ was collected. After evaporating of the solvent, the residue was dissolved in a small amount of chloroform and precipitated into methanol. The precipitate was collected and dried under high vacuum.
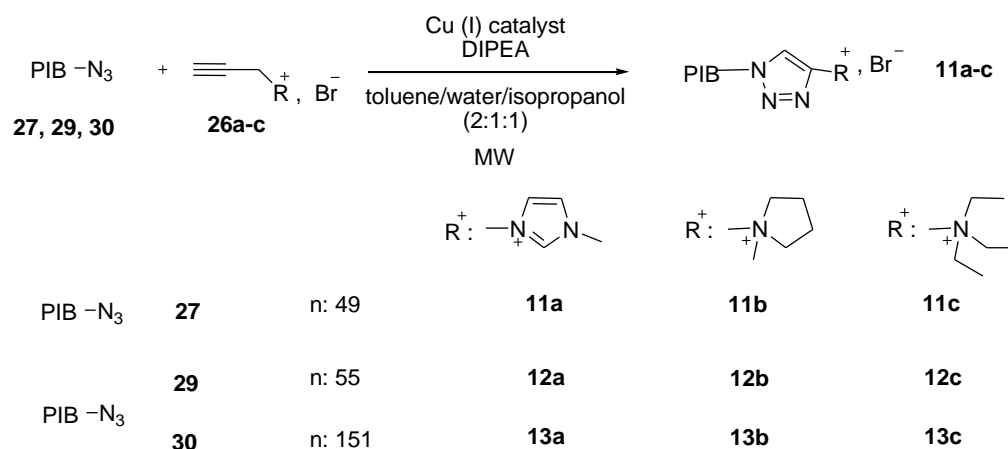
3-Methylimidazolium telechelic PIB bromide (11a)

Compound **26a** (12.09 mg, 0.06 mmol), azido telechelic PIB (**27**) ($M_n= 2920$ g/mol, $M_w/M_n= 1.1$) (100 mg, 0.03 mmol), CuI (10 mg) and DIPEA mixture was prepared and irradiated under 75 W, at 75 °C, for 16 h. Purification of the product according to the described procedure resulted to the desired polymer with a yield of 58%. $M_n= 3256$ g/mol, $M_w/M_n = 1.2$, ^{1}H NMR (400 MHz, $CDCl_3$, δ ppm): 10.70 (s, 1H) 8.47 (s, 1H), 7.63 (s, 1H), 7.09 (s, 1H), 5.86 (s, 2H), 4.29 (t, 2H, J= 7.5), 3.98 (s, 3H), 1.94-1.83 (m, 2H), 1.47-1.36 (m, 104H), 1.16-1.05 (m, 312H), 1.00-0.97 (m, 15H). ^{13}C NMR (100 MHz, $CDCl_3$, δ ppm): 139.74, 137.82, 125.23, 122.69, 122.46, 59.52, 59.39, 59.11, 58.83, 58.20, 55.94, 51.47, 44.40, 42.16, 38.31, 38.14, 38.07, 37.96, 37.81, 37.77, 36.58, 34.83, 32.57, 32.43, 31.23, 31.15, 30.81, 30.78, 29.14, 25.52.

1-Methylpyrrolidinium telechelic PIB bromide (11b)

Compound **26b** (12.24 mg, 0.06), azido telechelic PIB (**27**) (M_n= 2920 g/mol, M_w/M_n= 1.1) (100 mg, 0.03 mmol), CuI (8 mg) and DIPEA mixture was prepared and irradiated under 75 W, at 75 °C , for 16 h. The yield of the product after purification was 52%. M_n= 3259 g/mol, M_w/M_n= 1.2, ^{1}H NMR (400 MHz, CDCl$_3$, δ ppm): 8.52 (s, 1H), 5.02 (s, 2H), 4.34 (t, 2H, J= 7.5), 4.11-4.00 (m, 2H), 3.60- 3.50 (m, 2H), 3.24 (s, 3H), 2.40-2.18 (m, 4H), 1.98-1.81 (m, 2H), 1.47-1.36 (m, 104H), 1.16-1.05 (m, 312H), 1.00-0.97 (m, 15H). ^{13}C NMR (100 MHz, CDCl$_3$, δ ppm): 136,13, 128.42, 63.98, 59.53, 59.39, 59.13, 58.84, 58.21, 55.89, 51.58, 42.17, 38.31, 38.15, 38.08, 37.97, 37.83, 37.78, 34.83, 32.57, 32.43, 31.23, 31.15, 30.82, 30.78, 29.16, 25.53, 21.91.

_N,N,N_-Triethylammonium telechelic PIB bromide (11c)

Compound **26c** (13.20, 0.06 mmol), azido telechelic PIB (**27**) (M_n= 2920 g/mol, M_w/M_n= 1.1) (100 mg, 0.03 mmol), CuI (10 mg) and DIPEA mixture was prepared and irradiated under 70 W, at 75 °C, for 16. The yield of the product after purification was 74%. M_n= 3334 g/mol, M_w/M_n= 1.2, ^{1}H NMR (400 MHz, CDCl$_3$, δ ppm): 8.81 (s, 1H), 5.01 (s, 2H), 4.36 (t, 2H, J= 7.5), 3.48 (q, 6H, J= 7.3), 1.98-1.88 (m, 2H), 1.52 (t, 9H, J= 7.2), 1.45-1.36 (m, 102H), 1.15-1.05 (m, 306H), 0.99-0.95 (m, 15H). ^{13}C NMR (100 MHz, CDCl$_3$, δ ppm): 135.10, 128.39, 59.52, 59.39, 59.14, 58.83, 58.20, 55.90, 53.48, 51.95, 51.52, 42.14, 38.31, 38.23 , 38.14, 38.06, 37.96, 37.82, 37.77, 34.83, 32.57, 32.43, 31.23, 31.15, 30.82, 30.78, 29.15, 25.43, 7.85.

3-Methylimidazolium telechelic PIB bromide (12a)

Compound **26a** (0.13 g, 0.67 mmol), azido telechelic PIB (**29**) (M_n= 3200 g/mol, M_w/M_n= 1.2) (1.00 g, 0.33 mmol), CuI (12 mg), irradiation conditions: 80 W, 85 °C, 16 h. Yield of **12a**: 51% (0.51 g). M_n= 3449 g/mol, M_w/M_n=1.3. ^{1}H NMR (400 MHz, CDCl$_3$, δ ppm): 9.82 (s, 1H), 8.27 (s, 1H), 7.55 (s, 1H), 7.24 (d, J = 8.8 Hz, 2H), 7.12 (m, 1H), 6.77 (d, J = 8.6 Hz, 2H), 5.62 (s, 2H), 4.55 (m, 2H), 3.95 (m, 5H), 2.36 (m, 2H), 2.05–1.05 (m, 370H), 1.04-0.99 (s, 15H), 0.98–0.79 (m, 65H). ^{13}C NMR (100 MHz, CDCl$_3$, δ ppm): 156.0, 143.0, 140.1, 138.1, 127.1, 125.3, 122.7, 122.5, 113.7, 64.2, 59.5, 58.8, 58.2, 47.7, 44.4, 38.1, 36.5, 34.2, 32.4, 32.4, 31.2, 30.8, 30.0, 29.1, 28.0, 26.9, 23.4, 22.4. IR (cm^{-1}): 3449 (w), 2949 (s), 2892 (m), 1744 (w), 1643 (w), 1610 (w), 1511 (w), 1470 (s), 1388 (s), 1364 (s), 1229 (s), 1185 (w), 1049 (w), 949 (w), 829 (w), 760 (w), 626 (w).

1-Methylpyrrolidinium telechelic PIB bromide (12b)

Compound **26b** (0.20 g, 1.02 mmol), azido telechelic PIB (**29**) (M_n= 3200 g/mol, M_w/M_n= 1.2) (1.5 g, 0.50 mmol), CuI (19.4 mg, 0.102 mmol), 80 °C, 4 days. Yield of **12b**: 73% (1.1 g). (M_n= 3054 g/mol, M_w/M_n= 1.3). ^{1}H NMR (400 MHz, CDCl$_3$, δ ppm): 8.55 (s, 1H), 7.24 (d, J = 8.8 Hz, 2H), 6.78 (d, J = 8.7 Hz, 2H), 4.94 (s, 2H), 4.63 (t, J = 7.2 Hz, 2H), 3.97 (m, 4H), 3.50 (t, J = 5.2 Hz, 2H), 3.17 (s, 3H), 2.40 (m, 2H), 2.28 (m, 2H), 2.20 (m, 2H), 1.95–1.05 (m, 345H), 1.04-0.99 (s, 15H), 0.98–0.79 (m, 32H). ^{13}C NMR (100 MHz, CDCl$_3$, δ ppm): 156.0, 143.2, 136.3, 128.8, 127.1, 113.7, 64.0, 59.5, 59.2, 58.8, 58.2, 57.6, 49.4, 48.0, 38.2, 32.4, 31.2, 30.8, 30.7, 30.0, 29.1, 28.0, 26.9, 25.3, 22.7, 21.9, 20.3, 14.1. IR (cm^{-1}): 3449 (s), 2949 (s), 2892 (m), 1744 (w), 1643 (w), 1610 (w), 1511 (w), 1469 (s), 1388 (s), 1364 (s), 1229 (s), 1186 (w), 1047 (w), 949 (w), 827 (w), 732 (w), 638 (w).

N,N,N-Triethylammonium telechelic PIB bromide (12c)

Compound **26c** (0.22 g, 1.02 mmol), azido telechelic PIB (**29**) (M_n= 3200 g/mol, M_w/M_n= 1.2) (1.50 g, 0.50 mmol), CuI (19 mg), 80 °C, 4 days. Yield of **12c**: 82% (1.23 g). (M_n= 3142 g/mol, M_w/M_n= 1.3). ^{1}H NMR (400 MHz, CDCl$_3$, δ ppm): 8.66 (s, 1H), 7.22 (d, J = 8.7 Hz, 2H), 6.78 (d, J = 8.8 Hz, 2H) 4.78 (m, 4H), 4.63 (t, J = 5.7 Hz, 2H), 3.99 (t, J = 6.0 Hz, 6H), 3.99 (q, J = 6.4 Hz, 6H), 2.42 (m, 2H) 1.29 (t, J = 2.5 Hz, 9H), 1.95–1.05 (m, 340H), 1.04-0.99 (s, 15H), 0.98–0.79 (m,47 H). ^{13}C NMR (100 MHz, CDCl$_3$, δ ppm): 156.1, 143.1, 135.1, 128.7, 127.1, 113.7, 64.3, 59.5, 58.8, 58.2, 53.4, 51.9, 47.9, 38.2, 32.4, 31.2, 30.8, 30.7, 30.0, 29.1, 26.9, 25.3, 22.7, 20.3, 14.1, 7.8. IR (cm^{-1}): 3442 (m), 2949 (s), 2892 (m), 1511 (w), 1471 (s), 1388 (s), 1364 (s), 1229 (s), 1186 (w), 1050 (m), 1021 (m), 949 (w), 923 (w), 829 (w), 804 (w).

3-Methylimidazolium telechelic PIB bromide (13a)

Compound **26a** (0.06 g, 0.33 mmol), azido telechelic PIB (**30**) (M_n= 8600 g/mol, M_w/M_n= 1.3) (1.50 g, 0.16 mmol), CuI (6.7 mg), irradiation conditions: 80 W, 85 °C, 16 h. Yield of **13a**: 44% (0.66 g). (M_n= 9043 g/mol, M_w/M_n= 1.2). ^{1}H NMR (400 MHz, CDCl$_3$, δ ppm): 9.94 (s, 1H), 8.28 (s, 1H), 7.58 (s, 1H), 7.25 (d, J = 8.8 Hz, 2H), 7.13 (m, 1H), 6.80 (d, J = 8.7 Hz, 2H), 5.63 (s, 2H), 4.58 (m, 2H), 3.96 (m, 5H), 2.40 (m, 2H), 2.06–1.05 (m, 956H), 1.04-0.99 (s, 15H), 0.98–0.79 (m, 139H). ^{13}C NMR (100 MHz, CDCl$_3$, δ ppm): 155.0, 143.0, 140.1, 137.1, 127.1, 125.3, 122.5, 122.5, 113.7, 64.2, 59.5, 58.5, 58.2, 47.7, 44.4, 38.3, 36.5, 34.2, 32.4, 32.4, 31.2, 30.8, 30.0, 29.1, 28.0, 26.9, 23.2, 22.4. IR (cm^{-1}): 3449 (w), 2949 (s), 2892 (m), 1744 (w), 1643 (w), 1610 (w), 1511 (w), 1470 (s), 1388 (s), 1364 (s), 1229 (s), 1185 (w), 1049 (w), 949 (w), 829 (w), 760 (w), 626 (w).

1-Methylpyrrolidinium telechelic PIB bromide (13b)

Compound **26b** (0.07 g, 0.35 mmol), azido telechelic PIB (**30**) (M_n= 8600 g/mol, M_w/M_n= 1.3) (1.50 g, 0.17 mmol), CuI (6.8 mg), 80 °C, 4 days. Yield of **13b**: 58% (0.87 g). (M_n= 8428 g/mol, M_w/M_n= 1.2). ^{1}H NMR (400 MHz, CDCl$_3$, δ ppm): 8.61 (s, 1H), 7.24 (d, J= 8.8 Hz, 2H), 6.81 (d, J= 8.6 Hz, 2H), 4.98 (s, 2H), 4.64 (t, J= 7.2 Hz, 2H), 4.01 (m, 4H), 3.56 (t, J= 10.2 Hz, 2H), 3.19 (s, 3H), 2.42 (m, 2H), 2.29 (m, 2H), 2.22 (m, 2H), 1.97–1.05 (m, 847H), 1.04-0.99 (s, 15H), 0.98–0.79 (m, 202H). ^{13}C NMR (100 MHz, CDCl$_3$, δ ppm): 156.0, 144.2, 136.3, 128.4, 127.1, 113.7, 64.3, 59.5, 59.2, 58.8, 58.2, 57.6, 49.4, 48.5, 38.2, 32.4, 31.2, 30.8, 30.7, 30.0, 29.4, 28.0, 26.9, 25.3, 22.7, 21.9, 20.3, 14.1. IR (cm^{-1}): 3449 (s), 2949 (s), 2892 (m), 1744 (w), 1643 (w), 1610 (w), 1511 (w), 1469 (s), 1388 (s), 1364 (s), 1229 (s), 1186 (w), 1047 (w), 949 (w), 827 (w), 732 (w), 638 (w).

N,N,N-Triethylammonium telechelic PIB bromide (13c)

Compound **26c** (0.08 g, 0.37 mmol), telechelic PIB (**30**) (M_n= 8600 g/mol, M_w/M_n= 1.3) (1.50 g, 0.18 mmol), CuI (7.2 mg), 80 °C, 4 days. Yield of **13c**: 64% (0.96 g). (M_n=7925 g/mol, M_w/M_n= 1.2). ^{1}H NMR (400 MHz, CDCl$_3$, δ ppm): 8.66 (s, 1H), 7.22 (d, J = 8.7 Hz, 2H), 6.79 (d, J = 8.8 Hz, 2H) 4.76 (m, 4H), 4.64 (t, J = 7.1 Hz, 2H), 3.98 (t, J = 5.7 Hz, 2H), 3.32 (q, J = 7.2 Hz, 6H), 2.40 (m, 2H) 1.29 (t, J = 2.5 Hz, 9H), 1.95–1.05 (m, 878H), 1.04-0.99 (s, 15H), 0.98–0.79 (m,107 H). ^{13}C NMR (100 MHz, CDCl$_3$, δ ppm): 156.1, 143.3, 135.1, 128.7, 127.6, 113.7, 64.3, 59.8, 58.8, 58.2, 53.4, 52.3, 47.9, 38.2, 32.4, 31.2, 30.8, 30.7, 30.0, 29.5, 26.9, 25.3, 22.7, 20.3, 14.1, 7.8. IR (cm^{-1}): 442 (m), 2949 (s), 2892 (m), 1511 (w), 1471 (s), 1388 (s), 1364 (s), 1229 (s), 1186 (w), 1050 (m), 1021 (m), 949 (w), 923 (w), 829 (w), 804 (w).

General procedure for the synthesis of poly(isobutylene) based ionic liquids via anionic exchange reaction (14a-c, 15a-c)

Lithium bis(trifluoromethanesulfonyl)imide salt (2 equivalent) was dissolved in a 0.5 mL of methanol and subsequently was added into a solution of 1 equivalent **12a-c** and **13a-c** in 5mL of chloroform. The obtained mixture was stirred at room temperature. After 72 h. the solvent was removed. The obtained crude product was dissolved in minimal amount of CHCl$_3$ and washed with excess amount of water to remove the inorganic side product of LiBr. Finally, the product was precipitated into methanol to eliminate the excess of lithium bis(trifluoromethanesulfonyl)imide.

3-Methylimidazolium telechelic PIB bis(trifluoromethylsulfonyl)imide (14a)

Pale yellowish, highly viscous liquid, yield of **14a**: 96.7% (0.193 g). M_n= 3460 g/mol, M_w/M_n= 1.4, ^{1}H NMR (400 MHz, CDCl$_3$, δ ppm): 9.82 (s, 1H), 8.27 (s, 1H), 7.55 (s, 1H), 7.24 (d, J = 8.8 Hz, 2H), 7.12 (m, 1H), 6.77 (d, J = 8.6 Hz, 2H), 5.62 (s, 2H), 4.55 (m, 2H), 3.95 (m, 5H), 2.36 (m, 2H), 2.05–1.05 (m, 370 H), 1.04-0.99 (s, 15H), 0.98–0.79 (m, 65H). ^{13}C NMR (100 MHz, CDCl$_3$, δ ppm): 156.0, 143.0, 140.1, 137.0, 138.1, 127.1, 125.3, 122.7, 122.5, 113.7, 64.2, 47.7, 44.4, 36.5, 30.0. ^{19}F NMR (400 MHz, CDCl$_3$, δ ppm): -78.81. IR (cm^{-1}): 3581 (s), 2950 (s), 2922 (m), 2897 (s), 1639 (m), 1578 (w), 1465 (s), 1388 (m), 1348 (s), 1197 (s), 1136 (s), 1058 (s), 949 (w), 924 (w), 795 (w), 742 (w), 656 (m), 617 (m), 573 (m), 511 8 (w).

3-Methylpyrrolidinium telechelic PIB bis(trifluoromethylsulfonyl)imide (**14b**)

Pale yellowish, highly viscous liquid, yield of **14b**: 95% (0.19 g). M_n= 3403 g/mol, M_w/M_n= 1.4. ^{1}H NMR (400 MHz, CDCl$_3$, δ ppm): 8.55 (s, 1H), 7.24 (d, J= 8.8 Hz, 2H), 6.78 (d, J= 8.7 Hz, 2H), 4.94 (s, 2H), 4.63 (t, J= 7.2 Hz, 2H), 3.97 (m, 4H), 3.50 (t, J= 5.2 Hz, 2H), 3.17 (s, 3H), 2.40 (m, 2H), 2.28 (m, 2H), 2.20 (m, 2H), 1.95–1.05 (m, 345H), 1.04-0.99 (s, 15H), 0.98–0.79 (m, 32H). ^{13}C NMR (100 MHz, CDCl$_3$, δ ppm): 156.0, 143.2, 135.5, 136.3, 128.8, 127.1, 113.7, 64.3, 59.5, 58.2, 49.4, 48.0, 28.0. ^{19}F NMR (400 MHz, CDCl$_3$, δ ppm): -78.81. IR (cm^{-1}): 3592 (s), 2950 (s), 2925 (w), 2896 (m), 1661 (m), 1552 (w), 1511 (s), 1469 (s), 1389 (s), 1361 (s), 1349 (w), 1228 (s), 1195 (w), 1137 (s), 1058 (s), 949 (w), 923 (w), 829 (w), 794 (w), 655 (w), 671 (m), 572 (m), 512 (w).

N,N,N-Triethylammonium telechelic PIB bis(trifluoromethylsulfonyl)imide (14c)

Reddish brown, highly viscous liquid, yield of **14c**: 98.5% (0.197 g). M_n= 3315 g/mol, M_w/M_n= 1.4, ^{1}H NMR (400 MHz, CDCl$_3$, δ ppm): 8.66 (s, 1H), 7.22 (d, J= 8.7 Hz, 2H), 6.78 (d, J= 8.8 Hz, 2H) 4.78 (m, 4H), 4.63 (t, J= 5.7 Hz, 2H), 3.99 (t, J= 6.0 Hz, 6H), 3.99 (q, J= 6.4 Hz, 6H), 2.42 (m, 2H) 1.29 (t, J= 2.5 Hz, 9H), 1.95–1.05 (m, 340H), 1.04-0.99 (s, 15H), 0.98–0.79 (m,47 H). ^{13}C NMR (100 MHz, CDCl$_3$, δ ppm): 156.1, 143.1, 136.6, 135.1, 128.7, 127.1, 113.7, 64.3, 59.5, 58.2, 53.4, 32.4, 7.8. ^{19}F NMR (400 MHz, CDCl3, δ ppm): -78.81. IR (cm^{-1}): 3584 (s), 2950 (s), 2924 (m), 1661 (s), 1579 (w), 1549 (w), 1511 (w), 1469 (s), 1388 (s), 1360 (s), 1349 (w), 1228 (s), 1195 (s), 1138 (w), 1058 (s), 949 (w), 924 (w), 795 (w), 656 (m), 617 (w), 571 (w).

3-Methylmidazolium telechelic PIB bis(trifluoromethylsulfonyl)imide (15a)

Pale yellow, highly viscous liquid, yield of **15a** 93% (186 mg). M_n= 9326 g/mol, M_w/M_n= 1.4, ^{1}H NMR

(400 MHz, CDCl$_3$, δ ppm): 9.94 (s, 1H), 8.28 (s, 1H), 7.58 (s, 1H), 7.25 (d, J = 8.8 Hz, 2H), 7.13 (m, 1H), 6.80 (d, J = 8.7 Hz, 2H), 5.63 (s, 2H), 4.58 (m, 2H), 3.96 (m, 5H), 2.40 (m, 2H), 2.06–1.05 (m, 956H), 1.04-0.99 (s, 15H), 0.98–0.79 (m, 139H). ^{13}C NMR (100 MHz, CDCl$_3$, δ ppm): 156.0, 143.0, 140.1, 137.0, 138.1, 127.1, 125.3, 122.7, 122.5, 113.7, 64.2, 47.7, 44.4, 36.5, 30.0. ^{19}F NMR (400 MHz, CDCl$_3$, δ ppm): -78.81.,

3-Methyl-1-pyrrolidinium telechelic PIB bis(trifluoromethylsulfonyl)imide (15b)

Pale yellowish, highly viscous liquid, yield of **15b**: 94% (188 mg). M_n= 9453 g/mol, M_w/M_n= 1.4, ^{1}H NMR (400 MHz, CDCl$_3$, δ ppm): 8.61 (s, 1H), 7.24 (d, J= 8.8 Hz, 2H), 6.81 (d, J= 8.6 Hz, 2H), 4.98 (s, 2H), 4.64 (t, J= 7.2 Hz, 2H), 4.01 (m, 4H), 3.56 (t, J= 10.2 Hz, 2H), 3.19 (s, 3H), 2.42 (m, 2H), 2.29 (m, 2H), 2.22 (m, 2H), 1.97–1.05 (m, 847H), 1.04-0.99 (s, 15H), 0.98–0.79 (m, 202H). ^{13}C NMR (100 MHz, CDCl$_3$, δ ppm): 156.0, 143.2, 135.5, 136.3, 128.8, 127.1, 113.7, 64.3, 59.5, 58.2, 49.4, 48.0, 28.0. ^{19}F NMR (400 MHz, CDCl$_3$, δ ppm): -78.81.

N,N,N-Triethylammonium telechelic PIB bis(trifluoromethylsulfonyl)imide (15c)

Red brown, highly viscous liquid, yield of **15c**: 98% (196 mg). M_n= 8321 g/mol, M_w/M_n= 1.4, ^{1}H NMR (400 MHz, CDCl$_3$, δ ppm): 8.66 (s, 1H), 7.22 (d, J= 8.7 Hz, 2H), 6.79 (d, J= 8.8 Hz, 2H) 4.76 (m, 4H), 4.64 (t, J= 7.1 Hz, 2H), 3.98 (t, J= 5.7 Hz, 2H), 3.32 (q, J= 7.2 Hz, 6H), 2.40 (m, 2H) 1.29 (t, J= 2.5 Hz, 9H), 1.95–1.05 (m, 878H), 1.04-0.99 (s, 15H), 0.98–0.79 (m,107 H). ^{13}C NMR (100, MHz, CDCl$_3$, δ ppm): 156.1, 143.1, 136.6, 135.1, 128.7, 127.1, 113.7, 64.3, 59.5, 58.2, 53.4, 32.4, 7.8. ^{19}F NMR (400 MHz, CDCl$_3$, δ ppm): -78.81.

4. Summary

The aim of this work was to develop an efficient synthetic approach toward polymeric ionic liquids (POILs) and investigate the properties of the obtained materials with regard to the nature of the polymer, chain length, and the type of the associating cations and anions. In this respect, two different polymers, poly(ethylene glycol) and poly(isobutylene), with different molecular weights were selected as hydrophilic and hydrophobic polymers to be transformed to imidazolium, pyrrolidinium, and ammonium based polymeric ionic liquids.

Poly(ethylene glycol)-based ionic liquids (PEGILs)
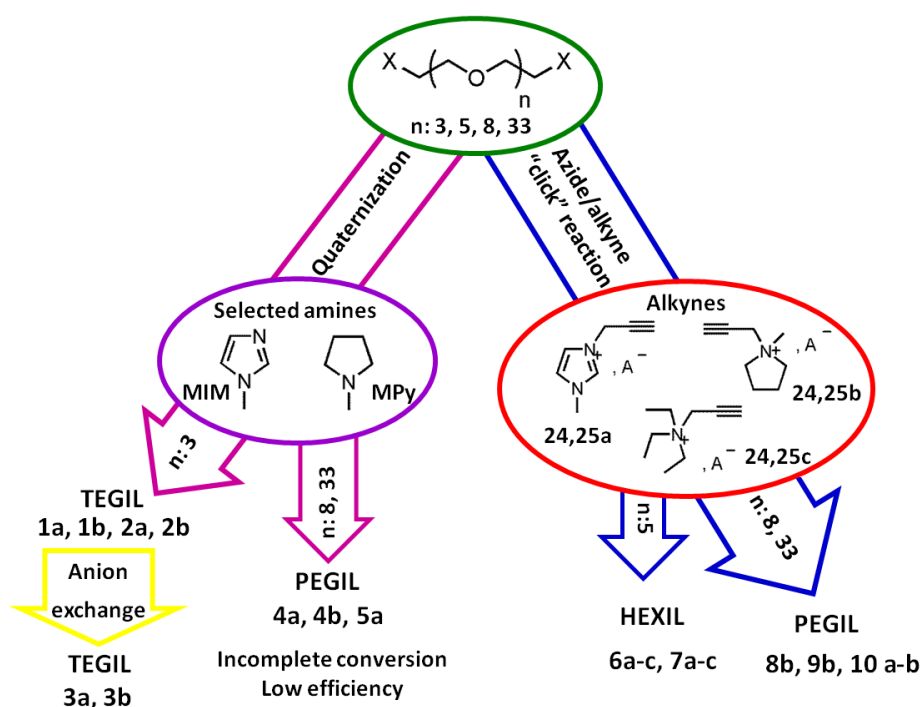
Figure 4.1. Schematic representation of different strategies toward synthesis of **TEGILs**, **HEXILs**, and **PEGILs**.

Poly(ethylene glycol)s with n=3 (**TEG**), 5 (**HEX**), 8, and 33 (**PEG**) were planned to react with the corresponding amines to obtain the poly(ethylene glycol)-based ionic liquids. Tetraethylene glycol (n=3) was selected as a model structure to evaluate the condition of the quaternization reaction for the synthesis of the poly(ethylene glycol)-based ionic liquids. As the chain length was short, the reaction succeeded smoothly and resulted in **1a,b**, **2a,b** with a reasonable yield. Further variation in the structure of the synthesized ionic liquids (**3a,b**) was achieved via anion exchange. With increasing

the polymer chain length, efficient synthesis of the projected **PEGILs** (**4a,b** and **5a**) became difficult due to incomplete conversion of the functional groups of the primary polymer chain. Thus, azide/alkyne "click" reaction was developed as a new strategy to attach the ionic moieties to the body of the polymer chain. For this reason, azido- derivative of hexaethylene glycol (n=5) was conducted with alkyne compounds bearing desired ionic moiety (**24, 25c**). The reaction of the azido-functionalized hexaethylene glycol with corresponding alkyne moieties in the presence of Cu (I) catalyst and microwave or conventional heating resulted in efficient synthesis of the projected products (**6a-c**, **7a-c**). A similar procedure was extended to poly(ethylene glycol)s with longer chain length (n=8, 33), where the quaternization reaction failed. Accordingly, azide/alkyne "click" reaction resulted in successful synthesis of poly(ethylene glycol)-based ionic liquids with different chain length as well as different cations and anions (**8,9b** and **10a,b**). The profound characterization of the all synthesized compounds was performed via spectroscopic methods. ^{1}H and ^{13}C NMR provided firm evidence of the existence and purity of the materials. Furthermore, ESI-TOF-MS analysis of the synthesized materials verified the presence of the projected structures for both oligomeric and polymeric ionic liquids. It is worth to mention that, ESI-TOF-MS analysis of the oligomeric ionic liquids revealed the formation of the variety of aggregates from ionic liquids associated with corresponding counter anions, Br$^-$, Cl$^-$, or combinations of two anions. TGA and DSC analysis also provided valuable information about thermal behavior of the synthesized materials. According to the results, all synthesized materials exhibited higher thermal stability (293-431 °C) comparing to their analogous oligomers or polymers without ionic moieties. Increasing chain length resulted in decreasing thermal stability. Pyrrolidinium derivatives demonstrated higher thermal stability comparing to imidazolium and ammonium where the anions and the chain length were identical. The influence of the associating anion on thermal stability of the synthesized ionic liquids determined as follow: Tf$_2$N$^-$ >MsO$^-$>Cl$^-$.

Poly(isobutylene)-based ionic liquids (PIBILs)

To investigate the influence of the ionic moieties on physical and mechanical properties of a hydrophobic polymer, a series of novel poly(isobutylene)-based ionic liquids were successfully synthesized (**11-13a,b,c**). The designed **PIBILs** were consisted of polymers with two different molecular weights (~8000 and ~3000 g.mol^{-1}). First, isobutylene was polymerized via living carbocationic polymerization (LCCP) and quenched with two different quenching agents which

results in alkene and bromo functionalized telechelic polymers. These polymers were converted to azido functionalized PIB (**27**, **29** and **30**) and were reacted with imidazolium, pyrrolidinium, and ammonium derivatives bearing alkyne moieties (**26a-c**). The azide/alkyne "click" reaction was performed under microwave irradiation, in the presence of CuI as a catalyst. Further variation in anion combination was achieved via anion exchange in the solution of lithium bistriflimide salt (**14-15a,b,c**).
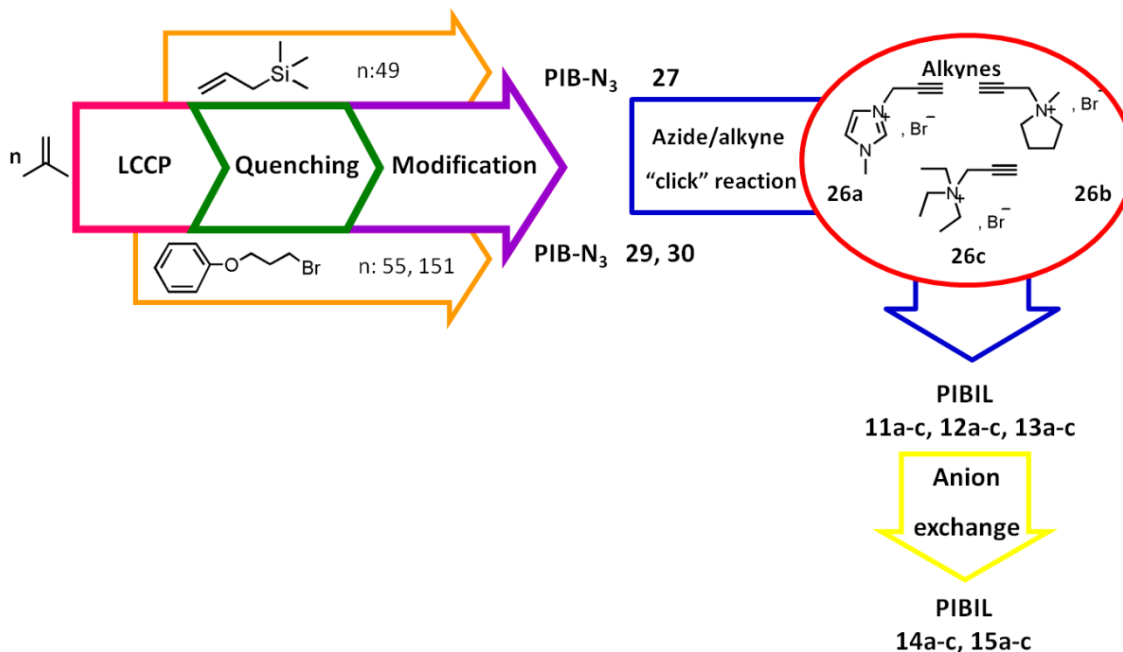
Figure 4.2. Schematic representation of different strategies toward synthesis of **PIBILs**.

All of the synthesized POILs were characterized by ^{1}H and ^{13}C NMR spectroscopy. ^{19}F NMR and IR spectroscopy were used to confirm the occurrence of the anion exchanges. Furthermore, the structure of the synthesized polymers was also proved by MALDI-TOF analysis. TGA analysis of the synthesized POILs demonstrated two decomposition points for most of the products. The first decomposition was detected in the range of 100-210 °C and attributed to the moisture and solvent residue trapped in the product, while the main decomposition occurred around 367–395 °C. Both cation and anion had influence on the thermal stability of the synthesized products. For the first series of the products the cation effect was significant as the anions were identical. However, for the second series of the materials the effect of the anion was more pronounced. In general, POILs containing bromide exhibited a higher thermal stability in comparison to bistriflimide counter anion.

Meanwhile, DSC analysis proved a slight increase in T_g of the products as a result of the presence of the ionic moieties. Furthermore, all synthesized PIBILs associated with bistriflimide anion exhibited an additional T_g as a result of the formation of the clusters according to EHM theory. Due to high polarity difference between ionic end group and hydrophobic nature of poly(isobutylene), the synthesized POILs constructed multiplets with restricted mobility regions resulted in cluster formation, similar to the behavior of ionomers. The occurrence of such phenomenon in all synthesized **PIBILs** except **15a-c** is proved by means of SAXS measurements. According to the results, the confirmed nanostructural organizations were detected in simple cubic confinement at room temperature. Furthermore, temperature dependent in situ SAXS measurements of the samples demonstrated a reversible temperature dependent order-disorder transition, in most of the synthesized **PIBILs**. The short relaxation time required for the restoration of the primary ordered structure was implying the self healing ability of the designed materials. Rheological measurements on the synthesized **PIBILs** confirmed the existence of the nanostructural organizations. According to the results, the constructed multiplets in the cluster were sliding on each other resulting in a rubbery plateau up to the temperature where the cluster was destroyed.
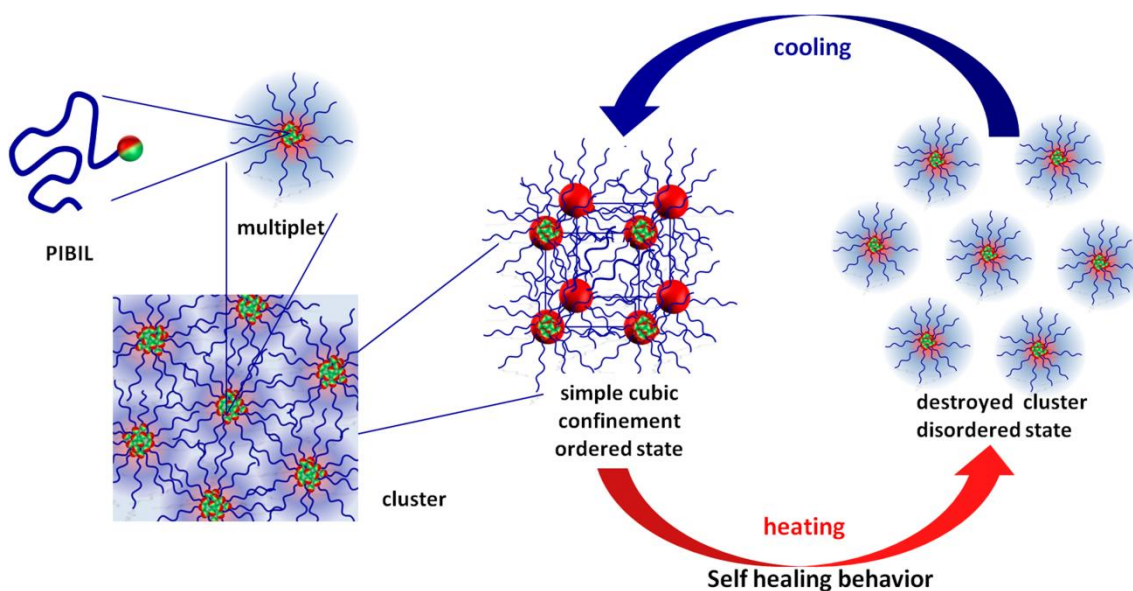
Figure 4.3. Schematic representation of the formation of multiplet and cluster resulted in ordered structure with simple cubic confinement. Increasing the temperature leads to the reversible destruction of the clusters and flow of the material as an indication of self healing behaviour.

.

1. Wasserscheid, P.; Welton, T. *Ionic liquids in synthesi;* 2nd ed.; Wiley-VCH: Weinheim, 2008.

2. Welton, T. *Chem. Rev.* **1999,** *99*, 2071-2083.

3. Sun, J.; Cheng, W.; Fan, W.; Wang, Y.; Meng, Z.; Zhang, S. *Catal. Today* **2009,** *148*, 361-367.

4. Hallett, J. P.; Welton, T. *Chem. Rev.* **2011,** *111*, 3508-3576.

5. Giernoth, R. *Angew. Chem. Int. Ed.* **2010,** *49*, 2834-2839.

6. Walden, P. *Bull. Acad. Sci. St. Petersburg* **1914**, 405-422.

7. Endres, F.; Zein El Abedin, S. *Phys. Chem. Chem. Phys.* **2006,** *8*, 2101-2116.

8. Lu, J.; Yan, F.; Texter, J. *Prog. Polym. Sci.* **2009,** *34*, 431-448.

9. Kubisa, P. *Prog. Polym. Sci.* **2004,** *29*, 3-12.

10. Armand, M.; Endres, F.; MacFarlane, D. R.; Ohno, H.; Scrosati, B. *Nat. Mater.* **2009,** *8*, 621-629.

11. MacFarlane, D. R.; Tachikawa, N.; Forsyth, M.; Pringle, J. M.; Howlett, P. C.; Elliott, G. D.; Davis, J. H.; Watanabe, M.; Simon, P.; Angell, C. A. *Energ. Environ. Sci.* **2014,** *7*, 232-250.

12. Tarascon, J. M.; Armand, M. *Nature* **2001,** *414*, 359-367.

13. Singh, V. V.; Nigam, A. K.; Batra, A.; Boopathi, M.; Singh, B.; Vijayaraghavan, R. *Int. J. Electrochem.* **2012,** *2012,* 1-19.

14. Li, Y. L.; Gross, M. L. *J. Am. Soci. Mass Spectrom.* **2004,** *15*, 1833-1837.

15. Tang, J.; Tang, H.; Sun, W.; Radosz, M.; Shen, Y. *Polymer* **2005,** *46*, 12460-12467.

16. Stojanovic, A.; Kogelnig, D.; Fischer, L.; Hann, S.; Galanski, M.; Groessl, M.; Krachler, R.; Keppler, B. K. *Aust. J. Chem.* **2010,** *63*, 511-524.

17. Welton, T. *Coord. Chem. Rev.* **2004,** *248*, 2459-2477.

18. Wasswerscheid, P.; Keim, W. *Angew. Chem. Int. Ed.* **2000,** *39*, 3772-3789.

19. Kim, D. W.; Chi, D. Y. *Angew. Chem.* **2004,** *116*, 489-491.

20. Zhou, F.; Liang, Y.; Liu, W. *Chem. Soc. Rev.* **2009,** *38*, 2590-2599.

21. Minami, I. *Molecules* **2009,** *14*, 2286-2305.

22. Plechkova, N. V.; Seddon, K. R. *Chem. Soc. Rev.* **2008,** *37*, 123-150.

23. Petkovic, M.; Seddon, K. R.; Rebelo, L. N.; Silva Pereira, C. *Chem. Soc. Rev.* **2011,** *40,* 1383-1403.

24. Marcilla, R.; Alberto Blazquez, J.; Rodriguez, J.; Pomposo, J. A.; Mecerreyes, D. *J. Polym. Sci. Pol. Chem.* **2004,** *42*, 208-212.

25. Marcilla, R.; Sanchez-Paniagua, M.; Lopez-Ruiz, B.; Lopez-Cabarcos, E.; Ochoteco, E.; Grande, H.; Mecerreyes, D. *J. Polym. Sci. Pol. Chem.* **2006,** *44*, 3958-3965.

26. Nakajima, H.; Ohno, H. *Polymer* **2005,** *46*, 11499-11504.

27. Firestone, M. A.; Green, O.; Grubjesic, S.; Lee, S. W. *Polym. Rev.* **2009,** *49*, 339-360.

28. Mecerreyes, D. *Prog. Polym. Sci.* **2011,** *36,* 1629-1648.

29. Yuan, J.; Antonietti, M. *Polymer* **2011,** *52*, 1469-1482.

30. Shaplov, A. S.; Vlasov, P. S.; Lozinskaya, E. I.; Ponkratov, D. O.; Malyshkina, I. A.; Vidal, F.; Okatova, O. V.; Pavlov, G. M.; Wandrey, C.; Bhide, A.; Schönhoff, M.; Vygodskii, Y. S. *Macromolecules* **2011**, *44,* 9792-9803.

31. Shaplov, A. S.; Lozinskaya, E. I.; Vygodskii, Y. S. In *Electrochemical Properties and Applications of Ionic Liquids*; Torriero, A. A. J.; Shiddiky, M. J. A., Eds; Nova Publishers: New York, 2001, p 203.

32. Ohno, H. *Macromol. Symp.* **2007,** *249-250*, 551-556.

33. Ohno, H. *Electrochim. Acta* **2001,** *46*, 1407-1411.

34. Yoshizawa, M.; Ogihara, W.; Ohno, H. *Polym. Adv. Technol.* **2002,** *13*, 589-594.

35. Ohno, H.; Ito, K. *Chem. Lett.* **1998,** *27*, 751-752.

36. Washiro, S.; Yoshizawa, M.; Nakajima, H.; Ohno, H. *Polymer* **2004,** *45*, 1577-1582.

37. Ohno, H.; Yoshizawa, M.; Ogihara, W. *Electrochim. Acta* **2004,** *50*, 255-261.

38. Chen, H.; Choi, J.-H.; Salas-de la Cruz, D.; Winey, K. I.; Elabd, Y. A. *Macromolecules* **2009,** *42*, 4809-4816.

39. Ogihara, W.; Suzuki, N.; Nakamura, N.; Ohno, H. *Polym. J.* **2006,** *38*, 117.

40. Yoshizawa, M.; Hirao, M.; Ito-Akita, K.; Ohno, H. *J. Mater. Chem.* **2001,** *11*, 1057-1062.

41. Schüler, F.; Kerscher, B.; Beckert, F.; Thomann, R.; Mülhaupt, R. *Angew. Chem. Int. Ed.* **2013,** *52*, 455-458.

42. Murugan, E.; Pakrudheen, I. *Appl. Catal. A.* **2012,** *439–440*, 142-148.

43. Kensuke, N.; Ryusuke, S.; Maki, Y.; Fadila Djouadi, B.; Yoko, A.; Yasuyuki, I.; Sonu Ram, S.; Kumar Sai, S.; Noriyoshi, M.; Shogo, T.; Shinichi, S. *Polym. J.* **2014,** *46*, 42-51.

44. Vygodskii, Y. S.; Shaplov, A. S.; Lozinskaya, E. I.; Lyssenko, K. A.; Golovanov, D. G.; Malyshkina, I. A.; Gavrilova, N. D.; Buchmeiser, M. R. *Macromol. Chem. Phys.* **2008,** *209*, 40-51.

45. Pont, A.-L.; Marcilla, R.; De Meatza, I.; Grande, H.; Mecerreyes, D. *J. Power Sources* **2009,** *188*, 558-563.

46. Nakai, Y.; Ito, K.; Ohno, H. *Solid State Ionics* **1998,** *113–115*, 199-204.

47. Ohno, H.; Nakai, Y.; Ito, K. *Chem. Lett.* **1998,** *27*, 15-16.

48. Sarma, N. S.; Dutta, A.; Dass, N. N. *Eur. Polym. J.* **2003,** *39*, 1071-1075.

49. Zhang, Q.; Wang, X.; Barrett, C. J.; Bazuin, C. G. *Chem. Mater.* **2009,** *21*, 3216-3227.

50. Wielema, T. A.; Engberts, J. B. F. N. *Eur. Polym. J.* **1987,** *23*, 947-950.

51. Hirao, M.; Ito, K.; Ohno, H. *Electrochim. Acta* **2000,** *45*, 1291-1294.

52. Ding, S.; Tang, H.; Radosz, M.; Shen, Y. *J. Polym. Sci. A Polym. Chem.* **2004,** *42*, 5794-5801.

53. Tang, H.; Tang, J.; Ding, S.; Radosz, M.; Shen, Y. *J. Polym. Sci. A Polym. Chem.* **2005,** *43*, 1432-1443.

54.   Han, H.; Chen, F.; Yu, J.; Dang, J.; Ma, Z.; Zhang, Y.; Xie, M. *J. Polym. Sci. A Polym. Chem.* **2007,** *45*, 3986-3993.

55.   Mori, H.; Yahagi, M.; Endo, T. *Macromolecules* **2009,** *42*, 8082-8092.

56.   Vijayakrishna, K.; Jewrajka, S. K.; Ruiz, A.; Marcilla, R.; Pomposo, J. A.; Mecerreyes, D.; Taton, D.; Gnanou, Y. *Macromolecules* **2008,** *41*, 6299-6308.

57.   Vijayakrishna, K.; Mecerreyes, D.; Gnanou, Y.; Taton, D. *Macromolecules* **2009,** *42*, 5167-5174.

58.   Batra, D.; Seifert, S.; Firestone, M. A. *Macromolecular Chemistry and Physics* **2007,** *208*, 1416-1427.

59.   Bara, J. E.; Lessmann, S.; Gabriel, C. J.; Hatakeyama, E. S.; Noble, R. D.; Gin, D. L. *Ind. Eng. Chem. Res.* **2007,** *46*, 5397-5404.

60.   Vygodskii, Y. S.; Shaplov, A. S.; Lozinskaya, E. I.; Vlasov, P. S.; Malyshkina, I. A.; Gavrilova, N. D.; Santhosh Kumar, P.; Buchmeiser, M. R. *Macromolecules* **2008,** *41*, 1919-1928.

61.   Vygodskii, Y. S.; Shaplov, A. S.; Lozinskaya, E. I.; Filippov, O. A.; Shubina, E. S.; Bandari, R.; Buchmeiser, M. R. *Macromolecules* **2006,** *39*, 7821-7830.

62.   Jaeger, W.; Wendler, U.; Lieske, A.; Bohrisch, J.; Wandrey, C. *Macromol. Symp.* **2000,** *161*, 87-96.

63.   Bohrisch, J.; Wendler, U.; Jaeger, W. *Macromol. Rapid Commun.* **1997,** *18*, 975-982.

64.   Wendler, U.; Bohrisch, J.; Jaeger, W.; Rother, G.; Dautzenberg, H. *Macromol. Rapid Commun.* **1998,** *19*, 185-190.

65.   Li, W.; Kang, J.; Li, X.; Fang, S.; Lin, Y.; Wang, G.; Xiao, X. *J. Photochem. Photobiol. A Chem.* **2005,** *170*, 1-6.

66.   Brodowski, G.; Horvath, A.; Ballauff, M.; Rehahn, M. *Macromolecules* **1996,** *29*, 6962-6965.

67.   Wittemann, M. *Chem. Commun.* **1998,** *5*, 623-624.

68.   Chiang, L. Y.; Swirczewski, J. W.; Ramanarayanan, T. A.; Mumford, J. D. *Chem. Mater.* **1992,** *4*, 245-247.

69.   Zhang, N.; Wu, R.; Li, Q.; Pakbaz, K.; Yoon, C. O.; Wudl, F. *Chem. Mater.* **1993,** *5*, 1598-1599.

70.   Huddleston, J. G.; Visser, A. E.; Reichert, W. M.; Willauer, H. D.; Broker, G. A.; Rogers, R. D. *Green Chem.* **2001,** *3*, 156-164.

71.   Gregor, H. P.; Gold, D. H. *J. of Phy. Chem.* **1957,** *61*, 1347-1352.

72.   Bohrisch, J.; Eisenbach, C.; Jaeger, W.; Mori, H.; Müller, A. E.; Rehahn, M.; Schaller, C.; Traser, S.; Wittmeyer, P. New Polyelectrolyte Architectures. In *Polyelectrolytes with Defined Molecular Architecture;* Schmidt, M., Ed. Springer Berlin Heidelberg: 2004; Vol. 165, pp 1-42.

73.   Eisenberg, A.; Rinaudo, M. *Polym. Bull.* **1990,** *24*, 671-671.

74.   Tang, S. K.; Baker, G. A.; Zhao, H. *Chem. Soc. Rev.* **2012,** *41*, 4030-4066.

75.   Ganapatibhotla, L. V. N. R.; Zheng, J.; Roy, D.; Krishnan, S. *Chem. Mater.* **2010,** *22*, 6347-6360.

76.   Golgovici, F.; Visan, T. *Chalcog. Lett.* **2011,** *8*, 487-497.

77. Fujii, K.; Asai, H.; Ueki, T.; Sakai, T.; Imaizumi, S.; Chung, U. i.; Watanabe, M.; Shibayama, M. *Soft Matter* **2012,** *8*, 1756-1759.

78. Döbbelin, M.; Azcune, I.; Bedu, M.; Ruiz de Luzuriaga, A.; Genua, A.; Jovanovski, V.; Cabañero, G.; Odriozola, I. *Chem. Mater.* **2012**. *24,* 1583-1590.

79. Matsumoto, K.; Endo, T. *J. Polym. Sci. A Polym. Chem.* **2011,** *49*, 3582-3587.

80. Wang, P.; Fang, J.; Qin, S.; Kang, Y.; Zhu, D. M. *J. Phys. Chem. C* **2009,** *113*, 13793-13800.

81. Fraga-Dubreuil, J.; Famelart, M. H.; Bazureau, J. P. *Org. Process Res. Dev.* **2002,** *6*, 374-378.

82. Bailey, F. E. *Poly(ethylene oxide);* Academic Press: New York, 1976.

83. Zalipsky, S. *Bioconjugate Chem.* **1995,** *6*, 150-165.

84. Dreborg, S.; Akerblom, E. B. *Crit. Rev. Ther. Drug Carr. Syst.* **1990,** *6*, 315-365.

85. Kubisa, P.; Biedroń, T. *Macromol. Chem. Phys.* **1996,** *197*, 31-40.

86. Kubisa, P.; Biedroń, T. *Macromol. Chem. Phys.* **1996,** *197*, 19-30.

87. Bazuin, C. G.; Eisenberg, A. *J. Chem. Educ.* **1981,** *58*, 938.

88. Bückmann, A. F.; Morr, M.; Johansson, G. *Macromol. Chem. Phys* **1981,** *182*, 1379-1384.

89. Ohno, H.; Ito, K. *Polymer* **1995,** *36*, 891-893.

90. Tominaga, Y.; Ito, K.; Ohno, H. *Polymer* **1997,** *38*, 1949-1951.

91. Anderson, J. L.; Ding, R. F.; Ellern, A.; Armstrong, D. W. *J. Am. Chem. Soc.* **2005,** *127*, 593-604.

92. Armstrong, D. W.; Anderson, J. High stability diionic liquid salts. US 20120215005 A1, August 23, 2008.

93. Han, X.; Armstrong, D. W. *Org. Lett.* **2005,** *7*, 4205-4208.

94. Jones, W. R.; Shogrin, B. A.; Jansen, M. J. *J. Synth. Lubr.* **2000,** *17*, 109-122.

95. Jin, C. M.; Ye, C. F.; Phillips, B. S.; Zabinski, J. S.; Liu, X. Q.; Liu, W. M.; Shreeve, J. M. *J. Mater. Chem.* **2006,** *16*, 1529-1535.

96. Huang, K.; Han, X.; Zhang, X.; Armstrong, D. *Anal. Bioanal. Chem.* **2007,** *389*, 2265-2275.

97. van den Broeke, J.; Winter, F.; Deelman, B.-J.; van Koten, G. *Org. Lett.* **2002,** *4*, 3851-3854.

98. Weyershausen, B.; Hell, K.; Hesse, U. *Green Chem.* **2005,** *7*, 283-287.

99. Geldbach, T. J.; Zhao, D.; Castillo, N. C.; Laurenczy, G.; Weyershausen, B.; Dyson, P. J. *J. Am. Chem. Soc.* **2006,** *128*, 9773-9780.

100. Peng, J. J.; Li, J. Y.; Bai, Y.; Gao, W. H.; Qiu, H. Y.; Wu, H.; Deng, Y.; Lai, G. Q. *J. Mol. Catal. A: Chem.* **2007,** *278*, 97-101.

101. Wu, C.; Peng, J.; Li, J.; Bai, Y.; Hu, Y.; Lai, G. *Catal. Commun.* **2008,** *10*, 248-250.

102. Chandrasekhar, S.; Narsihmulu, C.; Sultana, S. S.; Reddy, N. R. *Org. Lett.* **2002,** *4*, 4399-4401.

103. Zhi, H.; Lü, C.; Zhang, Q.; Luo, J. *Synfacts* **2009,** *2009*, 0930-0930.

104. Lu, T.; Mao, Y.; Yao, K.; Xu, J.; Lu, M. *Catal. Commun.* **2012,** *27*, 124-128.

105. Wang, P.-C.; Lu, M. *Tetrahedron Lett.* **2011,** *52*, 1452-1455.

106. Luo, J.; Zhang, Q. *Monatsh. Chem. Chem. Mon.* **2011,** *142*, 923-930.

107. Hu, Y. L.; Jiang, H.; Zhu, J.; Lu, M. *New J. Chem.* **2011,** *35*, 292-298.

108. Wang, Z.-g.; Jin, Y.; Cao, X.-h.; Lu, M. *New J. Chem.* **2014,** *38*, 4149-4154.

109. Petiot, P.; Charnay, C.; Martinez, J.; Puttergill, L.; Galindo, F.; Lamaty, F.; Colacino, E. *Chem. Commun.* **2010,** *46*, 8842-8844.

110. Jadhav, V. H.; Jeong, H.-J.; Lim, S. T.; Sohn, M.-H.; Kim, D. W. *Org. Lett.* **2011,** *13*, 2502-2505.

111. Liu, N.; Liu, C.; Jin, Z. *Green Chem.* **2012,** *14*, 592-597.

112. Wang, Y.; Luo, J.; Liu, Z. *J. Organomet. Chem.* **2013,** *739*, 1-5.

113. Wang, Y.; Luo, J.; Hou, T.; Liu, Z. *Aust. J. Chem.* **2013,** *66*, 586-593.

114. Brzezińska, K.; Chwiałkowska, W.; Kubisa, P.; Matyjaszewski, K.; Penczek, S. *Macromol. Chem. Phys.* **1977,** *178*, 2491-2494.

115. Matyjaszewski, K.; Penczek, S. *Macromol. Chem. Phys.* **1981,** *182* (6), 1735-1742.

116. Kubisa, P.; Penczek, S. *Macromol. Chem. Phys.* **1979,** *180* (7), 1821-1823.

117. Berti, C.; Colonna, M.; Binassi, E.; Fiorini, M.; Karanam, S.; Brunelle, D. J. *React. Funct. Polym.* **2010,** *70*, 366-375.

118. Colonna, M.; Berti, C.; Binassi, E.; Fiorini, M.; Sullalti, S.; Acquasanta, F.; Vannini, M.; Di Gioia, D.; Aloisio, I.; Karanam, S.; Brunelle, D. J. *React. Funct. Polym.* **2012,** *72*, 133-141.

119. Colonna, M.; Berti, C.; Binassi, E.; Fiorini, M.; Sullalti, S.; Acquasanta, F.; Vannini, M.; Di Gioia, D.; Aloisio, I. *Polymer* **2012,** *53*, 1823-1830.

120. Raynaud, J.; Absalon, C.; Gnanou, Y.; Taton, D. *J. Am. Chem. Soc.* **2009,** *131*, 3201-3209.

121. Biedroń, T.; Pietrzak, Ł.; Kubisa, P. *J. Polym. Sci. A Polym. Chem.* **2011,** *49*, 5239-5244.

122. Bates, F.; Fredrickson, G. *Phys. Today* **1999,** *52*, 32-38.

123. Mai, Y.; Eisenberg, A. *Chem. Soc. Rev.* **2012,** *41*, 5969-5985.

124. Eisenberg, A.; Hird, B.; Moore, R. B. *Macromolecules* **1990,** *23*, 4098-4107.

125. Cho, B.-K.; Jain, A.; Gruner, S. M.; Wiesner, U. *Science* **2004,** *305*, 1598-1601.

126. Hardacre, C.; Holbrey, J. D.; McMath, S. E. J.; Nieuwenhuyzen, M.; Hanke, C. *Am. Chem. Soc.* **2001,** *221*, 625-626.

127. Aerov, A. A.; Khokhlov, A. R.; Potemkin, I. *J. Phys. Chem. B* **2007,** *111*, 10189-10193.

128. Canongia Lopes, J. N. A.; Pádua, A. A. H. *J. Phys. Chem. B* **2006,** *110*, 3330-3335.

129. Triolo, A.; Russina, O.; Bleif, H.-J.; Di Cola, E. *J. Phys. Chem. B* **2007,** *111*, 4641-4644.

130. Del Pópolo, M. G.; Voth, G. A. *J. Phys. Chem. B* **2004,** *108*, 1744-1752.

131. Hardacre, C.; Holbrey, J. D.; McMath, S. E. J.; Bowron, D. T.; Soper, A. K. *J. Phys. Chem. B* **2003,** *118*, 273-278.

132. Urahata, S. M.; Ribeiro, M. C. C. *J. Chem. Phys.* **2004,** *120*, 1855-1863.

133. Wang, Y.; Voth, G. A. *J. Am. Chem. Soc.* **2005,** *127*, 12192-12193.

134. Canongia Lopes, J. N. A.; Pádua, A. A. H. *J. Phys. Chem. B* **2006,** *110*, 3330-3335.

135. Wilson, M.; Madden, P. A. *Phys. Rev. Lett.* **1994,** *72*, 3033.

136. Sanmartín Pensado, A.; Malfreyt, P.; Pádua, A. A. H. *J. Phys. Chem. B* **2009,** *113*, 14708-14718.

137. Deetlefs, M.; Hardacre, C.; Nieuwenhuyzen, M.; Padua, A. A.; Sheppard, O.; Soper, A. K. *J. Phys Chem. B* **2006,** *110*, 12055-12061.

138. FitzGerald, P. A.; Chatjaroenporn, K.; Zhang, X. L.; Warr, G. G. *Langmuir* **2011,** *27*, 11852-11859.

139. Leibler, L. *Macromolecules* **1980,** *13*, 1602-1617.

140. Helfand, E.; Wasserman, Z. R. *Polym. Eng. Sci.* **1977,** *17*, 582-586.

141. Helfand, E. *Macromolecules* **1975,** *8*, 552-556.

142. Fredrickson, G. H.; Helfand, E. *J. Chem. Phys.* **1987,** *87*, 697-705.

143. Stancik, C. M.; Lavoie, A. R.; Schütz, J.; Achurra, P. A.; Lindner, P.; Gast, A. P.; Waymouth, R. M. *Langmuir* **2003,** *20*, 596-605.

144. Weber, R. L.; Ye, Y.; Schmitt, A. L.; Banik, S. M.; Elabd, Y. A.; Mahanthappa, M. K. *Macromolecules* **2011,** *44*, 5727-5735.

145. Carrasco, P. M.; Ruiz de Luzuriaga, A.; Constantinou, M.; Georgopanos, P.; Rangou, S.; Avgeropoulos, A.; Zafeiropoulos, N. E.; Grande, H. J.; Cabañero, G. n.; Mecerreyes, D.; Garcia, I. *Macromolecules* **2011,** *44*, 4936-4941.

146. Scalfani, V. F.; Wiesenauer, E. F.; Ekblad, J. R.; Edwards, J. P.; Gin, D. L.; Bailey, T. S. *Macromolecules* **2012,** *45*, 4262-4276.

147. Coupillaud, P.; Fèvre, M.; Wirotius, A.-L.; Aissou, K.; Fleury, G.; Debuigne, A.; Detrembleur, C.; Mecerreyes, D.; Vignolle, J.; Taton, D. *Macromol. Rapid Commun.* **2014,** *35*, 422-430.

148. Hideharu, M.; Yuki, E.; Riina, K.; Kazuhiro, N. *Polymer Journal* **2012,** *44*, 550-560.

149. Choi, J.-H.; Ye, Y.; Elabd, Y. A.; Winey, K. I. *Macromolecules* **2013,** *46*, 5290-5300.

150. Yuan, J.; Soll, S.; Drechsler, M.; Müller, A. H. E.; Antonietti, M. *J. Am. Chem. Soc.* **2011,** *133*, 17556-17559.

151. Axenov, K. V.; Laschat, S. *Materials* **2011,** *4*, 206-259.

152. Yoshio, M.; Mukai, T.; Ohno, H.; Kato, T. *J. Am. Chem. Soc.* **2004,** *126*, 994-995.

153. Hoshino, K.; Yoshio, M.; Mukai, T.; Kishimoto, K.; Ohno, H.; Kato, T. *J. Polym. Sci. A Polym. Chem.* **2003,** *41*, 3486-3492.

154. Yoshio, M.; Kagata, T.; Hoshino, K.; Mukai, T.; Ohno, H.; Kato, T. *J. Am. Chem. Soc.* **2006,** *128*, 5570-5577.

155. Yamashita, A.; Yoshio, M.; Shimizu, S.; Ichikawa, T.; Ohno, H.; Kato, T. *J. Polym. Sci. A Polym. Chem.* **2014**, *53,* 366-371.

156. Zhao, F.; Pan, Z.; Wang, C.; Zhou, Y.; Qin, M. *Opt. Quant. Electron* **2014,** *46*, 1491-1498.

157. Hadjichristidis, N.; Pispas, S.; Pitsikalis, M. *Prog. Polym. Sci.* **1999,** *24*, 875-915.

158. Kim, J. S. Ionomers. In *Encyclopedia of Polymer Science and Technolog;* John Wiley & Sons, Inc., 2002.

159. Eisenberg, A. *Macromolecules* **1971,** *4*, 125-128.

160. Macknight, W. J.; Taggart, W. P.; Stein, R. S. *J. Polym. Sci. Polym. Symp.* **1974,** *45*, 113-128.

161. Yarusso, D. J.; Cooper, S. L. *Macromolecules* **1983,** *16*, 1871-1880.

162. Varley, R. Ionomers as Self Healing Polymers. In *Self Healing Materials*; van der Zwaag, S., Ed; Springer Netherlands: 2007; Vol. 100, pp 95-114.

163. Gao, Z.; Zhong, X. F.; Eisenberg, A. *Macromolecules* **1994,** *27*, 794-802.

164. Vanhoorne, P.; Jerome, R.; Teyssie, P.; Laupretre, F. *Macromolecules* **1994,** *27*, 2548-2552.

165. Peiffer, D. G.; Weiss, R. A.; Lundberg, R. D. *J. Polym. Sci. Polym. Phys. Ed.* **1982,** *20*, 1503-1509.

166. Nishida, M.; Eisenberg, A. *Macromolecules* **1996,** *29*, 1507-1515.

167. Schädler, V.; Franck, A.; Wiesner, U.; Spiess, H. W. *Macromolecules* **1997,** *30*, 3832-3838.

168. Sobry, R.; Fontaine, F.; Ledent, J.; Foucart, M.; Jérôme, R. *Macromolecules* **1998,** *31*, 4240-4252.

169. Vanhoorne, P.; Register, R. A. *Macromolecules* **1996,** *29*, 598-604.

170. Register, R. A.; Prud'homme, R. K., In *Ionomers: Synthesis, Structure, Properties and Applications;* Tant, M. R.; Mauritz, K. A.; Wilkes, G. L., Ed; Chapmann and Hall: New York, 1997.

171. Cooper, W. *J. Polym. Sci.* **1958,** *28*, 195-206.

172. Weiss, R. A.; Yu, W.-C. *Macromolecules* **2007,** *40*, 3640-3643.

173. Jéróme, R.; Broze, G. *Rubber Chem. Technol.* **1985,** *58*, 223-242.

174. Weiss, R. A.; Fitzgerald, J. J.; Kim, D. *Macromolecules* **1991,** *24*, 1064-1070.

175. Fitzgerald, J. J.; Weiss, R. A. *J. Macromol. Sci. C* **1988,** *28*, 99-185.

176. Bonotto, S.; Bonner, E. F. *Macromolecules* **1968,** *1*, 510-515.

177. Sakamoto, K.; MacKnight, W. J.; Porter, R. S. *J. Polym. Sci. B Polym. Phys.* **1970,** *8*, 277-287.

178. Ye, Y.-S.; Rick, J.; Hwang, B.-J. *J. Mater. Chem. A* **2013,** *1*, 2719-2743.

179. Yuan, J.; Antonietti, M. *Polymer* **2011,** *52*, 1469-1482.

180. Kim, D. W.; Chi, D. Y. *Angew. Chem.* **2004,** *116*, 489-491.

181. Kim, D. W.; Hong, D. J.; Jang, K. S.; Chi, D. Y. *Adv. Synth. Catal.* **2006,** *348*, 1719-1727.

182. Bergbreiter, D. E.; Su, H.-L.; Koizumi, H.; Tian, J. *J. Organomet. Chem.* **2011,** *696*, 1272-1279.

183. Byun, J.-W.; Lee, Y.-S. *Tetrahedron Lett.* **2004,** *45*, 1837-1840.

184. Zhang, Y.; Zhao, L.; Patra, P. K.; Hu, D.; Ying, J. Y. *Nano Today* **2009,** *4*, 13-20.

185. Tang, J.; Tang, H.; Sun, W.; Radosz, M.; Shen, Y. *J. Polym. Sci. A Polym. Chem.* **2005,** *43*, 5477-5489.

186. Magalhaes, T. O.; Aquino, A. S.; Vecchia, F. D.; Bernard, F. L.; Seferin, M.; Menezes, S. C.; Ligabue, R.; Einloft, S. *R. Soc. Chem. Adv.* **2014,** *4*, 18164-18170.

187. Fukushima, T.; Kosaka, A.; Ishimura, Y.; Yamamoto, T.; Takigawa, T.; Ishii, N.; Aida, T. *Science* **2003,** *300*, 2072-2074.

188. Wu, B.; Hu, D.; Kuang, Y.; Liu, B.; Zhang, X.; Chen, J. *Angew. Chem. Int. Ed.* **2009,** *48*, 4751-4754.

189. Pei, X.; Xia, Y.; Liu, W.; Yu, B.; Hao, J. *J. Polym. Sci. A Polym. Chem.* **2008,** *46*, 7225-7237.

190. Han, J.; Kim, H.; Kim, D. Y.; Jo, S. M.; Jang, S.-Y. *ACS Nano* **2010,** *4* (6), 3503-3509.

191. Kerscher, B.; Appel, A. K.; Thomann, R.; Mülhaupt, R. *Macromolecules* **2013,** *46*, 4395-4402.

192. Ishikawa, T.; Kobayashi, M.; Takahara, A. *ACS Appl. Mater. Interfaces* **2010,** *2*, 1120-1128.

193. Aboudzadeh, M. A.; Muñoz, M. E.; Santamaría, A.; Marcilla, R.; Mecerreyes, D. *Macromol. Rapid Commun.* **2012,** *33*, 314-318.

194. Varley, R. J.; van der Zwaag, S. *Acta Mater.* **2008,** *56*, 5737-5750.

195. Lindsten, G.; Wennerstrom, O.; Isaksson, R. *J. Org. Chem.* **1987,** *52*, 547-554.

196. Schwabacher, A. W.; Lane, J. W.; Schiesher, M. W.; Leigh, K. M.; Johnson, C. W. *J. Org. Chem.* **1998,** *63*, 1727-1729.

197. Yakuphanoglu, F.; Okutan, M.; Koysal, O.; Ozder, S.; Ocakoglu, K.; Icli, S. *J. Phys. Chem. B* **2005,** *109*, 24338-24342.

198. Huisgen, R.; Szeimies, G.; Möbius, L., *Chem. Ber.* **1967,** *100*, 2494.

199. Huisgen, R., *Pure & Appl. Chem.* **1989,** *61*, 613.

200. Kolb, H. C.; Finn, M. G.; Sharpless, K. B. *Angew. Chem. Int . Ed.* **2001,** *40*, 2004-2021.

201. Rostovtsev, V. V.; Green, L. G.; Fokin, V. V.; Sharpless, K. B. *Angew. Chem. Int. Ed.* **2002,** *41*, 2596-2599.

202. Binder, W. H.; Sachsenhofer, R. *Macromol. Rapid Commun.* **2007,** *28* (1), 15-54.

203. Binder, W. H.; Sachsenhofer, R. *Macromol. Rapid Commun.* **2008,** *29* (12-13), 952-981.

204. Binder, W. H.; Zirbs, R. "Click" Chemistry in Macromolecular Synthesis. In *Encyclopedia of Polymer Science and Technology*; John Wiley & Sons, Inc., 2009.

205. Binder, W. H.; Herbst, F. Click chemistry in polymer science. In *Yearbook of Science and Technology*; McGraw-Hill; Blumel, D., Eds.: New York, 2011.

206. Mansfeld, U.; Pietsch, C.; Hoogenboom, R.; Becer, C. R.; Schubert, U. S. *Polym. Chem.* **2010,** *1*, 1560-1598.

207. Liang, L.; Astruc, D. *Coord. Chem. Rev.* **2011,** *255*, 2933-2945.

208. Kempe, K.; Krieg, A.; Becer, C. R.; Schubert, U. S. *Chem. Soc. Rev.* **2012,** *41*, 176.

209. Harvison, M. A.; Lowe, A. B., *Macromol. Rapid Commun.* **2011,** *32*, 779.

210. Hsu, M. H.; Josephrajan, T.; Yeh, C. S.; Shieh, D. B.; Su, W. C.; Hwu, J. R. *Bioconjugate Chem.* **2007,** *18*, 1709-1712.

211. Aidhen, I. S.; Braslau, R. *Synth. Commun.* **1994,** *24*, 789-797.

212. Dyson, P. J.; McIndoe, J. S.; Zhao, D. *Chem. Commun.* **2003,** *4*, 508-509.

213. Dorbritz, S.; Ruth, W.; Kragl, U. *Adv. Synth. Cat.* **2005,** *347*, 1273-1279.

214. Nohara, D.; Ohkoshi, T.; Sakai, T. *Rapid Commun. Mass Spectrom.* **1998,** *12*, 1933-1935.

215. Nohara, D.; Bitoh, M. *J. Mass Spectrom.* **2000,** *35*, 1434-1437.

216. Bini, R.; Bortolini, O.; Chiappe, C.; Pieraccini, D.; Siciliano, T. *J. Phys. Chem. B* **2006,** *111*, 598-604.

217. Maton, C.; De Vos, N.; Stevens, C. V. *Chem. Soc. Rev.* **2013,** *42*, 5963-5977.

218. Forsyth, S. A.; Pringle, J. M.; MacFarlane, D. R. *Aust. J. Chem* **2004,** *57*, 113-119.

219. Baranyai, K. J.; Deacon, G. B.; MacFarlane, D. R.; Pringle, J. M.; Scott, J. L. *Aust. J. Chem.* **2004,** *57*, 145-147.

220. MacFarlane, D. R.; Forsyth, S. A.; Golding, J.; Deacon, G. B. *Green Chem.* **2002,** *4*, 444-448.

221. Tokuda, H.; Ishii, K.; Susan, M. A. B. H.; Tsuzuki, S.; Hayamizu, K.; Watanabe, M. *J. Phys. Chem. B* **2006,** *110*, 2833-2839.

222. Shirota, H.; Mandai, T.; Fukazawa, H.; Kato, T. *J. Chem. Eng. Data* **2011,** *56*, 2453-2459.

223. Payagala, T.; Huang, J.; Breitbach, Z. S.; Sharma, P. S.; Armstrong, D. W. *Chem. Mater.* **2007,** *19*, 5848-5850.

224. Tokuda, H.; Hayamizu, K.; Ishii, K.; Susan, M. A. B. H.; Watanabe, M. *J. Phys. Chem. B* **2005,** *109*, 6103-6110.

225. Zeng, Z.; Phillips, B. S.; Xiao, J.-C.; Shreeve, J. M. *Chem. Mater.* **2008,** *20* (8), 2719-2726.

226. Kondo, Y.; Koyama, T.; Sasaki, S., *Tribological Properties of Ionic Liquids*. *New Aspects for the Future*; Kadokawa, J. (Ed.), ISBN: 978-953-51-0937-2.

227. Minami, I. *Molecules* **2009,** *14*, 2286-2305.

228. Bermudez, M. D.; Jimenez, A. E.; Sanes, J.; Carrion, F. J. *Molecules* **2009,** *14*, 2888-2908.

229. Bermúdez, M.-D.; Carrión, F. J.; Iglesias, P.; Jiménez, A.-E.; Martínez-Nicolás, G.; Sanes, J. *Mater. Res. Soc. Symp. P.* **2008,** *1082*.

230. Jimenez, A. E.; Bermudez, M. D. *Tribol. Lett.* **2009,** *33*, 111-126.

231. Liu, W. M.; Ye, C. F.; Gong, Q. Y.; Wang, H. Z.; Wang, P. *Tribol. Lett.* **2002,** *13*, 81-85.

232. Ye, C. F.; Liu, W. M.; Chen, Y. X.; Yu, L. G. *Chem. Commun.* **2001,** *21*, 2244-2245.

233. Jimenez, A. E.; Bermudez, M. D. *Tribol. Lett.* **2010,** *40*, 237-246.

234. Qu, J.; Truhan, J. J.; Dai, S.; Luo, H.; Blau, P. J. *Tribol. Lett.* **2006,** *22*, 207-214.

235. Phillips, B. S.; Zabinski, J. S. *Tribol. Lett.* **2004,** *17*, 533-541.

236. Jiménez, A.-E.; Bermúdez, M. D. *Wear* **2008,** *265*, 787-798.

237. Yao, M.; Liang, Y.; Xia, Y.; Zhou, F. *ACS Appl. Mate. Interfaces* **2009,** *1*, 467-471.

238. Yu, G.; Zhou, F.; Liu, W.; Liang, Y.; Yan, S. *Wear* **2006,** *260*, 1076-1080.

239. Mo, Y.; Zhao, W.; Zhu, M.; Bai, M. *Tribol. Lett.* **2008,** *32*, 143-151.

240. Zhu, M.; Yan, J.; Mo, Y.; Bai, M. *Tribol. Lett.* **2008,** *29*, 177-183.

241. Palacio, M.; Bhushan, B. *Adv. Mater.* **2008,** *20*, 1194-1198.

242. Bhushan, B.; Palacio, M.; Kinzig, B. *J. Colloid and Interface Sci.* **2008,** *317*, 275-287.

243. Yu, G. Q.; Yan, S. Q.; Zhou, F.; Liu, X. Q.; Liu, W. M.; Liang, Y. M. *Tribol. Lett.* **2007,** *25*, 197-205.

244. Pagano, F.; Gabler, C.; Zare, P.; Mahrova, M.; Dörr, N.; Bayon, R.; Fernandez, X.; Binder, W.; Hernaiz, M.; Tojo, E.; Igartua, A. *Proc. Inst. Mech. Eng. J. Eng. Tribol* **2012,** *226*, 952-964.

245. Sigwalt, P.; Moreau, M. *Prog. Polym. Sci.* **2006,** *31*, 44-120.

246. Szwarc, M. 'Living' Polymers. *Nature* **1956,** *178*, 1168-1169.

247. Kennedy, J. P.; Ivan, B. *Designed Polymers by Carbocationic Macromolecular Engineering: Theory and Practice*. Hanser Publishers: Munich, New York, 1992.

248. Binder, W. H.; Kluger, C. *Macromolecules* **2004,** *37*, 9321-9330.

249. Bouteiller, L. *Assembly via Hydrogen Bonds of Low Molar Mass Compounds into Supramolecular Polymers Hydrogen Bonded Polymers*; Binder, W., H.; Ed.; Springer Berlin/Heidelberg: 2007; Vol. 207, pp 79-112.

250. Binder, W. H.; Kunz, M. J.; Kluger, C.; Hayn, G.; Saf, R. *Macromolecules* **2004,** *37*, 1749-1759.

251. Morgan, D. L.; Storey, R. F. *Macromolecules* **2009,** *42*, 6844-6847.

252. Adekunle, O.; Herbst, F.; Hackethal, K.; Binder, W. H. *J. Polym. Sci. Pol. Chem.* **2011,** *49*, 2931-2940.

253. Zare, P.; Stojanovic, A.; Herbst, F.; Akbarzadeh, J.; Peterlik, H.; Binder, W. H. *Macromolecules* **2012,** *45*, 2074-2084.

254. Weber, R. L.; Ye, Y.; Banik, S. M.; Elabd, Y. A.; Hickner, M. A.; Mahanthappa, M. K. *J. Polym. Sci. B Polym. Phys.* **2011,** *49*, 1287-1296.

255. Jovanovski, V.; Marcilla, R.; Mecerreyes, D. *Macromol. Rapid Commun.* **2010,** *31*, 1646-1651.

256. Treskow, M.; Pitawala, J.; Arenz, S.; Matic, A.; Johansson, P. *J. Phys. Chem. Lett.* **2012,** *3*, 2114-2119.

257. Kroon, M. C.; Buijs, W.; Peters, C. J.; Witkamp, G.-J. *Thermochim. Acta* **2007,** *465*, 40-47.

258. Xiao, D.; Hines, L. G.; Li, S.; Bartsch, R. A.; Quitevis, E. L.; Russina, O.; Triolo, A. *J. Phys. Chem. B* **2009,** *113*, 6426-6433.

259. Wang, Y.; Voth, G. A. *J. Am. Chem. Soc.* **2005,** *127*, 12192-12193.

260. Bodo, E.; Gontrani, L.; Caminiti, R.; Plechkova, N. V.; Seddon, K. R.; Triolo, A. *J. Phys.Chem. B* **2010,** *114*, 16398-16407.

261. Han, C. D.; Vaidya, N. Y.; Kim, D.; Shin, G.; Yamaguchi, D.; Hashimoto, T. *Macromolecules* **2000,** *33*, 3767-3780.

262. Varley, R. J.; van der Zwaag, S. *Acta Mater.* **2008,** *56*, 5737-5750.

263. Eisenbeg. A; King, M. *Macromolecules* **1971,** *4*, 204.

264. Moore, R. B.; Bittencourt, D.; Gauthier, M.; Williams, C. E.; Eisenberg, A. *Macromolecules* **1991,** *24*, 1376-1382.

265. Varley, R. J.; van der Zwaag, S. *Polym. Test.* **2008,** *27*, 11-19.

266. van Ruymbeke, E.; Vlassopoulos, D.; Mierzwa, M.; Pakula, T.; Charalabidis, D.; Pitsikalis, M.; Hadjichristidis, N. *Macromolecules* **2010,** *43*, 4401-4411.

267. Schädler, V.; Kniese, V.; Thurn-Albrecht, T.; Wiesner, U.; Spiess, H. W. *Macromolecules* **1998,** *31*, 4828-4837.

268. Vlassopoulos, D.; Pakula, T.; Fytas, G.; Pitsikalis, M. *J. Chem. Phys.* **1999,** *111*, 1760-1764.

269. Vlassopoulos, D.; Pitsikalis, M.; Hadjichristidis, N. *Macromolecules* **2000,** *33*, 9740-9746.

270. Fang, Z.; Wang, S.; Wang, S. Q.; Kennedy, J. P. *J. Appl. Polym. Sci.* **2003,** *88*, 1516-1525.

271. Antonietti, M.; Pakula, T.; Bremser, W. *Macromolecules* **1995,** *28*, 4227-4233.

272. Kaszás, G.; Györ, M.; Kennedy, J. P.; Tüdüs, F. *J. Macromol. Sci. Chem.* **1982,** *18*, 1367-1382.

273. Zare, P.; Mahrova, M.; Tojo, E.; Stojanovic, A.; Binder, W. H. *J. Polym. Sci. Pol. Chem.* **2013,** *51*, 190-202.

274. Binder, W. H.; Petraru, L.; Roth, T.; Groh, P.; Pálfi, V.; Keki, S.; Ivan, B. *Adv. Funct. Mater.* **2007,** *17*, 1317-1326.
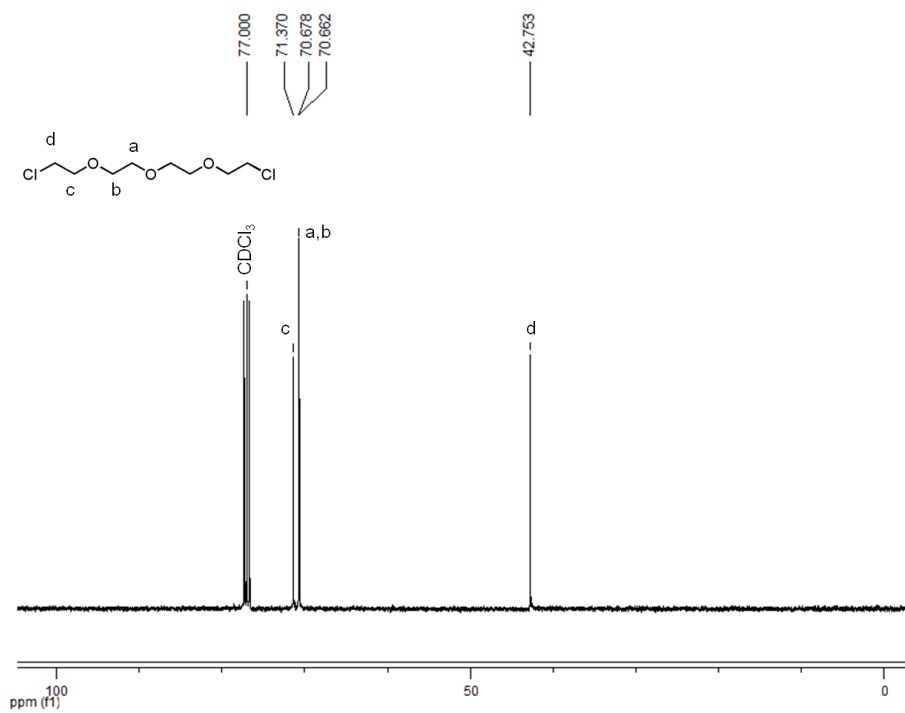
A1. ^{13}C NMR spectra of **17**
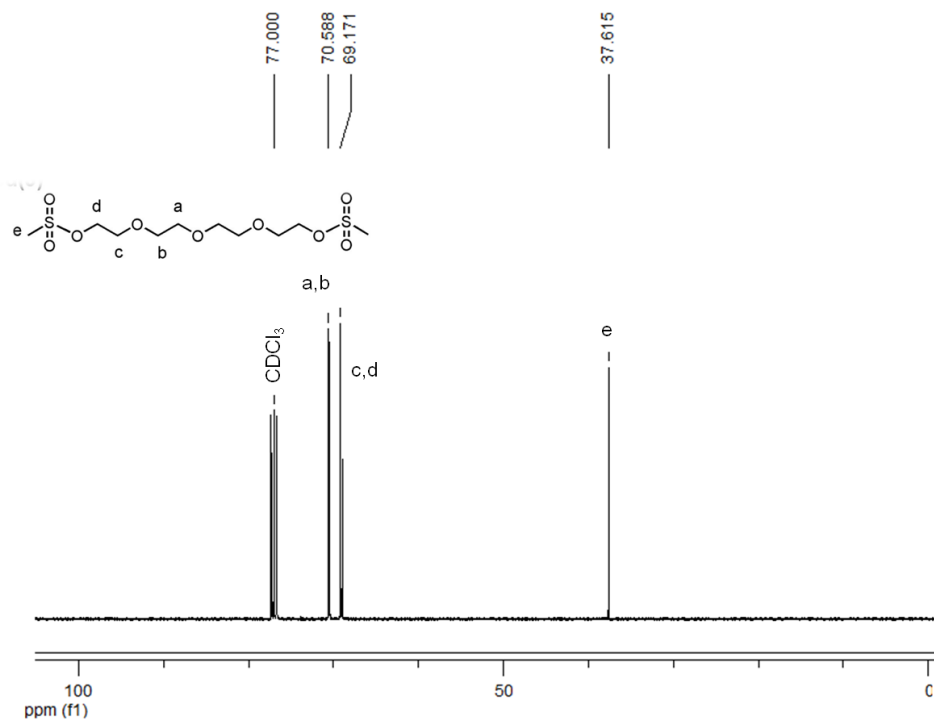
A2. ^{13}C NMR spectra of **18**
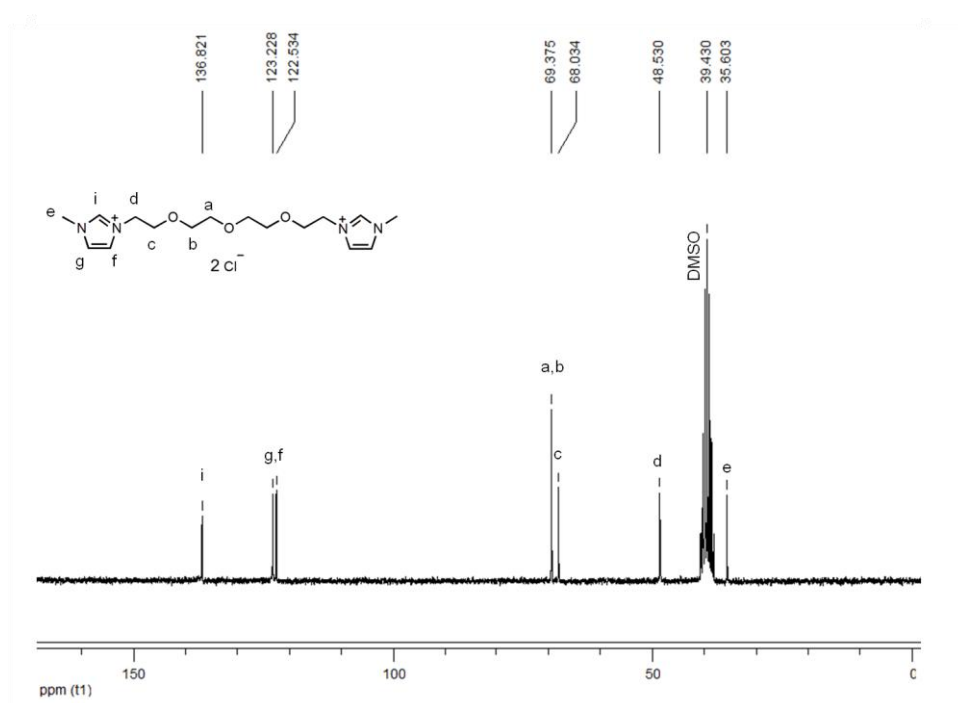
A3. ^{13}C NMR spectra of **1a**
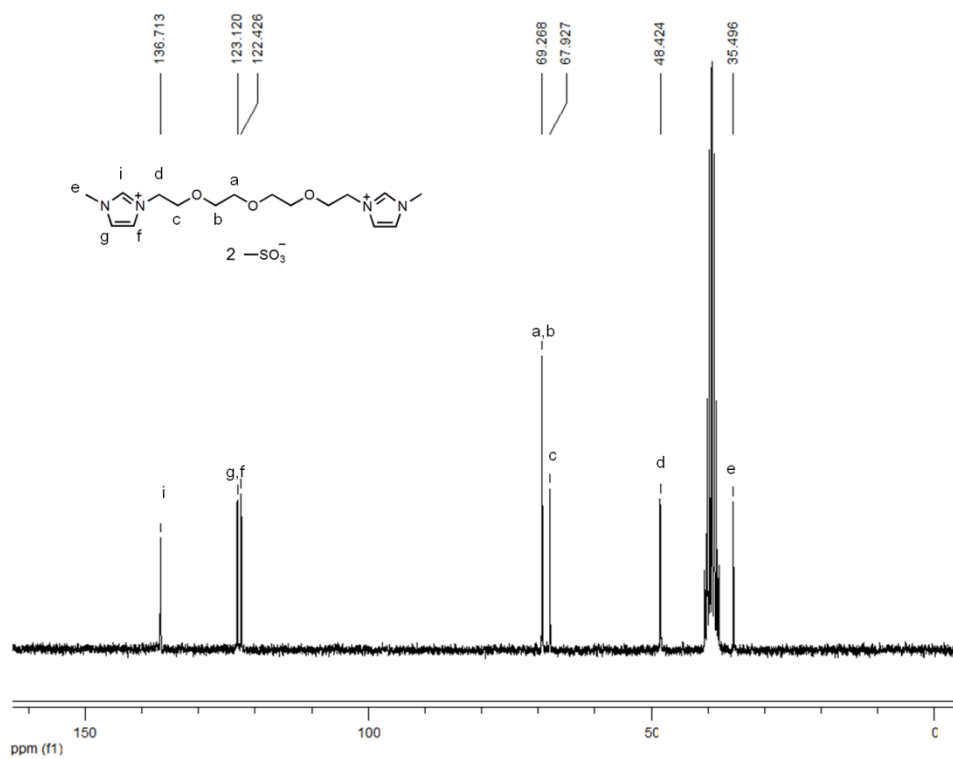
A4. ^{13}C NMR spectra of **2a**
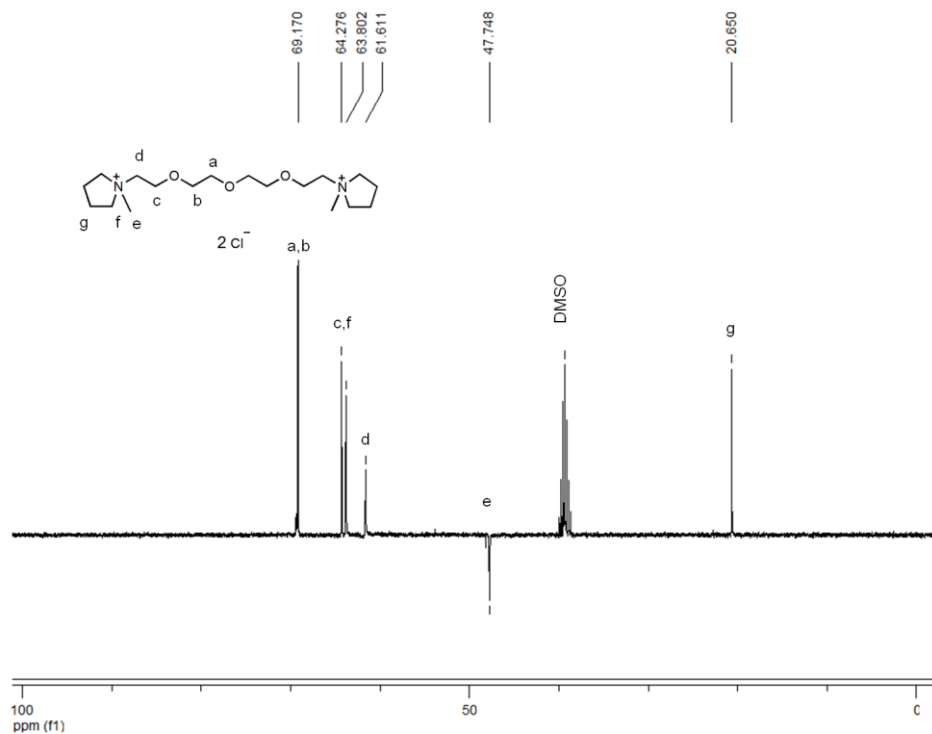
A5. ^{13}C NMR spectra of **1b**
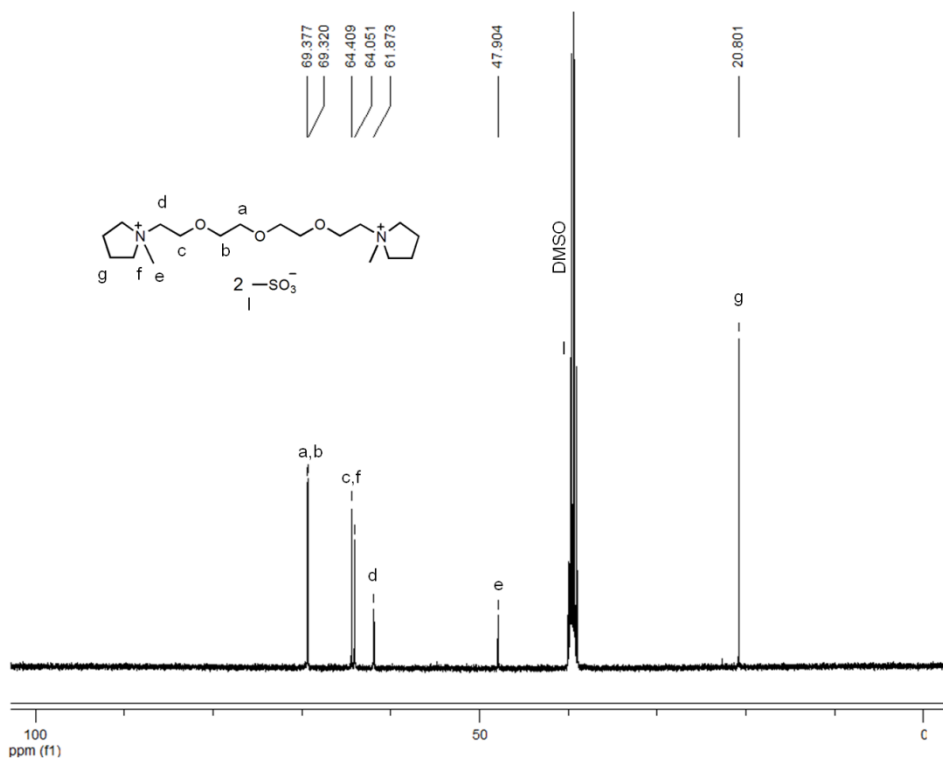
A6. ^{13}C NMR spectra of **2b**
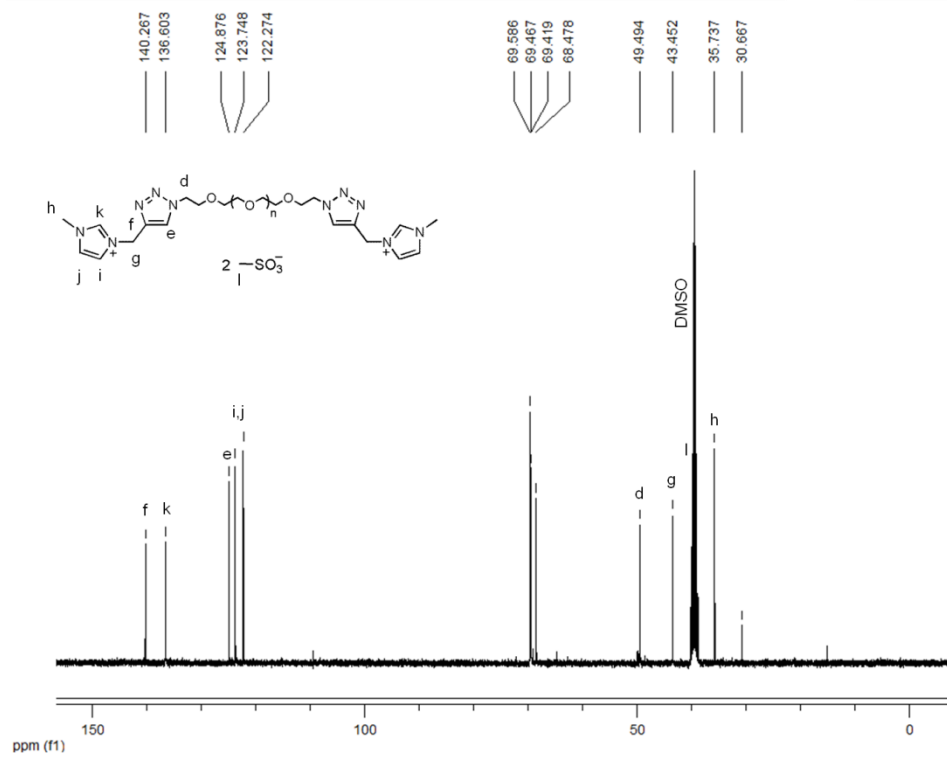
A7. ^{13}C NMR spectra of **6a**
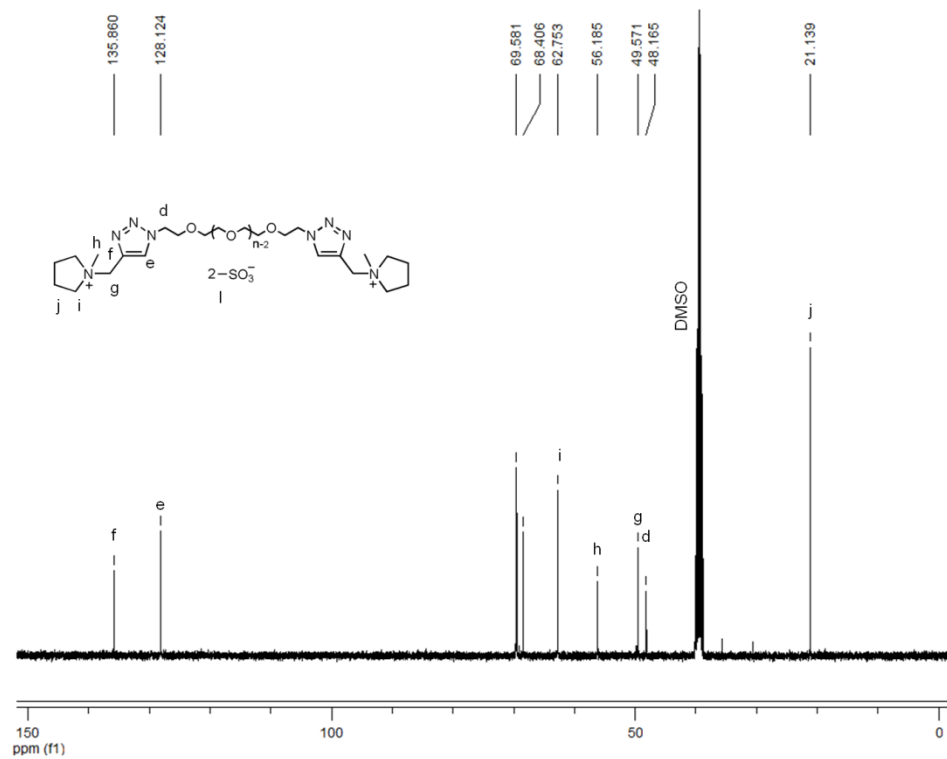
A8. ^{13}C NMR spectra of **6b**
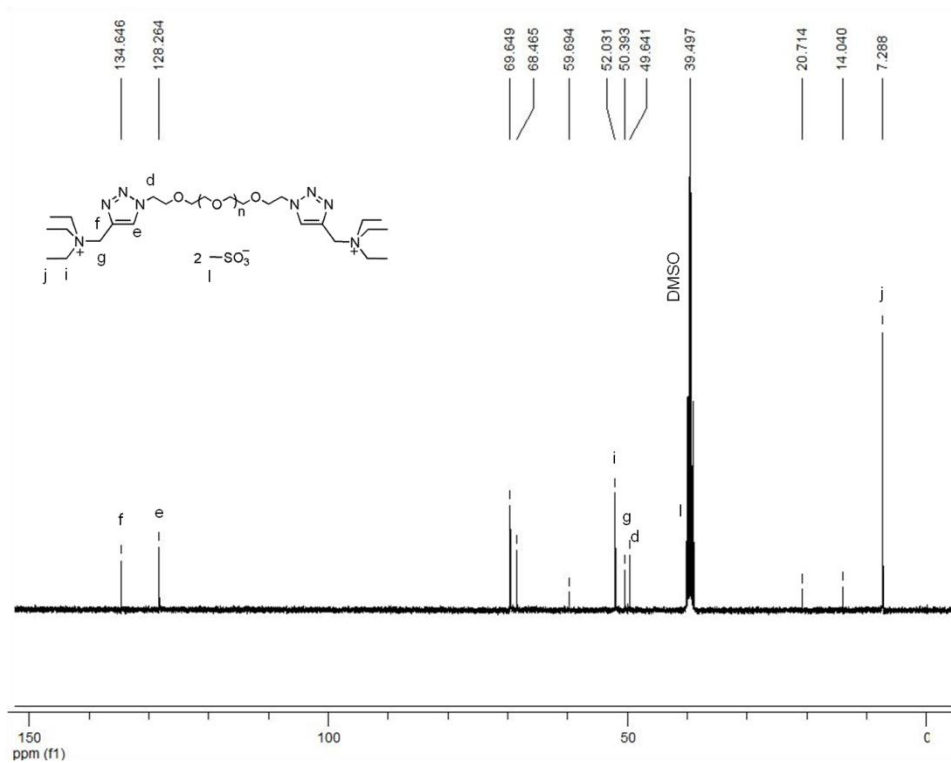
A9. ^{13}C NMR spectra of **6c.**

A10. ^{13}C NMR spectra of **7a.**

A11. ^{13}C NMR spectra of **7b.**
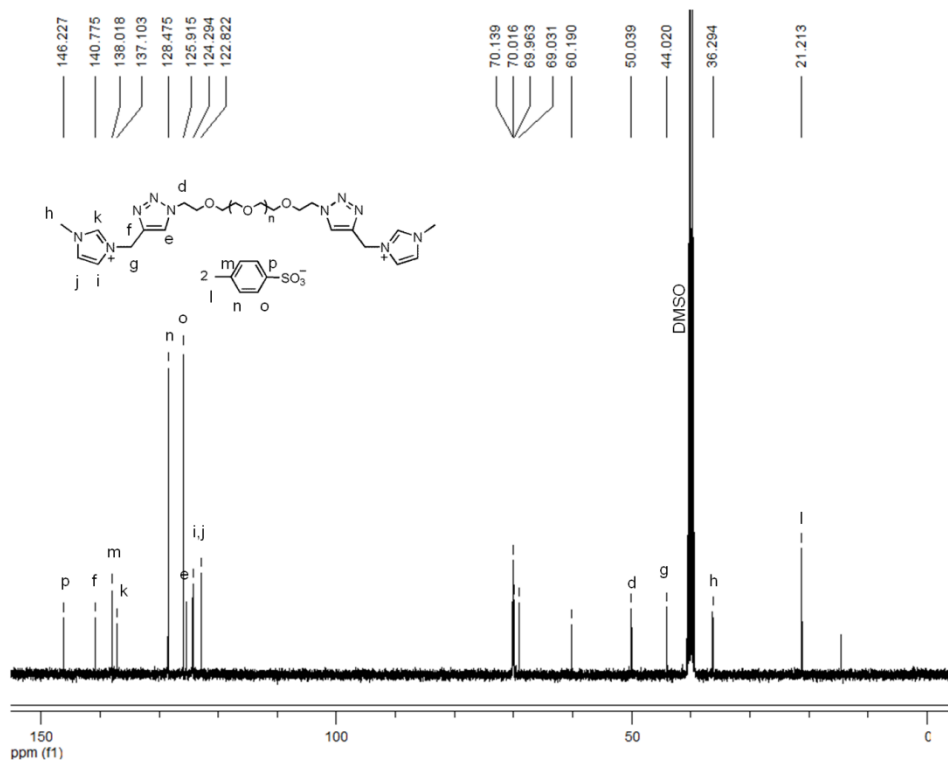
A12. ^{13}C NMR spectra of **7c.**
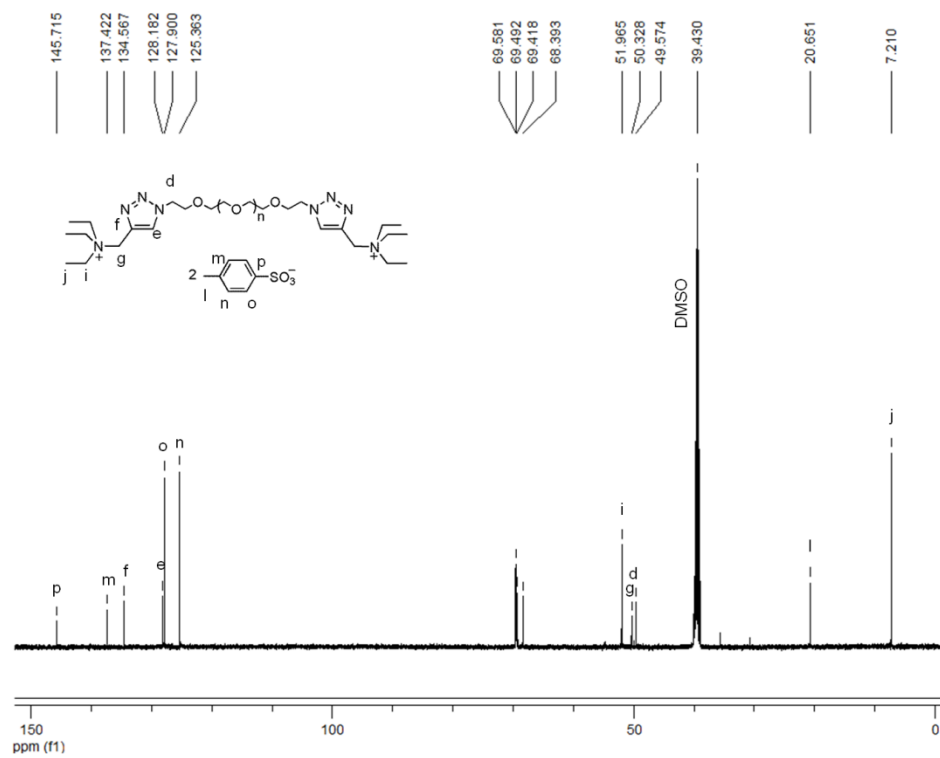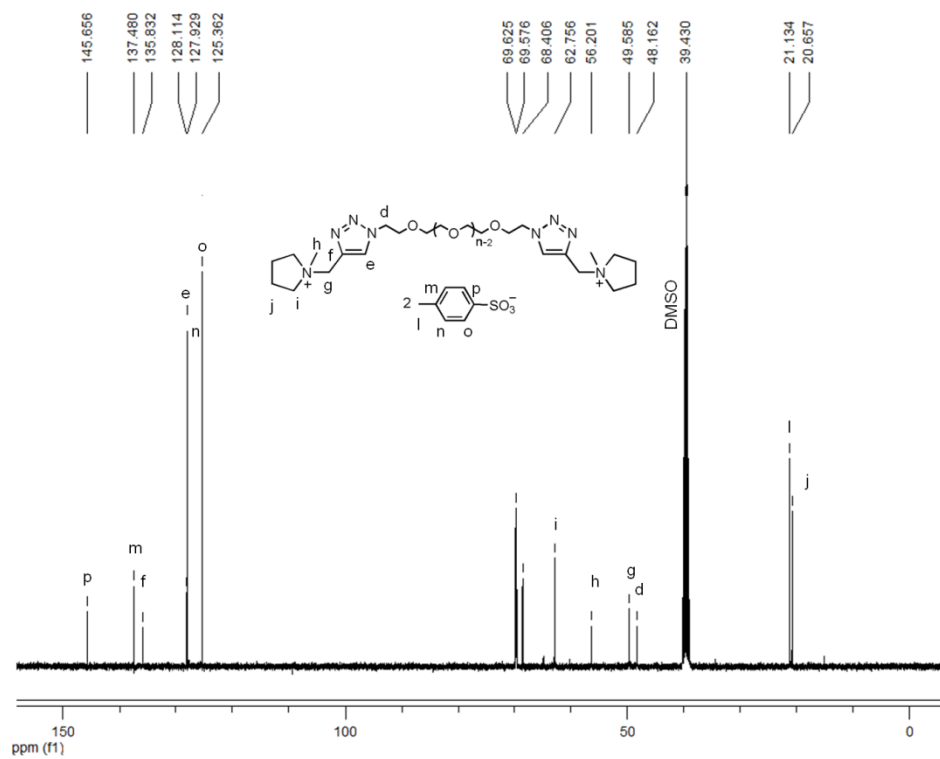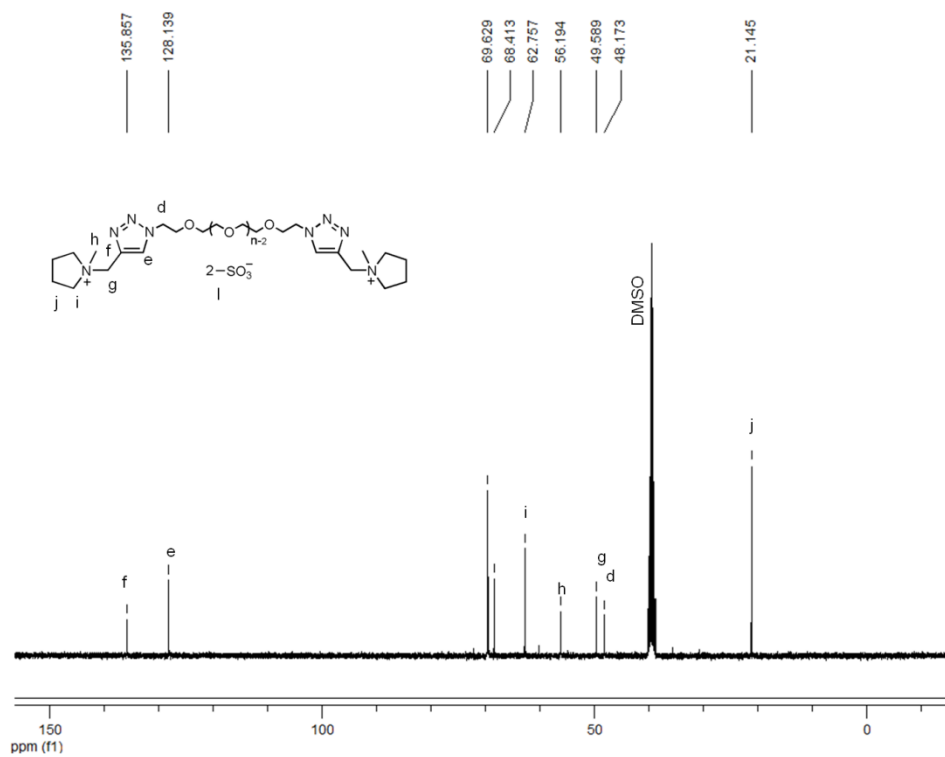
A13. ^{13}C NMR spectra of **8b.**
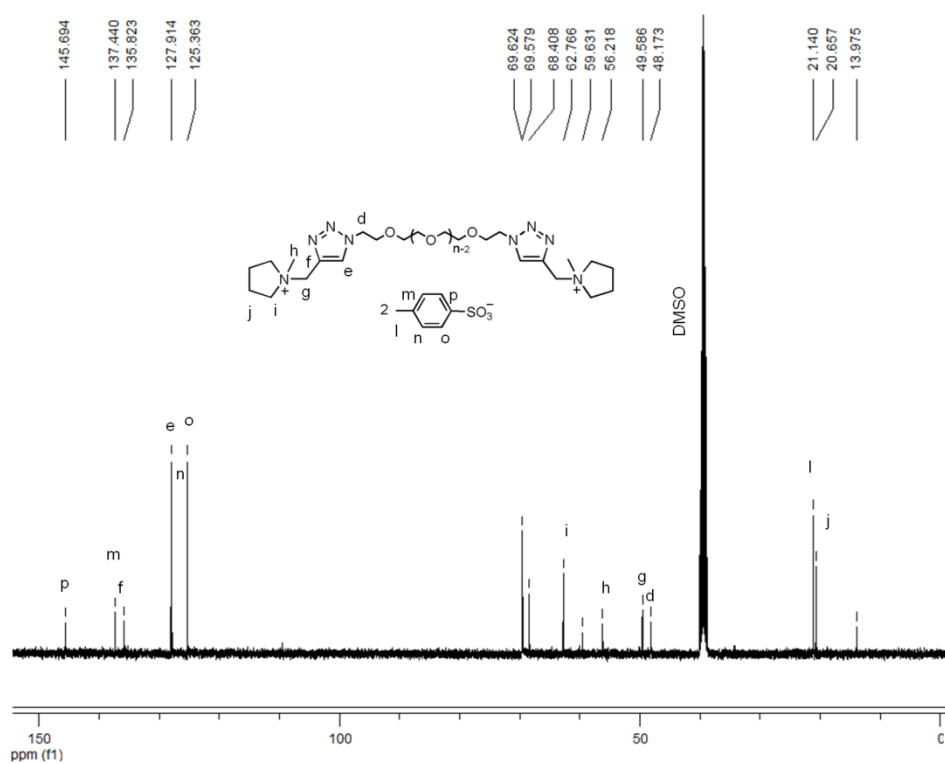
A14. ^{13}C NMR spectra of **9b.**
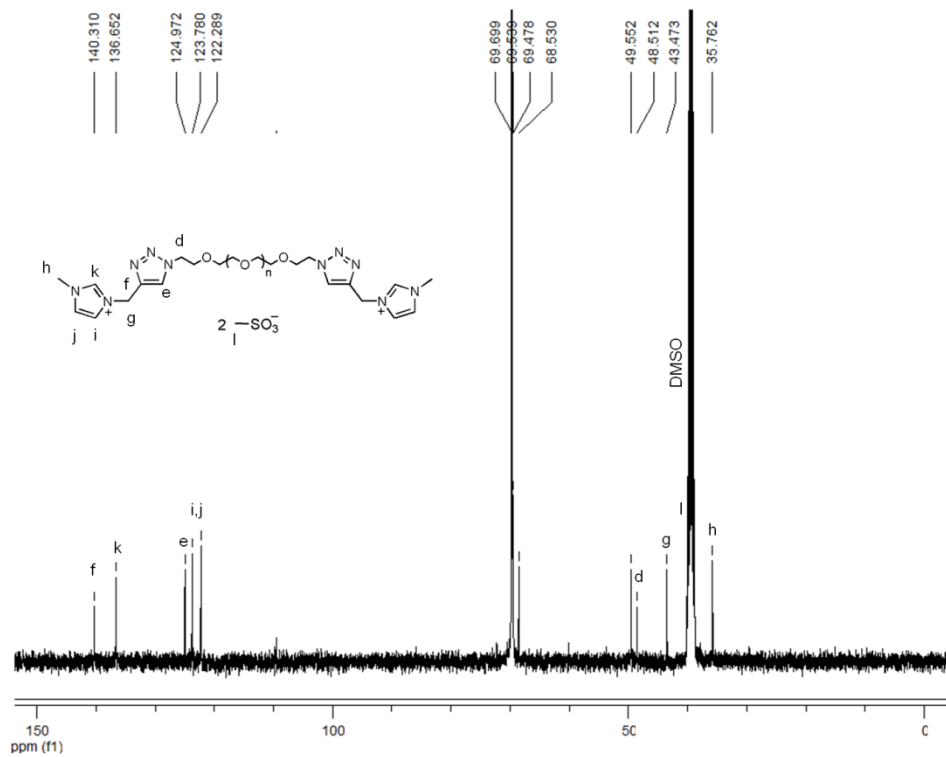
A15. ^{13}C NMR spectra of **10a.**
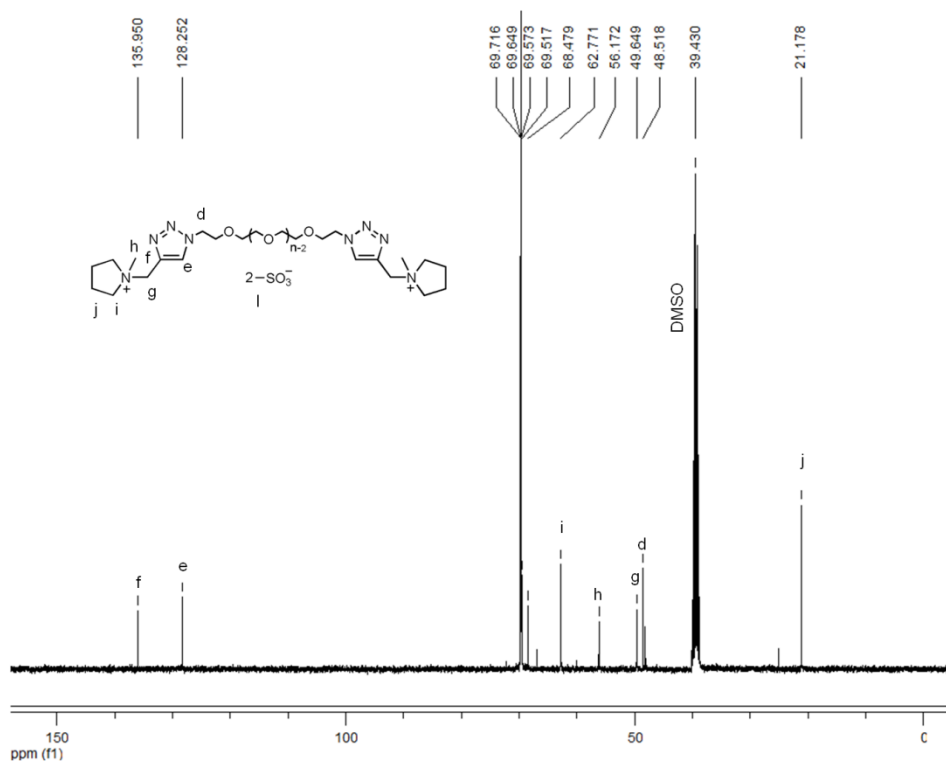
A16. ^{13}C NMR spectra of **10b.**

A17. Chemical formula and corresponding notations of the assigned signals detected by ESI-TOF for **PEGILs (8b, 9b, 10a, 10b).**

product	notation	Chemical formula
8b	$[C^{2+}]^{2+}$	$[(C_2H_4O)_nC_{18}H_{32}N_8]^{2+}$
	$[C^{2+}, A^-]^{1+}$	$[(C_2H_4O)_nC_{19}H_{35}N_8O_3S]^{1+}$
9b	$[C^{2+}]^{2+}$	$[(C_2H_4O)_nC_{18}H_{32}N_8]^{2+}$
	$[C^{2+}, A^-]^{1+}$	$[(C_2H_4O)_nC_{25}H_{39}N_8O_3S]^{1+}$
10a	$[C^{2+}]^{2+}$	$[(C_2H_4O)_nC_{16}H_{22}N_{10}]^{2+}$
	$[(C^{2+}, A^-)-H^•]^{•+}$	$[(C_2H_4O)_nC_{17}H_{24}N_{10}O_3S]^{•+}$
	$[(C^{2+}, A^-)-H+Na]^{1+}$	$[(C_2H_4O)_nC_{17}H_{24}N_{10}NaO_3S]^{1+}$
10b	$[C^{2+}]^{2+}$	$[(C_2H_4O)_nC_{18}H_{32}N_8]^{2+}$
	$[(C^{2+}, 2A^-)+CH_3OH]^{1+}$	$[(C_2H_4O)_nC_{21}H_{42}N_8O_7S2]^{1+}$
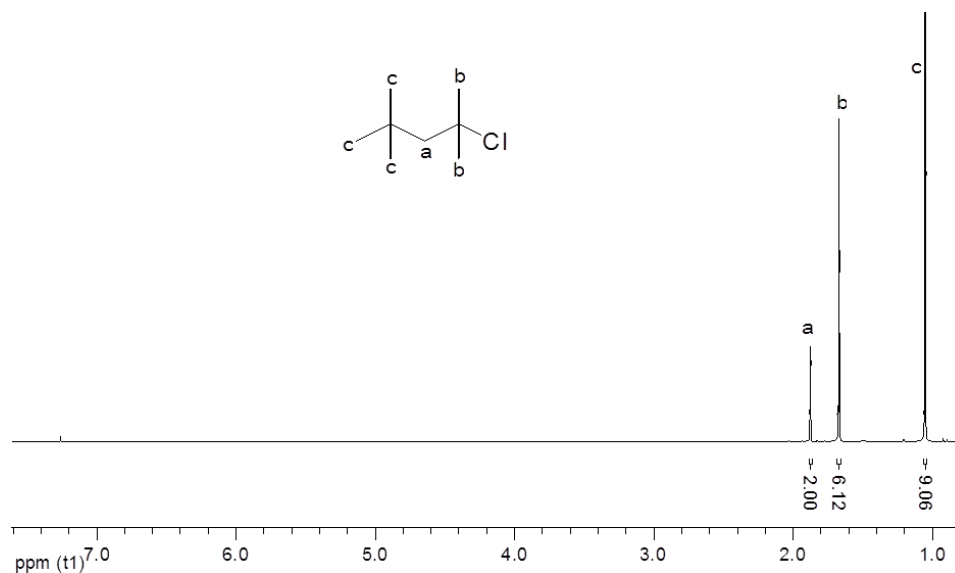
A18. ^{1}H NMR spectra of TMPCl.
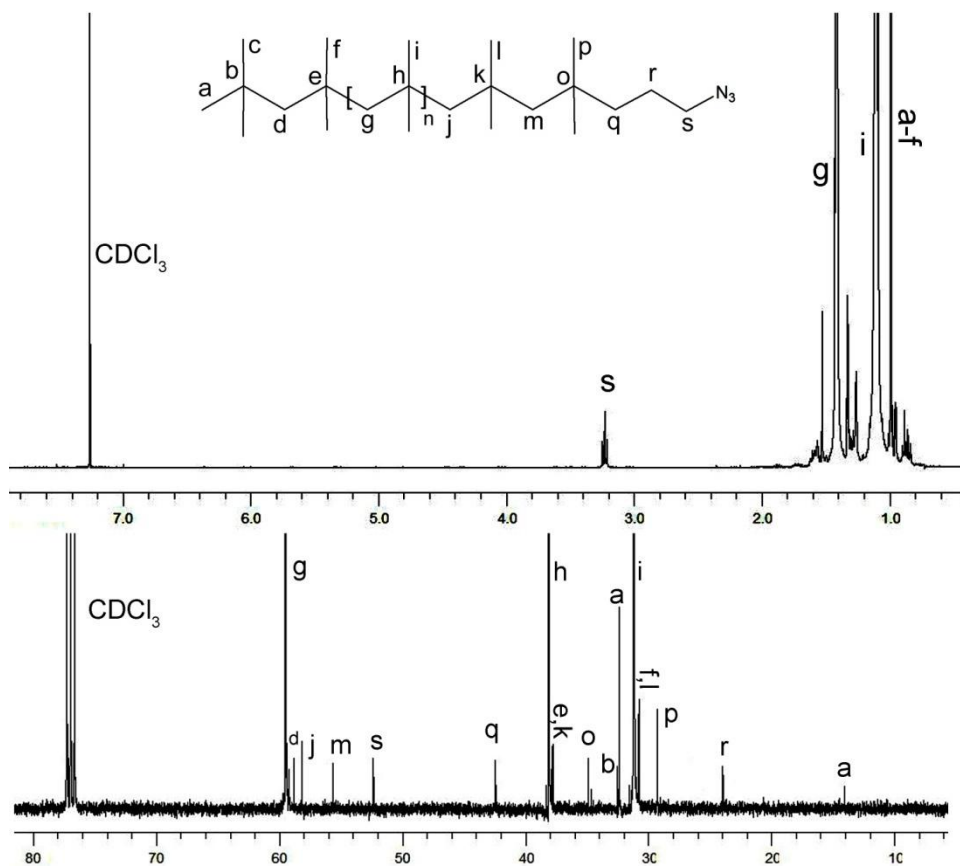
A19. ^{1}H and ^{13}C NMR spectra of **27.**
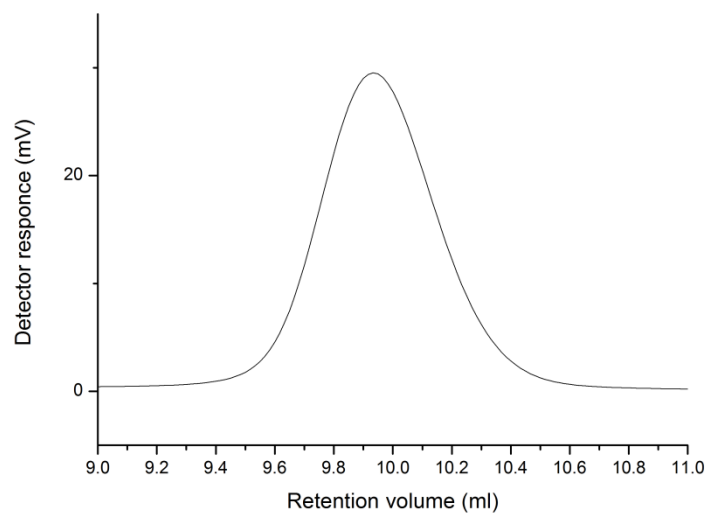
A20. GPC results of compound **27.**
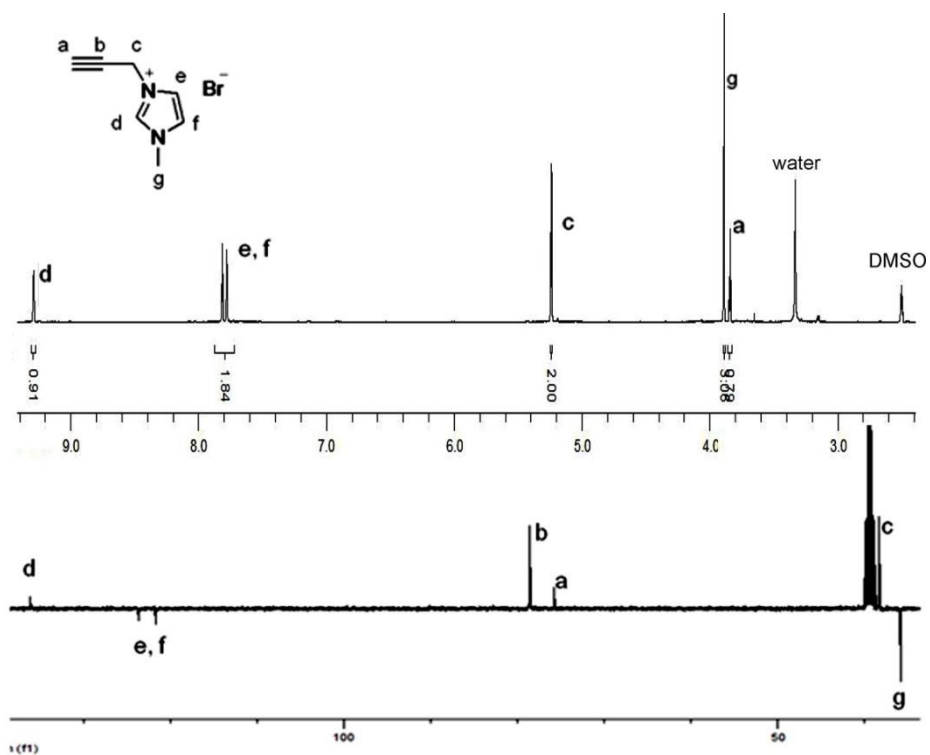
A21. ^{1}H and ^{13}C NMR spectra of **26a.**
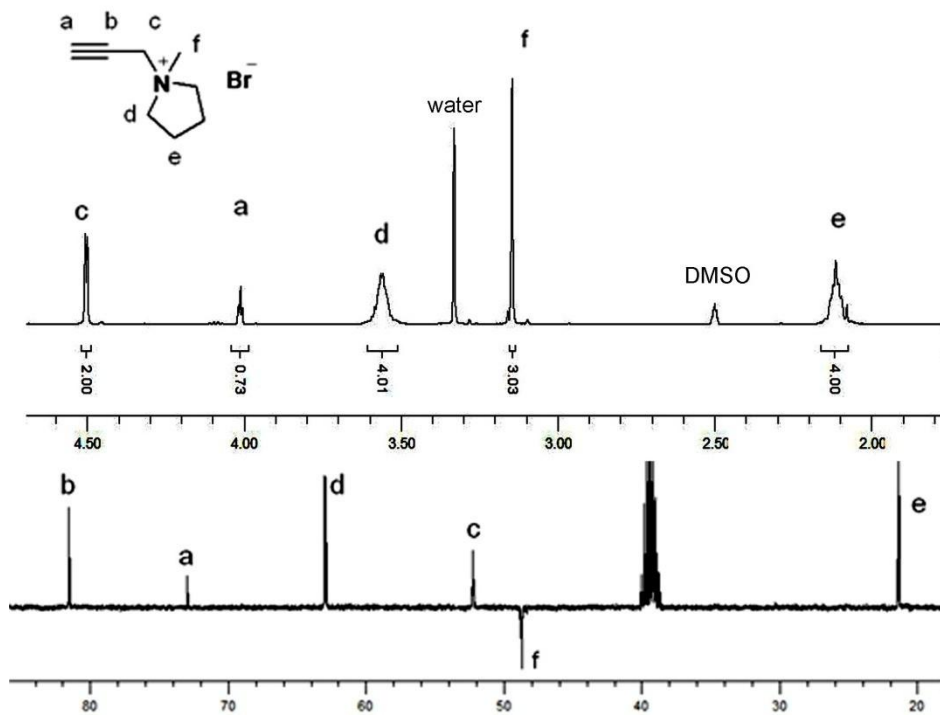
A22. ^{1}H and ^{13}C NMR spectra of **26b.**
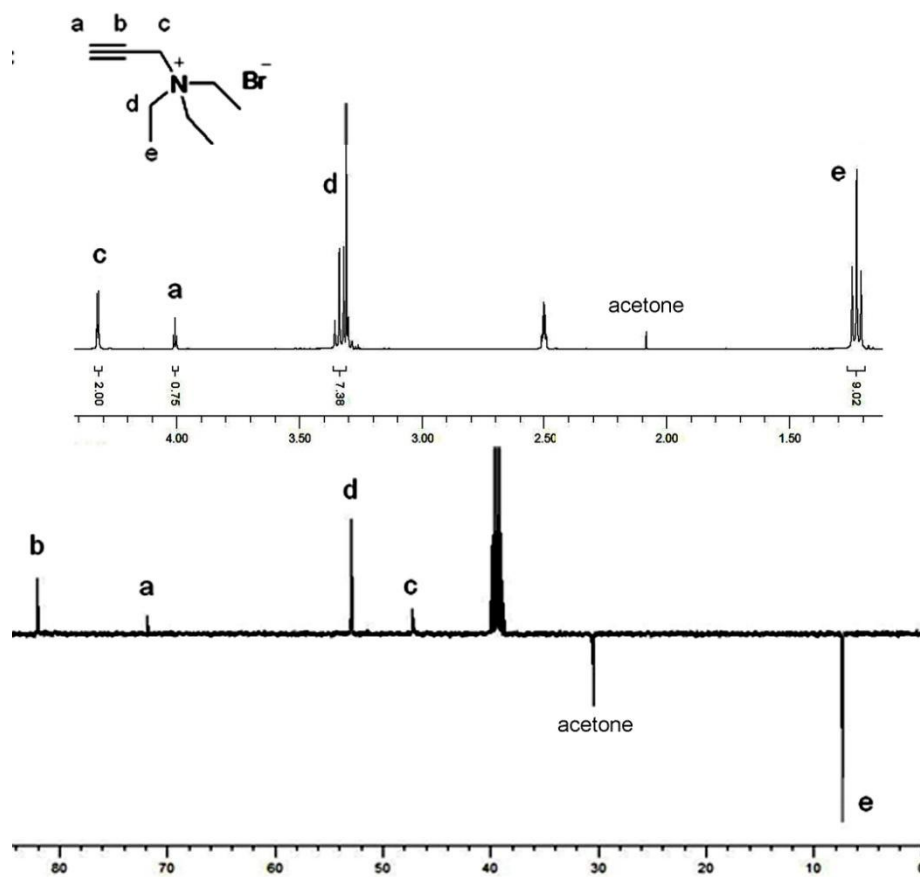
A23. ^{1}H and ^{13}C NMR spectra of **26c.**
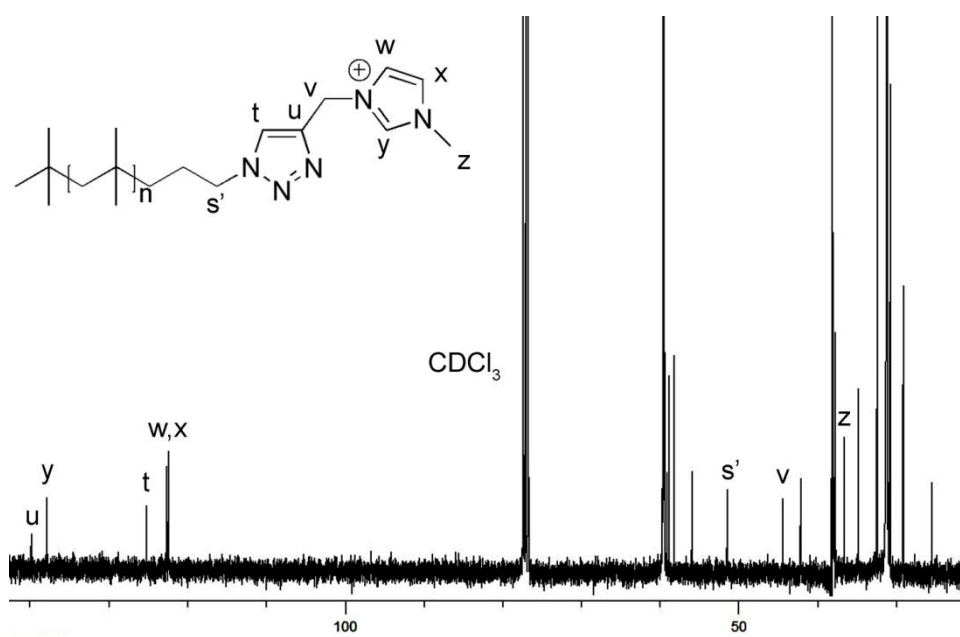
A24. ^{13}C NMR spectra of **11a.**
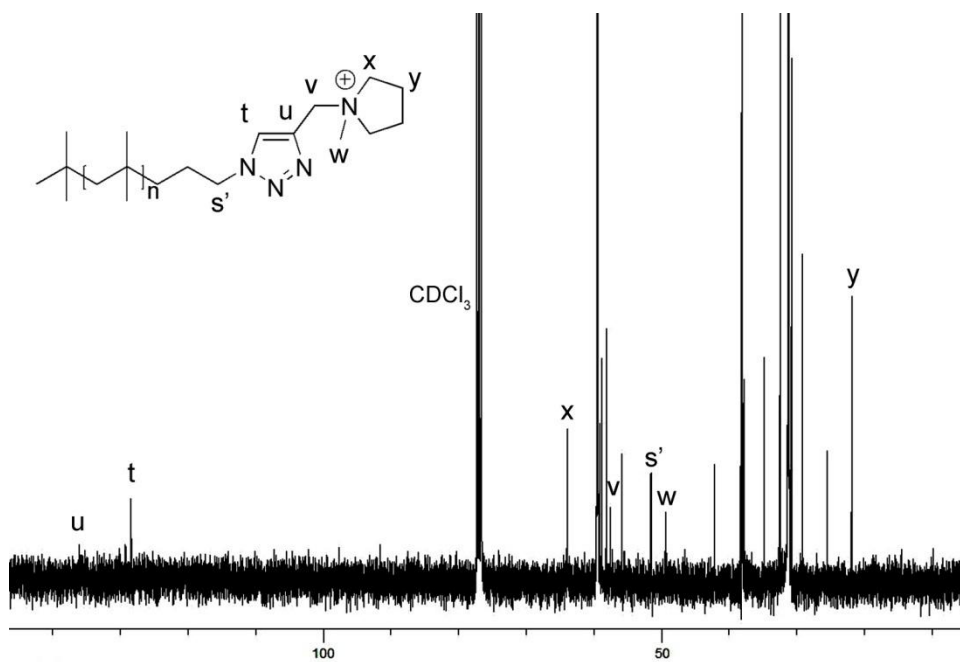
A25.^{13}C NMR spectra of **11b.**
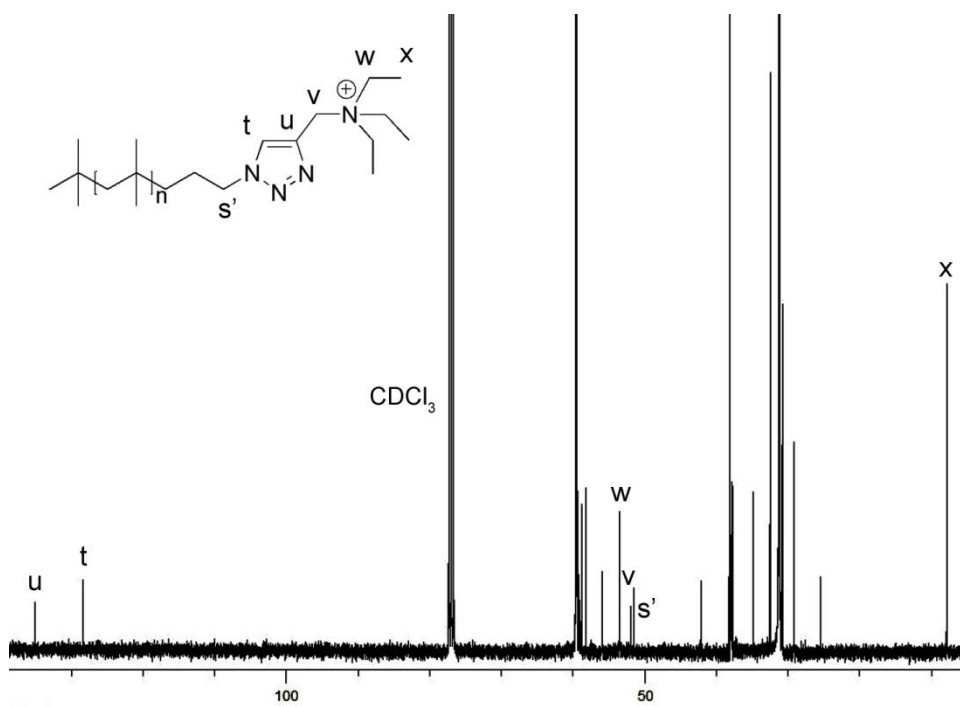
A26.^{13}C NMR spectra of **11c.**

A27. Conversions results of the reaction of 26a-26c with 27.

entry	product	catalyst	reaction condition	conversion(%)
1	3a	CuBr (0.05+0.05 mmol)[1]	100w/90˚C /10+10h	-[2]
2	3b		100w/90˚C /20h	-
3	3c		100w/90˚C /20h	-
4	3a	Cu(Pph$_3$)Br (0.02 mmol)	100w/90˚C /20h	57
5	3b		100w/90˚C /20h	43
6	3c		100w/90˚C /20h	30
7	3a	CuI (0.03 mmol)	70w/80˚C /16h	55
8	3a		75w/75˚C /16h	86
8	3b		70w/75˚C /16h	81
7	3c		75w/80˚C /16h	69[3]
9	3c		70w/75˚C /16h	74

[1] After 10 hours of irradiation, 0.05 mmol of catalyst was added and the irradiation was continued for 10 more hours.

[2] Conversion was checked by ^{1}H NMR (not a significant conversion detected by NMR)
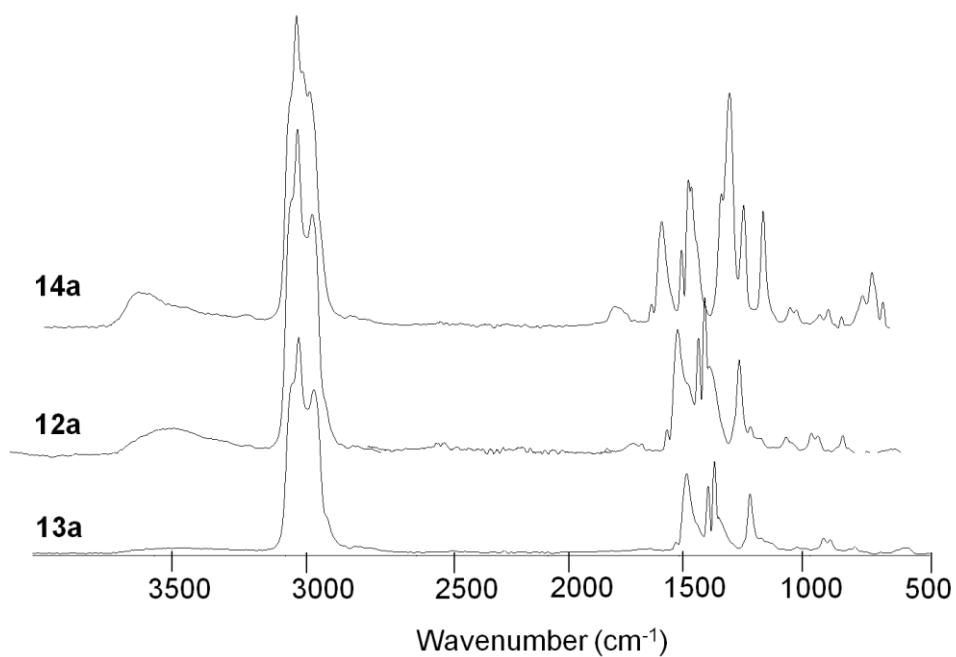
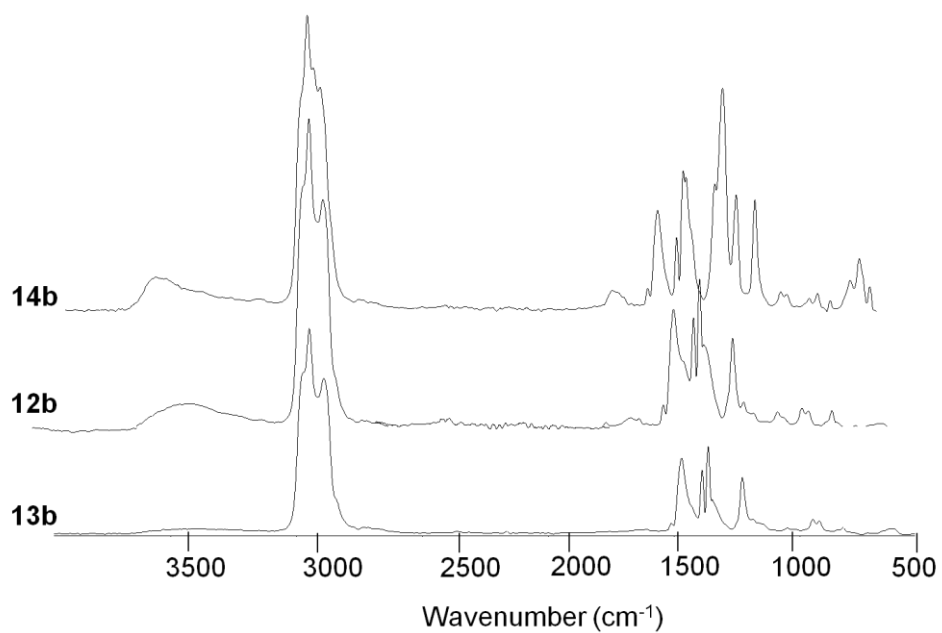[3]Hofmann elimination products were observed in the NMR.

A28. ^{13}C NMR spectra of **29.**

A29.¹H NMR spectra of **13a.**
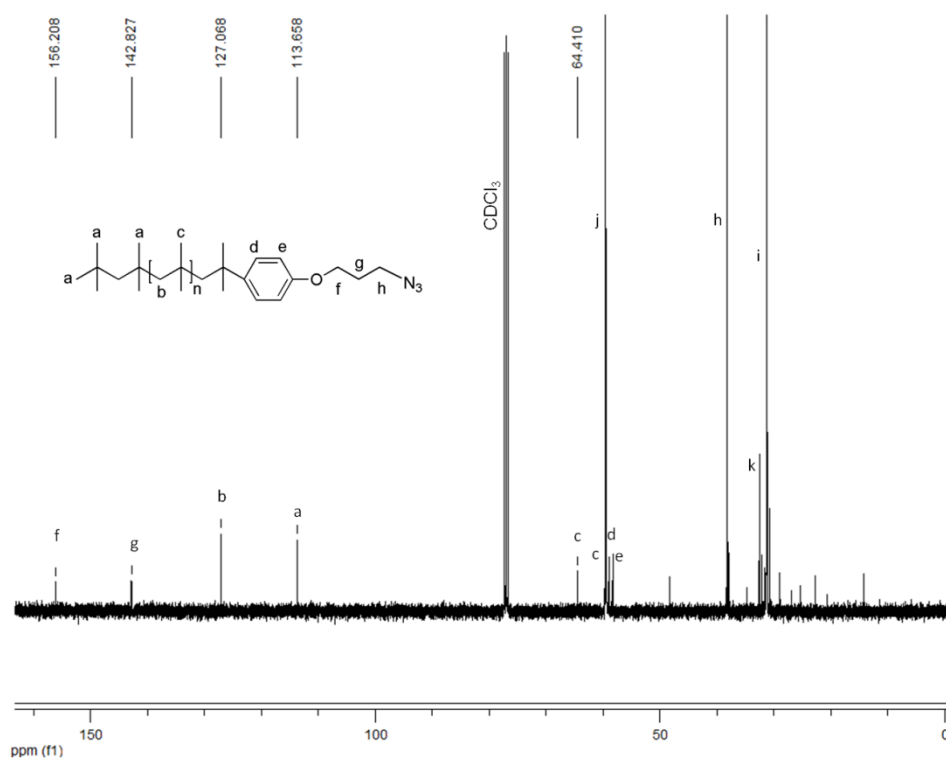
A30.¹³C NMR spectra of **13a.**
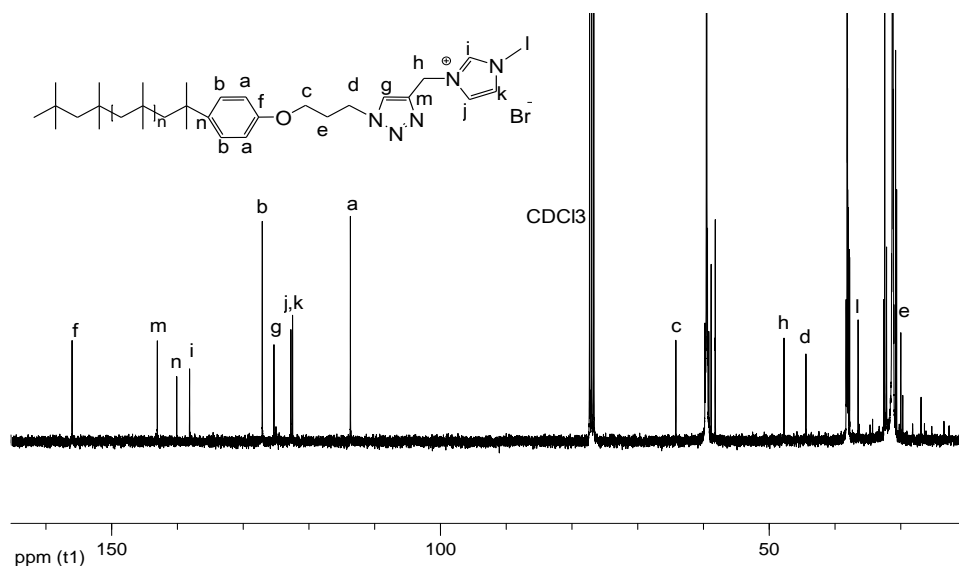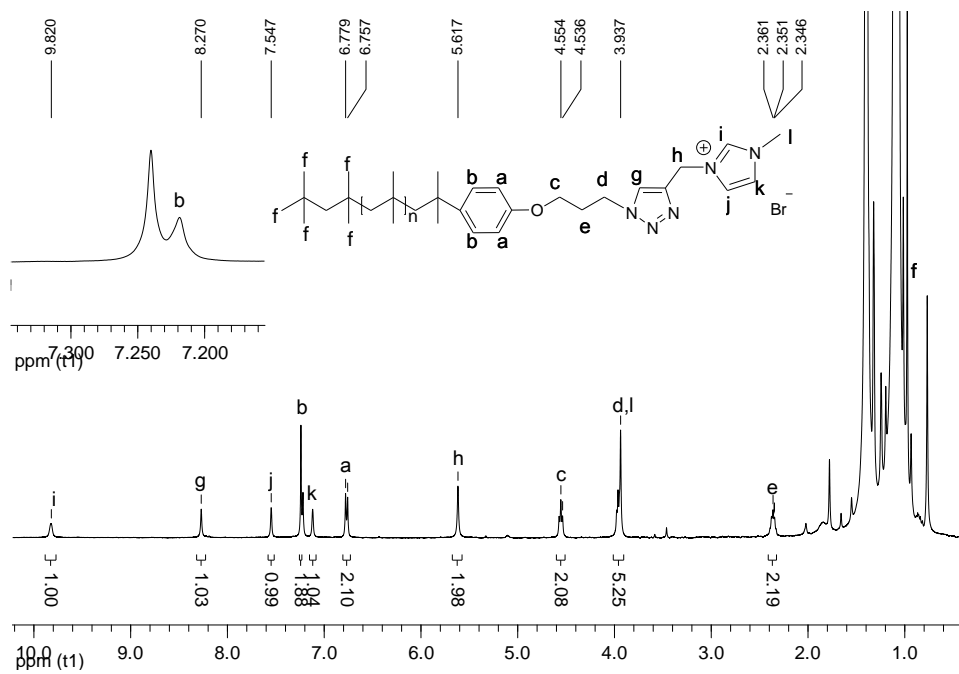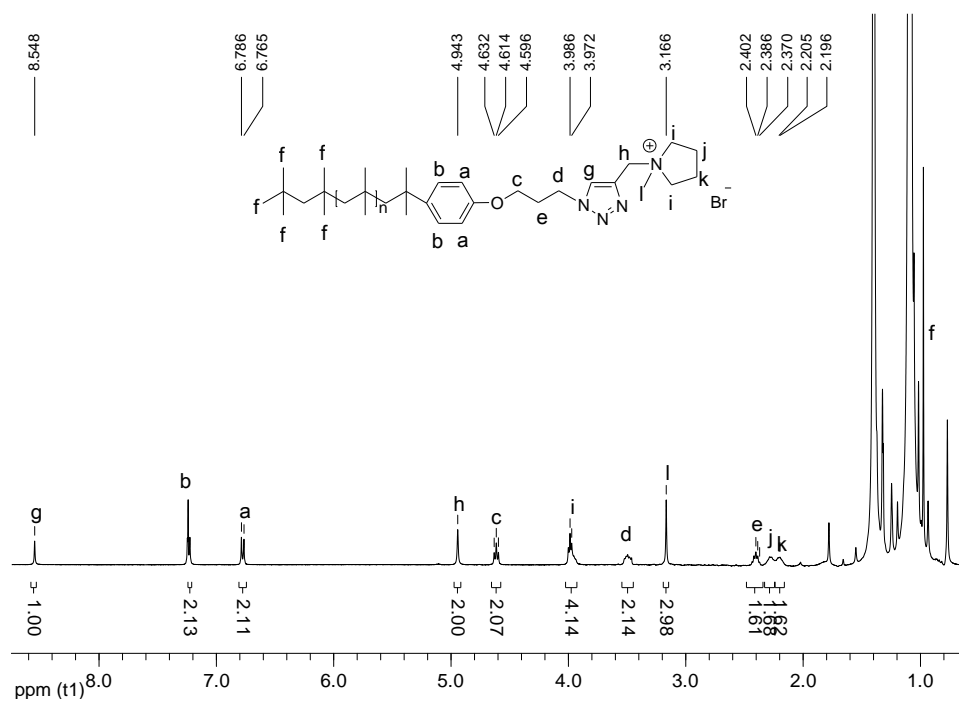
A31. ^{1}H NMR spectra of **13b.**
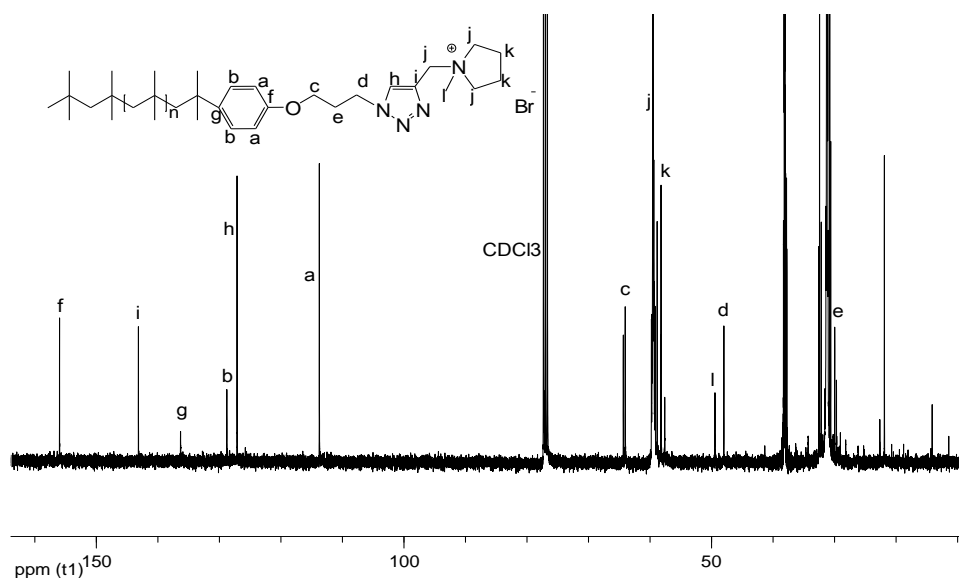
A32. ^{13}C NMR spectra of **13b.**
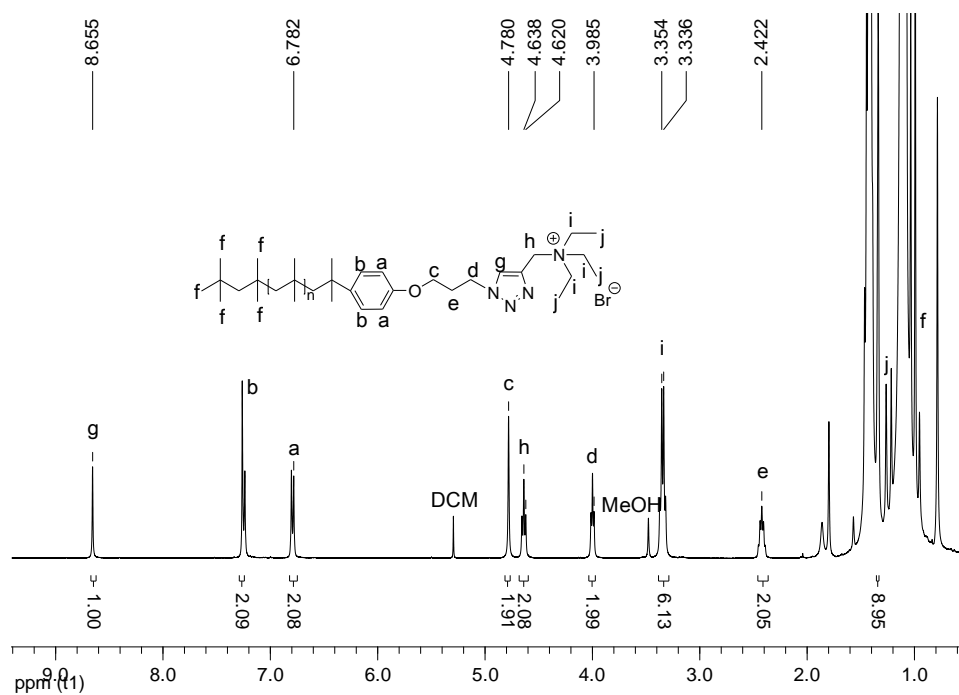
A33. ^{1}H NMR spectra of **13c.**
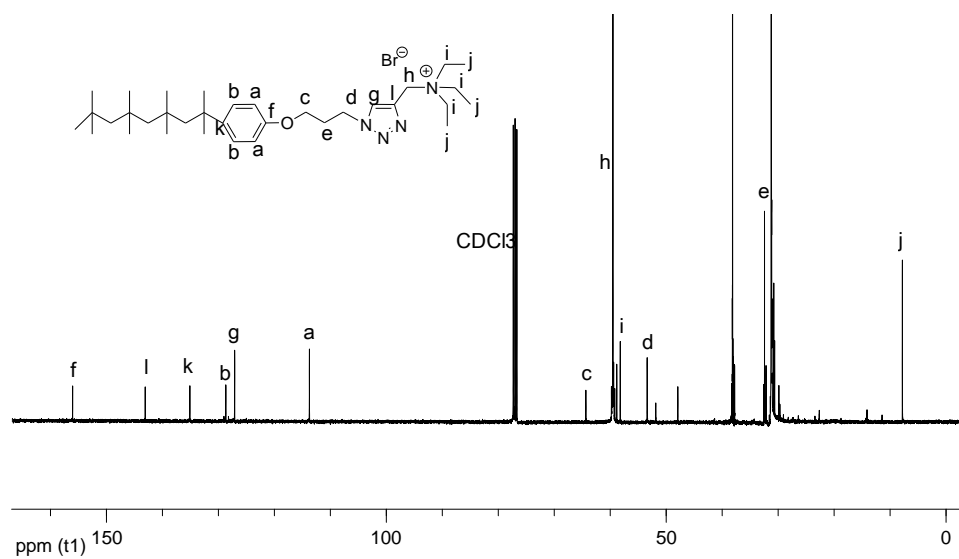
A34. ^{13}C NMR spectra of **13c.**
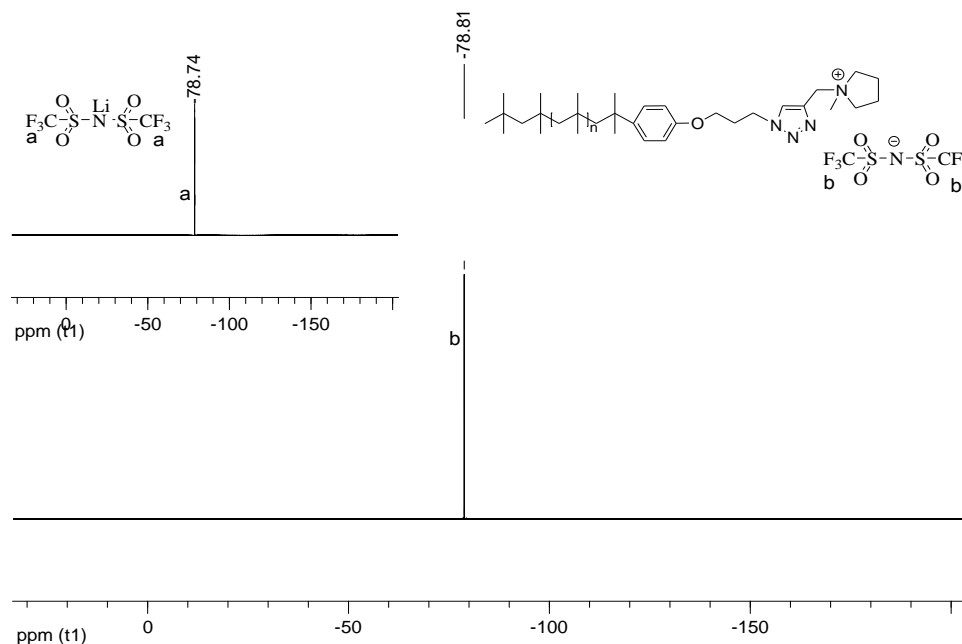
A35. ^{19}F NMR spectra of **14b.**
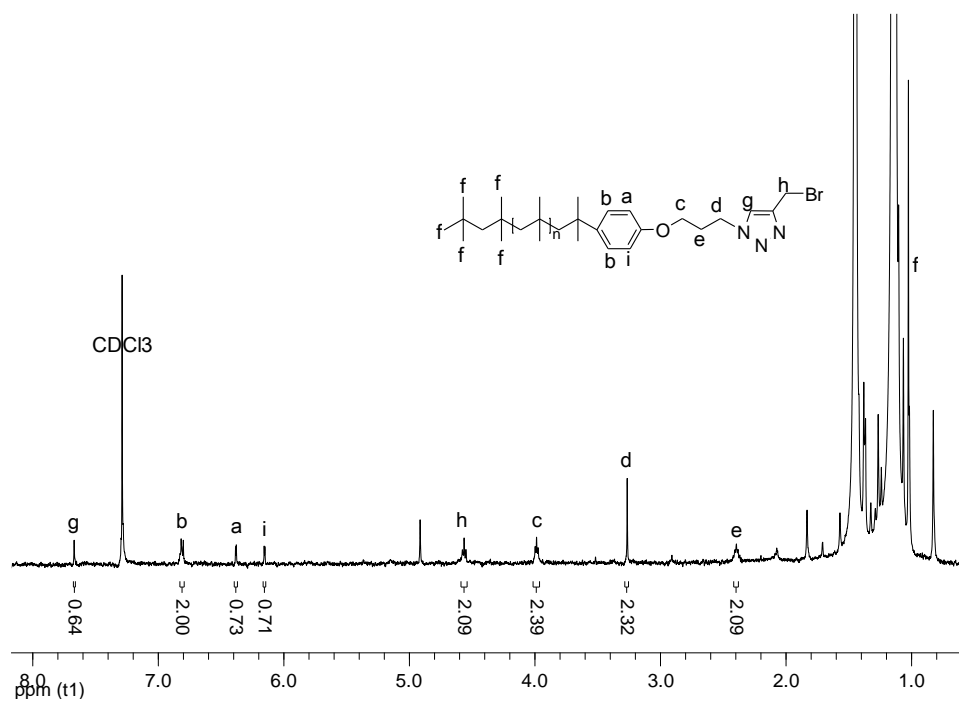
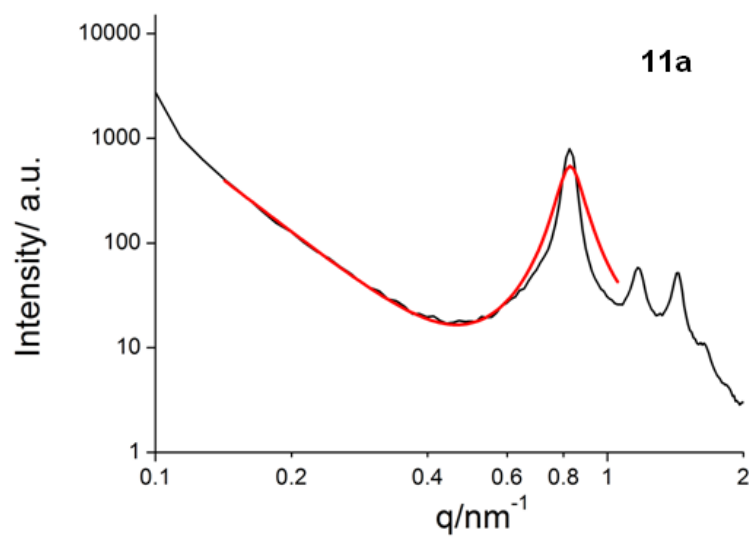**A36.** ^{1}H NMR spectra of decomposition product of **12a.**
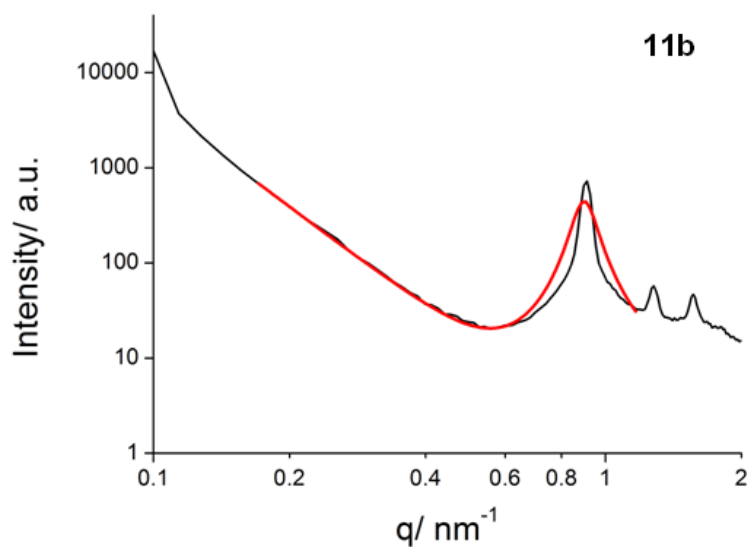
A37.[19]IR spectra of **12a-14a.**
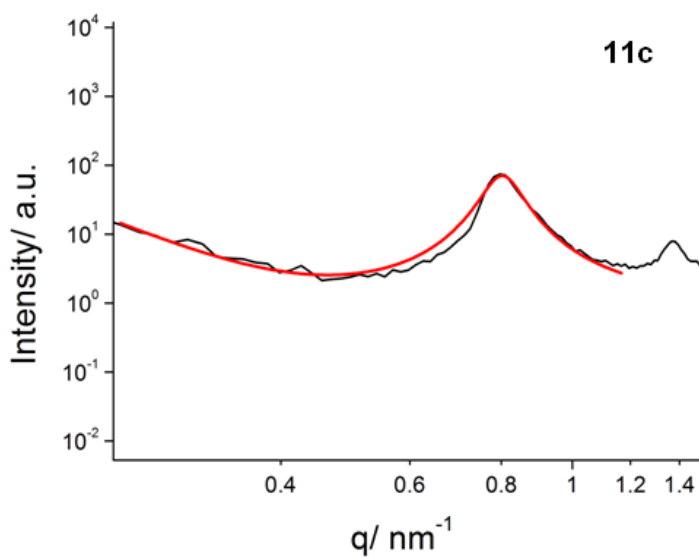

A38.[19]IR spectra of **12b-14b.**
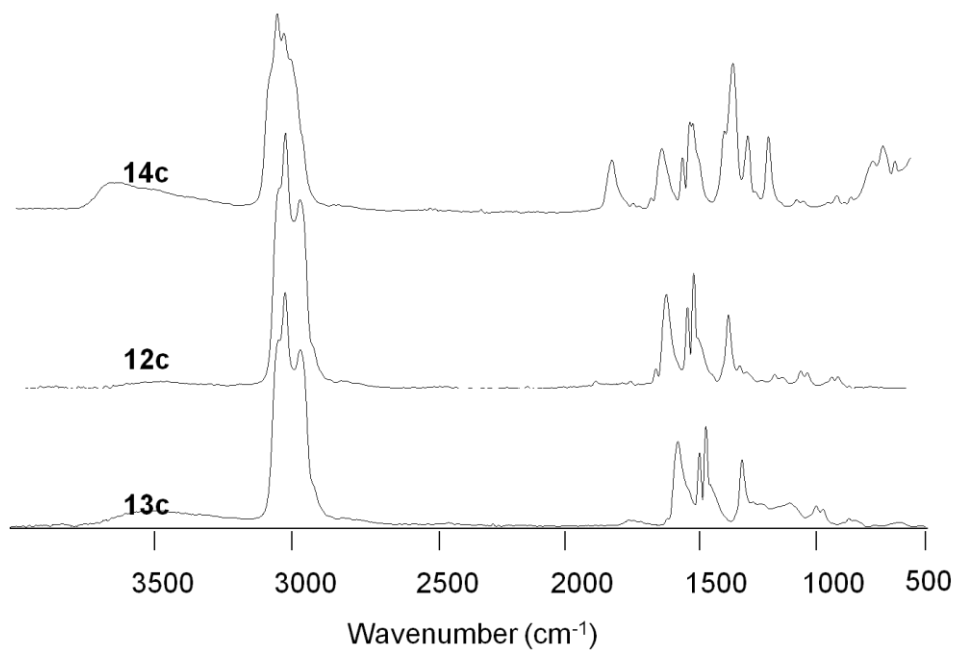
A39.[19]IR spectra of **12c-14c.**
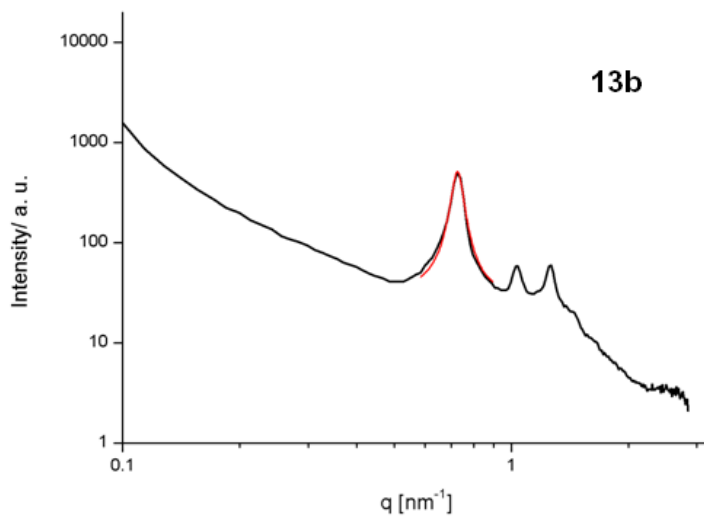

A40. SAXS profile for **11a** at 30°C with a fitted Leibler curve (red). The first peak was used for the calculation.
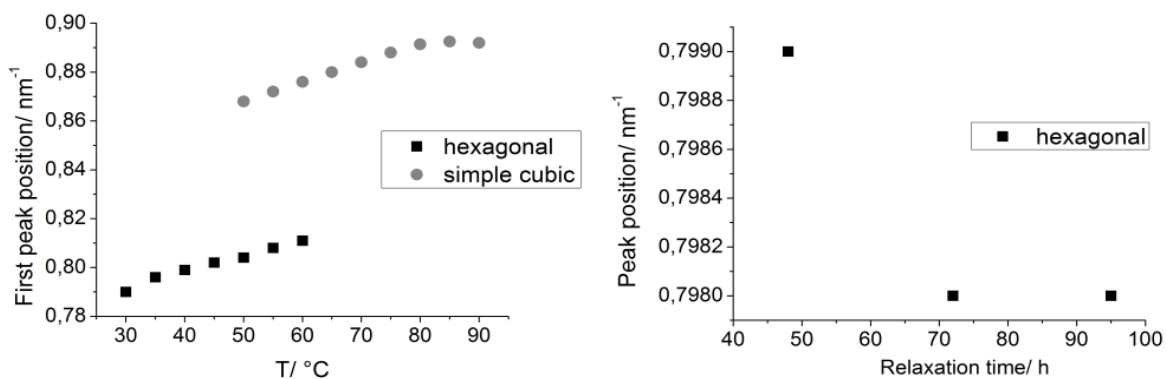
A41. SAXS profile for **11b** at 30°C with a fitted Leibler curve (red). The first peak was used for the calculation.


A42. SAXS profile for **11c** at 30°C with a fitted Leibler curve (red). The first peak was used for the calculation.

A43. SAXS profile for **13b** at 30°C with a fitted Leibler curve (red). The first peak was used for the calculation.

A44. Position of peak maximum and its variation with temperature (left figure) and subsequent relaxation at room temperature (right figure) obtained for **11c**, evaluated from *in-situ* SAXS measurements at different temperatures.
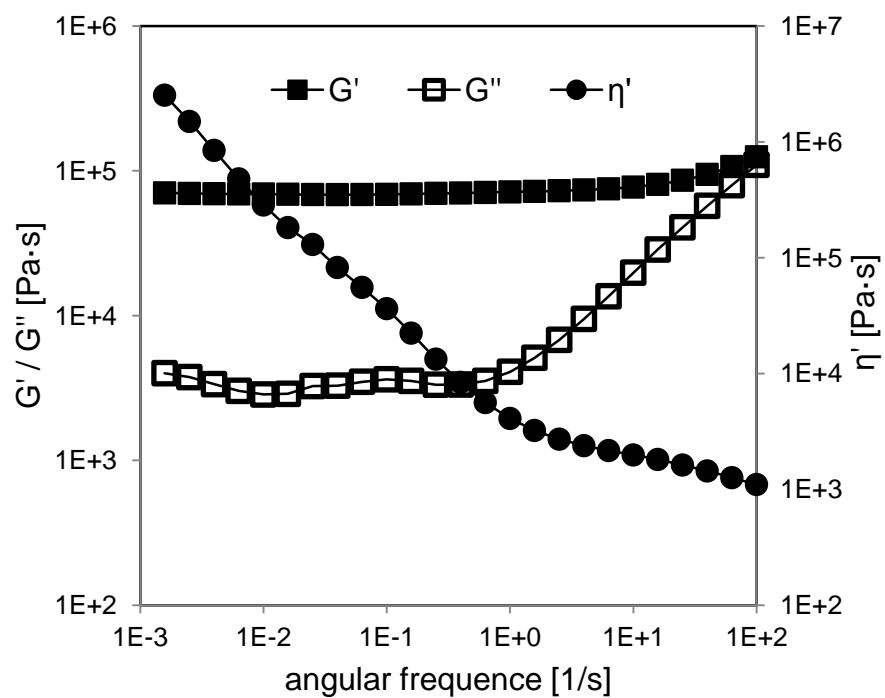
A44. Frequency-sweep measurement of **11a** at 20 °C.
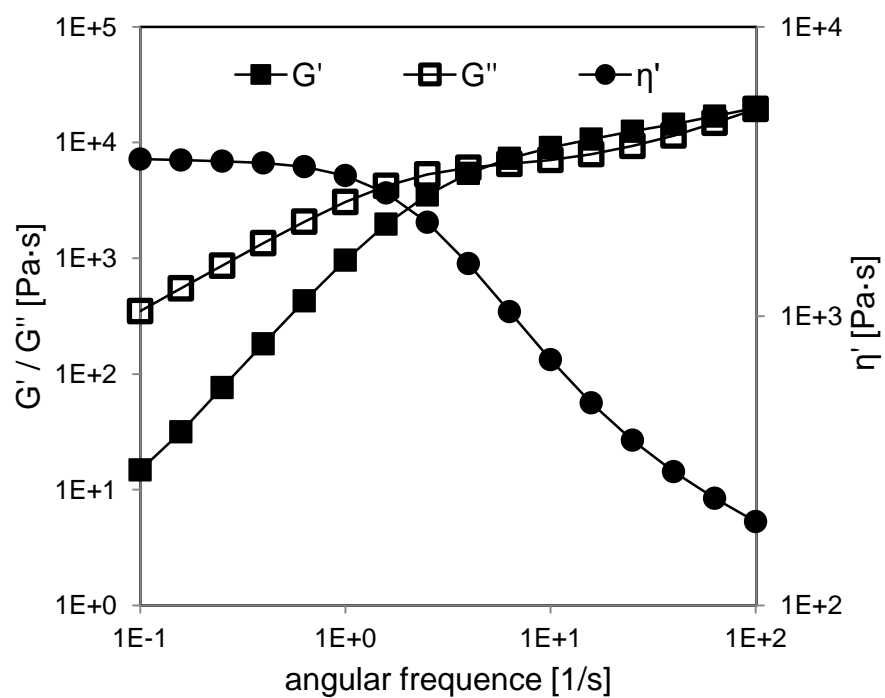
A45. Frequency-sweep measurement of **11b** at 20 °C.

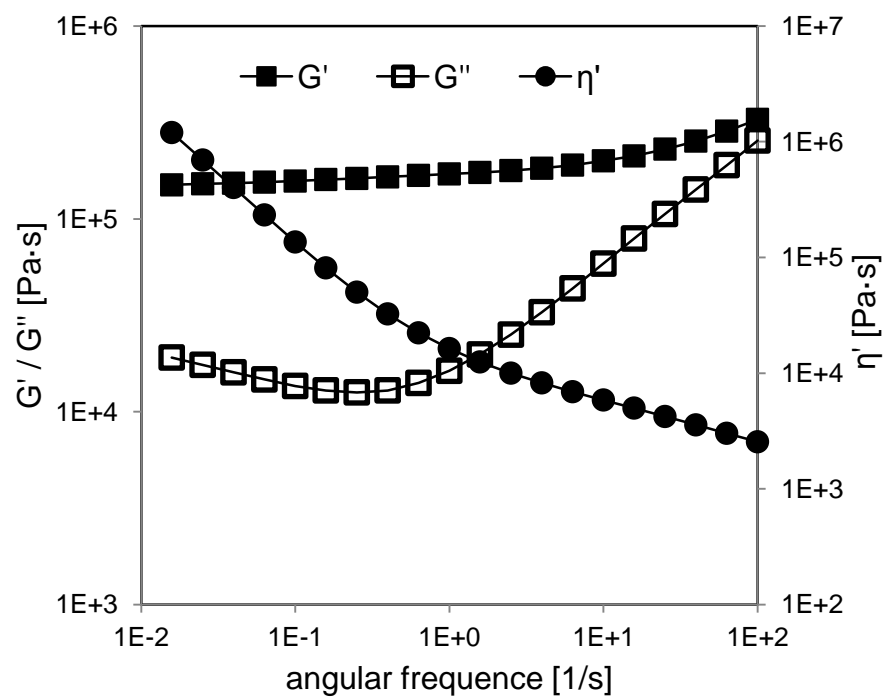**A46.** Frequency-sweep measurement of **11c** at 20 °C.

Eidesstattliche Erklärung

Hiermit erkläre ich, Parvin Zare, dass ich die vorliegende Arbeit selbstständig ohne fremde Hilfe angefertigt habe. Ich habe keine weiteren Quellen oder Hilfsmittel verwendet und die Werke von denen ich wörtlichen bzw. inhaltlichen Stellen entnommen habe, als solche kenntlich gemacht und angeführt.

Parvin Zare

Parvin Zare

Address:	Grosse Ulrichstr.45, 06108-D, Halle (Saale), Germany
E-mail:	parvin.zare@chemie.uni-halle.de
Telephone:	+4917662973403
Date of birth:	03.08.1981

Education

2009-Present   **Ph.D. candidate in Polymer Chemistry**

Martin Luther University of Halle-Wittenberg, Germany

Title: Synthesis and characterization of poly(ethylene glycol) and poly(isobutylene) based ionic liquids and SAXS investigations of their hierarchical structure

2005-2008   **M.Sc. degree in Organic Chemistry**

University of Tabriz, Tabriz, Iran

Title: Solvent-Free Microwave Assisted Synthesis of Functional Polymers Based on Poly(ethylene glycol)

2000-2004   **B.Sc. degree in Applied Chemistry**

University of Tabriz, Tabriz, Iran

Research experience

2013 (1 year)   **IASS project (Improving the Aircraft Safety by Self-Healing Structure and Protecting Nanofillers)**

funded by: European Commission under the 7th Framework Programme

2009-2012   **MINILUBES project (Mechanisms of interactions in nano-scale of novel ionic lubricants with functional surfaces)**

funded by: European Commission under the 7th Framework Programme

Fellowship

2009-2012   **Marie Curie fellowship as an"Early Stage Researcher"**

Martin Luther University of Halle-Wittenberg, Germany

Trainings

2012	**Entrepreneurship**	Prof. Robert D. Hisrich, Wiener Neustadt, Austria
2011	**Basics in Project Management**	Dr. Dagmar Zuci, Cardiff, UK
2010	**Nanotribology and Nanomechanics**	Prof. Bharat Bhushan, Vienna, Austria
2010	**Presentation workshop**	Tristan Jorde, Eibar, Spain

| **2010** | **Summer School on Ionic Liquids** | Katholieke Universiteit Leuven, Leuven, Belgium |

Skills

Language	**English**	Fluent	
	German	Intermediate	
	Turkish	Fluent	
	Farsi	Native	

Computer	**OS**	MS Windows
	Applications	MS Office, Coreldraw,Photoshop, Origin, Chem Draw, MestRec, Brucker Data Analysis

Laboratory **Organic synthesis and purification, Polymerization techniques**

Conducting rheology, DSC, TGA, GPC and DLS measurements

Data interpretation (NMR, IR, GPC, MALDI, ESI-MS, DSC, TGA, Rheology)

Additional skills Team work, Communication, Time management, Flexibility, Problem solving

Patent

- Aswath, P. B., Chen, X., Sharma, V. Igartua, M. A.; Pagano, F.; Binder, W.; **Zare, P.**; Doerr, N., **2013**, Synergistic mixtures of ionic liquids with other ionic liquids and/or with ashless thiophosphates for antiwear and/or friction reduction applications. **US patent 20130331305**

Publications

- Doehler, D.; **Zare, P**.; Binder. W. H., Hyperbranched polyisobutylenes for self-healing polymers. Polym. Chem., **2014**, 5, 992-1000.

- Stojanovic, A.; Appiah, C.; Doehler, D; Akbarzadeh, J.; **Zare, P.**; Peterlik, H.; Binder, W. H., Designing melt flow of poly(isobutylene)-based ionic liquids. J. Mater. Chem. A, **2013**, 1, 12159-12169.

- **Zare, P.**; Mahrova, M.; Tojo, E.; Stojanovic, A.; Binder, W. H., Ethylene glycol-based ionic liquids via azide/alkyne click chemistry. J. Polym. Sci. Part A : Chemistry, **2013**, 51 (1), 190-202.

- Pagano, F.; Gabler, C.; **Zare, P.**; Mahrova, M.; Doerr, N.; Bayon, R.; Fernandez, X.; Binder, W. H.; Hernaiz, M.; Tojo, E.; Igartua, A., Dicationic ionic liquids as lubricants. Proc. I. Mech. Eng., Part J: J. Engineering Tribology, **2012,** 226 (11), 952–964.

- **Zare, P.**; Stojanovic, A.; Herbst, F.; Akbarzadeh, J.; Peterlik, H.; Binder, W. H., Hierarchically Nanostructured Polyisobutylene-Based Ionic Liquids. Macromolecules, **2012**, 45 (4), 2074-2084.

Conferences

Proceedings

- Binder, W. H.; **Zare, P**.; Stojanovic, A., Poly(isobutylene)-based ionic liquids. Polymers and ionic liquids: Europolymer Conference (**EUPOC**), Gargnano, **2013**.

- **<u>Zare, P</u>.</u>**; Stojanovic, A., What are the strategies to synthesize polymeric ionic liquids? Minilubes symposium, Wiener Neustadt, **2012.**

Posters presentations

- <u>Stojanovic, A.</u>; **Zare, P**.; Herbst, F.; Akbarzadeh, J.; Peterlik, H.; Binder, W. H., Highly nanostructured polyisobutylene-based polymeric ionic liquids as novel selg-healing materials. 5th Congress on Ionic Liquids (**COIL-5**), Vilamoura, **2013**.

- **<u>Zare, P</u>.**; Appiah, C.; Stojanovic, A.; Binder, W. H., Nanostructured polyisobutylene-based ionic liquids: design of novel self-healing materials. Polymeric Materials (**P2012**), Halle (Saale), **2012**.

- **<u>Zare, P</u>.**; Mahrova, M.; Binder, W. H., Ethylene glycol-based ionic liquids as advanced lubricating systems. Polymeric Materials (**P2012**), Halle (Saale), **2012**.

- **Zare, P.**; <u>Stojanovic, A.</u>; Binder, W. H, Synthesis of novel poly(isobutylene)-based ionic liquids. 4th Congress on Ionic Liquids (**COIL-4**), Washington, DC, **2011**.

- <u>Mahrova, M.</u>; **Zare, P.**; Binder, W. H.; Tojo, E., New hexaethylene glycol and poly(ethylene glycol) based ionic liquids as potential lubricants. 4th Congress on Ionic Liquids (**COIL-4**), Washington, DC, **2011**.

- **<u>Zare, P</u>.**; Binder, W. H., Preparation of polymeric ionic liquids as potential lubricants. Polymeric Materials (**P2010**), Halle (Saale), **2010**.